การสังเคราะห์อนุภาคระดับนาโนเมตรของเงินโดยใช้การฉายรังสียูวีและ
การประยุกต์ในการตรวจหาสารฆ่าวัชพืช

นางขนิษฐา วัชราภรณ์

วิทยานิพนธ์นี้เป็นส่วนหนึ่งของการศึกษาตามหลักสูตรปริญญาวิทยาศาสตรดุษฎีบัณฑิต
สาขาวิชาวัสดุศาสตร์ ภาควิชาวัสดุศาสตร์
คณะวิทยาศาสตร์ จุฬาลงกรณ์มหาวิทยาลัย
ปีการศึกษา 2557

SYNTHESIS OF SILVER NANOPARTICLES USING UV IRRADIATION AND THEIR APPLICATION IN HERBICIDE DETECTION

Mrs. Kanitta Watcharaporn

A Dissertation Submitted in Partial Fulfillment of the Requirements
for the Degree of Doctor of Philosophy Program in Materials Science
Department of Materials Science
Faculty of Science
Chulalongkorn University
Academic Year 2014

Thesis Title	SYNTHESIS OF SILVER NANOPARTICLES USING UV IRRADIATION AND THEIR APPLICATION IN HERBICIDE DETECTION
By	Mrs. Kanitta Watcharaporn
Field of Study	Materials Science
Thesis Advisor	Associate Professor Vimolvan Pimpan, Ph.D.
Thesis Co-Advisor	Assistant Professor Mantana Opaprakasit, Ph.D.

Accepted by the Faculty of Science, Chulalongkorn University in Partial Fulfillment of the Requirements for the Doctoral Degree

.....Dean of the Faculty of Science
(Professor Supot Hannongbua, Dr.rer.nat.)

THESIS COMMITTEE

.....Chairman
(Assistant Professor Sirithan Jiemsirilers, Ph.D.)

.....Thesis Advisor
(Associate Professor Vimolvan Pimpan, Ph.D.)

.....Thesis Co-Advisor
(Assistant Professor Mantana Opaprakasit, Ph.D.)

.....Examiner
(Associate Professor Pranut Potiyaraj, Ph.D.)

.....Examiner
(Associate Professor Kawee Srikulkit, Ph.D.)

.....External Examiner
(Associate Professor Werasak Udomkichdecha, Ph.D.)

ขนิษฐา วัชราภรณ์ : การสังเคราะห์อนุภาคระดับนาโนเมตรของเงินโดยใช้การฉายรังสียูวีและการประยุกต์ในการตรวจหาสารฆ่าวัชพืช (SYNTHESIS OF SILVER NANOPARTICLES USING UV IRRADIATION AND THEIR APPLICATION IN HERBICIDE DETECTION) อ.ที่ปรึกษาวิทยานิพนธ์หลัก: รศ. ดร. วิมลวรรณ พิมพ์พันธุ์, อ.ที่ปรึกษาวิทยานิพนธ์ร่วม: ผศ. ดร. มัณฑนา โอภาประกาสิต, 165 หน้า.

งานวิจัยนี้เป็นการสังเคราะห์อนุภาคระดับนาโนเมตรของเงินด้วยการฉายรังสียูวีที่มีกำลังไฟฟ้าเท่ากับ 8 วัตต์ เป็นเวลา 1 ชั่วโมง ให้กับของผสมระหว่างสารละลายซิลเวอร์ไนเทรตและสารช่วยเสถียร โดยเลือกใช้สารช่วยเสถียร 5 ชนิด ได้แก่ กรดแทนนิก เกลือโซเดียมของกรดพอลิเมทาคริลิก เกลือโซเดียมของคาร์บอกซีเมทิลเซลลูโลส ไคโตซาน และเกลือโซเดียมของกรดฮิวมิก นอกจากนี้ ยังปรับเปลี่ยนค่าความเป็นกรด-ด่างเริ่มต้นของสารละลายสารช่วยเสถียรจาก 5.0, 6.0, 7.0, 8.0 ถึง 9.0 และอัตราส่วนโดยโมลของสารช่วยเสถียรต่อไอออนของเงินจาก 10:1, 1:1 ถึง 1:10 เพื่อศึกษาผลของพารามิเตอร์เหล่านี้ที่มีต่อกระบวนการสังเคราะห์

ผลการทดลองแสดงให้เห็นว่า สารช่วยเสถียรทั้ง 5 ชนิดสามารถทำหน้าที่เป็นสารรีดิวซ์ และการฉายรังสียูวีมีส่วนช่วยในปฏิกิริยารีดักชัน ภาพจากเครื่องอิเล็กตรอนไมโครสโกปีแบบส่องผ่าน แสดงให้เห็นว่า อนุภาคเงินทั้งหมดมีขนาดต่ำกว่า 50 นาโนเมตร และแสดงพีกที่เป็นลักษณะเฉพาะในการดูดกลืนแสงยูวีวิสซิเบิลในช่วงความยาวคลื่น 350-430 นาโนเมตร ขึ้นกับชนิด ปริมาณ และความเป็นกรด-ด่างของสารช่วยเสถียร คอลลอยด์อนุภาคระดับนาโนเมตรของเงินที่สังเคราะห์ได้ส่วนใหญ่มีสีเหลืองและมีอนุภาคที่เป็นทรงกลม อย่างไรก็ตาม คอลลอยด์อนุภาคระดับนาโนเมตรของเงินที่สังเคราะห์ด้วยไคโตซาน ที่อัตราส่วนโดยโมลของสารช่วยเสถียรต่อไอออนของเงินเท่ากับ 1:10 ค่าความเป็นกรด-ด่างเริ่มต้นเท่ากับ 5.0 และด้วยเกลือโซเดียมของกรดพอลิเมทาคริลิก ที่อัตราส่วนโดยโมลของสารช่วยเสถียรต่อไอออนของเงินเท่ากับ 1:10 ค่าความเป็นกรด-ด่างเริ่มต้นเท่ากับ 6.0 มีสีม่วงและมีอนุภาคที่เป็นทรงกลมและเป็นท่อน นอกจากนี้ ของผสมระหว่างอนุภาคที่เป็นทรงกลมและสามเหลี่ยมพบในคอลลอยด์ของอนุภาคระดับนาโนเมตรของเงินซึ่งมีเกลือโซเดียมของคาร์บอกซีเมทิลเซลลูโลสเป็นสารช่วยเสถียร เมื่อใช้อัตราส่วนโดยโมลของสารช่วยเสถียรต่อไอออนของเงินเท่ากับ 1:10 เมื่อพิจารณาจากความเสถียรของอนุภาคหลังเก็บไว้ 1 เดือน และลักษณะเฉพาะของการเป็นอนุภาคระดับนาโนเมตรของเงิน เช่น สี และ รูปร่าง ภาวะที่ดีที่สุดในการสังเคราะห์อนุภาคระดับนาโนเมตรของเงิน คือ ที่ความเป็นกรด-ด่างเท่ากับ 6 เมื่อใช้กรดแทนนิกเป็นสารช่วยเสถียร ณ อัตราส่วนโดยโมลของสารช่วยเสถียรต่อไอออนของเงินเท่ากับ 1:1 และที่ความเป็นกรด-ด่างเท่ากับ 6 เมื่อใช้เกลือโซเดียมของกรดพอลิเมทาคริลิก ณ อัตราส่วนโดยโมลของสารช่วยเสถียรต่อไอออนของเงินเท่ากับ 1:10

สุดท้าย เมื่อนำอนุภาคระดับนาโนเมตรของเงินที่สังเคราะห์ได้ไปทดสอบความสามารถในการตรวจหาสารฆ่าวัชพืช พบว่า อนุภาคระดับนาโนเมตรของเงินที่มีความสามารถในการรับรู้สารฆ่าวัชพืชชนิดไพราโซซัลโฟรอน-เอทิลและพาราควอตสูงสุด คือ ตัวอย่างที่สังเคราะห์ในภาวะมีกรดแทนนิก ณ อัตราส่วนโดยโมล ของสารช่วยเสถียรต่อไอออนของเงินเท่ากับ 1:1 ระดับความเป็นกรดที่ 6.0 และตัวอย่างที่สังเคราะห์ในภาวะมีเกลือโซเดียมของกรดพอลิเมทาคริลิก ณ อัตราส่วนโดยโมลของสารช่วยเสถียรต่อไอออนของเงินเท่ากับ 1:10 ระดับความเป็นกรดที่ 6.0 ตามลำดับ

ภาควิชา วัสดุศาสตร์	ลายมือชื่อนิสิต .....
สาขาวิชา วัสดุศาสตร์	ลายมือชื่อ อ.ที่ปรึกษาหลัก .....
ปีการศึกษา 2557	ลายมือชื่อ อ.ที่ปรึกษาร่วม .....

5173904923 : MAJOR MATERIALS SCIENCE
KEYWORDS: SILVER NANOPARTICLES / UV-IRRADIATION / TANNIC ACID / POLY (METHACRYLIC ACID SODIUM SALT) / CARBOXYMETHYL CELLULOSE SODIUM SALT / CHITOSAN / HUMIC ACID / HERBICIDE DETECTION

KANITTA WATCHARAPORN: SYNTHESIS OF SILVER NANOPARTICLES USING UV IRRADIATION AND THEIR APPLICATION IN HERBICIDE DETECTION. ADVISOR: ASSOC. PROF. VIMOLVAN PIMPAN, Ph.D., CO-ADVISOR: ASST. PROF. MANTANA OPAPRAKASIT, Ph.D., 165 pp.

In this research, silver nanoparticles were synthesized by exposing the mixture of silver nitrate and stabilizer solutions to 8 watts of UV-irradiation for one hour. Five stabilizers including tannic acid (TA), poly(methacrylic acid, sodium salt) (PMA), carboxymethyl cellulose sodium salt (CMC), chitosan (CS) and humic acid sodium salt (HA) were used. Initial pH of the stabilizer solution was varied from 5.0, 6.0, 7.0, 8.0 to 9.0 and the molar ratio of stabilizer to silver ions (MR) was varied from 10:1, 1:1 to 1:10 in order to study the effects of these parameters on the synthesis process.

The results showed that all five stabilizers acted as reducing agents and UV irradiation assisted the reduction process. All TEM images showed that the sizes of all synthesized particles were less than 50 nm. They exhibited the characteristic peaks of UV-Vis absorption in the wavelength of 350-430 nm depending on the type, the amount and the pH of the stabilizer. The synthesized silver nanoparticles colloids mostly had yellow color with spherical particles. However, the colloids of silver nanoparticles synthesized using CS at MR of 1:10 with pH of 5.0 and using PMA at MR of 1:10 with pH of 6.0 exhibited purple color with spherical and rod-like particles. In addition, the mixture of the particles having spherical and trigonal shapes was found in the colloids of CMC-stabilized silver nanoparticles synthesized using MR of 1:10. The suitable conditions for synthesizing the silver nanoparticles based on their stability after one month storage and their characteristics of being silver nanoparticles such as color and size were at pH of 6.0 when TA was used as a stabilizer at MR of 1:1 and at pH of 6.0 when PMA was used as a stabilizer at MR of 1:10.

Finally, the ability for herbicide detection of the synthesized silver nanoparticles was investigated. The silver nanoparticles that exhibited highest sensing abilities to pyrazosulfuron-ethyl and paraquat herbicides were the samples synthesized in the presence of TA with MR of 1:1 at pH of 6.0 and the sample synthesized in the presence of PMA with MR of 1:10 at pH of 6.0, respectively.

Department:	Materials Science	Student's Signature	.....
Field of Study:	Materials Science	Advisor's Signature	.....
Academic Year:	2014	Co-Advisor's Signature	.....

ACKNOWLEDGEMENTS

I would like to express my heartfelt gratitude to my advisor, Associate Professor Dr.Vimolvan Pimpan, for her continuing guidance and invaluable suggestions including her patience, consistency and continuing assistances during the whole process of the studies. My appreciation and thank are conveyed to the thesis committee comprising Assistant Professor Dr.Sirithan Jiemsirilers, Assistant Professor Dr.Mantana Opaprakasit, Associate Professor Dr.Kawee Srikulkit, Associate Professor Dr.Pranut Potiyaraj and Associate Professor Dr.Weerasak Udomkichdacha for their supportive guidance, invaluable advice and recommendations.

Without continuing support and encouragement from my collegues and friends at the Department of Textile Science, Agro-industry faculty, Kasetsart University including lecturers, and friends in the Department of Materials Science, Faculty of Science of Chulalongkorn University, this dissertation could not have evolved and appeared hereinafter.

My deep appreciation are extended to all my family members, particularly mom and dad, my husband Sitthirat and my son Peng, whose loving care, patience and understanding are sources of spiritual support and encouragement while empowering me with continuing enthusiasm throughout my Ph.D. studies.

Last but not least, I would like to express my deep appreciation and thank to all my teachers who have equipped me with invaluable knowledge, wisdom and experiences in the specific field of interest, kindly forgave me when I did something wrong and provided me ample opportunities to move on for a better and brighter future. Thank you with all my heart.

CONTENTS

Page

THAI ABSTRACT iv

ENGLISH ABSTRACT v

ACKNOWLEDGEMENTS vi

CONTENTS vii

LIST OF TABLES xi

LIST OF FIGURES xii

CHAPTER I INTRODUCTION 1

CHAPTER II THEORY AND LITERATURE REVIEW 3

2.1 Silver nanoparticles 3

2.1.1 Definition and properties of nanoparticles 3

2.1.2 Synthesis methods 6

2.1.2.1 Chemical reduction 6

2.1.2.2 Irradiation assisted method 9

2.1.2.3 Thermal assisted method 11

2.1.2.4 Microwave assisted method 12

2.1.3 Control of the nanoparticles size 14

2.2 Stabilizers 15

2.2.1 Tannic acid 16

2.2.2 Poly(methacrylic acid sodium salt) 18

2.2.3 Carboxymethyl cellulose sodium salt 20

2.2.4 Chitosan 21

2.2.5 Humic acid 24

Page

2.3 Applications of silver nanoparticles 25
2.3.1 Herbicide detection 25
2.3.1.1 Pyrazosulfuron-ethyl herbicide 26
2.3.1.2 Paraquat. 27
2.3.2 Other applications 27
CHAPTER III EXPERIMENT 32
3.1 The experimental scope 32
3.2 Materials 33
3.3 Instruments 34
3.4 Synthesis of silver nanoparticles 34
3.4.1 Determination of the UV lamp power for the synthesis of silver nanoparticles 34
3.4.2 Synthesis of silver nanoparticles using different stabilizers and conditions 35
3.5 Characterization and testing of silver nanoparticles 37
3.5.1 Analysis of optical characteristics 37
3.5.2 Analysis of morphology 38
3.5.3 Herbicide sensing tests 39
CHAPTER IV RESULTS AND DISCUSSION 40
4.1 Characteristics of silver nanoparticles stabilized by tannic acid. 40
4.1.1 Optical characteristics 40
4.1.1.1 Effect of UV lamp power 40
4.1.1.2 Effect of initial pH of tannic acid solution 46
4.1.1.3 Effect of molar ratio of tannic acid to silver ions 50

Page

4.1.1.4 Role of UV radiation in the synthesis 52
4.1.2 Morphology 55
4.1.3 Stability 59
4.2 Characteristics of silver nanoparticles stabilized by poly (methacrylic acid, sodium salt) 65
4.2.1 Optical characteristics 65
4.2.1.1 Effect of initial pH of poly (methacrylic acid, sodium salt) solution 65
4.2.1.2 Effect of molar ratio of poly(methacrylic acid, sodium salt) to silver ions 69
4.2.1.3 Role of UV radiation in the synthesis 71
4.2.2 Morphology 73
4.2.3 Stability 78
4.3 Characteristics of silver nanoparticles stabilized by carboxymethyl cellulose, sodium salt 85
4.3.1 Optical characteristics 86
4.3.1.1 Effect of initial pH of carboxymethyl cellulose sodium salt solution 86
4.3.1.2 Role of UV radiation in the synthesis 87
4.3.2 Morphology 90
4.3.3 Stability 92
4.4 Characteristics of silver nanoparticles stabilized by chitosan 95
4.4.1 Optical characteristics 96
4.4.1.1 Effect of radiation time 96

Page

4.4.1.2 Role of UV radiation in the synthesis 98
4.4.2 Morphology 100
4.4.3 Stability 101
4.4.1.2 Role of UV radiation in the synthesis 102
4.4.2 Morphology 104
4.4.3 Stability 105
4.5 Characteristics of silver nanoparticles stabilized by humic acid 107
4.5.1 Optical characteristics 107
4.5.1.1 Effect of initial pH of humic acid solution 107
4.5.1.2 Role of UV radiation in the synthesis 110
4.5.2 Morphology 112
5.2 Stability 114
4.6 Herbicide sensing ability of silver nanoparticles 117
4.6.1 Sensing to pyrazosulfuron-ethyl herbicide 117
4.6.2 Sensing to paraquat herbicide 131
CHAPTER V CONCLUSIONS AND RECOMMENDATIONS 140
5.1 Conclusions 140
5.2 Recommendations 143
REFERENCES 144
APPENDIX A 155
APPENDIX B 156
VITA 165

LIST OF TABLES

page

Table 2.1 Optical plasmonic sensors 29

Table 3.1 Chemicals used in this research 33

Table 3.2 Instruments used in this research 34

Table 3.3 Experimental conditions used for the synthesis of silver nanoparticles. 36

Table 4.1 Positions of UV-Vis spectra of the silver nanoparticles synthesized using different initial pH of TA solution and three molar ratios of TA to silver ions 47

Table 4.2 Positions of UV-Vis spectra of the silver nanoparticles synthesized using different initial pH of PMA solution and three molar ratios of PMA to silver ions 69

Table 4.3 Positions of UV-Vis spectra of the silver nanoparticles synthesized using different initial pH of CMC solution and molar ratio of CMC to silver ions at 1:10 87

LIST OF FIGURES

page

Figure 2.1 Schematic of a localized surface plasmon of a metal sphere..... 4

Figure 2.2 Absorption spectra of the silver nanoparticles having different shapes: (a) sphere, (b) cube, (c) tetrahedron, (d) triangular plate and (f) rectangular bar 5

Figure 2.3 Illustration of repulsive force separated silver nanoparticles by the adsorbed borohydride 7

Figure 2.4 Schematic reaction of silver ions reduced by sodium borohydride in the presence of humic acid 7

Figure 2.5 The molecular structure of tannic acid 16

Figure 2.6 The reaction mechanism of the reduction of a silver ion using tannic acid as a reducing agent 17

Figure 2.7 The molecular structure of poly(methacrylic acid sodium salt)..... 19

Figure 2.8 The molecular structure of carboxymethyl cellulose sodium salt 20

Figure 2.9 The molecular structure of chitosan..... 22

Figure 2.10 The molecular structure of humic acid..... 24

Figure 2.11 Molecular structure of pyrazosulfuron-ethyl 26

Figure 2.12 Molecular structure of paraquat 27

Figure 2.13 Schematic of the reduction process of silver ions by dopamine 31

Figure 2.14 Molecular structure of Dopamine, L-Dopa and Adrenaline..... 31

Figure 3.1 The experimental scope..... 32

Figure 3.2 The procedure used for the synthesis of silver nanoparticles 35

Figure 3.3 SPECORD 250 UV-Vis Spectrophotometer..... 37

Figure 3.4 Transmission Electron Microscopes 38

Figure 3.5 The procedure of herbicide sensing test 39

Figure 4.1 UV-Vis spectra of silver nanoparticles colloids synthesized using 8 and 10 watts of UV lamp in the presence of TA at pH of 5.0 43

Figure 4.2 UV-Vis spectra of silver nanoparticles colloids synthesized using 8 and 10 watts of UV lamp in the presence of TA at pH of 6.0 44

Figure 4.3 UV-Vis spectra of silver nanoparticles colloids synthesized using 8 and 10 watts of UV lamp in the presence of TA at pH of 7.0 44

Figure 4.4 UV-Vis spectra of silver nanoparticles colloids synthesized using 8 and 10 watts of UV lamp in the presence of TA at pH of 8.0 45

Figure 4.5 UV-Vis spectra of silver nanoparticles colloids synthesized using 8 and 10 watts of UV lamp in the presence of TA at pH of 9.0 45

Figure 4.6 Appearances of silver nanoparticles colloids synthesized using different initial pH of TA solution and three molar ratios of TA to silver ions 46

Figure 4.7 UV-Vis spectra of silver nanoparticles colloids synthesized using different initial pH of TA solution and three molar ratios (MR) of TA to silver ions; a) MR of 10:1 with dilution ratio of 1:200, b) MR of 1:1 with dilution ratio of 1:25 and c) MR of 1:10 with dilution ratio of 1:25 48

Figure 4.8 UV-Vis spectra of TA-stabilized silver nanoparticles colloids synthesized using three molar ratios of TA to silver ions at with different pH: a) 5.0, b) 6.0, c) 7.0, d) 8.0 and e) 9.0 51

Figure 4.9 Appearances of silver nanoparticles colloids synthesized without any reducing agent using different light sources a) at dark, b) natural light (indoor) and c) UV lamp 52

Figure 4.10 UV-Vis spectra of silver nanoparticles colloids synthesized without any reducing agent using different light sources a) at dark, b) natural light (indoor) and c) UV lamp 53

Figure 4.11 Appearances of TA-stabilized silver nanoparticles colloids synthesized at pH of 8.0 using different light sources: a) pure TA solution, b) at dark, c) natural light (indoor) and d) UV lamp..... 54

Figure 4.12 UV-Vis spectra of TA-stabilized silver nanoparticles colloids synthesized at pH of 8.0 using different light sources: a) pure TA solution, b) at dark, c) natural light (indoor) and d) UV lamp..... 54

Figure 4.13 TEM images of TA-stabilized silver nanoparticles synthesized using different initial pH of TA solution and molar ratio of TA to silver ions at 10:1..... 56

Figure 4.14 TEM images of TA-stabilized silver nanoparticles synthesized using different initial pH of TA solution and molar ratio of TA to silver ions at 1:1..... 57

Figure 4.15 TEM images of TA-stabilized silver nanoparticles synthesized using different initial pH of TA solution and molar ratio of TA to silver ions at 1:10..... 58

Figure 4.16 Appearances of TA-stabilized silver nanoparticles colloids after synthesis and after stored for one month..... 59

Figure 4.17 UV-Vis spectra of TA-stabilized silver nanoparticles colloids synthesized using molar ratio of TA to silver ions at 10:1 after synthesis and after stored for one month 61

Figure 4.18 UV-Vis spectra of TA-stabilized silver nanoparticles colloids synthesized using molar ratio of TA to silver ions at 1:1 after synthesis and after stored for one month 62

Figure 4.19 UV-Vis spectra of TA-stabilized silver nanoparticles colloids synthesized using molar ratio of TA to silver ions at 1:10 after synthesis and after stored for one month 63

Figure 4.20 TEM images of TA-stabilized silver nanoparticles synthesized with MR of TA to silver ions at 1:1 after one month storage. 64

Figure 4.21 Appearances of silver nanoparticles colloids synthesized using different initial pH of PMA solution and three molar ratios of PMA to silver ions 66

Figure 4.22 UV-Vis spectra of silver nanoparticles colloids synthesized using different initial pH of PMA solution and three molar ratios of PMA to silver ions 68

Figure 4.23 UV-Vis spectra of PMA-stabilized silver nanoparticles colloids synthesized using three molar ratios of PMA to silver ions at with different pH: a) 5.0, b) 6.0, c) 7.0, d) 8.0 and e) 9.0 70

Figure 4.24 Appearances of PMA-stabilized silver nanoparticles colloids synthesized at pH of 8.0 using different light sources: a) pure PMA solution, b) at dark, c) natural light (indoor) and d) UV lamp 71

Figure 4.25 UV-Vis spectra of PMA-stabilized silver nanoparticles colloids synthesized at pH of 8.0 using different light sources: a) pure PMA solution, b) at dark, c) natural light (indoor) and d) UV lamp 72

Figure 4.26 TEM images of PMA-stabilized silver nanoparticles synthesized using different initial pH of PMA solution and molar ratio of PMA to silver ions at 10:1 75

Figure 4.27 TEM images of PMA-stabilized silver nanoparticles synthesized using different initial pH of PMA solution and molar ratio of PMA to silver ions at 1:1 76

Figure 4.28 TEM images of PMA-stabilized silver nanoparticles synthesized using different initial pH of PMA solution and molar ratio of PMA to silver ions at 1:10 77

Figure 4.29 Appearances of PMA-stabilized silver nanoparticles colloids after synthesis and after stored for one month 80

Figure 4.30 UV-Vis spectra of PMA-stabilized silver nanoparticles colloids synthesized using molar ratio of PMA to silver ions at 10:1 after synthesis and after stored for one month 82

Figure 4.31 UV-Vis spectra of PMA-stabilized silver nanoparticles colloids synthesized using molar ratio of PMA to silver ions at 1:1 after synthesis and after stored for one month 83

Figure 4.32 UV-Vis spectra of PMA-stabilized silver nanoparticles colloids synthesized using molar ratio of PMA to silver ions at 1:10 after synthesis and after stored for one month 84

Figure 4.33 Appearances of 1.0 and 0.1 mM of carboxymethyl cellulose, sodium salt solutions 85

Figure 4.34 Appearance of incompletely dissolved CMC in 1.0 mM of carboxymethyl cellulose, sodium salt in aqueous solution 85

Figure 4.35 Appearances of silver nanoparticles colloids synthesized using different initial pH of CMC solution and molar ratios of CMC to silver ions at 1:10 86

Figure 4.36 UV-Vis spectra of silver nanoparticles colloids synthesized using different initial pH of CMC solution and molar ratio of CMC to silver ions at 1:10 87

Figure 4.37 Appearances of CMC-stabilized silver nanoparticles colloids synthesized at pH of 8.0 using different light sources: a) pure CMC solution, b) at dark, c) natural light (indoor) and d) UV lamp 88

Figure 4.38 UV-Vis spectra of CMC-stabilized silver nanoparticles colloids synthesized at pH of 8.0 using different light sources: a) pure CMC solution, b) at dark, c) natural light (indoor) and d) UV lamp 88

Figure 4.39 TEM images of CMC-stabilized silver nanoparticles synthesized using different initial pH of CMC solution and molar ratio of CMC to silver ions at 1:10 91

Figure 4.40 Appearances of CMC-stabilized silver nanoparticles colloids synthesized using molar ratio of CMC to silver ions at 1:10 after synthesis and after stored for one month 93

Figure 4.41 UV-Vis spectra of CMC-stabilized silver nanoparticles colloids synthesized using molar ratio of CMC to silver ions at 1:10 after synthesis and after stored for one month..... 94

Figure 4.42 Appearance of 0.1 mM of chitosan in 1.0 % v/v of acetic acid solutions at pH of a) 6.0 and b) 7.0 96

Figure 4.43 Appearances of silver nanoparticles colloids synthesized using initial pH of chitosan at 5.0 (left), and 6.0 (right) after UV radiation for one hour 96

Figure 4.44 Appearances of silver nanoparticles colloids synthesized using 0.1 mM CS in 1.0 % v/v acetic acid solution at initial pH of 5.0 at various radiation times of 1, 2, 4, 8, 15, 20, 25, 30, 40, 50 and 60 minutes 97

Figure 4.45 UV-Vis spectra of silver nanoparticles colloids synthesized using 0.1 mM CS in 1.0 % v/v acetic acid solution at initial pH of 5.0 at various radiation times of 1, 2, 4, 8, 15, 20, 25, 30, 40, 50 and 60 minutes 97

Figure 4.46 Appearances of CS-stabilized silver nanoparticles colloids synthesized at pH of 5.0 using different light sources: a) at dark for 2 min, b) at dark for 4 min, c) natural light for 2 min, d) natural light for 4 min, e) UV lamp for 2 min and f) UV lamp for 4 min..... 98

Figure 4.47 UV-Vis spectra of CS-stabilized silver nanoparticles colloids synthesized at pH of 5.0 using different light sources: a) at dark for 2 min, b) at dark for 4 min, c) natural light for 2 min, d) natural light for 4 min, e) UV lamp for 2 min and f) UV lamp for 4 min 99

Figure 4.48 TEM images of CS-stabilized silver nanoparticles colloids synthesized using 0.1 mM CS in 1.0 % v/v acetic acid solution at initial pH of 5.0 and radiation time of 2 minutes 100

Figure 4.49 Appearances of CS-stabilized silver nanoparticles colloids synthesized using 0.1 mM CS in 1.0 % v/v acetic acid solution at initial pH of 5.0 at various radiation times of 1, 2, 4, 8, 15, 20, 25, 30, 40, 50 and 60 minutes after synthesis and after stored for one month.....101

Figure 4.50 UV-Vis spectra of silver nanoparticles colloids synthesized using 0.1 mM CS in 1.0 % v/v acetic acid solution at initial pH of 5.0 at various radiation times of 1, 2, 4, 8, 15, 20, 25, 30, 40, 50 and 60 minutes 102

Figure 4.51 Appearances of CS-stabilized silver nanoparticles colloids synthesized at pH of 5.0 using different light sources: a) at dark for 2 min, b) at dark for 4 min, c) natural light for 2 min, d) natural light for 4 min, e) UV lamp for 2 min and f) UV lamp for 4 min 103

Figure 4.52 UV-Vis spectra of CS-stabilized silver nanoparticles colloids synthesized at pH of 5.0 using different light sources: a) at dark for 2 min, b) at dark for 4 min, c) natural light for 2 min, d) natural light for 4 min, e) UV lamp or 2 min and f) UV lamp for 4 min 103

Figure 4.53 TEM images of CS-stabilized silver nanoparticles colloids synthesized using 0.1 mM CS in 1.0 % v/v acetic acid solution at initial pH of 5.0 and radiation time of 2 minutes 104

Figure 4.54 Appearances of CS-stabilized silver nanoparticles colloids synthesized using 0.1 mM CS in 1.0 % v/v acetic acid solution at initial pH of 5.0 at various radiation times of 1, 2, 4, 8, 15, 20, 25, 30, 40, 50 and 60 minutes after synthesis and after stored for one month.....105

Figure 4.55 UV-Vis spectra of CS-stabilized silver nanoparticles colloids synthesized using 0.1 mM CS in 1.0 % v/v acetic acid solution at initial pH of 5.0 at various radiation times of 1, 2, 4, 8, 15, 20, 25, 30, 40, 50 and 60 minutes after synthesis and after stored for one month.....106

Figure 4.56 Appearances of humic acid solutions at different concentrations 107

Figure 4.57 Appearances of silver nanoparticles colloids synthesized using different initial pH of HA solution and two concentrations of HA: a) 0.0072 mM and b) 0.0007 mM. 108

Figure 4.58 UV-Vis spectra of silver nanoparticles colloids synthesized using different initial pH of HA solution and two concentrations of HA: a) 0.0072 mM and b) 0.0007 mM. 109

Figure 4.59 Appearances of HA-stabilized silver nanoparticles colloids synthesized at pH of 9.0 and 0.0007 mM of HA solution using different light sources: a) pure CMC solution, b) at dark, c) natural light (indoor) and d) UV lamp 111

Figure 4.60 UV-Vis spectra of HA-stabilized silver nanoparticles colloids synthesized at pH of 9.0 and 0.0007 mM of HA solution using different light sources: a) pure CMC solution, b) at dark, c) natural light (indoor) and d) UV lamp 111

Figure 4.61 TEM images of HA-stabilized silver nanoparticles colloids synthesized using 0.0072 mM of HA solution 113

Figure 4.62 Appearances of HA-stabilized silver nanoparticles colloids after synthesis and after stored for one month 114

Figure 4.63 UV-Vis spectra of HA-stabilized silver nanoparticles colloids synthesized using 0.0072 mM of HA solution after synthesis and after stored for one month 115

Figure 4.64 UV-Vis spectra of HA-stabilized silver nanoparticles colloids synthesized using 0.0007 mM of HA solution after synthesis and after stored for one month 116

Figure 4.65 Appearances of TA-stabilized silver nanoparticles colloids synthesized using initial pH of 6.0 and MR of 10:1 exposed to various amount of PSE herbicide (ppm) 117

Figure 4.66 UV-Vis spectra of TA-stabilized silver nanoparticles colloids synthesized using initial pH of 6.0 and MR of 10:1 exposed to various amount of PSE herbicide (ppm).....117

Figure 4.67 Appearances of TA-stabilized silver nanoparticles colloids synthesized using initial pH of 6.0 and MR of 1:1 exposed to various amount of PSE herbicide (ppm).....118

Figure 4.68 UV-Vis spectra of TA-stabilized silver nanoparticles colloids synthesized using initial pH of 6.0 and MR of 1:1 exposed to various amount of PSE herbicide (ppm).....118

Figure 4.69 Appearances of TA-stabilized silver nanoparticles colloids synthesized using initial pH of 6.0 and MR of 1:10 exposed to various amount of PSE herbicide (ppm).....119

Figure 4.70 UV-Vis spectra of TA-stabilized silver nanoparticles colloids synthesized using initial pH of 6.0 and MR of 1:10 exposed to various amount of PSE herbicide (ppm).....119

Figure 4.71 Appearances of TA-stabilized silver nanoparticles colloids synthesized using initial pH of 5.0 and MR of 1:1 exposed to various amount of PSE herbicide (ppm).....120

Figure 4.72 UV-Vis spectra of TA-stabilized silver nanoparticles colloids synthesized using initial pH of 5.0 and MR of 1:1 exposed to various amount of PSE herbicide (ppm).....120

Figure 4.73 Appearances of TA-stabilized silver nanoparticles colloids synthesized using initial pH of 6.0 and MR of 1:10 exposed to various amount of PSE herbicide (ppm).....121

Figure 4.74 UV-Vis spectra of TA-stabilized silver nanoparticles colloids synthesized using initial pH of 6.0 and MR of 1:10 exposed to various amount of PSE herbicide (ppm).....121

Figure 4.75 Appearances of PMA-stabilized silver nanoparticles colloids synthesized using initial pH of 6.0 and MR of 1:10 exposed to various amount of PSE herbicide (ppm)..... 122

Figure 4.76 UV-Vis spectra of PMA-stabilized silver nanoparticles colloids synthesized using initial pH of 6.0 and MR of 1:10 exposed to various amount of PSE herbicide (ppm)..... 122

Figure 4.77 Appearances of CMC-stabilized silver nanoparticles colloids synthesized using initial pH of 6.0 and MR of 1:10 exposed to various amount of PSE herbicide (ppm)..... 123

Figure 4.78 UV-Vis spectra of CMC-stabilized silver nanoparticles colloids synthesized using initial pH of 6.0 and MR of 1:10 exposed to various amount of PSE herbicide (ppm)..... 123

Figure 4.79 Appearances of CS-stabilized silver nanoparticles colloids synthesized using initial pH of 5.0, radiation time of 4 mins and MR of 1:10 exposed to various amount of PSE herbicide (ppm)..... 124

Figure 4.80 UV-Vis spectra of CS-stabilized silver nanoparticles colloids synthesized using initial pH of 5.0, radiation time of 4 mins and MR of 1:10 exposed to various amount of PSE herbicide (ppm)..... 124

Figure 4.81 Appearances of HA-stabilized silver nanoparticles colloids synthesized using 0.0007 mM of HA at initial pH of 6.0 exposed to various amount of PSE herbicide (ppm)..... 125

Figure 4.82 UV-Vis spectra of HA-stabilized silver nanoparticles colloids synthesized using 0.0007 mM of HA at initial pH of 6.0 exposed to various amount of PSE herbicide (ppm)..... 125

Figure 4.83 Dissociation of pyrazosulfuron-ethyl acid..... 126

Figure 4.84 Hydrolysis of pyrazosulfuron-ethyl herbicide..... 127

Figure 4.85 Reaction showing the role of heterocyclic amine as basic substance.... 128

Figure 4.86 Schematic interaction between pyrazosulfuron ethyl and TA-stabilized silver nanoparticles. (TA= Tannic acid, PSE= pyrazosulfuron ethyl, B^+= cationic of heterocyclic amine). 128

Figure 4.87 TEM images of TA-stabilized silver nanoparticles synthesized using molar ratio of TA to silver ions at 1:1 with different initial pH of TA after exposed to 400 ppm of PSE herbicide; a) pH of 6.0 and b) pH of 5.0 130

Figure 4.88 Appearances of TA-stabilized silver nanoparticles colloids synthesized using initial pH of 6.0 and MR of 1:1 exposed to various amount of PQ herbicide (ppm)..... 132

Figure 4.89 UV-Vis spectra of TA-stabilized silver nanoparticles colloids synthesized using initial pH of 6.0 and MR of 1:1 exposed to various amount of PQ herbicide (ppm)..... 132

Figure 4.90 Appearances of PMA-stabilized silver nanoparticles colloids synthesized using initial pH of 6.0 and MR of 1:10 exposed to various amount of PQ herbicide (ppm)..... 133

Figure 4.91 UV-Vis spectra of PMA-stabilized silver nanoparticles colloids synthesized using initial pH of 6.0 and MR of 1:10 exposed to various amount of PQ herbicide (ppm)..... 133

Figure 4.92 Appearances of CMC-stabilized silver nanoparticles colloids synthesized using initial pH of 6.0 and MR of 1:10 exposed to various amount of PQ herbicide (ppm)..... 134

Figure 4.93 UV-Vis spectra of CMC-stabilized silver nanoparticles colloids synthesized using initial pH of 6.0 and MR of 1:10 exposed to various amount of PQ herbicide (ppm). 134

Figure 4.94 Appearances of CS-stabilized silver nanoparticles colloids synthesized using initial pH of 5.0, radiation time of 4 mins and MR of 1:10 exposed to various amount of PQ herbicide (ppm)..... 135

Figure 4.95 UV-Vis spectra of CS-stabilized silver nanoparticles colloids synthesized using initial pH of 5.0, radiation time of 4 mins and MR of 1:10 exposed to various amount of PQ herbicide (ppm)..... 135

Figure 4.96 Appearances of HA-stabilized silver nanoparticles colloids synthesized using 0.0007 mM of HA at initial pH of 6.0 exposed to various amount of PQ herbicide (ppm)..... 136

Figure 4.97 UV-Vis spectra of HA-stabilized silver nanoparticles colloids synthesized using 0.0007 mM of HA at initial pH of 6.0 exposed to various amount of PQ herbicide (ppm)..... 136

Figure 4.98 TEM images of PMA stabilized silver nanoparticles synthesized with molar ratio of PMA to silver ions at 1:10 with initial pH of PMA at 6.0 after exposed to PQ herbicide; a) 0 ppm and b) 400 ppm..... 138

Figure 4.99 The illustration of the charge-transfer interaction at nanoparticles surface between PMA-stabilized silver nanoparticles and PQ herbicide. 139

CHAPTER I
INTRODUCTION

Recently, the development of silver nanoparticles is widely interested since they can be used in many applications such as optics, optoelectrics, antibacterial materials, and chemical/biochemical sensors. This is because of their unique optical characteristics, electrical and chemical properties as well as antibacterial ability. These advantageous characteristics and properties come from their very small sizes which are in the range of 1-100 nm and depend on their particles size, shape, inter-particle spacing and the dielectric constant of their surroundings.

The synthesis of silver nanoparticles plays an important role to their properties. Many synthesizing methods have been studied. Most of the conventional methods use the reducing agents such as sodium citrate, citric acid, ascorbic acid and sodium borohydride in conjunction with a stabilizer. The selection of a stabilizer is also important. When silver nanoparticles are applied as chemical sensors, the strategies are based on the changes in dielectric constant of the surroundings by varying the solution medium. This can change the size of the nanoparticles which results in changing color of the solution. This phenomenon can be developed by using a stabilizer which contains oxygen-rich functional groups such as carbonyl, carboxylic and hydroxyl groups in order to make the nanoparticles sensitive to ionic strength of the targeting chemicals [1].

However, there are some concerns about the chemical reduction method such as the difficulty in removing unreacted reducing agent and/or stabilizer which can affect the characteristics and properties of the resulting silver nanoparticles. Therefore, it is better to use fewer chemicals in order to minimize this problem. Instead of using a reducing agent and a stabilizer, several chemicals that can act as both reducing agent and stabilizer have been employed. In order to promote the reduction of silver ions by these chemicals, many techniques such as thermal assisted [2], microwave assisted [3] and UV radiation assisted methods [4, 5] have been developed. Since thermal assisted method has a problem concerning

non-uniform heat distribution [3] and microwave assisted method is not suitable for controlling the size of silver nanoparticles when some type of stabilizer is used [3, 6], UV radiation assisted method is selected for this research.

In this research, silver nanoparticles are synthesized using UV irradiation in the presence of a stabilizer that potentially acts as a reducing agent in order to reduce the amount and/or type of the chemicals used in the synthesis of silver nanoparticles. Five chemicals including tannic acid, poly(methacrylic acid, sodium salt), carboxymethyl cellulose, sodium salt, chitosan and humic acid sodium salt are chosen because they contain a lot of oxygen-rich functional groups and have highly steric structures that can help stabilizing the nanoparticles and may promote sensing ability of the nanoparticles. Previous works usually reported the synthesis and the application of silver nanoparticles at specific conditions [1-4], but in this research, the molar ratio of the stabilizer to silver ions and pH of the system are varied in order to determine the optimum conditions for synthesizing silver nanoparticles and making them stable. In addition, varying pH of the system can increase the opportunity to use the silver nanoparticles for herbicide sensing application. This is because each herbicide has its own characteristics and properties. For example, some herbicides only dissolve in acidic condition; consequently, for detecting these herbicides, silver nanoparticles have to be in acidic condition.

Therefore, the objectives of this research are summarized as follows:

1. To synthesize silver nanoparticles using UV irradiation in the presence of a stabilizer

2. To study the effects of the type and the amount of stabilizers and pH of the solution on the characteristics and stability of the synthesized silver nanoparticles.

3. To study the ability for herbicide detection of the synthesized silver nanoparticles.

CHAPTER II
THEORY AND LITERATURE REVIEW

2.1 Silver nanoparticles

2.1.1 Definition and properties of nanoparticles

Nanoparticles are very small particles which have the diameters in the range of 1-100 nanometers. Their size-related characteristics and properties such as chemical, optical and electrical properties are greatly different from those of their bulk materials.

For example, the colloids or sols of silver nanoparticles are in yellow color and those of gold nanoparticles normally appears in red or purple color [7]. These optical characteristics of silver and gold nanoparticles are affected by localized surface plasmon absorption (LSPR). LSPR is caused by an excitation of the oscillated conductive electrons of the metallic nanoparticles which is induced by the incident light as shown in Figure 2.1. The light causes the electrons of the nanoparticles to delocalize and then form the electrical field opposite to the light wave. At specific frequencies, the electron oscillation is in resonance with the light wave. This phenomenon is called LSPR [8, 9].

The position, shape and intensity of the LSPR are the functions of several factors including the morphology, the dielectric constant of the surrounding medium as well as inter-particles coupling [10]. Figure 2.2 shows the absorption spectra obtained from various shapes of the silver nanoparticles [11]. However, this phenomenon is observed when nanoparticles size is larger than a few ten nanometers [10, 12-15]. Typical shapes of the silver nanoparticles are sphere, square, rod, and polygonal which can be varied by the synthesis methods. Spherical shape is most typically shape, normally obtained via fast reduction methods using strong

reducing agents such as sodium borohydride [1, 14, 16] or using microwave-assisted reduction [3, 6]. Polygonal, square and rod are usually synthesized by two-steps method or using weaker reducing agents or others techniques. Tian X. and coworkers [17] used two-steps method to synthesize polygonal silver nanoparticles by seeding with sodium borohydride at first, followed by seed mediated step involving the reduction of silver ions with tannin. Pal S. and coworkers [18] synthesized rod-like shape silver nanoparticles by seeding with sodium borohydride, and then mediated with sodium citrate. Sun Y. and coworker [19] synthesized single crystal cube silver nanoparticles by reducing silver nitrate with ethylene glycol at 160°C in the presence of poly(vinyl pyrolidone). Moreover, Lee, G.P. and coworkers [20] reported the shapes of the citrate-mediated silver nanoparticles were varied from spherical, hexagonal to triangonal shapes.

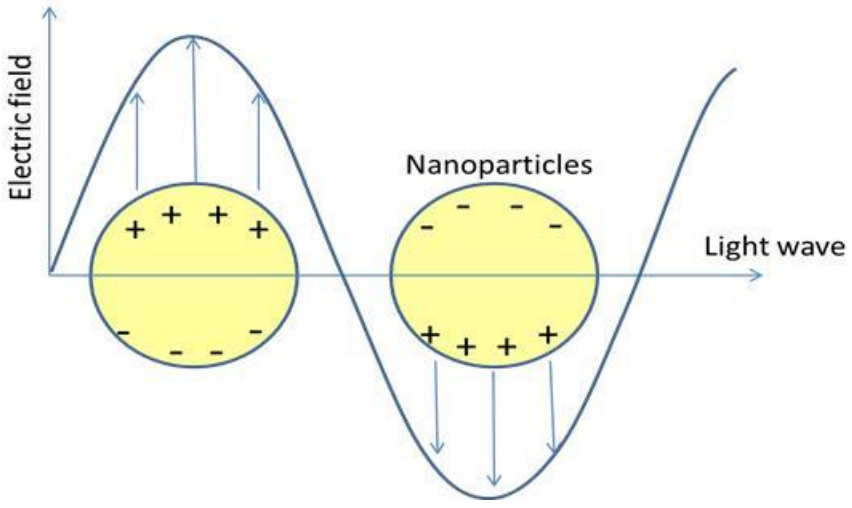

Figure 2.1 Schematic of a localized surface plasmon of a metal sphere [9]

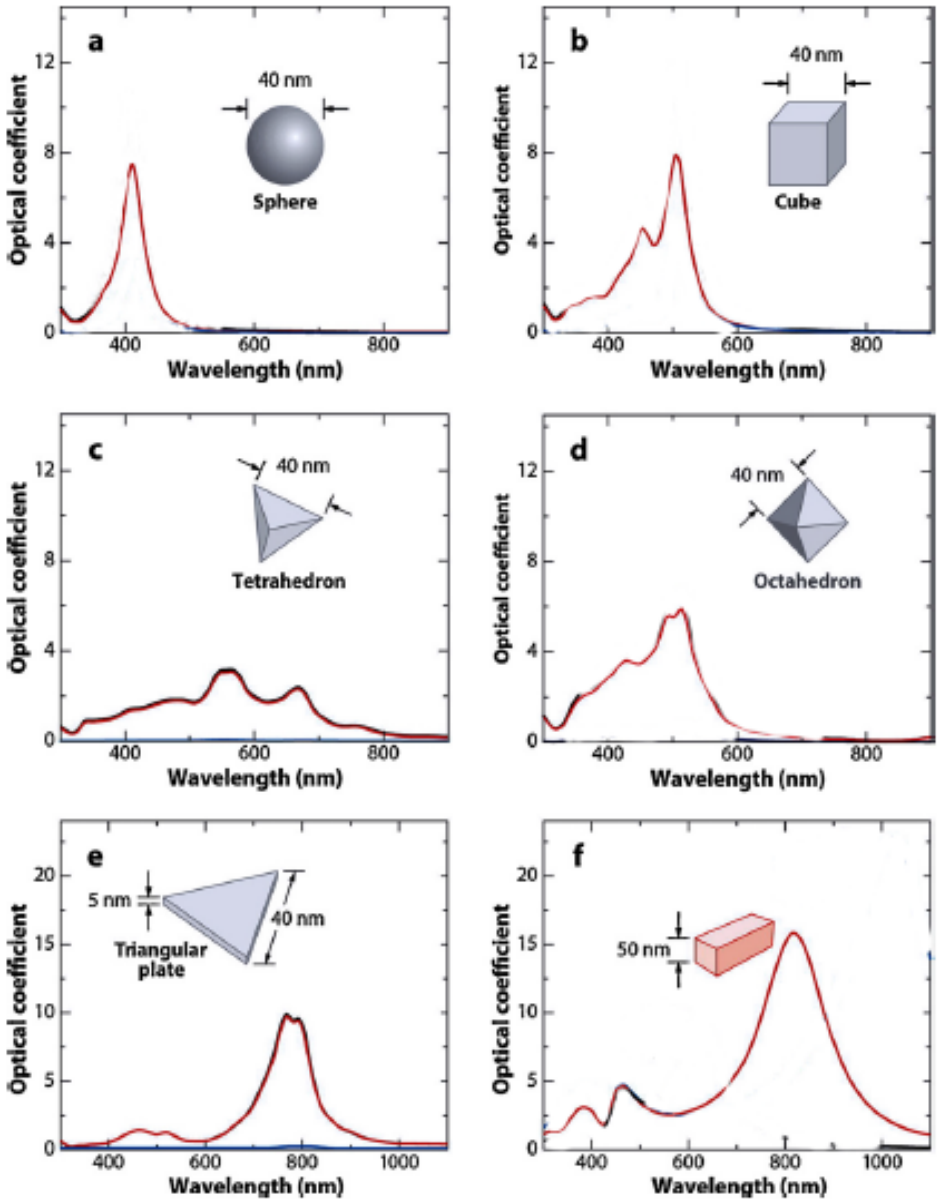

Figure 2.2 Absorption spectra of the silver nanoparticles having different shapes: (a) sphere, (b) cube, (c) tetrahedron, (d) triangular plate and (f) rectangular bar [11]

2.1.2 Synthesis methods

One of the important concerns in the development of silver nanoparticles is to synthesize the uniform nanoparticles with a well-controlled mean size and narrow size distribution. In most cases, the system for fabricating silver nanoparticles consists of a silver salt precursor, a reducing agent, and a stabilizer. Silver nitrate is usually applied as a salt precursor. The reduction of silver ions to silver nanoparticles can be done using wide variety of methods such as chemical reduction, irradiation assisted reduction, thermal assisted reduction and microwave assisted reduction.

2.1.2.1 Chemical reduction

Reduction of silver ions by using a reducing agent is the most widely used method for synthesizing silver nanoparticles. Several reducing agents such as sodium citrate or citric acid [15], ascorbic acid [21], and sodium borohydride [1, 22, 23] have been employed. The most powerful reducing agent is sodium borohydride. It mostly yields silver nanoparticles having diameter smaller than 10 nm. While more controllable size of silver nanoparticles is obtained when ascorbic acid and citric acid are used [15, 21], the reduction with borohydride gives more uniform nanoparticles.

Solomon D.S. and coworkers [7] synthesized silver nanoparticles by using sodium borohydride as both reducing agent and stabilizer. They revealed that the sodium borohydride solution turned yellow right after adding silver nitrate solution into it. They proposed the reduction reaction of the silver nitrate as shown in eq. 2.1 and proposed the illustration of how silver nanoparticles were kept in the suspension as shown in Figure 2.3. The diameter of the obtained silver nanoparticles was about 10-14 nm.

$$AgNO_3 + NaBH_4 \longrightarrow Ag + \frac{1}{2}H_2 + \frac{1}{2}B_2H_6 + NaNO_3 \quad \text{.....(eq. 2.1)}$$

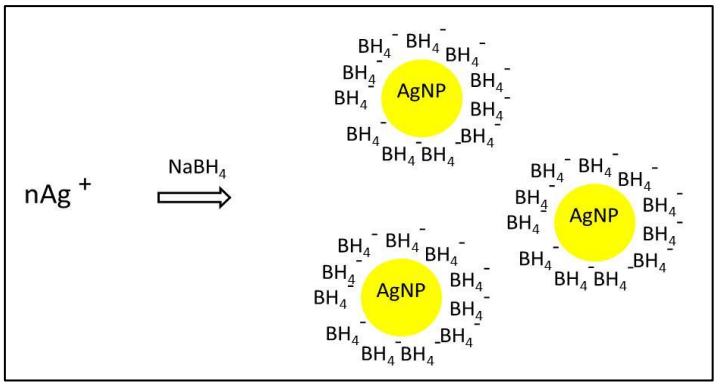

Figure 2.3 Illustration of repulsive force separated silver nanoparticles by the adsorbed borohydride [7]

Dubas S.T. and Pimpan V. [1] suggested a schematic reaction of silver ions reduced by sodium borohydride in the presence of humic acid acting as a stabilizer as shown in Figure 2.4. They also revealed that humic acid had chelating potential to metallic ions. The interaction between humic acid and silver ions was explained by high content of nitrogen and oxygen which were electron donors. As soon as sodium borohydride was added, the solution turned yellow. This confirmed the formation of silver nanoparticles. The size of the silver nanoparticles was 5 nm in diameter.

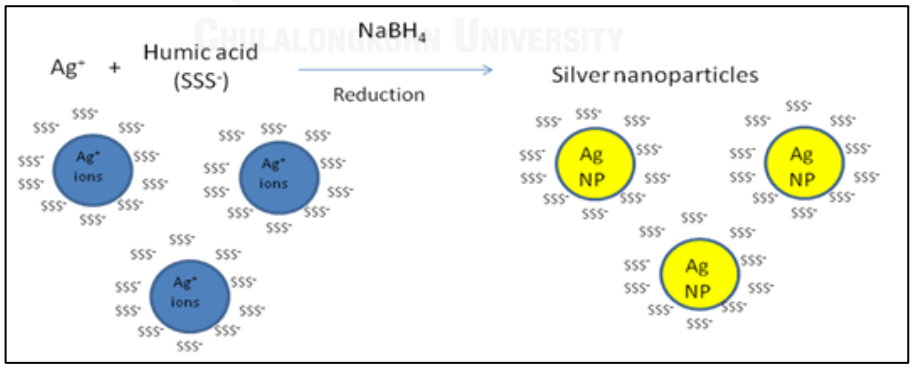

Figure 2.4 Schematic reaction of silver ions reduced by sodium borohydride in the presence of humic acid [1]

These reports indicate that very small silver nanoparticles can be obtained due to the high reactivity of sodium borohydride since it induces fast nucleation process right after it is introduced to the system. Unfortunately, fast nucleation process is less effective when the size of the nanoparticles is concerned. Reaction parameters such as molar ratio of the reducing agent to silver precursor, pH or temperature can be used for making silver nanoparticles with desired particle size.

Huang T. and coworker [14] developed a rapid simple one-pot synthesis method to produce twelve colloidal silver nanoparticles that exhibited the rainbow color, using sodium citrate as a stabilizer, poly(vinyl pyrolidone) for controlling the shape of particles and sodium borohydride as a reducing agent. By varying sodium borohydride concentration, the amount of nucleation increased and this can be used to control size and shape of the silver nanoparticles.

However, there are some concerns about unreacted reducing agent which remains in the system and cannot be easily removed. Oliveira J. F. and coworker [24] revealed that excess of sodium borohydride after synthesis competed with citrate (as a capping agent) and caused the aggregation of silver nanoparticles. Therefore, it is better to use less reducing agent or avoid using them. Other methods to synthesize silver nanoparticles have been developed by using some chemicals that can act as both reducing agent and stabilizer with or without the assistance of other input energy depending on the reactivity of such chemicals.

2.1.2.2 Irradiation assisted method

To reduce the amount and/or type of chemicals in the synthesis of silver nanoparticles, UV radiation and γ-ray radiation are some of the radiations applied for assisting the reduction of silver ions.

Dubas S.T. and Pimpan V. [4] exposed the mixture of silver nitrate and poly(methacrylic acid), (PMA) to UV radiation. Their results show that the color of PMA-stabilized silver nanoparticles synthesized from this method was purple which was different from yellow color of PMA-stabilized silver nanoparticles produced by chemicals reduction with sodium borohydride. They explained that it was due to the incomplete reduction of the silver ions which perturbed to the dielectric of the surroundings causing the change in the color of silver nanoparticles colloid.

Spadaro D. and coworkers [5] used UV radiation to enhance the chemical process in the synthesis of silver nanoparticles. They revealed that varying UV lamp power affected the reaction mechanisms. PMA-Ag^{+} co-ordination or PMA polymerization occurred can obstruct the formation of nanoparticles nucleation and growth. They reported that using lower energy of radiation slowed down PMA polymerization resulting in more space to the natural metal-ligand co-ordination which made the growth of the nanoparticles to be easier.

Other studies on the irradiation assisted reduction of silver ions in chitosan solutions were also reported [25, 26]. It was found that the UV-radiated products exhibited intense yellow color than those synthesized with less amount of silver nitrate solution. The color intensity increased as a function of silver nitrate content and γ-ray irradiation dose. The hydrated electron generated by water radiolysis (eq. 2.2) can reduce silver ions to silver atom (eq. 2.3) [26]. The neutral silver atom reacts with silver ion to form relative stabilized silver clusters as shown in eq. 2.4, 2.5 and 2.6 [27, 28].

Previous studies on γ-ray irradiation method done by Yoksan, R., Chen, P. and Janata, E. revealed the reduction mechanism of silver ions [25-28]. The irradiation–reduced process can be written as follows:

$$n\ H_2O \xrightarrow{\gamma\text{-rays}} e^-_{aq} + H^\bullet + OH^\bullet + H_3O + H_2 + \ldots \quad \text{(eq. 2.2)}$$

$$Ag^+ + e^-_{aq} \xrightarrow{\text{reduction}} Ag^0 \quad \text{(eq. 2.3)}$$

Neutral silver atom (Ag^0) is found to react with Ag^+ to form the stabilized silver cluster as shown in eq. 2.4, 2.5, 2.6 [25, 27, 28]

$$Ag^0 + Ag^+ \xrightarrow{\text{reduction}} Ag_2^+ \quad \text{(eq. 2.4)}$$

$$Ag^0 + Ag^+ \xrightarrow{\text{reduction}} Ag_2^+ \quad \text{(eq. 2.5)}$$

$$Ag^0 + Ag_n^+ \xrightarrow{\text{reduction}} Ag_n^+ \quad \text{(eq. 2.6)}$$

Though irradiation can assist in the reduction of the silver ions to silver atom and formed silver cluster, high energy radiation can result in other unwanted reactions such as chain growth or chain scission of the stabilizer.

Huang L. and coworkers [29] reported the UV-induced synthesis of silver nanoparticles in alkali carboxymethylated chitosan solution. The structure of carboxymethylated chitosan (CMCTS) is similar to those of an amino acid since CMCTS has both amino groups and carboxylic agroups in the molecule. They used laser photolysis technique to investigate the formation mechanism of silver nanoparticles in CMCTS solution. They reported three main reactions as shown below.

$$CMCTS \longrightarrow (\ CMCTS\ )^* \quad \text{(eq. 2.7)}$$

$$(CMCTS)^* \longrightarrow CMCTS^+ + e^-_{aq} \quad \text{(eq. 2.8)}$$

$$CMCTS + e^-_{aq} \longrightarrow \bullet CMCTS^- \quad \text{(eq. 2.9)}$$

They also reported that e^-_{aq} produced according to eq. 2.8 was a reducing agent for metal cat ions such as Ag^+ and Au^{3+} [29] as given in eq.2.10.

$$Ag^{+} + e^{-}_{aq} \xrightarrow{\text{reduction}} Ag^{0} \qquad \text{(eq. 2.10)}$$

Zhai, M. and coworkers [30] studied the formation of hydrate electron by laser photolysis of carboxymethylated chitin derivatives in aqueous solution. This work also supported that e^{-}_{aq} was produced from $-NHCOCH_3$ groups of CMCTS under the irradiation laser beam [30]. e^{-}_{aq} acted as a reducing agent for silver as shown in eq. 2.10. Therefore, CMCTS can be used as both reducing agent and stabilizing agent to synthesize silver nanoparticles by UV radiation.

Moreover, it was reported that the silver atom formed at the beginning of the reduction process had an absorption band at 360 nm [31], then shifted to 310 nm and 265 nm due to the formation of Ag_2^{+} [32]. Oligomeric clusters appeared step by step and form stable complexes with CMCTS due to electronic attraction between silver cluster and CMCTS. When these complexes were further reduced, larger cluster and finally silver nanoparticles occurred [33]. The growth processes of the particles are shown in eq. 2.11-2.13.

$$Ag^{0} + Ag^{+} \xrightarrow{\text{reduction}} Ag_2^{+} \qquad \text{(eq. 2.11)}$$

$$Ag_2^{+} + Ag^{0} \xrightarrow{\text{reduction}} Ag_3^{+} \qquad \text{(eq. 2.12)}$$

$$Ag_3^{+} + Ag^{0} \xrightarrow{\text{reduction}} Ag_4^{+} \xrightarrow{(n-4)Ag^{0}} Ag_n^{+} \qquad \text{(eq. 2.13)}$$

2.1.2.3 Thermal assisted method

To avoid using a reducing agent, researchers have used heat or thermal energy to drive the reduction of the silver ions. For example, Akaighe N. and coworker [2] synthesized silver nanoparticles via the reduction of silver ions in the presence of humic acid at various temperatures. Their results showed that increasing temperature reduced the reaction time used to synthesize silver nanoparticles and yielded

the nanoparticles with narrower size distribution. The characteristic surface plasmon resonance (SPR) of silver nanoparticles observed by UV-Vis spectroscopy appeared within 2-4 days at 22°C whereas at 90°C the SPR appeared within 90 minutes.

Hebeish, A. A. and coworkers [34] synthesized silver nanoparticles using thermal-assisted reduction in the presence of carboxymethyl cellulose. They reported that at 50°C, the reduction of silver was not completed. However, increasing the reaction temperature to 70–90°C resulted in the disappearance of the characteristic peak representing silver ions, indicating its complete transformation into silver.

Xue B. and coworkers [35] reported that the thermal-assisted reduction had the problem with non-uniform distribution of the heat. Therefore, microwave has been used to overcome this weakness since it provides homogeneous heating and promotes the nucleation of silver nanoparticles [3].

2.1.2.4 Microwave assisted method

Due to the advantage of using microwave as previously mentioned, several researchers have focused on synthesizing silver nanoparticles using this method. For example, Chen J. and coworkers [3] synthesized silver nanoparticles using carboxymethyl cellulose salt (CMC) as both reducing and stabilizing agents. They proposed that the synthesis of CMC-stabilized silver nanoparticles without catalyst or heat, was nearly impossible to achieve. However, using microwave-assisted method resulted in uniform and stable nanoparticles. The results also suggested that there was not much effect from CMC concentration on the nanoparticles size.

Hu B. and coworkers [6] synthesized silver nanoparticles using microwave assisted techniques for 10 second. They used basic amino acids, such as L-lysine or

L-arginine, as reducing agents and used soluble starch as a protecting agent. They claimed that their method can be applied to large-scale production, for example, a reaction yielding 0.1 g of nearly monodisperse silver nanoparticles can be performed in a 80 mL microwave sealed vessel.

Aswathy, B. and coworkers [36] synthesized silver nanoparticles using microwave assisted method. They used vanillin as a reducing agent and anionic surfactants such as Dioctyl sodium sulfosuccinate (Aerosol OT) and Sodium Dodecyl Sulfate as capping agents. UV-Visible absorption spectra showed a broad SPR band consisting of two peaks suggesting the formation of silver nanoparticle with bimodal size distribution. These results later confirmed by TEM images which showed the particles having spherical and hexagonal shapes

Chen, J. and coworkers [3] synthesized silver nanoparticles using microwave assisted method. They used carboxymethyl cellulose sodium salt as both reducing agent and stabilizer. The obtained silver nanoparticles showed small size distribution and well-stabilized particles with critical size of 15 nm. They also found that increasing carboxymethyl cellulose sodium salt had small effect on the size and size distribution of the obtained nanoparticles. On the other hand, increasing silver nitrate concentration, bigger particles with broader size distribution were obtained.

By comparison between four different synthesis methods, it can be concluded that the reduction by chemical method have been widely used but due to environmental concern nowadays, using less reducing agent is more preferable. On the other hand, thermal assisted reduction has a problem with non-uniform distribution of the heat during synthesis resulting in various sizes of silver nanoparticles [3]. Microwave assisted method is not suitable for controlling the size of silver nanoparticles when some type of stabilizer is used [3]. From those reasons, it can be suggested that the UV irradiation method is considerable good synthesis method as it uses less reducing agent.

2.1.3 Control of the nanoparticles size

The control of the size of the obtained silver nanoparticles can be made by changing the reaction parameters such as the type of reducing agent, the amount of reducing agent or pH. Those parameters affect the nucleation and growth processes of the silver nanoparticles.

Martinez, G. A. and coworkers [37] synthesized silver nanoparticles with different sizes using gallic acid as both reducing and stabilizing agents. The results showed that 7 and 29 nm silver nanoparticles were obtained with the reaction condition at pH 11 and 10, respectively. At these pH values, phenol groups were ionized so that the reduction was fast and the particles obtained were spherical.

Watcharaporn, K. and coworkers [38] studied the effect of UV radiation and pH of tannic acid solution in the synthesis of silver nanoparticles. It was found that using UV radiation resulted in silver nanoparticles with smaller particles and narrower size distribution at every pH (6.0, 7.0 and 8.0). They also revealed that smaller particles without agglomeration were obtained with alkali condition.

Dong X. and coworkers [39] synthesized silver nanoparticles by citrate reduction under the range of pH from 5.7 to 11.1. The results showed that under high pH, the product was composed of both spherical and rod-like silver nanoparticles as a result of the faster reduction rate of the precursor. Under low pH, the product was mainly dominated by triangle or polygon silver nanoparticles due to the slower reduction rate of the precursor. Moreover, to obtain spherical shape nanoparticles, a 2-step reduction method was carried out at high and low pH, respectively. According to Lamer model which suggest that to obtain spherical shape silver nanoparticles, the synthesis mechanism prefer fast nucleation follow with slow growth of the particles [40].

2.2 Stabilizers

In order to use fewer chemicals with environmental concern, less toxic chemicals were more preferable. Moreover, choosing the stabilizer for silver nanoparticles is not only aimed for stabilizing the particles against the aggregation but also designed for more functions such as reducing the silver ions, as well as immobilizing on the surface of nanoparticles for selective detection of targeted chemicals. For using silver nanoparticles in detection applications, the strategy is based on either the change in dielectric constant of the surrounding by changing solution medium or by complex formation at the surface of the particles or the change in the distance available between particles. Consequently, to make it easier for capping the nanoparticles and sensing to the change in dielectric constant of the surroundings, the stabilizer should have the sensitivity to ionic strength of the surroundings which may obtain from functional groups in the molecule such as carbonyl group (-C=O), carboxylic group (-COOH) and hydroxyl group (-OH) [1]. In addition, the molecular structure of a stabilizer should be large or has high steric hindrance to prevent the nanoparticles from aggregation.

In this research, 5 stabilizers were chosen based on their potential to possibly act as a reducing agent for synthesizing silver nanoparticles. The selected stabilizers were tannic acid, poly(methacrylic acid sodium salt), carboxymethyl cellulose sodium salt, chitosan and humic acid sodium salt.

2.2.1 Tannic acid

Tannic acid (TA) has been studied extensively for its antioxidant properties [41], and used as a chelating agent for inorganic cations [42]. The molecular structure of tannic acid is shown in Figure 2.5. It consists of glucose unit in the middle and linked to polygalloyl ester chains with ester bond. TA is a weak acid and known as a weak reducing agent that can grow seeds into nanoparticles at room temperature [17, 43, 44]. Tannic acid is known to partially hydrolyzed under mild acidic or mild alkali conditions into glucose and gallic acid. Although, gallic acid is more reactive to reduce silver ions at alkali condition at room temperature, the stability of the gallic acid stabilized silver nanoparticles was very poor [37]. On the other hand, glucose is a weak reducing agent at room temperature but it is a good stabilizer at alkali condition [45]. Those findings suggest that tannic acid could be acted as an effective reducing agent and stabilizer in alkali condition at room temperature.

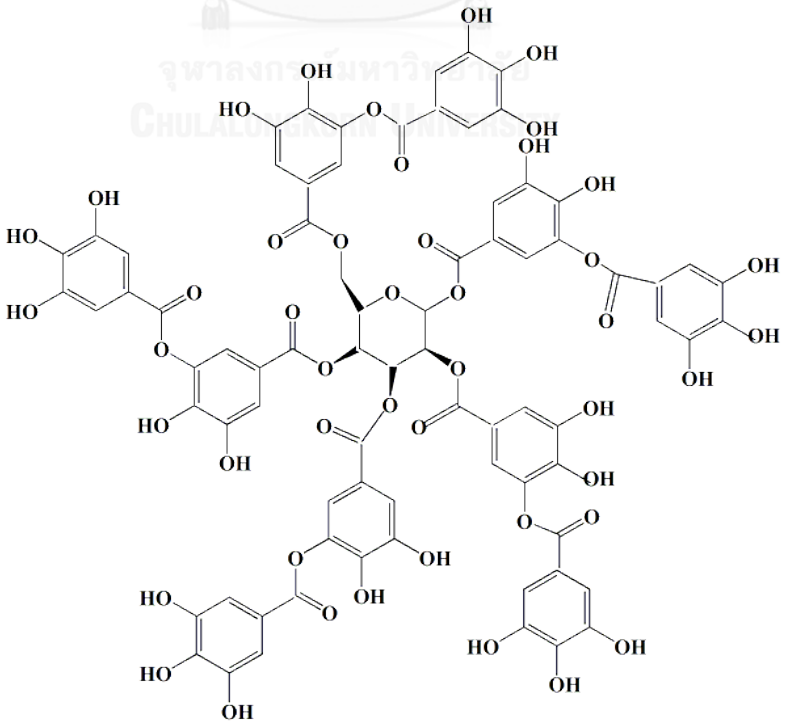

Figure 2.5 The molecular structure of tannic acid

As shown in Figure 2.5, TA has 25 hydroxyl groups presenting in the phenolic compound position. At least two hydroxyl groups at ortho or para positions to each other give off two electrons oxidation convert from phenolic form to quinone form which corresponds for reduction of metal ions later [46]. Consequently, the probable reaction mechanism for the formation of silver nanoparticles by TA reduction of silver nitrate solution can be represent as shown in Figure 2.6 [47].

Yi Z. and coworkers [44] synthesized silver nanoparticles at room temperature using various concentrations of TA at pH of 7.0 and reaction time of 5 hours, without any irradiation. The size of the obtained silver nanoparticles was in the range of 50-500 nm. Their morphology was influenced by both the concentrations of TA and pH of solution. Some conditions yielded the mixture of spherical and polygonal particles.

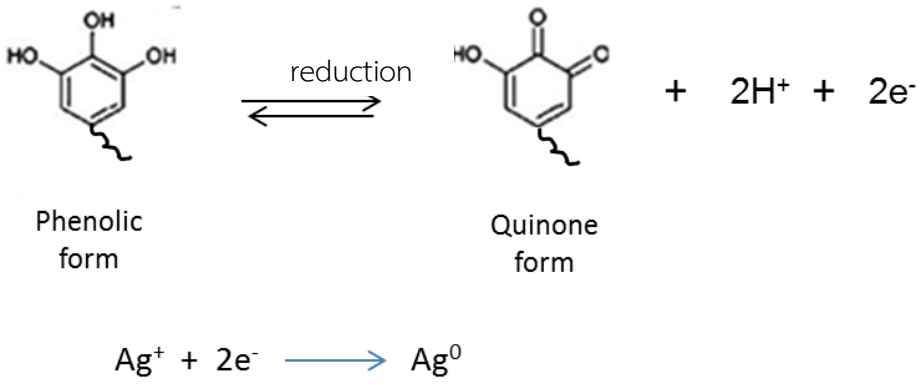

Figure 2.6 The reaction mechanism of the reduction of a silver ion using tannic acid as a reducing agent [47]

Dadosh T. [16] reported his method to synthesize uniform silver nanoparticles stabilized with tannic acid. He used tri-sodium citrate as a reducing agent. The synthesis was done in two steps. First, for seeding process, the mixture was heated at 60°C for 3 minutes or until it turned yellow. Then for the growth step,

the mixture was boiled for 20 minutes, cooled down and stored at 4°C. Uniform nanoparticles having diameters in the range of 18-30 nm were obtained. The diameter of the obtained nanoparticles increased with decreasing TA concentration.

Srivaraman S.K. and coworkers [43] synthesized silver nanoparticles at room temperature using various concentrations of TA at pH of 8.0. It was found that as soon as tannic acid was poured into silver nitrate solution, the mixture turned dark brown readily in a few seconds. These confirmed the occurrence of silver nanoparticles. The sizes ofthe obtained silver nanoparticles were in the range of 3-22 nm. The particle size increased with increasing the molar ratio of TA to silver nitrate.

2.2.2 Poly(methacrylic acid sodium salt)

The molecular structure of poly(methacrylic sodium salt) (PMA) is shown in Figure 2.7. PMA is soluble in water and dissociated into anionic polyelectrolyte. Each molecule contains a lot of $-COO^-$ groups, which gives ability to interact to silver ions. Previous work showed that PMA has ability to coordinate to the metal nanoparticles [48]. In addition, an intrinsic polymer structure and the steric effect of the methyl groups leaded to metal clusters linking to the carboxylic parts of the macromolecules [49]. Moreover, polymers in solution have been used in order to prevent the aggregation of silver nanoparticles due to their strong interactions after nucleation [50, 51]. Furthermore, it was accepted that being good reducing agent, the chemicals should possess of phenol or aldehyde group as a reactive site. Those groups are the electron donor site [52]. In the case of PMA-stabilized silver nanoparticles synthesis, it is unclear about the involvement of PMA in

the reduction mechanism. However, successful syntheses of silver nanoparticles were reported.

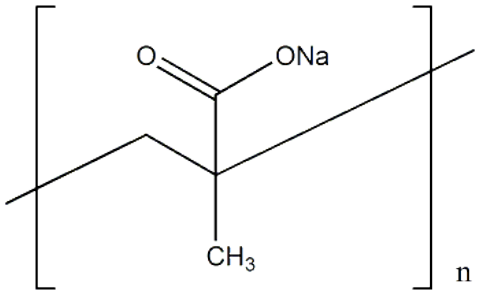

Figure 2.7 The molecular structure of poly(methacrylic acid sodium salt)

Dubas S.T. and coworker [4] synthesized silver nanoparticles using low power UV-radiation (8 watt) assisted method in the presence of PMA solution at pH of 4.0 (using acetic-acetate buffer) with the radiation time of 60 minutes. The obtained silver nanoparticles showed purple color with the diameter around 8 nm with spherical shape.

Spadaro D. and coworkers [53] synthesized silver nanoparticles using PMA as reducing and capping agents with UV radiation assisted method at pH of 8.5. They suggest two steps processed in order to control the size distribution of the particles. First step promoted quick reduction of silver ions with nanoparticles nucleation through relatively low energy UV irradiation (6 watt) for one hour. Second step used UV irradiation at higher energy density (25 watt) for 5 hours in order to allow quick cross-linking of PMA which freezed out any further modification of silver nanoparticles distribution. This method made nanoparticles more stable and allows narrower size distribution of nanoparticles with the diameter less than 10 nm. The obtained silver nanoparticles of the first step, yields yellow color sol. Without the second step, the result shows more agglomeration. However, this method took about 6 hours to synthesize silver nanoparticles which could be improved for shorter reaction time.

2.2.3 Carboxymethyl cellulose sodium salt

Carboxymethyl cellulose or cellulose gum is an artificial-nature polymer derived from cellulose. Carboxymethyl celluylose is a copolymer of two units: ß-D-glucose and D-glucopyranose 6-O-(carboxymethyl)-monosodium salt which are connected via ß-1,4-glycosidic bonds [54]. Normally it is used in the form of carboxymethyl celluylose sodium salt (CMC) as shown in Figure 2.8. CMC is an anionic polysaccharide that comes from cellulose. It is a salt of strong acid and weak base which has pKa around 4.0 [3]. The negatively charged solubilized CMC facilitates the attraction of the positively charged metal ions to its polymeric chains followed by reduction with the existing reducing groups [34].

CMC is used in thickener in food industry and also used in non-food products such as toothpaste, water-based paint, textiles sizing, etc. Moreover, CMC can be used as cation-exchange resin in ion-exchange chromatograph for purification proteins [55].

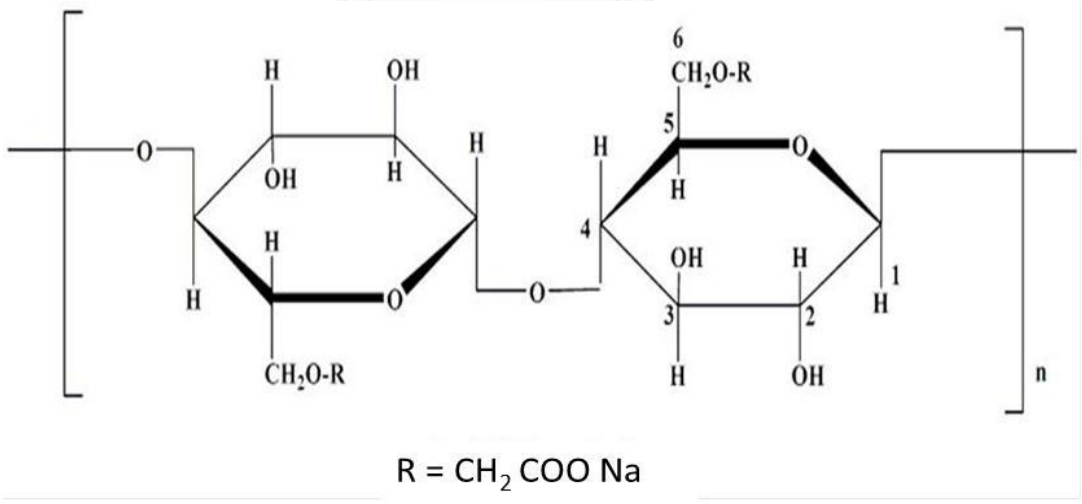

Figure 2.8 The molecular structure of carboxymethyl cellulose sodium salt

Chen J. and coworker [3] synthesized silver nanoparticles using CMC as both reducing agent and stabilizer with microwave assisted method. Their results showed that the concentration of CMC had very small effect on the size distribution, whereas high concentration of $AgNO_3$ resulted in bigger particle and broaden size distribution.

Hebeish, A. A. and coworkers [34] synthesized silver nanoparticles using CMC as both reducing agent and stabilizer with thermal assisted method (70 °C) for 1 hour. By varying pH from 6.0 to 12.5, the results showed that the UV-Vis absorbance maximum peak appeared around 405 nm, but shifted to higher wavelength as pH condition decreased. While varying CMC concentration (0.3-1.5 %w/v), at pH of 12.5 and temperature of 70 °C for 1 hour, the results showed that, similar plasmon bands were formed at 405 nm. Their absorbance intensities gradually increased when CMC concentration increased. They reported that CMC consists of modified cellulose chains containing reducing groups of carboxylate groups. The negatively charge solubilizes CMC and provides attraction to the silver cations followed by reduction with the existing reducing groups [34] However, they did not mention specifically for their reducing groups or the reducing mechanism.

2.2.4 Chitosan

Chitosan (CS) the second most abundant polysaccharide biopolymer obtained by deacetylation of the highly abundant biopolymer chitin. Typically chitin, has the degree of acetylation (DA) of 0.90, this indicates the presence of amino groups (as some amount of deacetylation) might take place during extraction, chitin may also consist of 5-15% amino groups [56]. CS consists of glucosamine and N-acetyl glucosamine units linked together by ß-1,4-glucosidic bonds with a typical DA of less than 0.35 as shown in Figure 2.9 [57]. The physical properties of CS depend on a number of parameters such as molecular weight (from approximately 10,000 to 1 million Dalton), degree of deacetylation (DD) in

range of 50-95%, sequence of the amino and the acetamido groups and the purity of the product [58, 59].

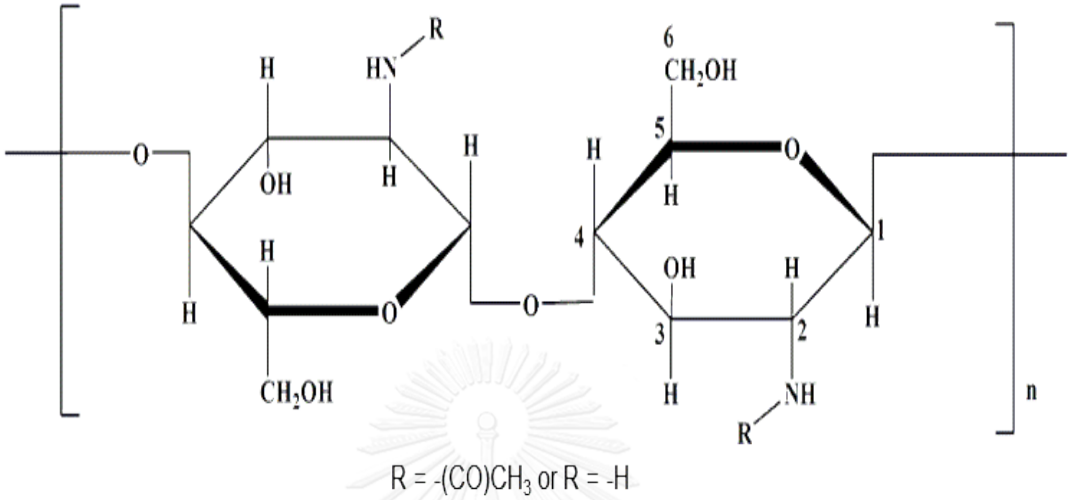

Figure 2.9 The molecular structure of chitosan

In last ten years, the used of biopolymers in research has been started more intensive due to their advantages such as non-toxic, environmental friendly, renewability of sources and also abundant in nature. Moreover, biopolymers are used in a variety of applications in biotechnology and in environment protection due to their biocompatibility and biodegradability. In research involving silver-chitosan nanocomposite, silver nanoparticles were synthesized via various methods using chitosan as a stabilizer [60-62].

Yoksan, R. and coworker [25] synthesized silver nanoparticles by using CS as a stabilizer with γ-ray irradiation assisted method at room temperature. The obtained nanoparticles were spherical with an average size of 7- 30 nm. However, the UV-Vis spectra shows broaded distribution curve, and TEM images also confirmed that the obtained silver nanoparticles were varied in sizes. The nanoparticles size synthesized with 0.1 %w/v CS is smaller than the results from 0.5 %w/v CS.

However, the nanoparticles synthesized in 0.5% w/v CS solution stable more than 3 months, whereas the other precipitated out within a few weeks.

Bozanic, D. K. and coworkers [60] synthesized silver nanoparticles stabilized with CS with two step process. First, silver-CS complex were prepared by mixing CS solution with silver nitrate solution for 6 hours at room temperature. Then silver-CS nanocomposites were prepared by using D-glucose as the reducing agent mixed with the silver-CS complex solution, stirred for 30 min., then thermally treated in microwave at 750 watt for 30 seconds. Upon second step process, the mixture rapidly changes color from purple to yellow. The obtained nanoparticles were found in spherical shape and approximately 10 nm in diameter.

Huang, H. and coworkers [62] synthesize silver nanoparticles stabilized with CS using sodium borohydride as a reducing agent in the presence of chitosan. They reported that when silver ions were mixed with chitosan solution, those silver ions could be attracted to chitosan molecules via electrostatic interactions at electron rich hydroxyl and ether groups. Silver nanoparticles were formed by the reduction of silver ions with sodium borohydride. The results showed that it is possible to control the size and size distribution by adjusting the amount of silver ions rather than the amount of chitosan in solution.

Yi, H. and coworkers [63] reviewed about the biofabriction with chitosan. Although chitin is insoluble in most organic solvents, CS is soluble in dilute acidic solutions below pH of 6.0. Since CS is considered a strong base as it has primary amino groups with a pKa near neutrality, the soluble-insoluble transition occurs at pH around 6.3 [63]. At low pH, the amine groups are protonated into $-NH_3^+$ form, and this make CS being water-soluble cationic polyelectrolyte. This cationic polyelectrolyte should be good for stabilizing the particles because those cations do not form a complex with silver ions left in the mixture.

2.2.5 Humic acid

Humic acid (HA) is organic macromolecule which results from microbiological decomposition of plants and animals. Chemical structure of HA is shown in Figure 2.10. It is natural anionic polyelectrolyte, due to the polar functional groups such as phenolic–hydroxyl groups, quinones, hydroxyls, carbohydrates sub-unit and the presence of carboxylic acids [64]. Those functional groups influence the interaction with metals ions which lead to the formation of self-assemble structures [65]. Moreover, the reduction potential of HA can be enhanced with pH condition [66]. The phenolic–hydroxyl groups and quinones functional groups could serve as reduction sites for metal ions.

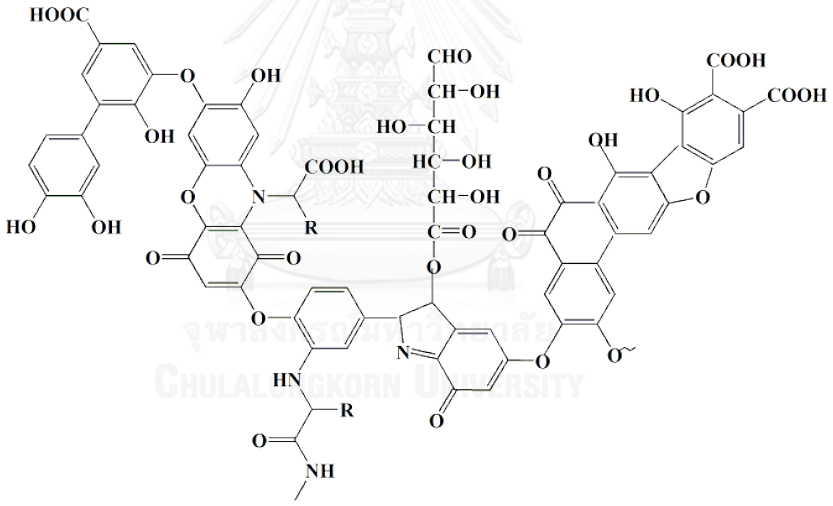

Figure 2.10 The molecular structure of humic acid

Dubas, S.T. and coworker [1] synthesized silver nanoparticles by using HA as a stabilizer with sodium borohydride as a reducing agent at room temperature. The results showed that with increasing HA from 0.001 to 0.1 %wt and fixed silver nitrate content at 0.01 %wt, the UV-Vis spectra exhibited maximum peaks at wavelength around 400 nm. The plasmon band shifted to higher wavelength as the amount of humic acid increased.

Peter, K. J. Prashob and coworkers [64] synthesized silver nanoparticles by using HA as a stabilizer with thermal assisted method. The mixture were heated in an air oven at 85-90 °C while maintaining pH at 11.5 and reduction time varied from 15 minutes to 1 hour depending on the silver nitrate concentration. UV-Vis spectra show maximum peaks at 412 nm, as HA concentration increased, the results show another peak around 320 and 370 nm. TEM images showed the obtained silver nanoparticles with various sizes.

2.3 Applications of silver nanoparticles

Silver nanoparticles have been used widely in variety applications due to their unique characteristics and properties such as antibacterial, electrical and optical properties. The applications based on each property can be summarized as follows:

2.3.1 Herbicide detection

The most common method to detect herbicide which has low volatility and thermal instability is high performance liquid chromatograph (HPLC) method. This technique is based on solvent extraction method. It requires a period of time to extract the chemicals and costly in solvent preparation. Moreover, it requires HPLC instrument, which is not convenient for onsite analysis. Alternative analysis is to use nanoparticles as previously reported by Dubas S.T. and coworker [1]. It is known that LSPR of nanoparticles can be shifted to the other wavelengths when the size or shape of the nanoparticles and/or the surroundings are changed. Using this advantage, the detection of the target chemicals such as the following herbicides is possible.

2.3.1.1 Pyrazosulfuron-ethyl herbicide

Pyrazosulfuron-ethyl herbicide (PSE) was chosen as a targeting herbicide. It's chemical structure is shown in Figure 2.11.

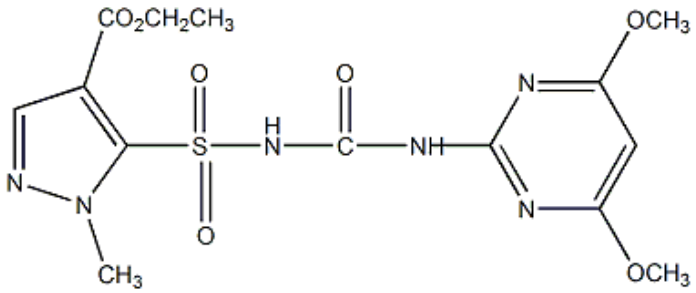

Figure 2.11 Molecular structure of pyrazosulfuron-ethyl

PSE or (ethyl-5-[(4,6-dimethoxypyrimidin-2-ylcarbamoyl) sulfamoyl] -1-thylpyrazole-4-carboxylate) is a herbicide in the class of sulfonylurea. It is used widely for weed control in variety of crops and vegetables including wheat, barley, rice, maize, soybeans, flax, plantation crops, blueberries, potatoes and tomatoes [27]. It is active to annual broad leaf weeds and barnyard grass. Due to its high activity at low application rate and low toxicity to mammal, it becomes more popular, nowadays [67]. It has very low solubility in water; 9.76 mg/l at 20°C, but solubility in acetone is 33.7 g/l at 20°C [68] . Sulfonylureas are weak acids. And they are subjected to pH dependent hydrolysis of sulfonylurea linkage. The rate of hydrolysis can be hundreds of times faster under acidic conditions [27]. In this study, PSE solution was prepared in acetone solution.

2.3.1.2 Paraquat.

Paraquat (PQ) or (1,1'-Dimethyl-4,4'-bipyridinium dichloride) is classified as a viologen, a family of redox-active heterocycles or similar structure as shown in Figure 2.12.

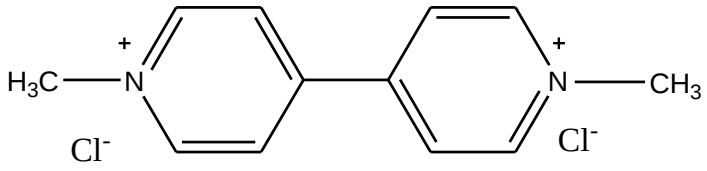

Figure 2.12 Molecular structure of paraquat

PQ is one of the most widely used herbicides. It is non-selective killing green plant tissues on contact. It is toxic to animals and human. Previous research reported that it also links to Parkinson's disease [69] . It has high solubility in water. From its structure, it is an electron acceptor in redox and radical reactions.

2.3.2 Other applications

Silver nanoparticles have been used extensively as anti-bacteria products, food containers, textile finishing and environmental applications. This encouraged the textile industry to use silver nanoparticles in different textile fabrics. The cotton fibers were applied with silver nanoparticles exhibited high anti-bacterial activity against *Escherichia coli* [70, 71]. Anti-bacteria textile fabrics were easily achieved using nanosized colloidal silver particles (2-5nm) by padding on cotton and polyester fabrics. These fabrics showed fastness properties to laundering against *S. aureus* and *K. pneumonia [72]*. Moreover polyester nonwovens were applied with 10 ppm colloidal silver particles (means diameter of 2-5 nm) . It was shown that a smaller particles size yielded better bateriostasis on the silver particles padded on nonwoven fabrics [73]. An anti-bacteria water filter was studied by coated silver nanoparticles

onto polyurethane foams. This foam can be washed several times without loss of nanoparticles. It showed that the filtered water had no bacterium (*E.coli*) although the input water had a bacteria input loaded [74].

Furthermore, the thermal properties of silver nanoparticles were applied for conductive ink. The thermal behavior of the ink-jet printed conductive films composed of Ag particles was investigated. The use of the metallic nanoparticles allows the formation of the highly conductive patterns by ink-jet printing followed by heat-treatment at temperatures much lower than the bulk melting temperature [75]. Moreover, the electrochemical properties of silver nanoparticles were applied for nanoscale sensors which offered fast respond times and lower detection limits. The silver nanoparticles were electrodeposited onto suitable substrates with gold interdigital electrodes realizing amperometric sensors that showed a high sensitivity to hydrogen peroxide [76].

Catalytic activities of nanoparticles differ from the chemical properties of their bulk materials. For instance, Kohler and coworkers [77] revealed that the bleaching of the organic dyes by potassium peroxodisulphate in aqueous solution at room temperature was enhanced by silver nanoparticles. Furthermore, silver nanoparticles were used to catalyze the chemiluminescence from lumino-hydrogen peroxide system with catalytic activity better than gold (Au) and platinum (Pt) colloids.

However, several types of sensors have been developed based on of the plasmonic properties of silver nanoparticles, for instance, extremely high molar extinction coefficients and enhanced local inherent electromagnetic fields near the surface of nanoparticles on the others. These properties are inherent to a given detection mechanism and a given detection technique, which can classified this sensor behavior in two main groups depends on the type of interaction between the nanoparticles and the analyze molecule and method of evaluated. The first group concerns sensors with LSPR shift, due to the interaction between nanoparticle and

target molecule. Within this group, two different sensors may be distinguished, depending on the origin of LSPR changes: aggregation sensor and refractive index sensors. For aggregation sensors, the LSPR shift occurs due to the plasmon coupling of nanoparticles. For refractive index sensors, the LSPR shift occurs due to change in local refractive index of medium [78]. The second group of sensors is based on the electromagnetic field enhancement of metal nanoparticle, which called surface enhanced spectroscopies, such as Surface Enhanced Raman Spectroscopy (SERS) and Metal Enhance Fluorescence (MEF). This classification of plasmonic sensors are summarized in Table 2.1 [78].

Table 2.1 Optical plasmonic sensors [78]

Sensor	**Mechanism**		**Evaluated technique**
Aggregation	LSPR shift	Near field electromagnetic coupling	UV-Vis spectroscopy
Refractive index		Local refractive index changes	UV-Vis spectroscopy Dark field microscopy
SERS	Local electricfield enhancement		Raman Spectroscopy
MEF			Fluorescence spectroscopy

However, in the application for chemical detection of the silver nanoparticles for this work, the aggregation sensor was interested and the following were previous works on chemical sensing of the silver nanoparticles. The aggregation sensors can be achieved by functionalizing the nanoparticles surface with ligands that can specific binding with the target molecules [78].

From Table 2.1, it implies that for aggregation mechamism, the nanoparticles normally grow bigger by the aggregation after interacting with the target chemicals. The size of the silver nanoparticles should be small at the beginning in order to get the unique optical characteristics of silver nanoparticles after modified with target chemicals. Moreover, it is known that the smaller particles the more reactivity particles are.

Furthermore, Hormozi Nezhad, M. R. and coworkers [79] reported the simple one-pot synthesis process of silver nanoparticles in the presence of PVP as a stabilizing agent which produced silver nanoparticles that can detect Dopamine, L-Dopa and adrenaline (called as catecholamines). They are biogenic amines which act as neurotransmitters in the function of brain and nerve signal transduction or hormones. They are widely used in treatment of Parkinson's disease, hypertension and cardiac surgery [80]. To diagnostics of diseases and control medicine, the catecholamine level in biological fluids was measured. In recent years, many methods have been reported to determination of catecholamine, such as electrochemistry, high performance liquid chromatography (HPLC) and mass spectrometry [79]. In their studied, the system consisted of silver nitrate ($AgNO_3$) solution, which included PVP as stabilizer, in alkali condition. Different catecholamines such as Dopamine (1), L-Dopa (2) and Adrenaline (3) act as reducing agents for reduction of silver ions to form silver nanoparticles as shown in Figure 2.13. Molecular structures of the catecholaines were shown in Figure 2.14.

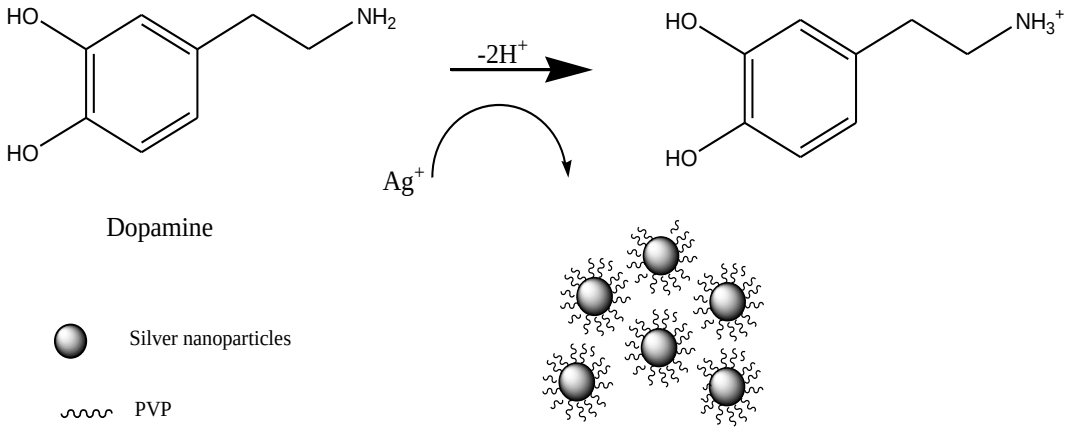

Figure 2.13 Schematic of the reduction process of silver ions by dopamine [79]

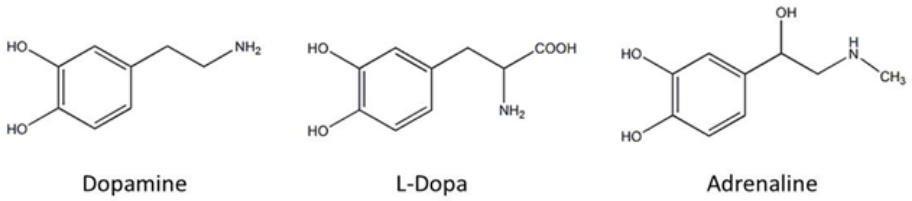

Figure 2.14 Molecular structure of Dopamine, L-Dopa and Adrenaline [79]

CHAPTER III

EXPERIMENT

3.1 The experimental scope

This research was divided into two parts as shown in Figure 3.1. The first part was the synthesis of silver nanoparticles. The second part was the characterization and testing of silver nanoparticles.

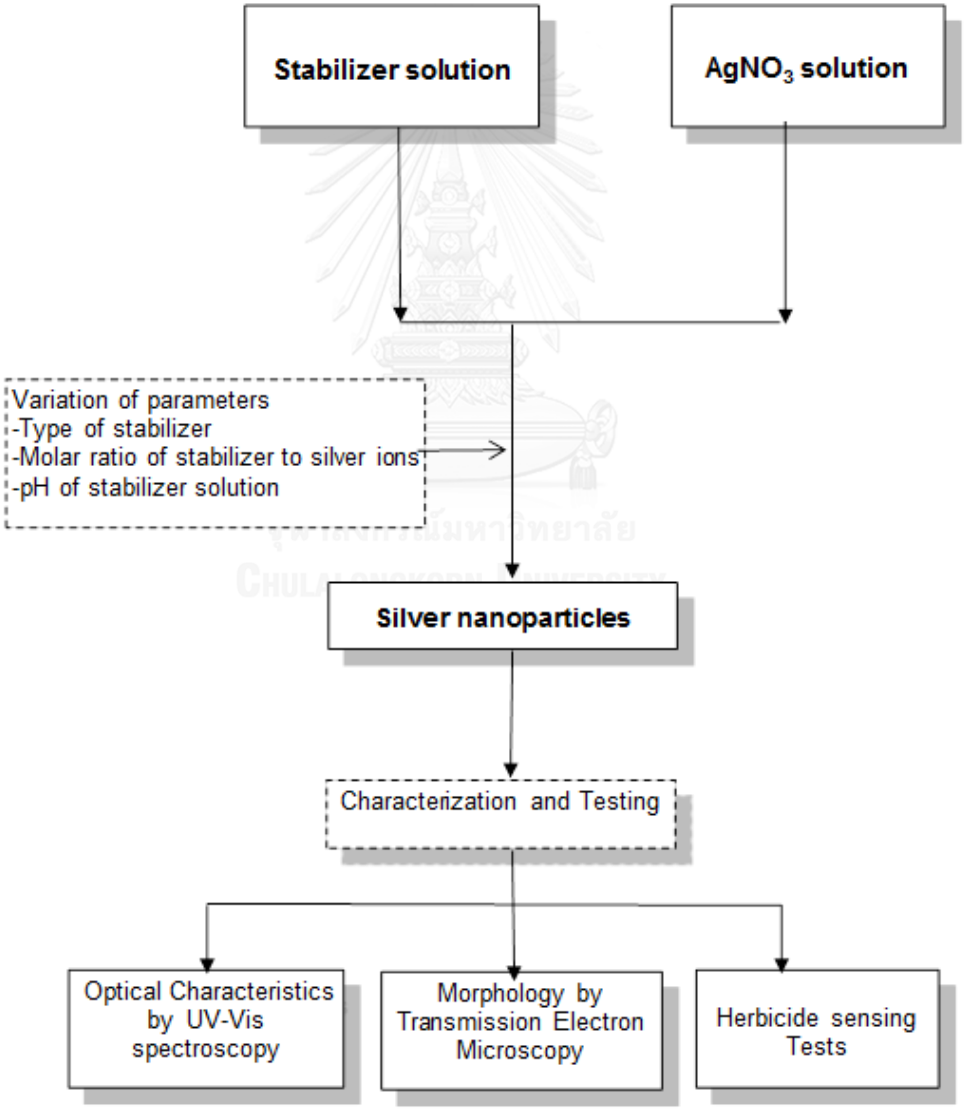

Figure 3.1 The experimental scope

3.2 Materials

In this research, all chemicals as listed in Table 3.1 were used without any further purification.

Table 3.1 Chemicals used in this research

No.	Chemicals	Grade	Manufacturer
1.	Acetic acid; M_w= 60.05 g/mol	Analytical reagent	Merck
2.	Acetone; M_w= 58.05 g/mol	Analytical reagent	RCI Labscan
3.	Carboxymethyl cellulose sodium salt; M_w= 90,000	Analytical reagent	Fluka
4.	Chitosan; M_w= 80,000 g/mol, DD = 90%	Analytical reagent	Seafresh Ltd., Thailand
5.	Humic acid sodium salt; M_w=124,758 g/mol	Analytical reagent	Sigma-Aldrich
6.	Paraquat herbicide; 27.6%	Commercial grade	Syngeta
7.	Poly (methacrylic acid, sodium salt) 30%, M_w= 9,500 g/mol	Analytical reagent	Sigma-Aldrich
8.	Potassium carbonate; M_w= 138.205 g/mol	Analytical reagent	Ajak
9.	Pyrazosulfuron-ethyl herbicide; 10%	Commercial grade	Sotus International Ltd.
10.	Sodium acetate; M_w= 136.08 g/mol	Analytical reagent	Ajak
11.	Silver nitrate; M_w= 169.08 g/mol	Analytical reagent	Merck
12.	Sulfuric acid; M_w= 98.079 g/mol	Analytical reagent	Merck
13.	Tannic acid; M_w= 1701.20 g/mol	Analytical reagent	Sigma-Aldrich

3.3 Instruments

Table 3.2 shows the list of the instruments used in this research.

Table 3.2 Instruments used in this research

Instrument	Model	Manufacturer
1. UV lamp	G10T8(10watts), G8T5(8 watts)	Tokiava lamp
2. pH meter	pH 510	EUTECH instrument
3. UV-Vis Spectrophotometer (UV-Vis)	SPECORD 250	Analytikjena
4. Tranmission Electron Microscope (TEM)	JEM 2100	JEOL
5. Tranmission Electron Microscope (TEM)	JEM 1400	JEOL

3.4 Synthesis of silver nanoparticles

The effects of three reaction parameters on the synthesis of silver nanoparticles were investigated. These parameters included the type of the stabilizer, the initial pH condition of the stabilizer solution and the molar of the stabilizer to silver ions.

3.4.1 Determination of the UV lamp power for the synthesis of silver nanoparticles

In order to determine the power of UV lamp used for synthesizing silver nanoparticles, 8 and 10 watts UV lamps were used for radiation in the synthesis of silver nanoparticles in the presence of tannic acid (TA). 5 ml of 4 mM silver nitrate solution was poured into 20 ml of TA solution using molar ratio (MR) of TA to silver ions at 1:1. pHs of TA solutions were varied from 5.0, 6.0 7.0, 8.0 to 9.0 using acetic acid or potassium carbonate solutions. After stirring for 5 minutes, the solution

was exposed to UV radiation for 60 minutes and then the silver nanoparticles were obtained. The synthesizing procedure can be summarized according to Figure 3.2.

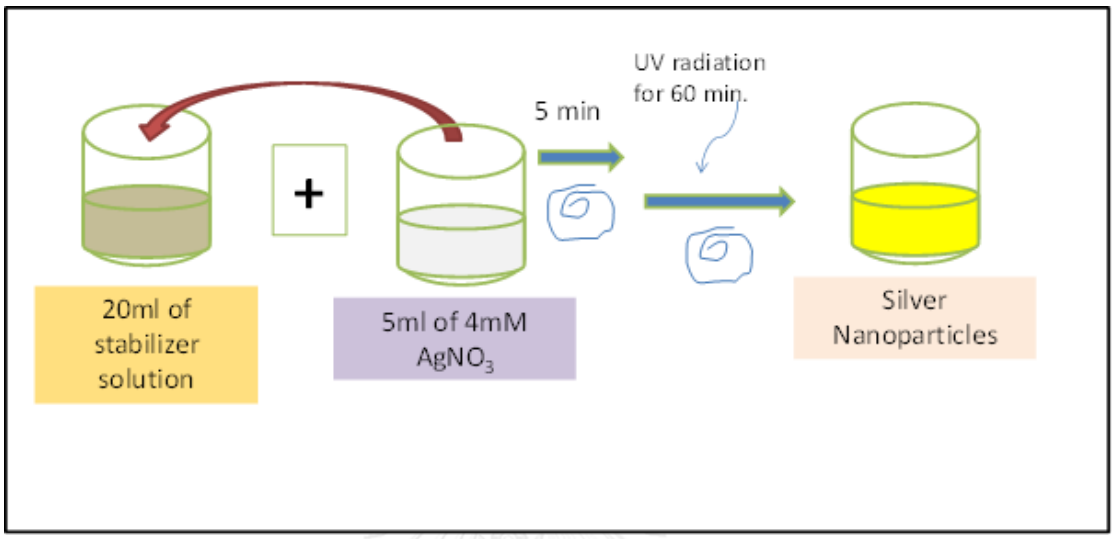

Figure 3.2 The procedure used for the synthesis of silver nanoparticles

3.4.2 Synthesis of silver nanoparticles using different stabilizers and conditions

Silver nanoparticles were synthesized according to the procedure shown in Figure 3.2 using UV lamp power determined from section 3.3.1. Five chemicals including tannic acid (TA), poly(methacrylic acid, sodium salt) (PMA), carboxymethyl cellulose, sodium salt (CMC), chitosan (CS) and humic acid (HA) were used. Initial pH of stabilizer solution and molar ratio of the stabilizer to silver ions were varied. The conditions used for each stabilizer are given in Table 3.3. pHs of the stabilizer solutions were varied from 5.0, 6.0 7.0, 8.0 to 9.0 using acetic acid or potassium carbonate solutions. For the stabilizers with lower molecular weight which were TA and PMA, the molar ratio was varied at 3 values. On the other hand, for the stabilizers with high molecular weight which were CMC, CS and HA,

the molar ratio with less amount of the stabilizers was applied due to the difficulty in dissolving the stabilizers when higher amount was used.

Furthermore, to determine the role of UV radiation in the synthesis, the control experiments were done for each stabilizer. Two samples of the mixture of stabilizer solution and silver nitrate solution were prepared using the same amount of the chemicals as shown in Figure 3.2. One was kept in the dark for 60 minutes and the other was exposed to natural light for 60 minutes. Then the optical characteristics of the obtained products were compared with those of their UV-irradiated counterparts.

Table 3.3 Experimental conditions used for the synthesis of silver nanoparticles.

Stabilizer	Stabilizer concentration mM	pH of stabilizer solution	Stabilizer solution (ml)	4mM Silver nitrate solution (ml)
TA	10.0	5.0, 6.0, 7.0, 8.0, 9.0	20	5
	1.0			
	0.1			
PMA	10.0	5.0, 6.0, 7.0, 8.0, 9.0	20	5
	1.0			
	0.1			
CMC	0.1	5.0, 6.0, 7.0, 8.0, 9.0	20	5
CS	0.1	5.0	20	5
HA	0.0072	5.0, 6.0, 7.0, 8.0, 9.0	20	5
	0.0007			

3.5 Characterization and testing of silver nanoparticles

3.5.1 Analysis of optical characteristics

UV-Vis absorption measurements were used for determining LSPR of the synthesized silver nanoparticles. These synthesized silver nanoparticles colloids were analyzed using UV-Vis spectrophotometer (SPECORD 250, Analytikjena) as shown in Figure 3.3. The absorption spectra were exhibited in the wavelengths ranging from 250 to 700 nm. This measurement was used to analyze the size, the size distribution, the agglomeration and also the stability of the silver nanoparticles. As previously mentioned in Chapter II, size of the nanoparticles is related to their LSPR. Bigger particles or agglomerated particles show the maximum absorbance at higher wavelength position. Uniformity of the obtained nanoparticles or size distribution is indicated by narrow absorbance peak. On the other hand, broader peak indicates the variation in the size or shape of the nanoparticles.

In this research, the stability of the nanoparticles was evaluated by comparing the absorption spectra of the nanoparticles after synthesis and after stored for one month. If the stability of nanoparticles was good, these spectra should be similar.

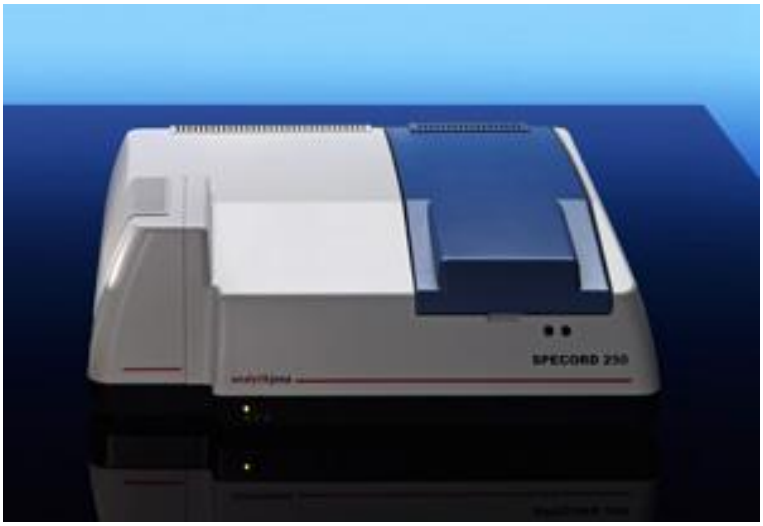

Figure 3.3 SPECORD 250 UV-Vis Spectrophotometer

3.5.2 Analysis of morphology

The morphology of the synthesized silver nanoparticles was analyzed using 2 Transmission Electron Microscopes (TEM) model JEOL: JEM 2100 and JEOL: JEM1400 as shown in Figure 3.4. TEM is suitable especially for analyzing the morphology of nanoparticles. It is a technique where a sample is bombarded by high energy electrons. Then a lot of electrons produce the image which are projected onto a fluorescent panel and show the images of the very small samples in nanometer size. Sample preparation was done by a dropped coat method. A drop of silver nanoparticles colloid was dropped on copper grid. The droplet was left for 5 minutes then the solution was wiped out of the grid and it was left to dry in the desiccator. All samples were measured without any further treatment.

Figure 3.4 Transmission Electron Microscopes

3.5.3 Herbicide sensing tests

Pyrazosulfuron-ethyl and paraguat were two herbicides used for herbicide sensing tests. The former is a non-polar substance and the latter has high solubility in water. The herbicide sensing ability was done by mixing 1.0 ml of the synthesized silver nanoparticles colloid with 1.0 ml of herbicide solution as shown in Figure 3.5. Then the mixture was shaken for 5 minutes and observed for the difference in the color of the mixtures. The amounts of herbicide were varied from 0, 50, 100, 200 to 400 ppm. UV-Vis spectroscopy was used to monitor the change in the absorbance peaks of the samples.

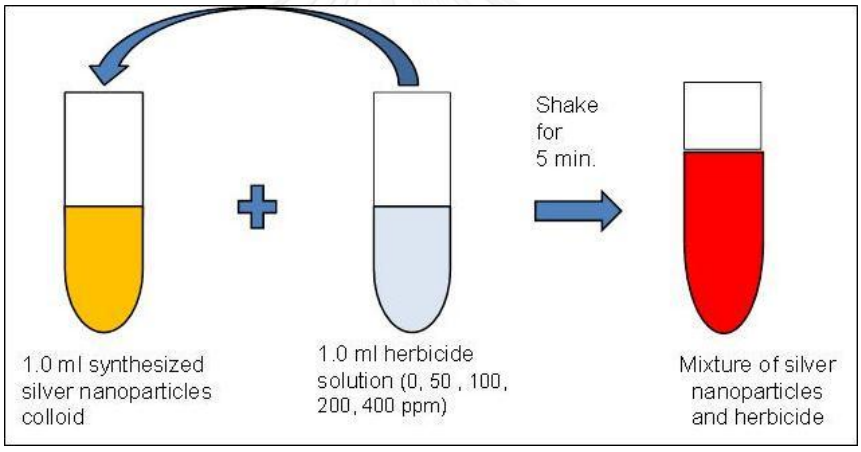

Figure 3.5 The procedure of herbicide sensing test

CHAPTER IV
RESULTS AND DISCUSSION

In this chapter, all results from every section of the experimental parts are reported and discussed. This chapter includes six parts of the experiments with their sub-sections. First five parts relates to the characteristics of the synthesized silver nanoparticles. The last part relates to the herbicide sensing tests of the synthesized silver nanoparticles. All abbreviations in this works are presented in the appendix A.

4.1 Characteristics of silver nanoparticles stabilized by tannic acid.

4.1.1 Optical characteristics

4.1.1.1 Effect of UV lamp power

In order to avoid side effect of UV irradiation to the stabilizer molecules, UV lamps with low energy were chosen to synthesize silver nanoparticles. Spadaro, D. and coworker [53] reported that when 6 watts of UV lamp was used, the nucleation and growth of the nanoparticles occurred without any modification to the stabilizer whereas when 25 watts of UV lamp was used, some modifications of the stabilizer occurred. In addition, previous studies suggested that low energy of UV lamp resulted in a slow growth rate of the nanoparticles yielding more controllable or uniform nanoparticles [4, 81]. In this research, 8 and 10 watts of UV lamps were applied for the synthesis of silver nanoparticles in the presence of TA solution at 5 different pH conditions (5.0, 6.0, 7.0, 8.0 and 9.0). The reduction of silver ions under UV irradiation was evidenced by the change in the color of the nanoparticles colloids from very pale yellow to yellow and then dark orange. The formation of silver nanoparticles was confirmed by the presence of LSPR

absorption peak in UV-Vis spectra around 430 nm which is typical for the nanoparticles having diameter less than 30 nm [48].

Due to the unique optical characteristics of silver nanoparticles, a great deal of information about the physical state of the nanoparticles can be obtained by analyzing UV-Vis spectra of silver nanoparticles in solution. As the diameter increases, the absorption peak shifts to longer wavelength and broadens. The peak wavelength and the peak width yield a unique spectral fingerprint for a plasmonic nanoparticles with specific size and shape [82].

In order to determine the UV lamp power for further synthesis, the differences of the UV-Vis spectra between two colloids obtained from using different UV lamps (same pH condition) were analyzed. In this research, two criteria were used for selecting the UV power. First criterion was the lowest UV power that can assist the reduction of silver ions. Second criterion was the UV power that had lowest side effect to the stabilizer molecules.

UV-Vis spectra after synthesis and after one month storage of TA-stabilized silver nanoparticles colloids synthesized with initial pH of TA solutions at 5.0, 6.0, 7.0, 8.0 and 9.0 were given in Figures 4.1-4.5, respectively. In the case of acidic conditions at pH 5.0 and 6.0, it was found that the silver nanoparticles synthesized using 2 UV powers exhibited similar UV-Vis spectra after synthesis and after one month storage. Their maximum absorption peaks at around 425 nm representing the silver nanoparticles reduced and stabilized by TA and at around 275 nm representing TA as shown in Figures 4.1 and 4.2. When compared to neutral and alkali conditions, it seemed that the silver nanoparticles synthesized using pH of 5.0 and 6.0 exhibited higher stability than those obtained from other pH conditions since their UV-Vis spectra after synthesis and after one month storage are similar as previously mentioned.

It can be seen from Figure 4.3 that UV-Vis spectra after synthesis of the silver nanoparticles synthesized with TA at initial pH of 7.0 using 8 and 10 watts of UV lamps are comparable. The characteristic peaks of both silver nanoparticles appear at wavelength around 425 nm. However, after one month storage, an increase in the intensity of the wavelength at 425 nm and the appearance of the intensity of the wavelength around 375 nm indicate the formation of the nanoparticles still occurred after UV irradiation. The peak at 375 nm suggests the formation of the nanoparticles that were slightly different from those having the characteristic peaks around 425 nm. This may be due to the generation of e^-_{aq} during UV irradiation. After irradiation was finished, these e^-_{aq} still remained in the system and can reduce silver ion as previously reported during storage [29]. The nanoparticles synthesized using 10 watts of UV lamp exhibit higher intensity of the wavelength around 375 nm than those synthesized using 8 watts of UV lamp indicating higher amount of silver nanoparticles were formed. This may be because higher energy of 10 watts can generate more e^-_{aq} than 8 watts. This phenomenon was not observed in acidic conditions since it is difficult for electron to solely present in acidic system as shown inFigures 4.1 and 4.2.

Figures 4.4 and 4.5 shows that besides the occurrence of the nanoparticles obtained from the reduction by TA, using alkali conditions at pH of 8.0 and 9.0 also yielded the silver nanoparticles based on the reduction by gallic acid. The characteristic peaks of gallic acid and its nanoparticles can be observed at around 257 nm and 350-400 nm, respectively. After stored for one month,

the reaction still occurred resulting in an increase in the intensity of the characteristic peaks of the nanoparticles. Since gallic acid is formed from tannic acid in alkali condition as previously mentioned in Chapter 2, there were no characteristic peaks of gallic acid when pH of 5.0, 6.0 and 7.0 were used as shown in Figures 4.1-4.3. However, it is clearly seen from Figure 4.5 that at pH 9.0,

the intensities of UV-Vis spectra corresponding to the stabilizers and silver nanoparticles in the range of 250 - 400 nm are slightly lower when 10 watts of UV lamp was used. This may be because using higher energy of UV radiation affected the stabilizer molecules [53].

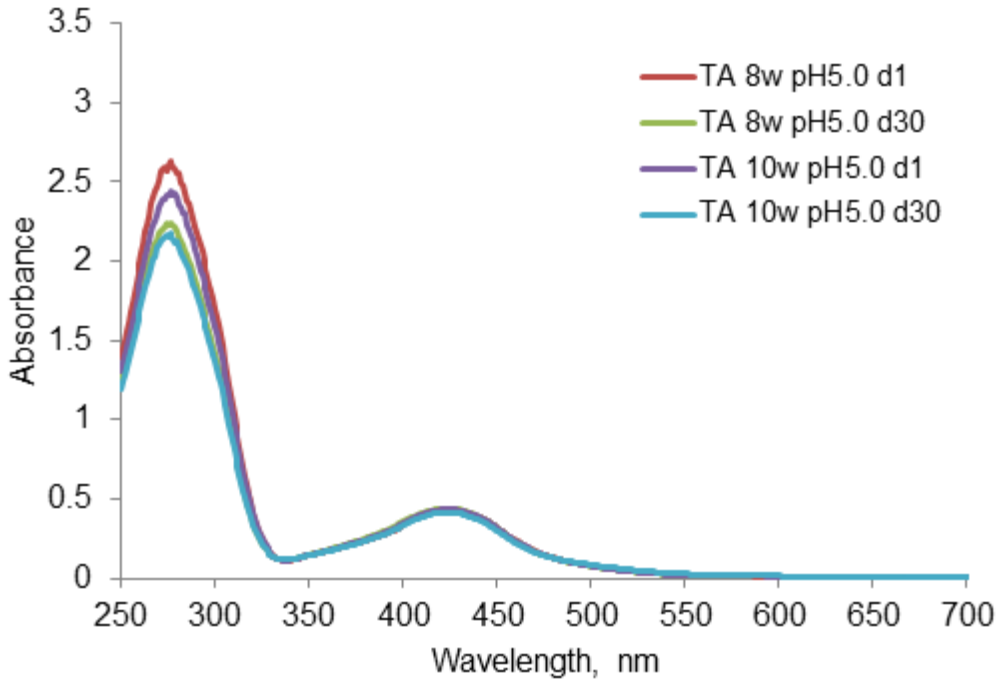

Figure 4.1 UV-Vis spectra of silver nanoparticles colloids synthesized using 8 and 10 watts of UV lamp in the presence of TA at pH of 5.0

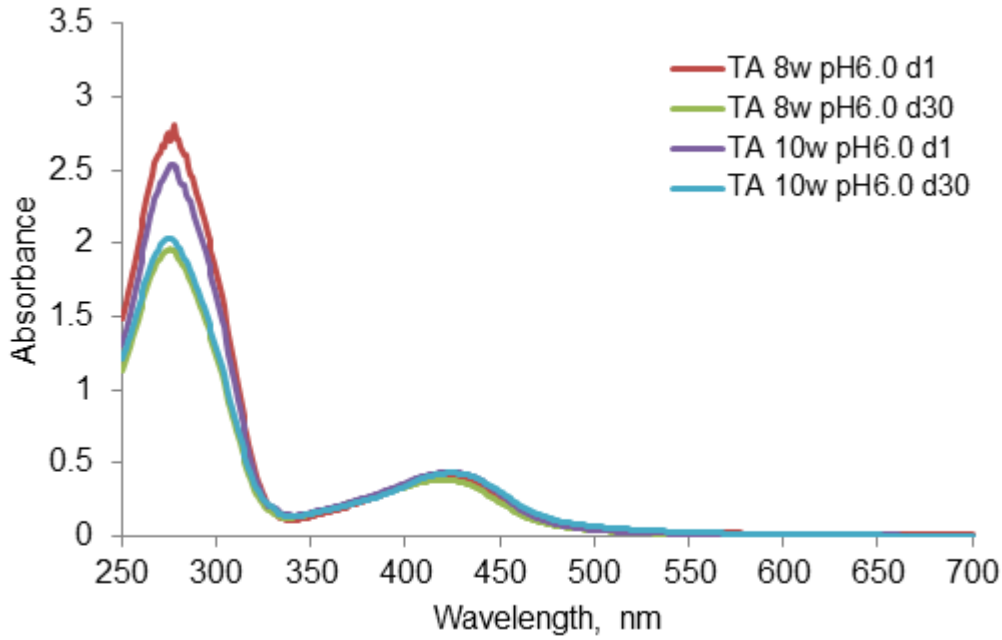

Figure 4.2 UV-Vis spectra of silver nanoparticles colloids synthesized using 8 and 10 watts of UV lamp in the presence of TA at pH of 6.0

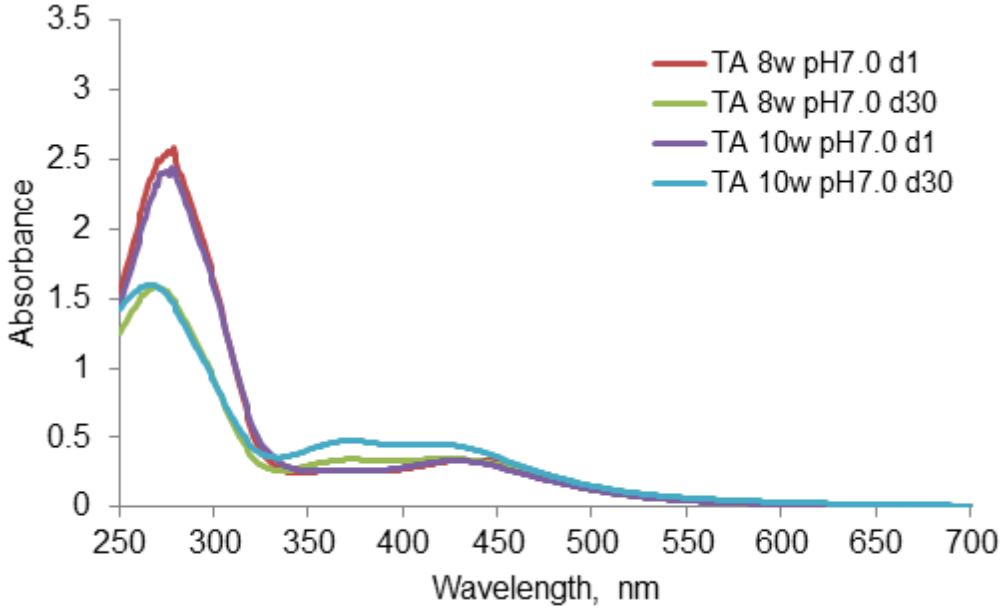

Figure 4.3 UV-Vis spectra of silver nanoparticles colloids synthesized using 8 and 10 watts of UV lamp in the presence of TA at pH of 7.0

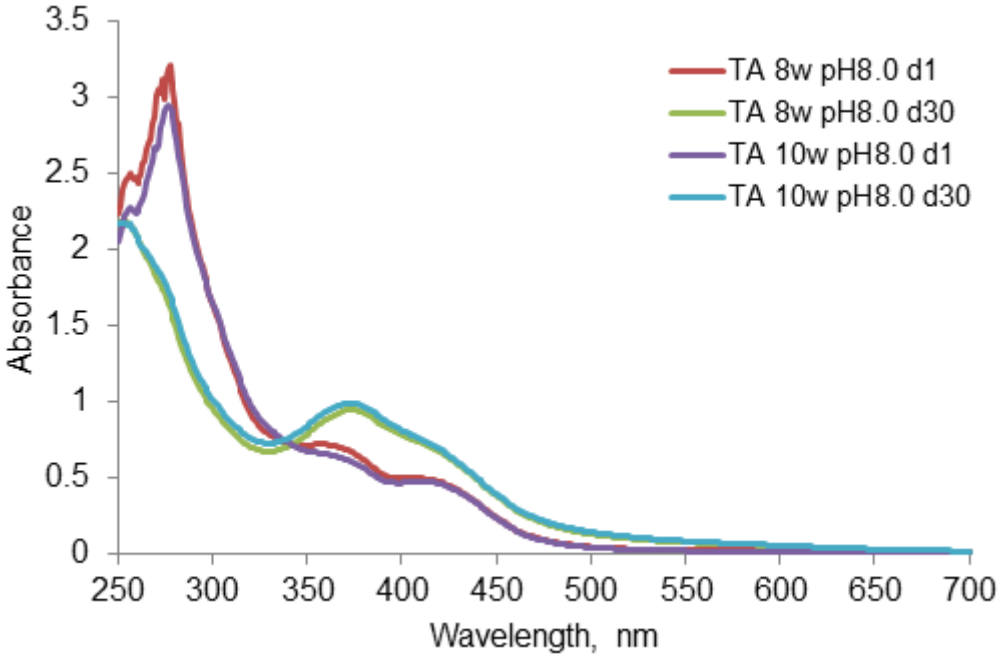

Figure 4.4 UV-Vis spectra of silver nanoparticles colloids synthesized using 8 and 10 watts of UV lamp in the presence of TA at pH of 8.0

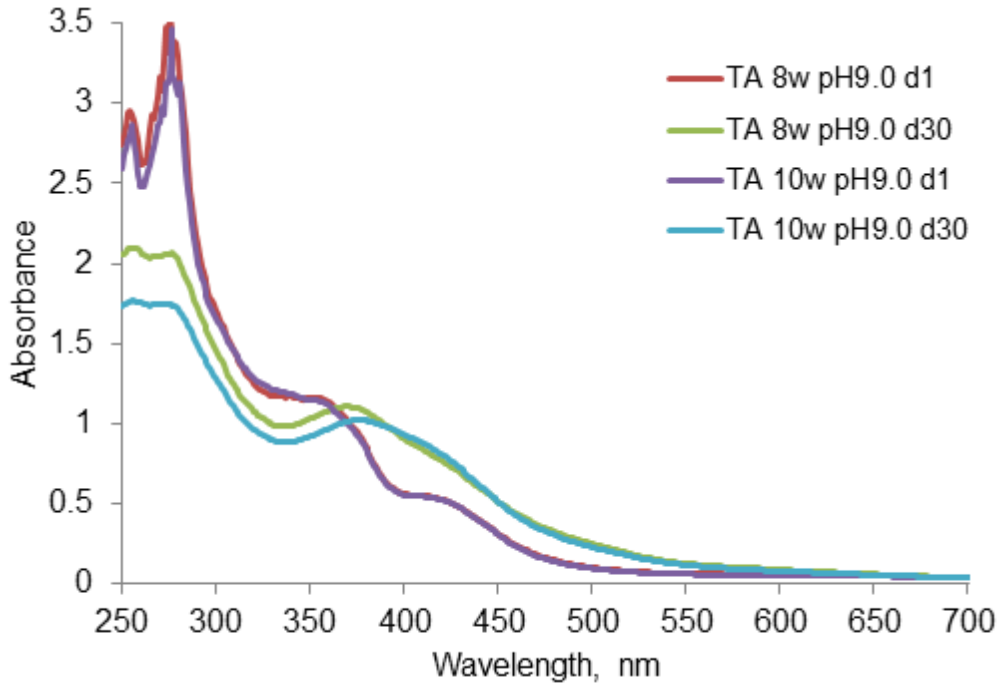

Figure 4.5 UV-Vis spectra of silver nanoparticles colloids synthesized using 8 and 10 watts of UV lamp in the presence of TA at pH of 9.0

It can be concluded based on the previous mentioned criteria that the power of 8 watts is enough to assist the reduction of silver ions and it shows less side effect of UV radiation to the stabilizer molecules. Therefore, UV lamp generating the power of 8 watts was chosen to use in further experiments.

4.1.1.2 Effect of initial pH of tannic acid solution

The appearances of the synthesized silver nanoparticles colloids are shown in Figure 4.6. Their optical characteristics were analyzed by UV-Vis spectroscopy and the results are given in Table 4.1 and Figure 4.7.

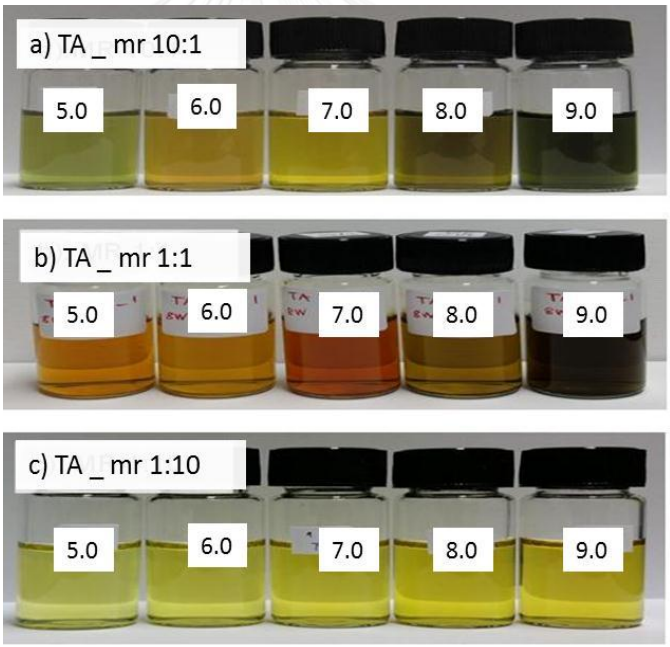

Figure 4.6 Appearances of silver nanoparticles colloids synthesized using different initial pH of TA solution and three molar ratios of TA to silver ions

Table 4.1 Positions of UV-Vis spectra of the silver nanoparticles synthesized using different initial pH of TA solution and three molar ratios of TA to silver ions

Peak position (Wavelength,nm)	pH 5.0	pH 6.0	pH 7.0	pH 8.0	pH 9.0
mr 10:1	275, 424	275, 424	275, 428	257, 275, 428	257,275, 310, 428
mr 1:1	275, 424	275, 422	275,435	257, 275, 355, 408	257, 275, 355,409
mr 1:10	275, 421	275, 419	275, 420	275, 421	257, 275, 410

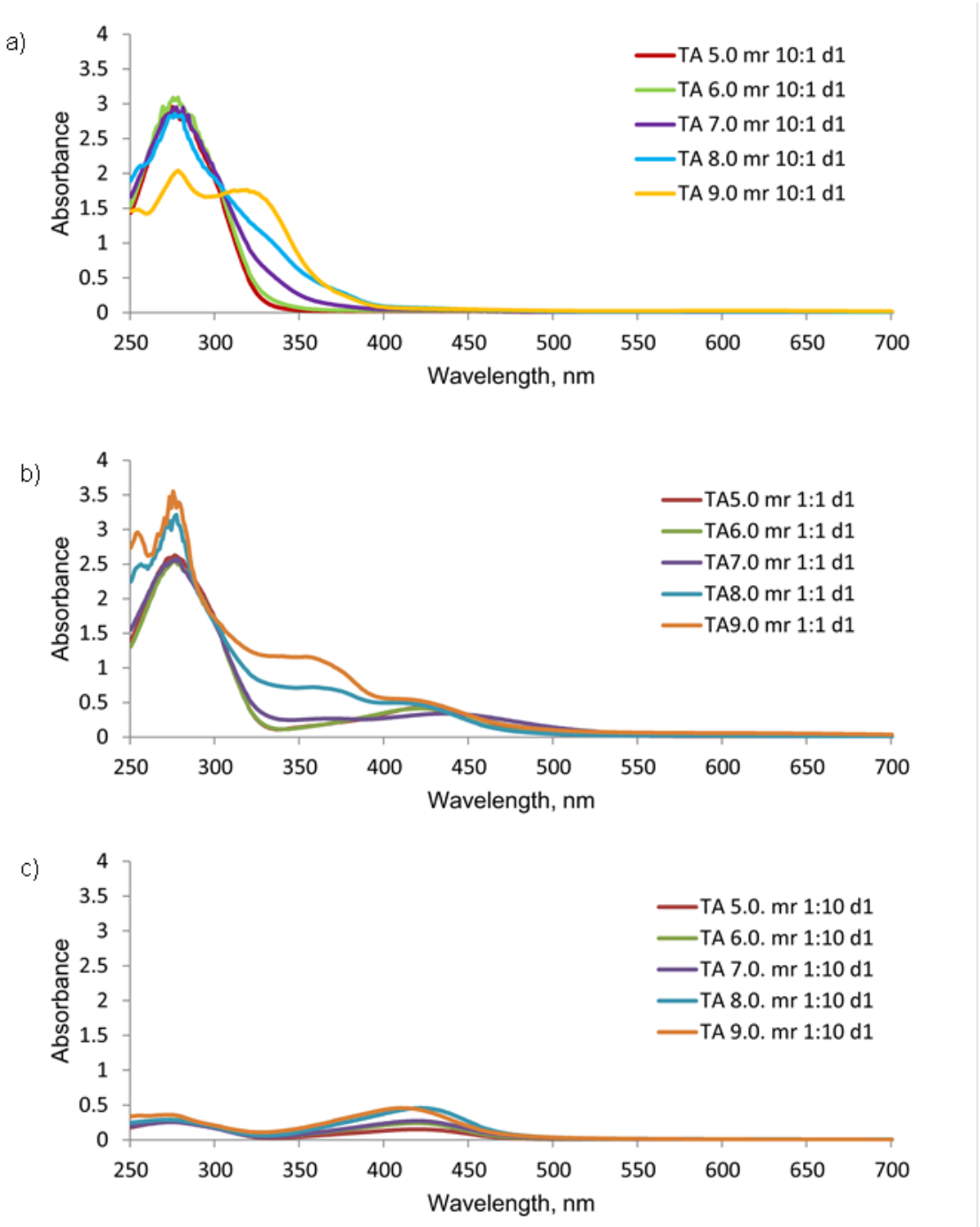

Figure 4.7 UV-Vis spectra of silver nanoparticles colloids synthesized using different initial pH of TA solution and three molar ratios (MR) of TA to silver ions; a) MR of 10:1 with dilution ratio of 1:200, b) MR of 1:1 with dilution ratio of 1:25 and c) MR of 1:10 with dilution ratio of 1:25

UV-Vis spectra showed that the main characteristic peaks of silver nanoparticles can be divided into two groups. First group of the characteristic peak at about 400-450 nm is attributed to silver nanoparticles stabilized with TA. The second group of the characteristic peak at about 300-350 nm is attributed to silver nanoparticles stabilized with gallic acid. This can be explained by the occurrence of gallic acid in this system. Previous work revealed that at alkali condition, TA was hydrolyzed into gallic acid which can be confirmed byUV-Vis characteristic peak of gallic acid at 257 nm [83] and TA around 270 nm [43]. Since gallic acid reduced silver ions into silver atom rapidly at room temperature, more spherical and smaller particles were obtained [44]. For pH conditions of 5.0, 6.0 and 7.0, there were no intensities around 350 nm which possibly represented silver nanoparticles which were reduced and stabilized by gallic acid whereas the peaks around 400-450 nm found in all spectra represents silver nanoparticles which were reduced and stabilized by TA itself.

4.1.1.3 Effect of molar ratio of tannic acid to silver ions

Figure 4.8 shows that the effect of molar ratio is clearly seen especially in alkali conditions of pH 8.0 and 9.0; hence, where gallic acid involves. At these conditions, the intensity of the characteristic peaks corresponding to the silver nanoparticles based on the reduction by gallic acid increases with increasing the amount of stabilizer. This is because the amount of gallic acid is related to TA content since it is a hydrolyzed product of TA at alkali condition [6]. On the other hand, at acidic and neutral conditions, the silver nanaoparticles based on the reduction by TA were the main product. The molar ratio slightly affected the formation of the nanoparticles as seen from Figures 4.8 a)-c) that the intensities of the characteristic peaks of these nanoparticles synthesized using MR of 10:1, 1:1 and 1:10 are not much different. However, at pH of 5.0 and 6.0, using MR of 1:1 resulted in the highest intensity of the characteristic peak of silver nanoparticles at around 425 nm This may be because in acidic solution, if the amount of TA is too high as in this case, about 10:1, the mobility of TA molecules may be difficult for the reduction and stabilization processes. Therefore, lower amount of silver nanoparticles was obtained at this ratio when compared to MR of 1:1.

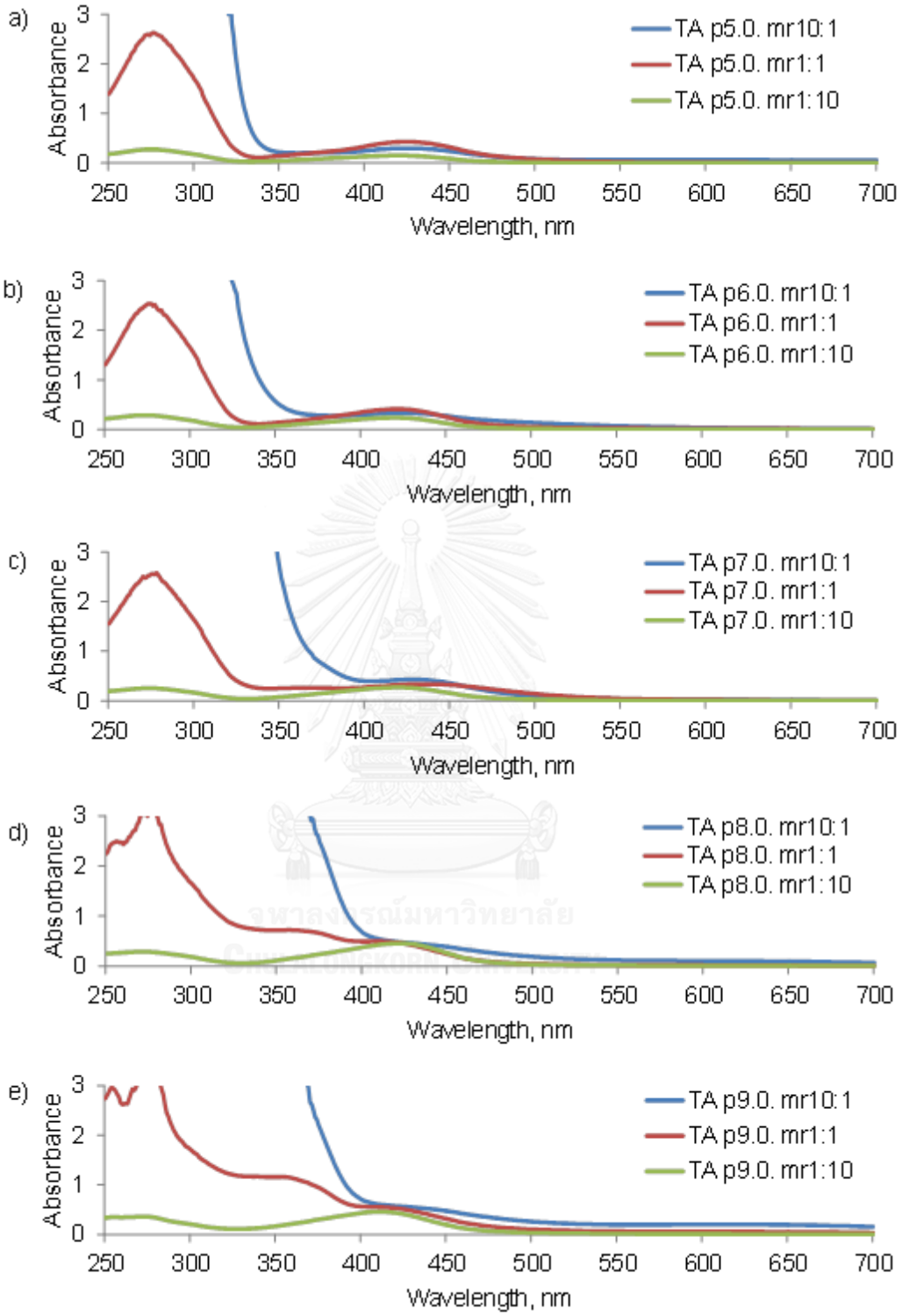

Figure 4.8 UV-Vis spectra of TA-stabilized silver nanoparticles colloids synthesized using three molar ratios of TA to silver ions at with different pH: a) 5.0, b) 6.0, c) 7.0, d) 8.0 and e) 9.0

4.1.1.4 Role of UV radiation in the synthesis

Figure 4.9 shows that no color of all the silver nanoparticles colloids synthesized using different light sources without adding any reducing agent was observed. However, UV-Vis spectra shown in Figure 4.10 indicated that without UV radiation there was no sign of silver nanoparticles formation. With natural light, it can reduce very little amount of silver ions to form silver nanoparticles. On the other hand, slightly higher amount of silver nanoparticles was formed after exposing to UV radiation. These results indicate that UV radiation can assist the reduction of silver ions into silver nanoparticles. However, low amount of silver nanoparticles was obtained. Therefore, it is necessary to use the reducing agent/stabilizer in the system in order to increase the product.

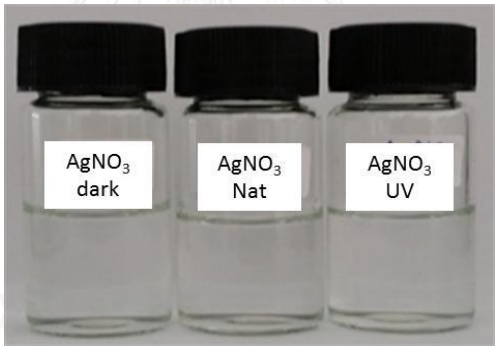

Figure 4.9 Appearances of silver nanoparticles colloids synthesized without any reducing agent using different light sources a) at dark, b) natural light (indoor) and c) UV lamp

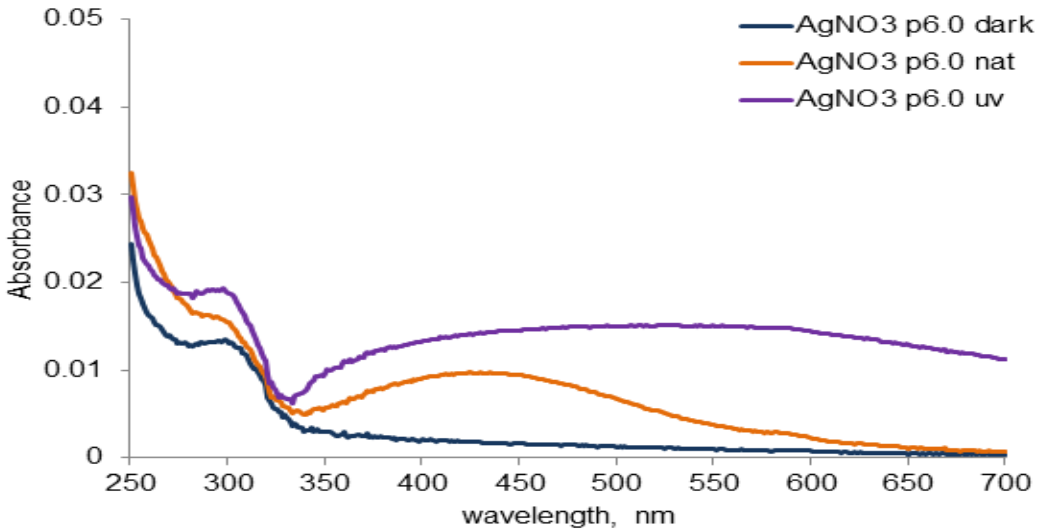

Figure 4.10 UV-Vis spectra of silver nanoparticles colloids synthesized without any reducing agent using different light sources a) at dark, b) natural light (indoor) and c) UV lamp

When TA was used, the silver nanoparticles colloids exhibit yellow color as shown in Figure 4.11. Their UV-Vis spectra given in Figure 4.12 show the differences between the samples at the wavelength range of 320-400 nm. Higher absorbance intensity in the wavelength range of 350-400 nm was observed when natural light was used. On the other hand, without any light (dark), the spectrum shows lowest absorbance intensity between 320-350 nm, but shows highest absorbance intensity between 350-390 nm. The latter wavelength range represents silver nanoparticles reduced by gallic acid (without any light) whereas the former range (320-350 nm) represents silver nanoparticles reduced by gallic acid with the assistance of light. This figure also shows that the absorbance intensities of the silver nanoparticles synthesized using natural light and UV radiation in the range of 300-350 nm are not different. On the other hand, in the wavelength range of 350-390 nm, the spectrum of UV- radiated sample shows higher absorbance than the sample synthesized under natural light. Moreover, the results indicate that the amount of gallic acid is highest when synthesizing in the dark and is lowest when synthesizing under natural light.

This indicates that TA can reduce silver ion to silver atom without using any light since it has a lot of phenol groups in its structure as mentioned in section 2.2.1.

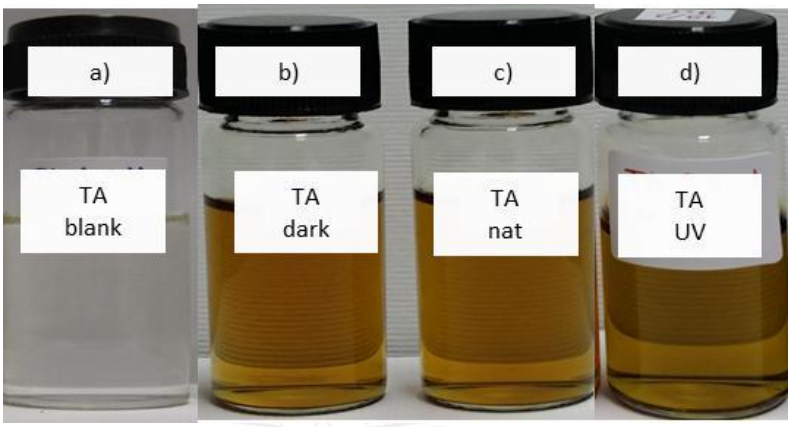

Figure 4.11 Appearances of TA-stabilized silver nanoparticles colloids synthesized at pH of 8.0 using different light sources: a) pure TA solution, b) at dark, c) natural light (indoor) and d) UV lamp

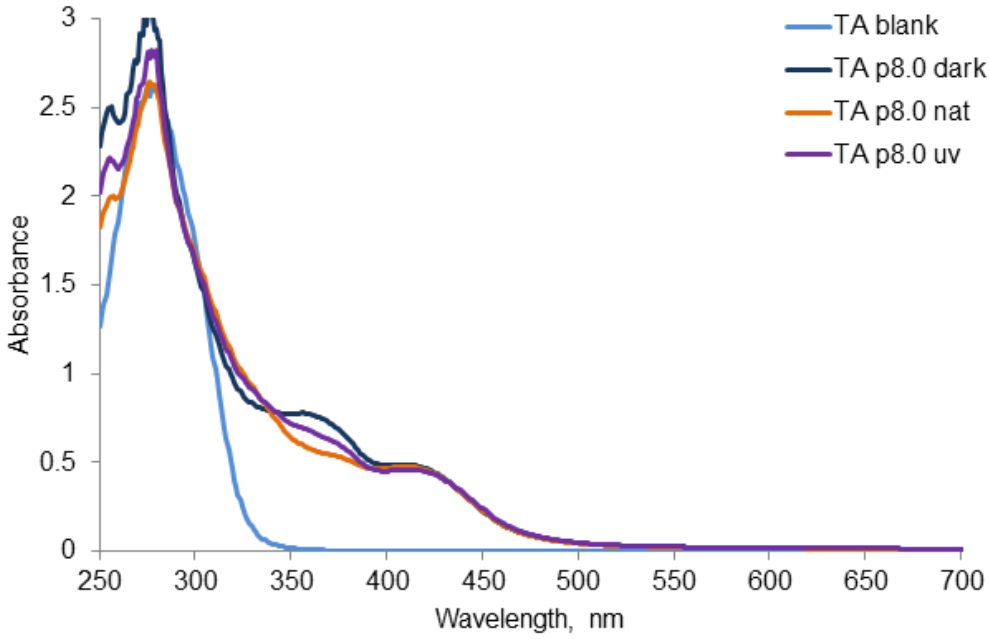

Figure 4.12 UV-Vis spectra of TA-stabilized silver nanoparticles colloids synthesized at pH of 8.0 using different light sources: a) pure TA solution, b) at dark, c) natural light (indoor) and d) UV lamp

4.1.2 Morphology

TEM images of TA-stabilized silver nanoparticles shown in Figures 4.13-4.15 confirm the occurrence of nanoparticles. At molar ratios of 10:1 and 1:1, bigger nanoparticles were obtained when pH of 5.0, 6.0 and 7.0 were employed. This supports the observation of their characteristic peak in UV-Vis spectra. It is clearly seen from Figure 4.13 that gallic acid-stabilized silver nanoparticles are smaller than TA-stabilized silver nanoparticles.

On the other hand, at molar ratios of 1:10, the sizes of the silver nanoparticles synthesized using initial pH of 5.0, 6.0, 7.0 and 8.0 are comparable as shown in Figure 4.15. However, the nanoparticle synthesized using initial pH of 9.0 exhibited smaller in size. This is probably due to more gallic acid occurred in this sample than the others as its UV-Vis spectrum shows higher absorbance intensity at 257 nm compared to the others as shown in Figure 4.7 c).

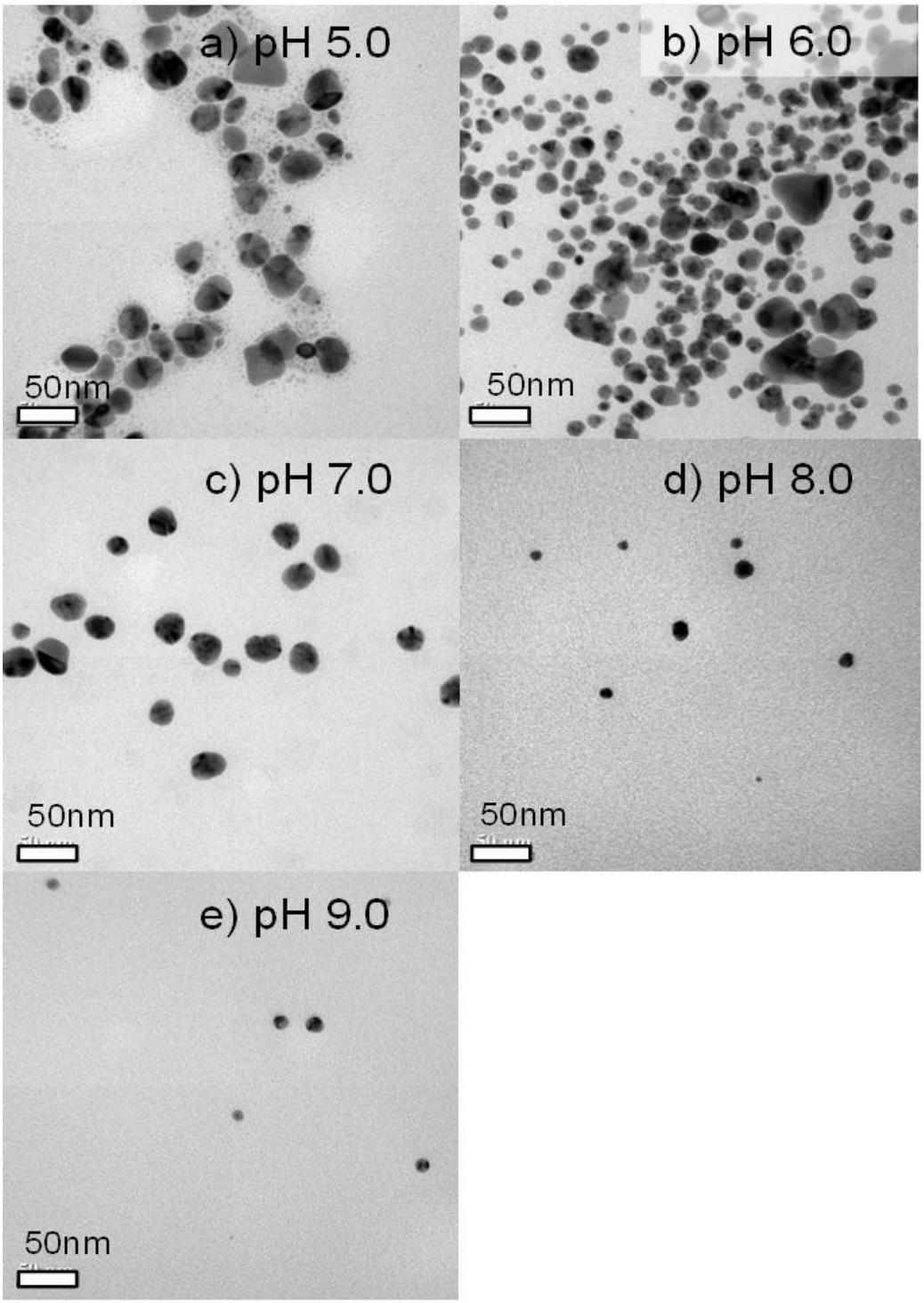

Figure 4.13 TEM images of TA-stabilized silver nanoparticles synthesized using different initial pH of TA solution and molar ratio of TA to silver ions at 10:1

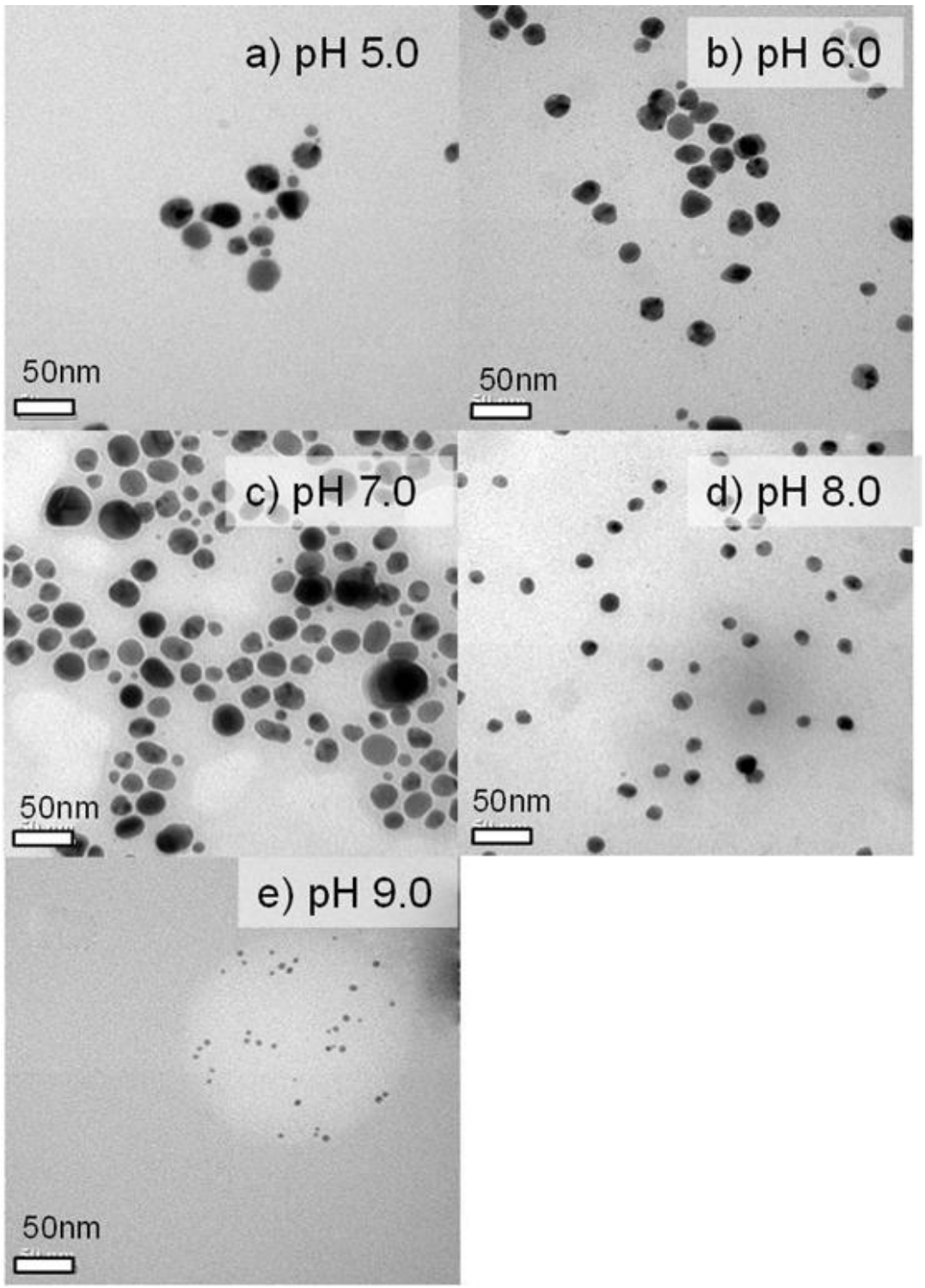

Figure 4.14 TEM images of TA-stabilized silver nanoparticles synthesized using different initial pH of TA solution and molar ratio of TA to silver ions at 1:1

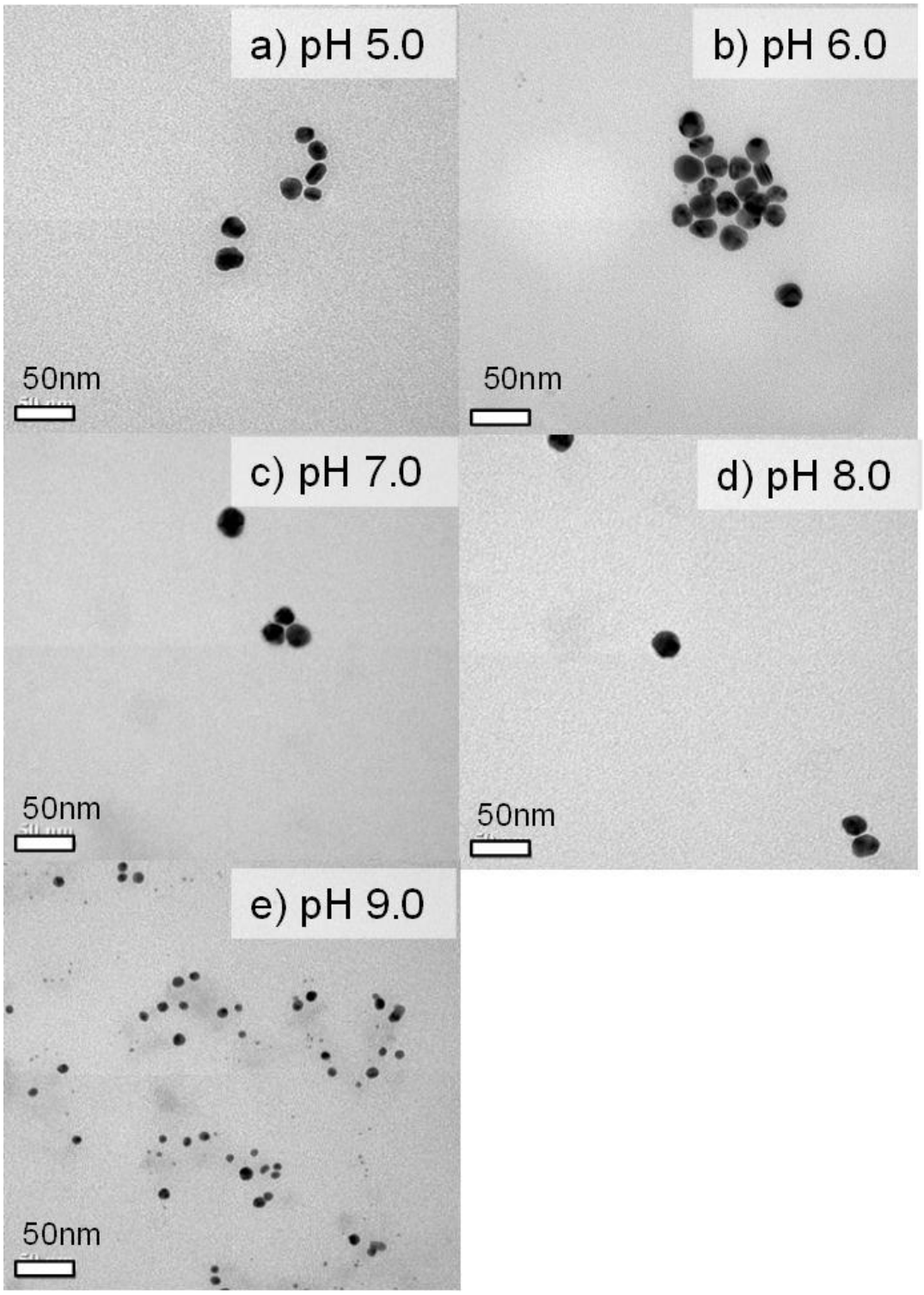

Figure 4.15 TEM images of TA-stabilized silver nanoparticles synthesized using different initial pH of TA solution and molar ratio of TA to silver ions at 1:10

4.1.3 Stability

The stability of the synthesized silver nanoparticles was observed after stored for one month at room temperature. Figure 4.16 shows that after one month, the colors of most of the silver nanoparticles colloids become darker especially those synthesized using MR of 10:1 at pH of 7.0, 8.0 and 9.0 and those synthesized using MR of 1:1 at pH of 8.0 and 9.0. In addition, the agglomeration of silver particles occurred resulting in the sediment atthe bottom of the bottles. On the other hand, those synthesized using MR of 1:10 exhibited a slight change in the color at every pH conditions.

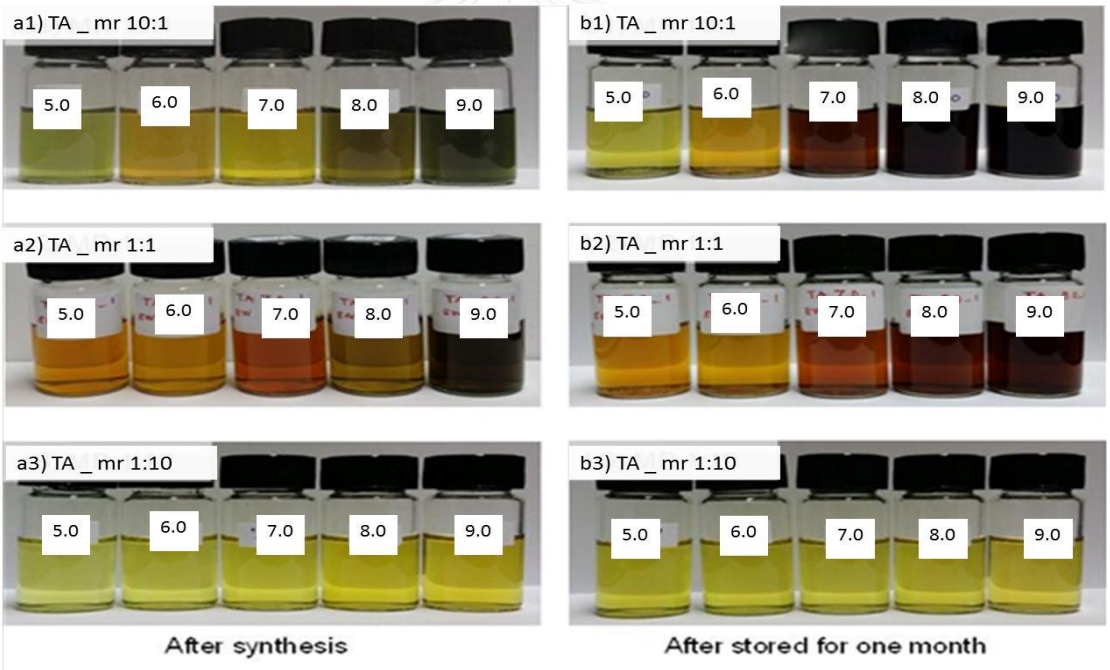

Figure 4.16 Appearances of TA-stabilized silver nanoparticles colloids after synthesis and after stored for one month

These above results can be confirmed by UV-Vis spectra as shown in Figures 4.17-4.19. It was found that when MR of 1:1 was used, the stability of TA-stabilized silver nanoparticles occurred when no gallic acid and/or gallic acid-stabilized silver nanoparticles present in the system. This is because TA is a better stabilizer than gallic acid as previously mentioned in Chapter II. Since TA is normally hydrolyzed into gallic acid at alkali condition, using pH of 5.0 and 6.0 can minimize this transformation and yielded the silver nanoparticles with high stability. On the other hand, when pH of 8.0 and 9.0 were used, TA was hydrolyzed into gallic acid and this resulted in the silver nanoparticles with low stability. It can be seen from Figure 4.20 that after one month storage, the nanoparticles become bigger. However, while this phenomenon was similar when MR 10:1 was used, but it was different when MR of 1:10 was applied. It was found that at this ratio, only characteristic peaks of TA-stabilized silver nanoparticles were observed in every pH condition. This indicated no involvement of gallic acid in the synthesis process. After one month storage, the samples synthesized using pH of 5.0, 6.0 and 7.0 showed an increase in the absorbance of these characteristic peaks. This may be probably because the amount of silver ions left in the mixture due to very slow reaction was higher than those synthesized at higher pH. The reduction of the silver ions still occurred further after finished the UV radiation. On the other hand, at pH of 8.0 and 9.0, the reduction of silver ions was mostly complete during the UV radiation; consequently, less reduction of the silver ions during storage occurred.

Moreover, the change in the color of the colloids after stored for one month depends on the numbers of gallic acid-stabilized and TA-stabilized silver nanoparticle as shown in UV-Vis spectra. This is why the change in the color of the samples synthesized using MR of 10:1 was much more than the others due to they produced more gallic acid than the others.

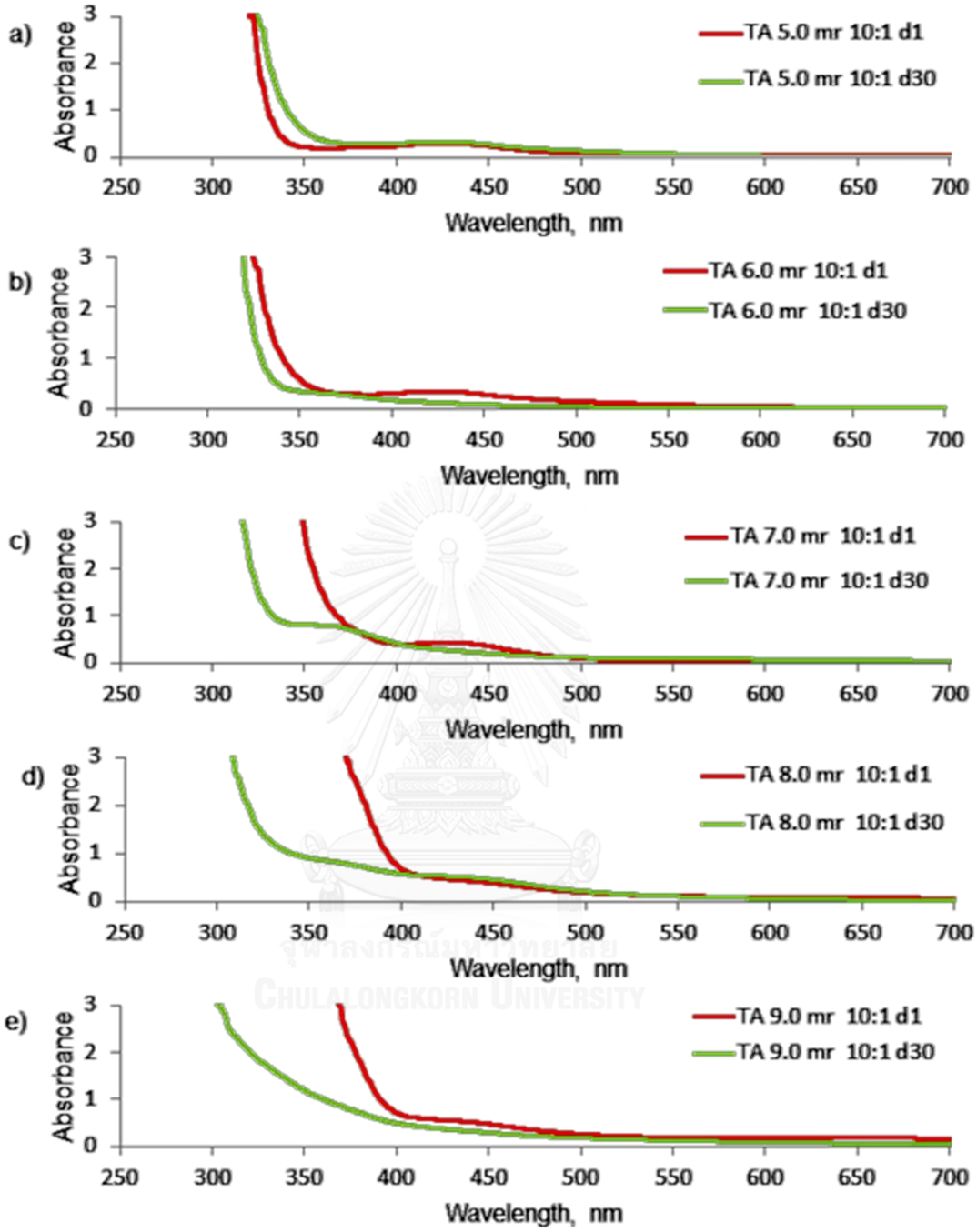

Figure 4.17 UV-Vis spectra of TA-stabilized silver nanoparticles colloids synthesized using molar ratio of TA to silver ions at 10:1 after synthesis and after stored for one month

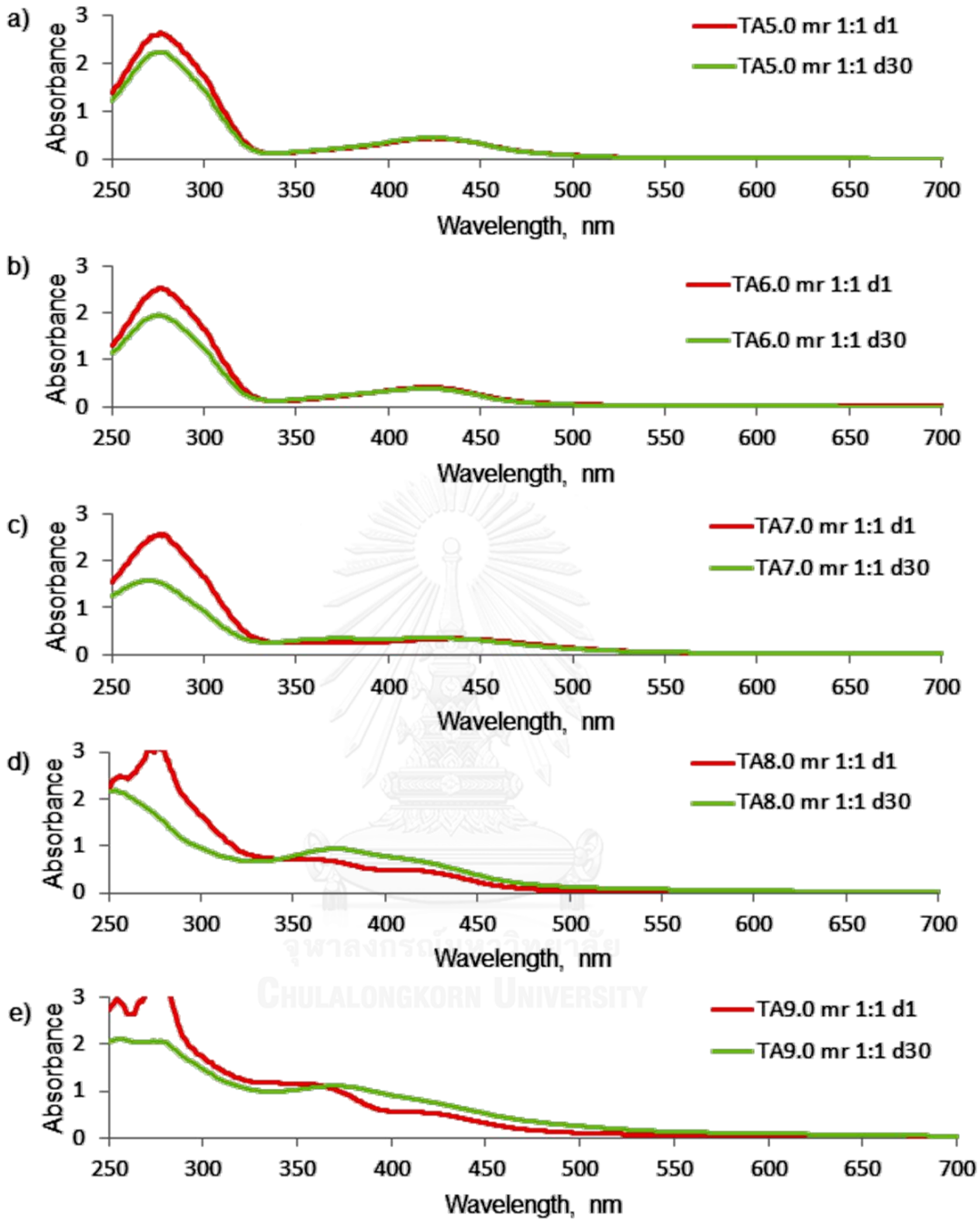

Figure 4.18 UV-Vis spectra of TA-stabilized silver nanoparticles colloids synthesized using molar ratio of TA to silver ions at 1:1 after synthesis and after stored for one month

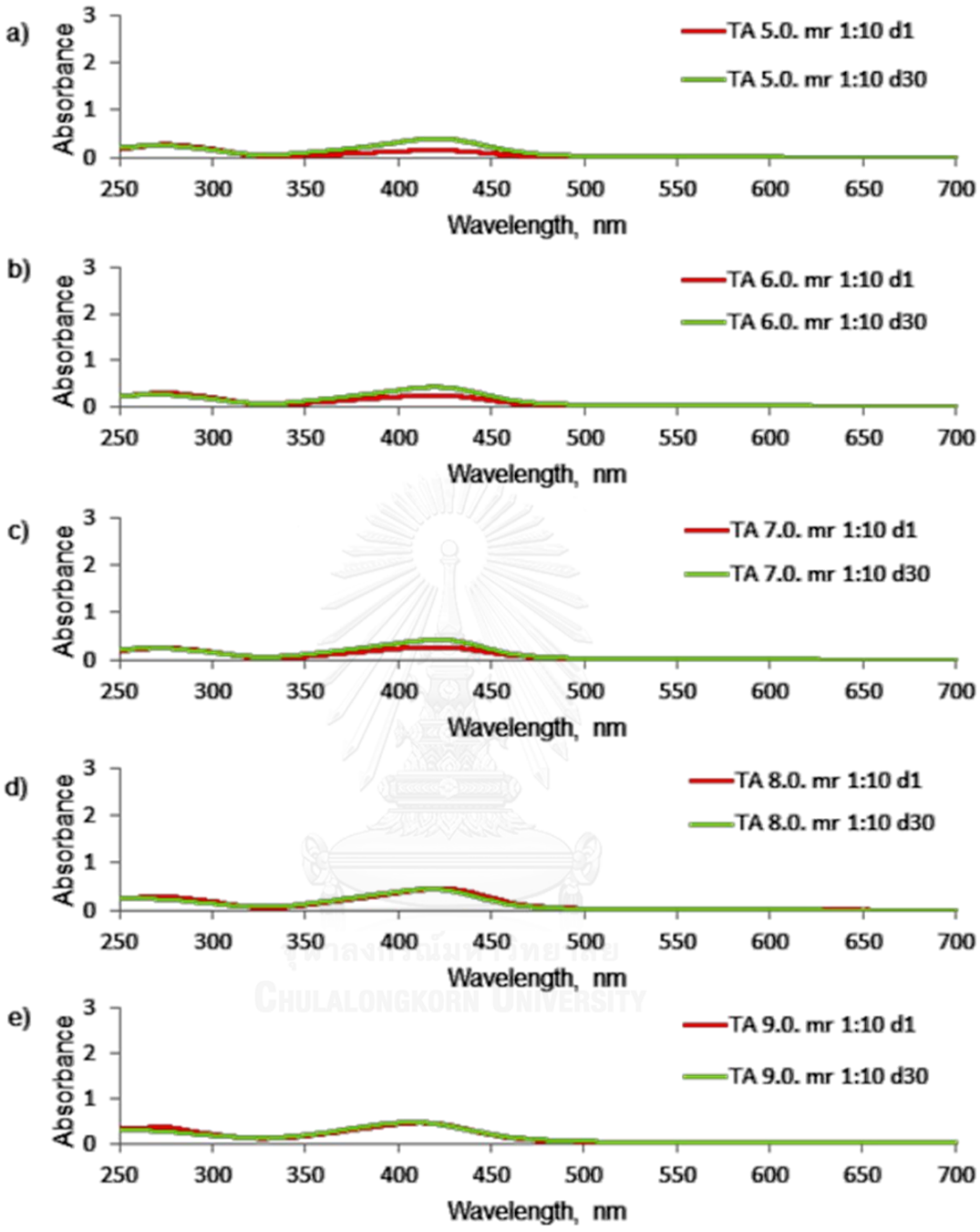

Figure 4.19 UV-Vis spectra of TA-stabilized silver nanoparticles colloids synthesized using molar ratio of TA to silver ions at 1:10 after synthesis and after stored for one month

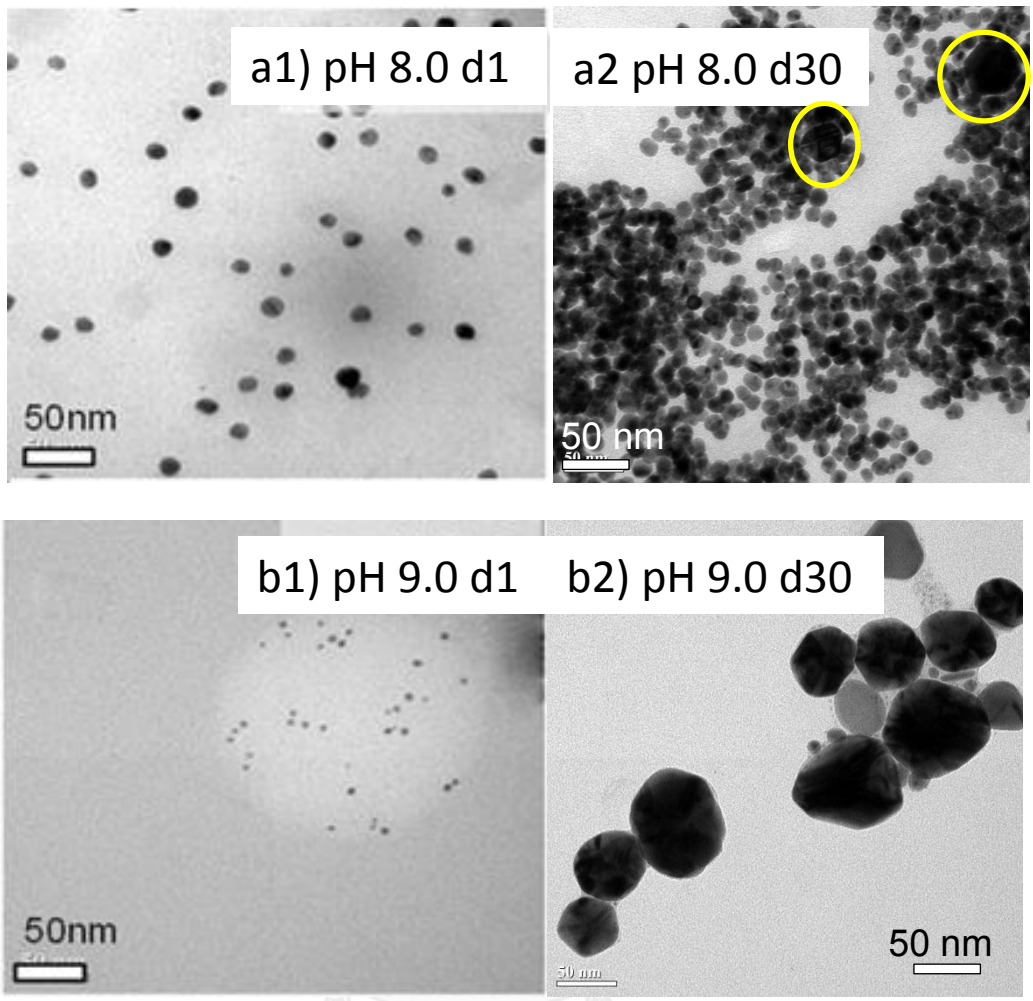

Figure 4.20 TEM images of TA-stabilized silver nanoparticles synthesized with MR of TA to silver ions at 1:1 after one month storage.

4.2 Characteristics of silver nanoparticles stabilized by poly (methacrylic acid, sodium salt)

4.2.1 Optical characteristics

4.2.1.1 Effect of initial pH of poly (methacrylic acid, sodium salt) solution

PMA-stabilized silver nanoparticles were synthesized using the same procedure as was employed to TA-stabilized silver nanoparticles. It can be seen from Figure 4.21 that the color of the silver nanoparticles colloids is darker with increasing the pH of PMA solution. This is because higher dissociation of PMA occurs when pH is increased than its pK_a. Poly (methacrylic acid) has pK_a at 5.6 [84]. Within the same pH condition, the samples synthesized using MR of 10:1 are darker than those synthesized using other MR. This is because increasing the amount of PMA means increasing the amount of reducing agent. As a result, higher amount of silver nanoparticles is obtained. When pH of 8.0 and 9.0 were used, UV-Vis spectra show that the characteristic peaks of samples of MR 10:1 and 1:1 were closed to each other compared to those of the sample of MR 1:10 as shown in Figure 4.22 and Table 4.2. This is because PMA is a long chain molecular structure, somehow the reduction rates of MR 10:1 and 1:1 were slower than MR 1:10 due to the mobility of PMA was poorer.

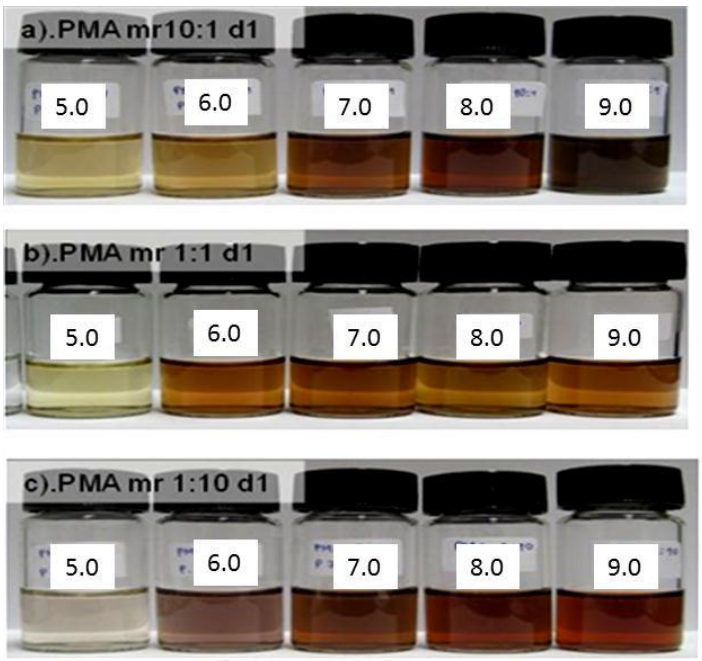

Figure 4.21 Appearances of silver nanoparticles colloids synthesized using different initial pH of PMA solution and three molar ratios of PMA to silver ions

Figure 4.22 shows the spectra of PMA-stabilized silver nanoaprticles and their peak positions are summarized in Table 4.2. It can be seen that at MR of 10:1, there are no characteristic peaks of silver nanoparticles appearing on UV-Vis spectra when pH of 5.0 and 6.0 were used in the synthesis. However, when initial pH of PMA solutions was elevated to 7.0, 8.0 and 9.0, the characteristic peaks of silver nanoparticles appear at the wavelength of 405 nm.

Figure 4.22 b) shows the UV-Vis spectra of the silver nanoparticles synthesized with MR of 1:1. The absorbance characteristic peak shifted to the longer wavelength compared to the sample of MR 10:1. Due to the sample of MR 1:1 has less amount of PMA to reduced silver ions, then this sample has slower reduction rate of silver ions. this resulted in larger particles obtained from MR 1:1 compared to MR 10:1. There was no characteristic of silver nanoparticles occurred in the sample synthesized with pH of 5.0. With pH of 6.0, 7.0, 8.0 and 9.0 presented absorbance characteristic peaks of silver nanoparticles at 414, 410, 409 and 409 nm, respectively.

Figure 4.22 c) shows the UV-Vis spectra of the silver nanoparticles synthesized with MR 1:10. The characteristic peaks shifted to the longer wavelength compared to the sample of MR 1:1. This because the chain mobility of MR 1:10 is more free and made the reduction easier. The lack of formation of silver nanoparticles in sample of MR 1:1 compared to sample of MR 1:10 may be explained by a high concentration of PMA can be obstacles the silver ions reduction and nucleation [5]. There was no characteristic peak of silver nanoparticles occurred in the sample synthesized with pH of 5.0, same as the other MR conditions. Moreover, the absorbance intensities increased as pH of PMA solutions were elevated. But the peak positions shifted to shorter wavelength when pH of PMA solutions was elevated. This is due to as pH increased higher than pK_a of PMA (5.6), the reduction rate increased. This is because higher pH made PMA stay in dissociated form more than neutral form due to the acid dissociation equilibrium [85].

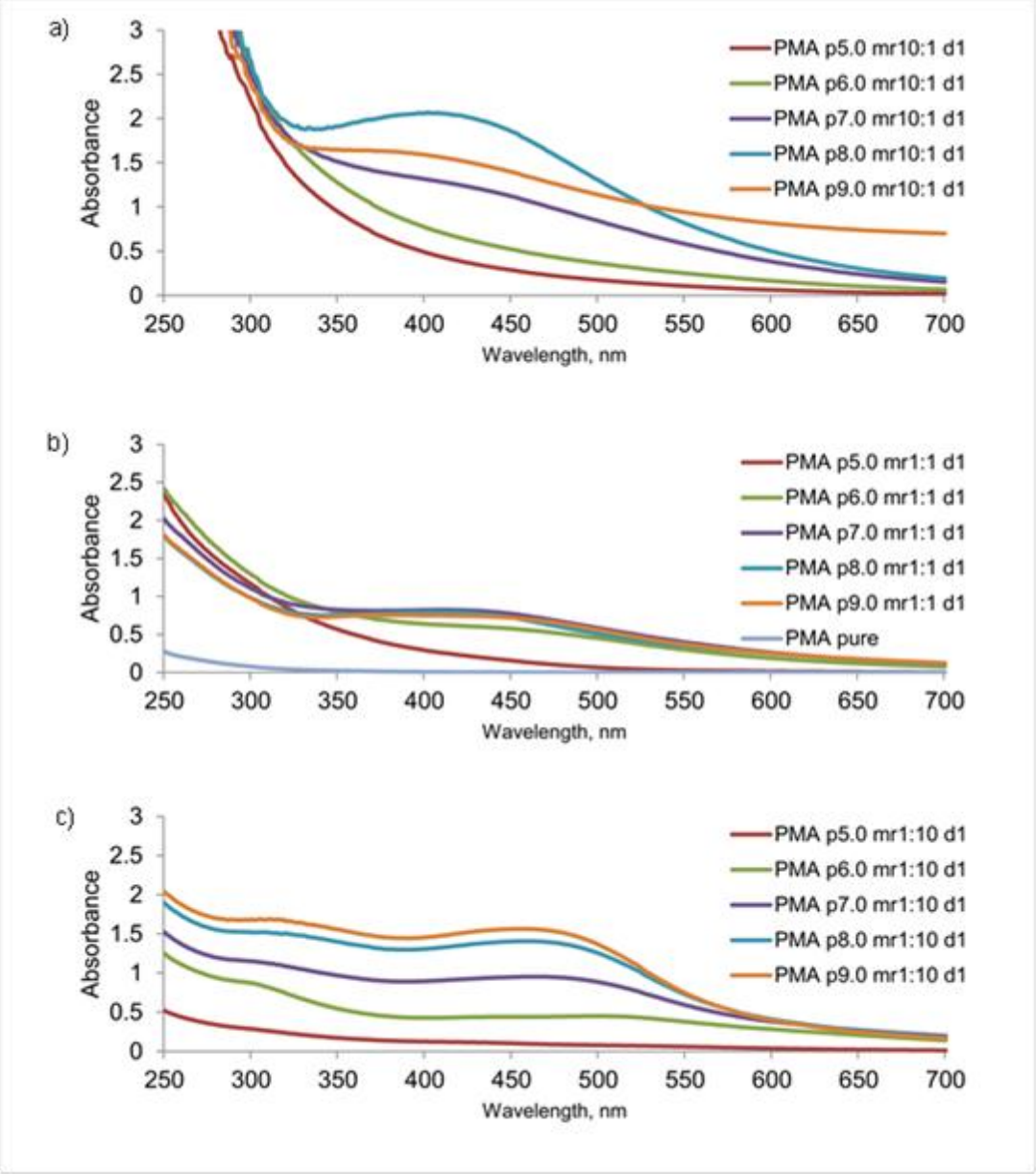

Figure 4.22 UV-Vis spectra of silver nanoparticles colloids synthesized using different initial pH of PMA solution and three molar ratios of PMA to silver ions

Table 4.2 Positions of UV-Vis spectra of the silver nanoparticles synthesized using different initial pH of PMA solution and three molar ratios of PMA to silver ions

Peak position (Wavelength,nm)	pH 5.0	pH 6.0	pH 7.0	pH 8.0	pH 9.0
mr 10:1	-	-	405	405	405 Broaden pk 350-700
mr 1:1	-	414	410	409	409 Broaden pk 330-550
mr 1:10	-	297, 501	300, 461	311, 458	311, 456

4.2.1.2 Effect of molar ratio of poly(methacrylic acid, sodium salt) to silver ions

Figure 4.23 showed that at initial pH of PMA at 5.0, there was no characteristic peak of silver nanoparticles in every MR spectra. At initial pH of 6.0, MR 1:1 and 1:10 showed a characteristic peak of silver nanoparticles at 450, 520 nm, respectively. This can be explained that at pH of 6.0 with MR 10:1, there was less silver nanoparticles formation probably due to less mobility of the PMA. At pH of 7.0, sample of MR 1:1 started to show characteristic peak around 420 nm. As initial pH of PMA was elevated to 8.0, every spectrum showed higher absorbance intensities. However, when initial pH of PMA was elevated to 9.0, the absorbance intensities of MR 10:1 were decreased and the spectra line showed sign of agglomeration.

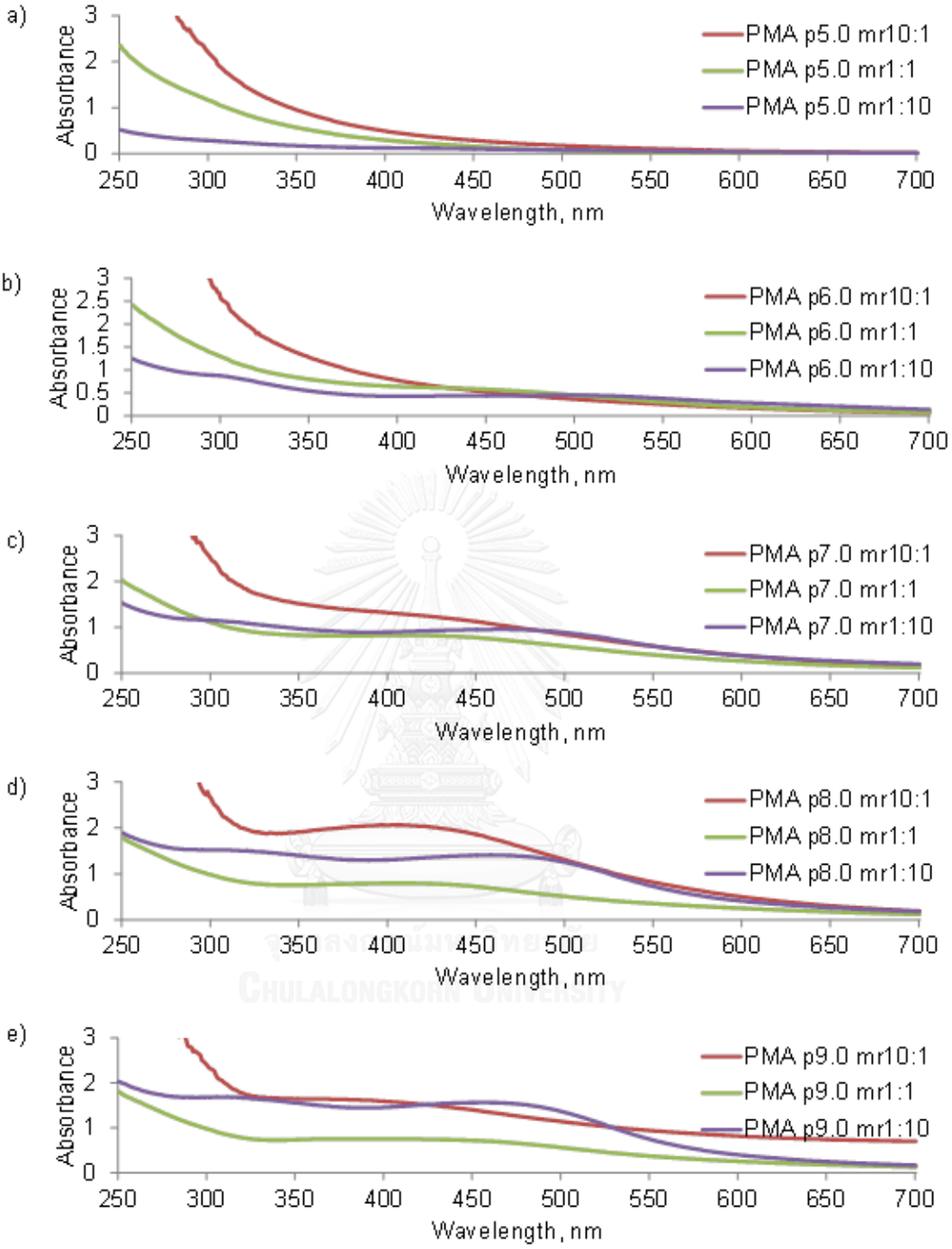

Figure 4.23 UV-Vis spectra of PMA-stabilized silver nanoparticles colloids synthesized using three molar ratios of PMA to silver ions at with different pH: a) 5.0, b) 6.0, c) 7.0, d) 8.0 and e) 9.0

4.2.1.3 Role of UV radiation in the synthesis

Figure 4.24 shows that PMA can reduce silver ions to form silver nanoparticles without the assistance of any light since its sample exhibited yellow color similar to that synthesized using natural light. When UV radiation was applied, PMA-stabilized silver nanoparticles colloid synthesized under UV radiation exhibiting the darkest color indicating an increase in the reduction of silver ions. These results can be confirmed by UV-Vis spectra as shown in Figure 4.25. Therefore, it can be concluded that UV radiation promotes the synthesis of silver nanoparticles and PMA can acts as both reducing agent and stabilizer.

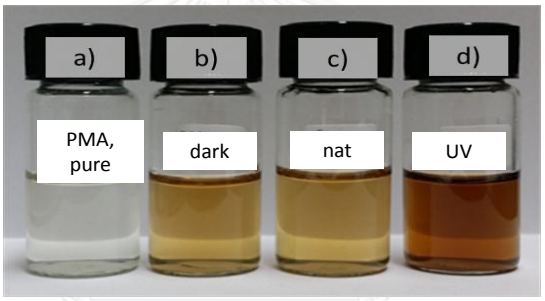

Figure 4.24 Appearances of PMA-stabilized silver nanoparticles colloids synthesized at pH of 8.0 using different light sources: a) pure PMA solution, b) at dark, c) natural light (indoor) and d) UV lamp

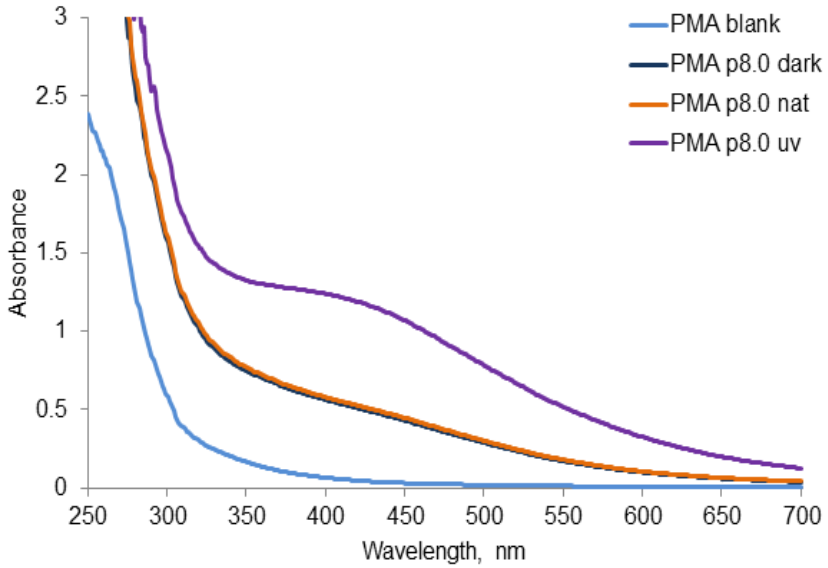

Figure 4.25 UV-Vis spectra of PMA-stabilized silver nanoparticles colloids synthesized at pH of 8.0 using different light sources: a) pure PMA solution, b) at dark, c) natural light (indoor) and d) UV lamp

The mechanism of the reduction process can be explained as follows. It was known that PMA has lots of functional groups of COO^- depends on pH condition of the system [85]. For each acid group, it has acid dissociation reaction as follow:

$$A\text{-}COO^- + H_2O \longleftrightarrow A\text{-}COOH + OH^- \qquad \text{(eq. 4.1)}$$

From the above equation, it is shown that the dissociation groups are increased as pH condition increased. On the other hand, as pH is decreased, the neutral forms are less dissociated [85].

Moreover, theorectically, it was known that among the carboxylic derivatives, carboxylate groups are the least reactive towards nucleophillic acyl substitution. It is also less reactive than carboxylic acid group. Due to the negatively charged oxygen one carboxylate group has lots of electron cloud to donate, therefore the carbonyl carbon is not very elecrophillic [86]. Then the nucleophile is probably attached to the end group of $-COO^-$ instead.

Furthermore, the OH^- ions can react with silver ions to give silver oxide: Ag_2O [87] as follow:

$$2\ Ag^+ + 2\ OH^- \longleftrightarrow Ag_2O + H_2O^- \qquad \text{(eq. 4.2)}$$

In this study, the reduction mechanism of PMA stabilized silver nanoparticles with initial pH of PMA solution above 7.0, were probably started with two silver ions attached to the $-COO^-$ and then leaving out to form Ag_2O and leaved the new end group of aldehyde functional group. Then this aldehyde end group reduced silver oxide to form silver nanoparticles by itself as shown in eq 4.3 [88]:

eq. 4.3

Those mechanism also explained why there were less silver nanoparticles formation when synthesized with initial pH of PMA at 5.0 and 6.0.

4.2.2 Morphology

TEM measurements were carried out to observe the morphology of the silver nanoparticles synthesized under different initial pH condition of PMA and their images were shown in Figure 4.26, 4.27 and 4.28. Almost all of the samples were in nanoparticles size.

Figure 4.26 shows TEM images of the synthesized silver nanoparticles with the MR of 10:1. Although, the samples synthesized with initial pH of PMA at 5.0 and 6.0, there was no characteristic peak of silver nanoparticles, TEM images showed that there were some silver nanoparticles in those samples but they were not uniformly.

Figure 4.27 shows TEM images of the synthesized silver nanoparticles with the MR of 1:1. Silver nanoparticles synthesized with MR of 1:1 were almost the same size. These confirmed the UV-Vis spectra that showed the characteristic peak at 409 - 414 nm as shown in Figure 4.22 b.

Figure 4.28 shows TEM images of the synthesized silver nanoparticles with the MR of PMA to silver ions as 1:10. TEM images showed that the silver nanoparticles synthesized with initial pH of PMA at pH of 6.0 were different from the others as they were spherical and rod shape as shown in Figure 4.28 b1) and b2) while the others were only spherical shape. This can be explained with the incomplete reduction of silver ions [4].This may be explained with the dissociation equilibrium, since it has pKa of 5.6 [84]. At pH of 5.0 it was lower than pKa then most of the PMA tended to stay in neutral form. This caused least formation of silver nanoparticles at this condition due to less reactive of the neutral form to the silver ions. However, as initial pH of PMA solution was elevated to pH of 6.0 which a little higher than pKa of PMA (5.6), there was probably incomplete dissociation of PMA. The reduction of silver ions at this condition was slower than those of higher pH conditions. Moreover, there are more silver ions left in the system after UV irradiation, and this silver ions may be perturb the electric surround of the silver nanoparticles [4]. These TEM results confirmed UV-Vis spectra that showed different positions of the characteristic peaks of this sample at 501 nm. While the other conditions were shown at 461, 458 and 456 nm as pH increased to 7.0, 8.0 and 9.0, respectively as shown in Figure 4.22 c).

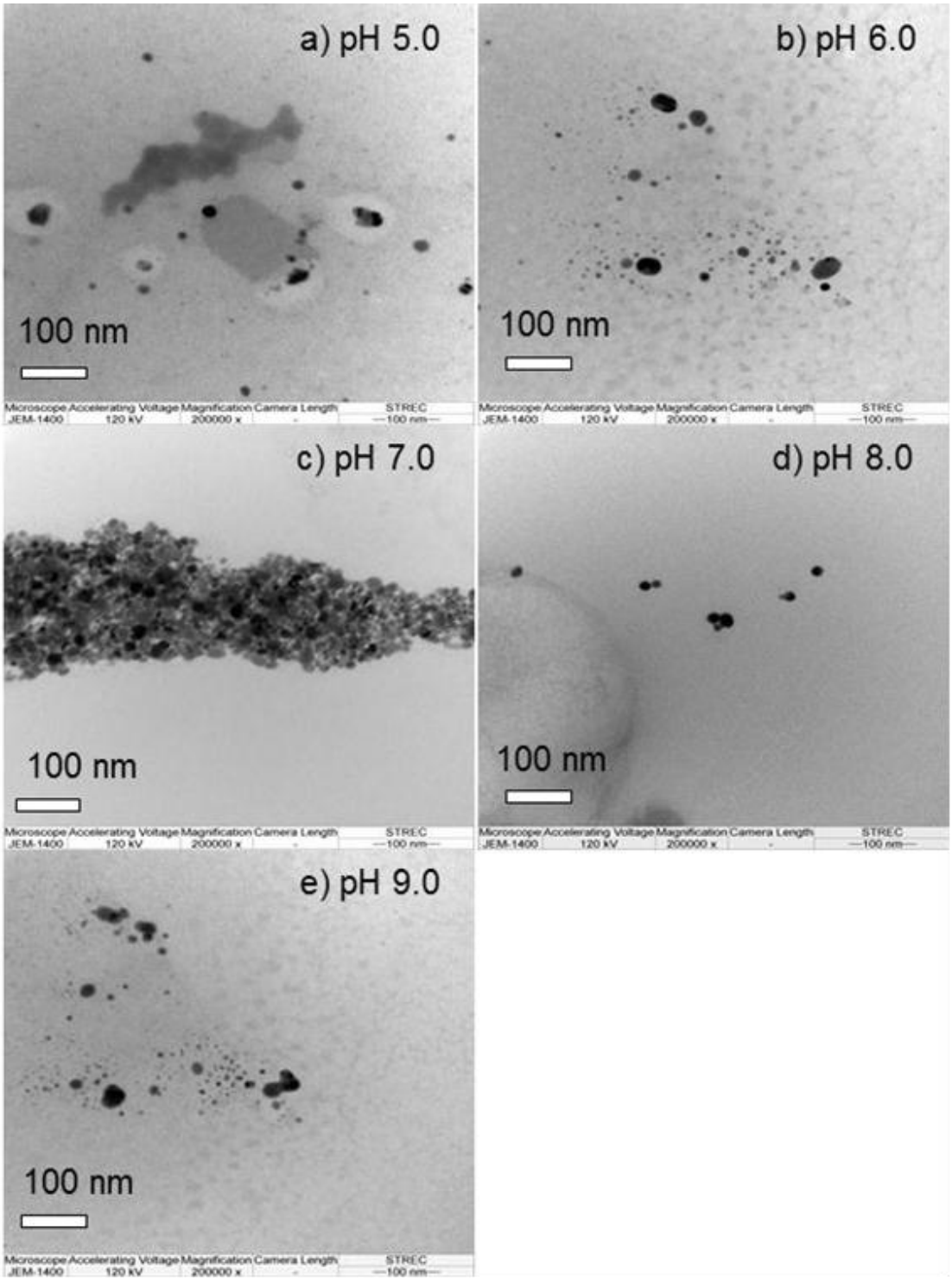

Figure 4.26 TEM images of PMA-stabilized silver nanoparticles synthesized using different initial pH of PMA solution and molar ratio of PMA to silver ions at 10:1

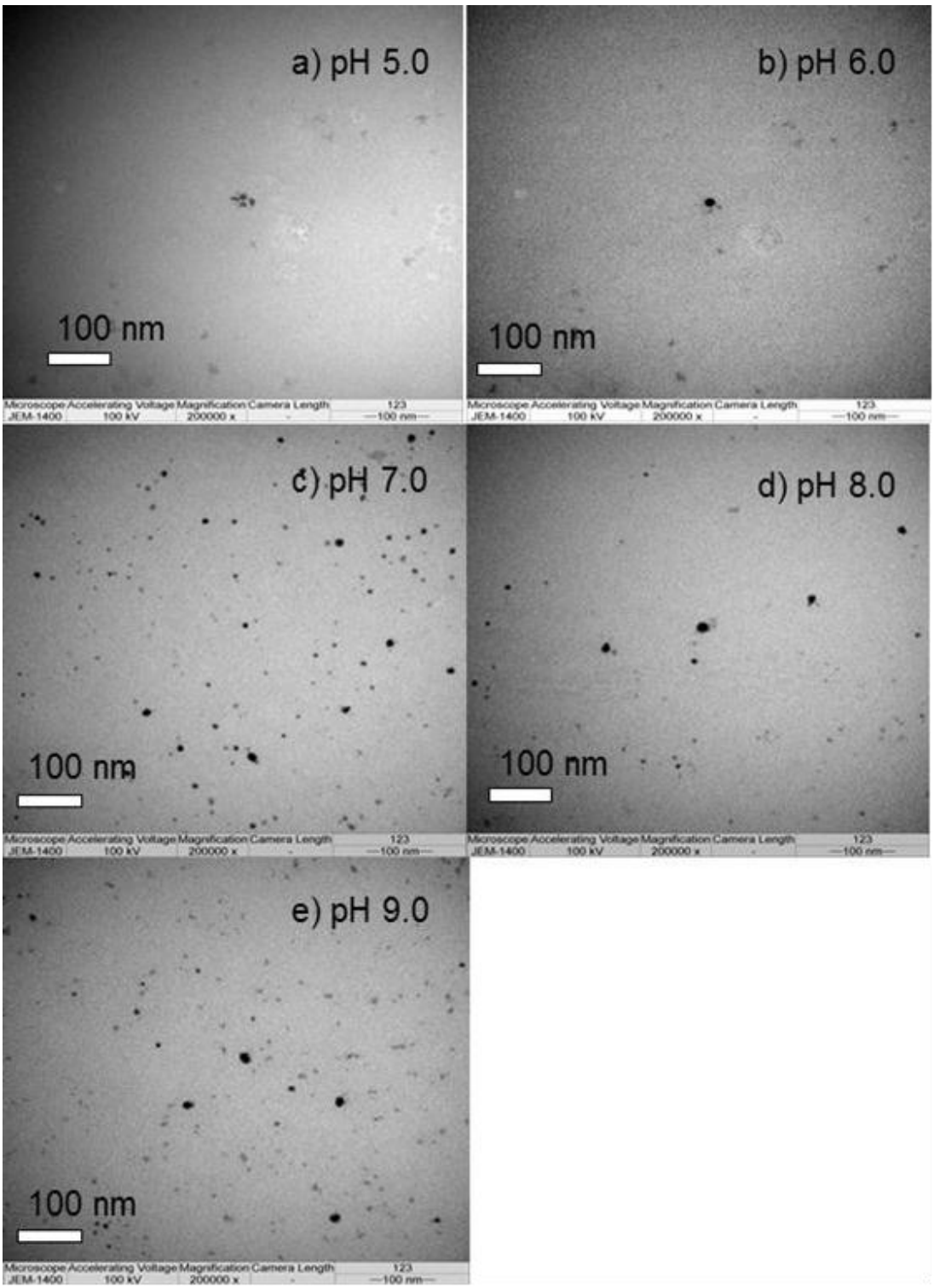

Figure 4.27 TEM images of PMA-stabilized silver nanoparticles synthesized using different initial pH of PMA solution and molar ratio of PMA to silver ions at 1:1

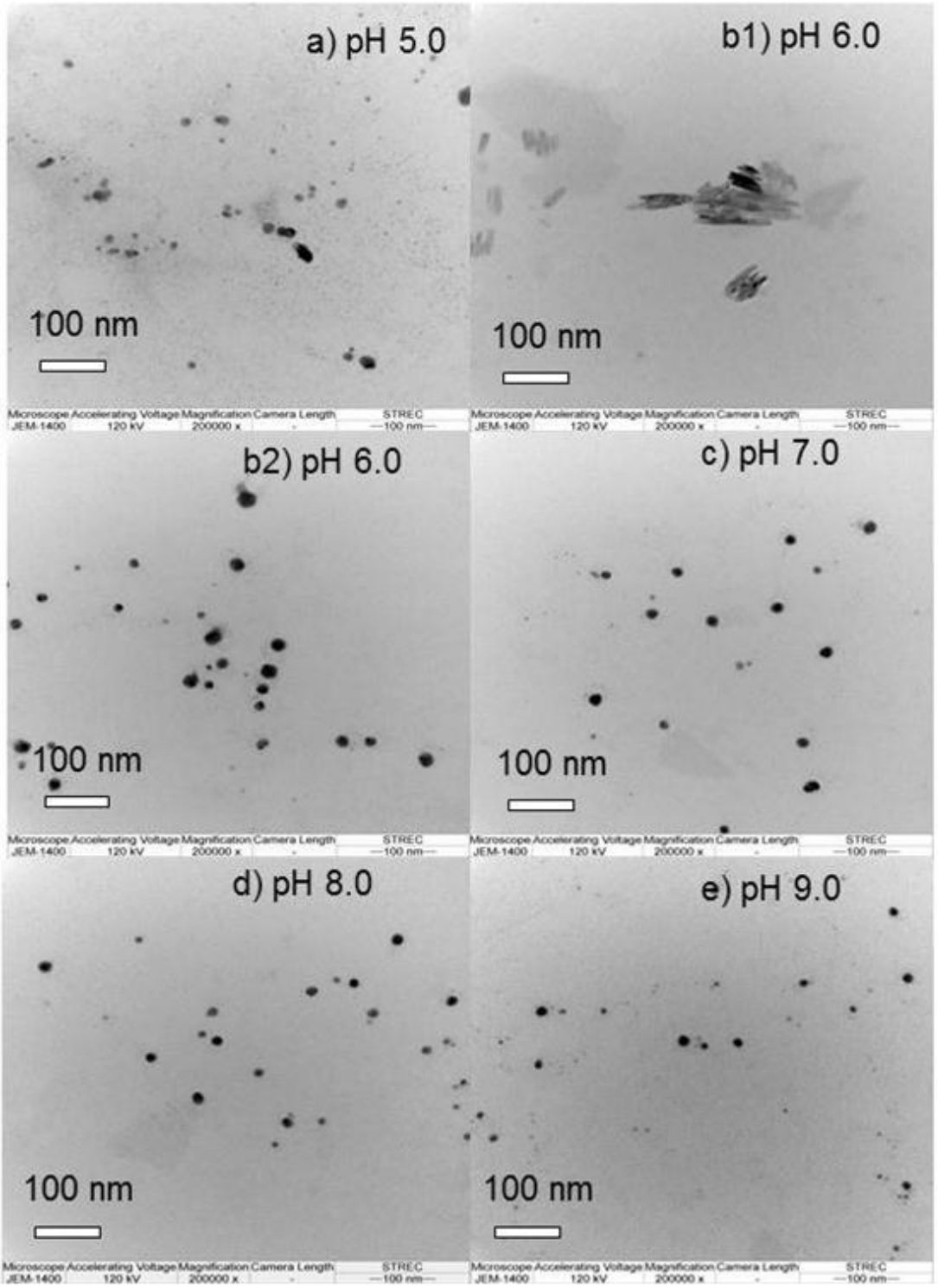

Figure 4.28 TEM images of PMA-stabilized silver nanoparticles synthesized using different initial pH of PMA solution and molar ratio of PMA to silver ions at 1:10

Dubas, S. T. and coworker [4] reported that the purple colloids of PMA-stabilized silver nanoparticles was due to the incomplete reduction of silver ions which perturbed the dielectric surround of the nanoparticles. The unreacted silver ions can interact with carboxylic groups (COO^-) on the surface of the nanoparticles and form Ag^+/COO^- complex. Then this nanoparticles colloid was justified by the less hydrophilic environment due tothe complex formation. This resulted in red shifted of the absorbance spectrum to 501 nm instead of 456-461 nm. However, the synthesized silver nanoparticles were showed two types of particles which were spherical and rod-like particles. While Dubas reported only spherical with largest diameter of 10 nm. This is probably due to different in synthesis condition. Moreover, it was showed that with the Dubas's condition, there was higher amount of silver nanoparticles formation.

4.2.3 Stability

The stability of PMA-stabilized silver nanoparticles was observed after stored for one month at room temperature. It is shown in Figure 4.29 that the color of silver nanoparticles colloids synthesized using MR of 10:1 changed to pale yellow with sediment at the bottom, after stored for one month except for that synthesized using pH of 5.0. These results were confirmed by UV-Vis spectra as shown in Figure 4.30. In this figure, every sample showed lower absorption spectra and the characteristic peaks of silver nanoparticles disappeared after stored for one month except for that synthesized using pH of 5.0. This suggests that with MR of 10:1, silver nanoparticles showed low stability. They agglomerated into bigger particles and sank down as sediment as shown in Figure 4.28 a). On the other hand, at pH of 5.0, the reduction rate was very slow by the acid dissociation equilibrium [84]; consequently, the reduction still occurred during storage.

For MR of 1:1, after stored for one month, silver nanoparticles were darker in every condition as shown in Figure 4.31 b2). These results confirmed with the UV-Vis spectra as shown in Figure 4.31. All UV-Vis spectra showed that every samples presented higher absorbance spectra after stored for one month and the characteristic peaks appeared after stored for one month in the range of 409-414 nm in all samples excepted those from initial pH of PMA at 5.0 condition. This was probably due to with less amount of PMA at MR of 1:1, made reduction of silver ions slower than MR 10:1 condition. After one hour UV radiation, there were silver ions left in the system. Then they were continuously reduced during storage. However, UV-Vis spectra results showed that with MR 1:10, there were higher amount of silver nanoparticles formed than MR 1:1 as shown in Figure 4.32. This was probably due to in the case that less amount of PMA allowed better mobility of PMA chain to react with silver ions. Then the reduction rate was faster than in MR 1:1. However, in pH of 5.0 and 6.0, the reduction rates were very slow resulting in the formation of bigger particles in these two conditions.

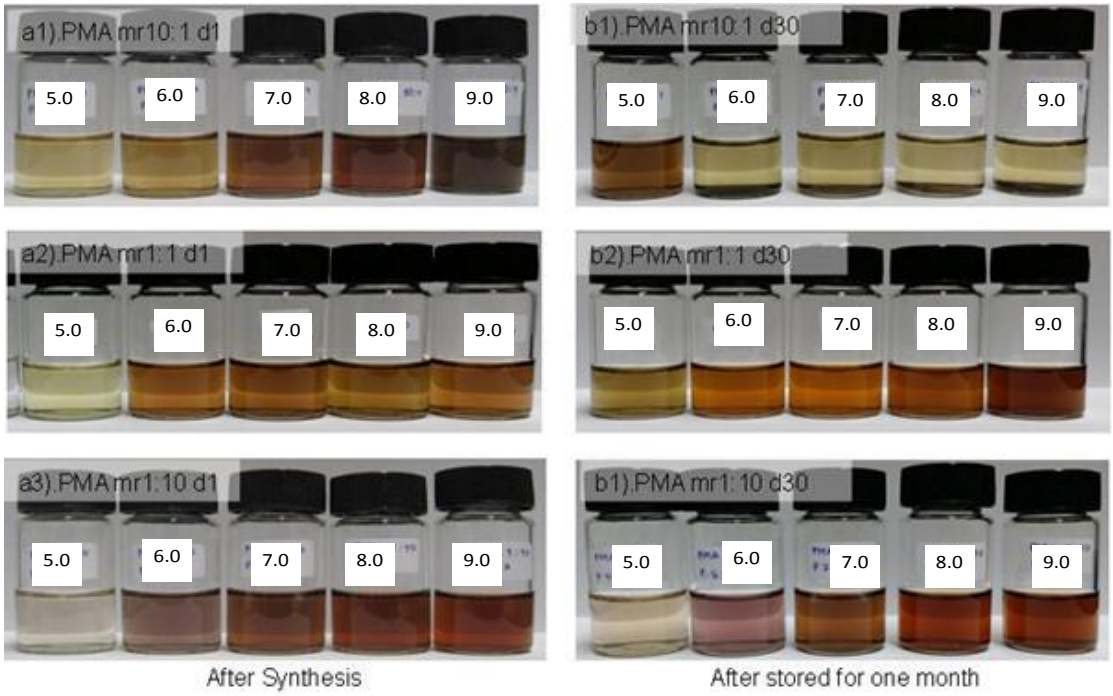

Figure 4.29 Appearances of PMA-stabilized silver nanoparticles colloids after synthesis and after stored for one month

In the case of MR of 1:10, after stored for one month, no sediment was observed and the color of the colloids looked almost the same. These results confirmed by UV-Vis spectra as shown in Figure 4.32. The samples of pH of 5.0 and 6.0 exhibited not much different in absorption spectra after stored for one month. However, the characteristic peaks of the samples synthesized with initial pH of PMA at 7.0, 8.0 and 9.0 shifted to the shorter wavelength from 461, 458 and 456 to 420, 417 and 418, respectively. It was showed that at this MR, the silver nanoparticles colloids synthesized with initial pH of PMA at 6.0 showed light purple color which was different to the others.

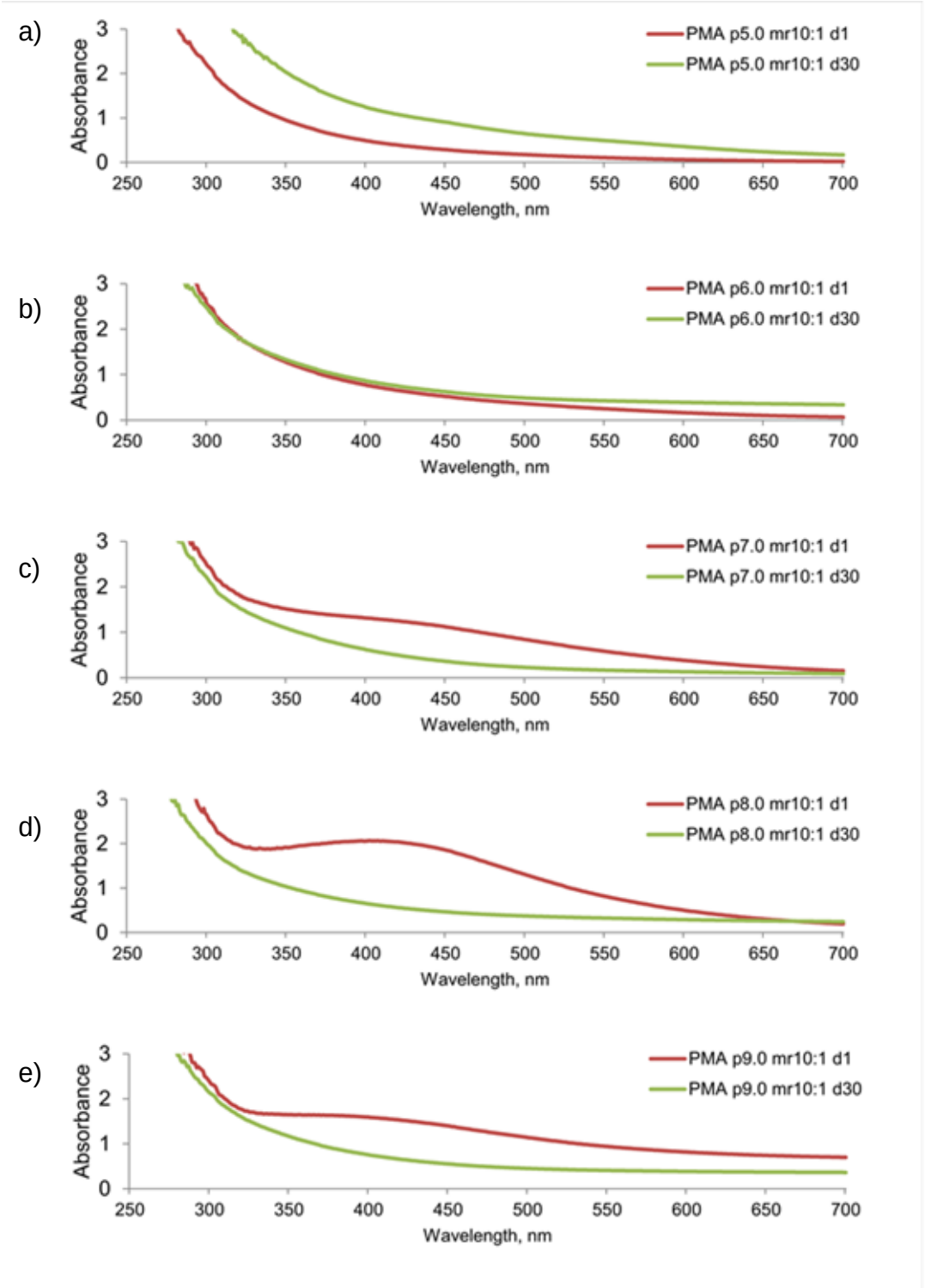

Figure 4.30 UV-Vis spectra of PMA-stabilized silver nanoparticles colloids synthesized using molar ratio of PMA to silver ions at 10:1 after synthesis and after stored for one month

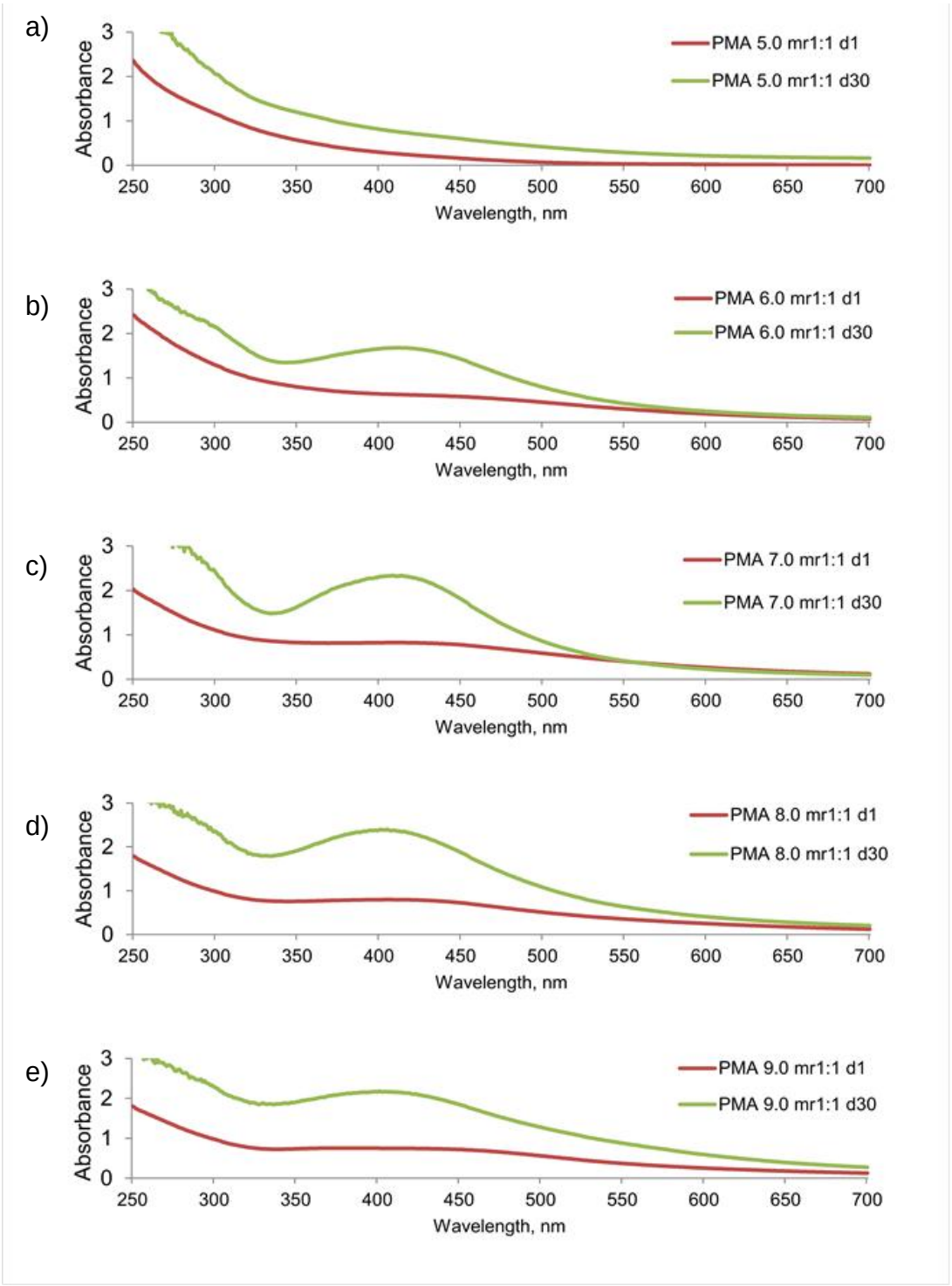

Figure 4.31 UV-Vis spectra of PMA-stabilized silver nanoparticles colloids synthesized using molar ratio of PMA to silver ions at 1:1 after synthesis and after stored for one month

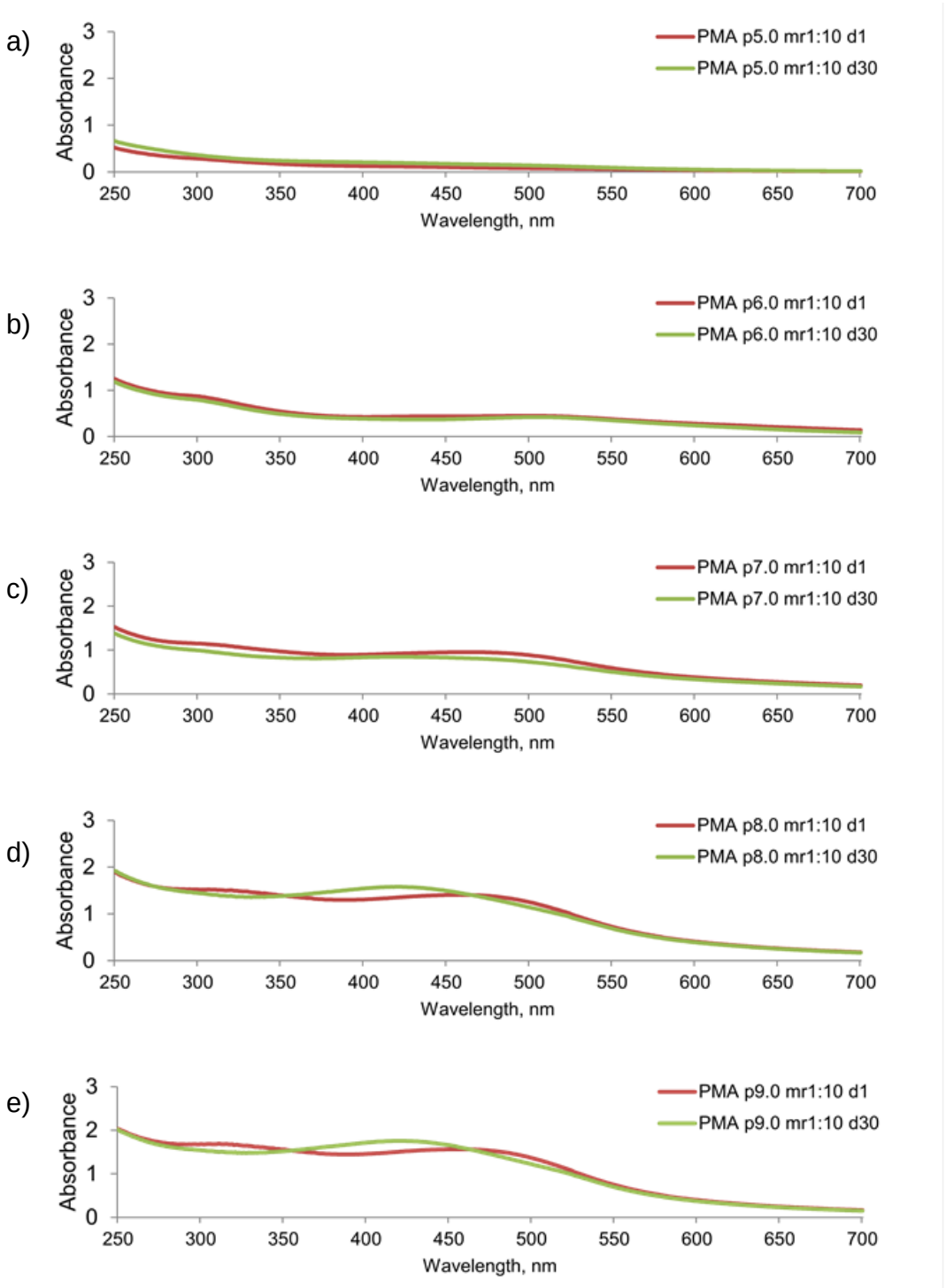

Figure 4.32 UV-Vis spectra of PMA-stabilized silver nanoparticles colloids synthesized using molar ratio of PMA to silver ions at 1:10 after synthesis and after stored for one month

4.3 Characteristics of silver nanoparticles stabilized by carboxymethyl cellulose, sodium salt

Due to high molecular weight of CMC (MW of CMC =90,000), large amount of CMC was needed to make the solutions with the concentrations of 1.0 and 10.0 mM (9 g per 100 ml and 90 g per 100 ml). As shown in Figure 4.33, 1.0 mM of CMC solution appears as a gel-like as it can hold air bubble in its high viscous solution compared to that of 0.1 mM. Moreover, there was incompletely dissolved CMC in the mixture as shown in Figure 4.34. Only CMC concentration of 0.1 mM can be completely dissolved into its aqueous solution. Therefore, only MR of 1:10 was used in the synthesis of silver nanoparticles using CMC solution.

Figure 4.33 Appearances of 1.0 and 0.1 mM of carboxymethyl cellulose, sodium salt solutions

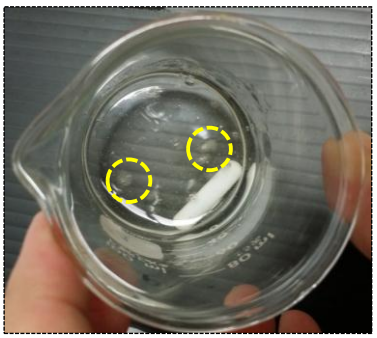

Figure 4.34 Appearance of incompletely dissolved CMC in 1.0 mM of carboxymethyl cellulose, sodium salt in aqueous solution

4.3.1 Optical characteristics

4.3.1.1 Effect of initial pH of carboxymethyl cellulose sodium salt solution

It is clearly seen from Figure 4.35 that there was less evidence representing the formation of silver nanoparticles in the synthesis since all mixtures have very pale color. However, UV-Vis absorption spectra shown in Figure 4.36 indicate that there were some silver nanoparticles formed. The summary of the peak positions are given in Table 4.3.

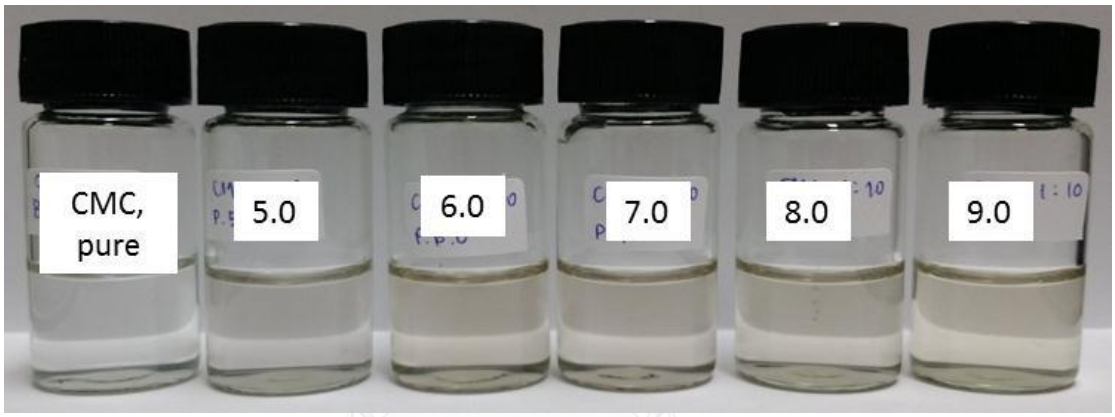

Figure 4.35 Appearances of silver nanoparticles colloids synthesized using different initial pH of CMC solution and molar ratios of CMC to silver ions at 1:10

UV-Vis absorption spectra exhibit very broaden peaks in the samples synthesized using initial pH of CMC solutions at 5.0, 6.0 and 7.0. This indicates that those nanoparticles were non-uniform with bigger particles than the other two conditions. On the other hand, at pH of CMC solutions at 8.0 and 9.0, UV-Vis absorbance peaks which respectively occur at 430-590 and 430-515 nm were narrower.

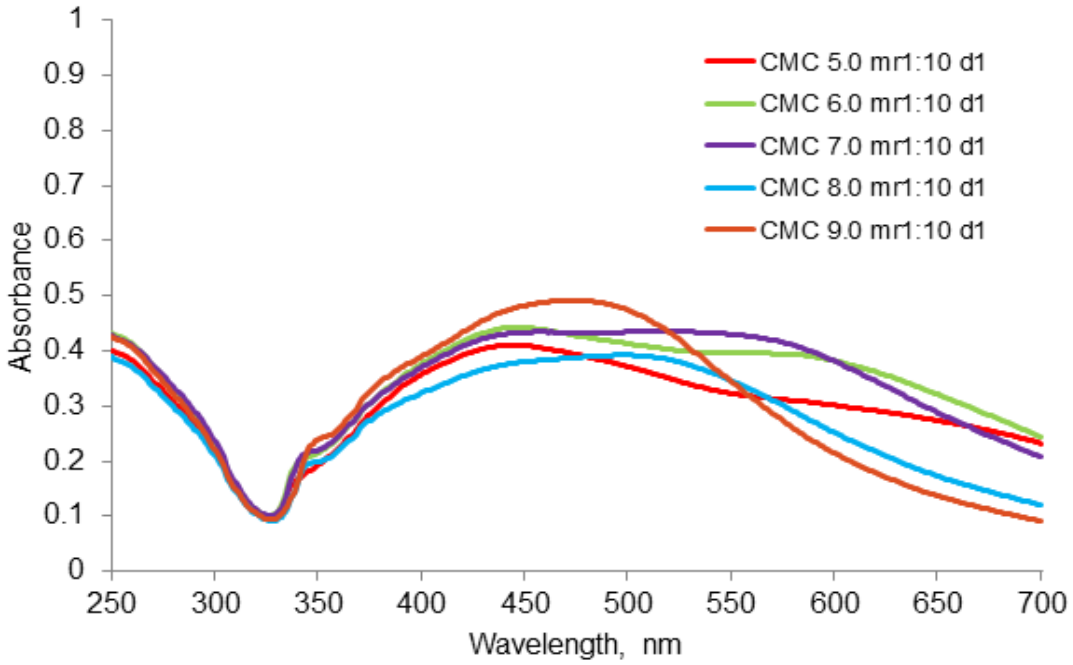

Figure 4.36 UV-Vis spectra of silver nanoparticles colloids synthesized using different initial pH of CMC solution and molar ratio of CMC to silver ions at 1:10

Table 4.3 Positions of UV-Vis spectra of the silver nanoparticles synthesized using different initial pH of CMC solution and molar ratio of CMC to silver ions at 1:10

Peak position (Wavelength, nm)	pH 5.0	pH 6.0	pH 7.0	pH 8.0	pH 9.0
MR 1:10	444 Broaden pk	581 Broaden pk	461 Broaden pk	430-590 Broaden pk	472

4.3.1.2 Role of UV radiation in the synthesis

From Figures 4.37 and 4.38, It can be seen that without UV radiation, CMC can slightly reduce very little amount of silver ions to form silver nanoparticles. Less formation of silver nanoparticles was observed for dark and natural light condition with the initial pH of CMC solution at 8.0. However, upon exposure to

UV radiation, there is the characteristic peak of silver nanoparticles appearing in the spectra with broaden peak having the maximum peak at 450 nm.

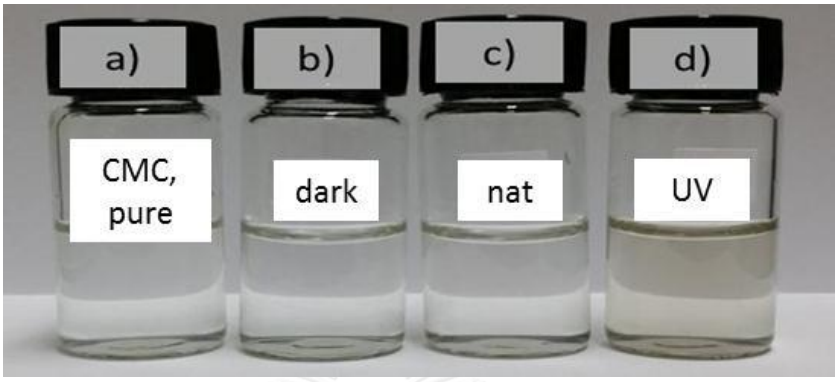

Figure 4.37 Appearances of CMC-stabilized silver nanoparticles colloids synthesized at pH of 8.0 using different light sources: a) pure CMC solution, b) at dark, c) natural light (indoor) and d) UV lamp

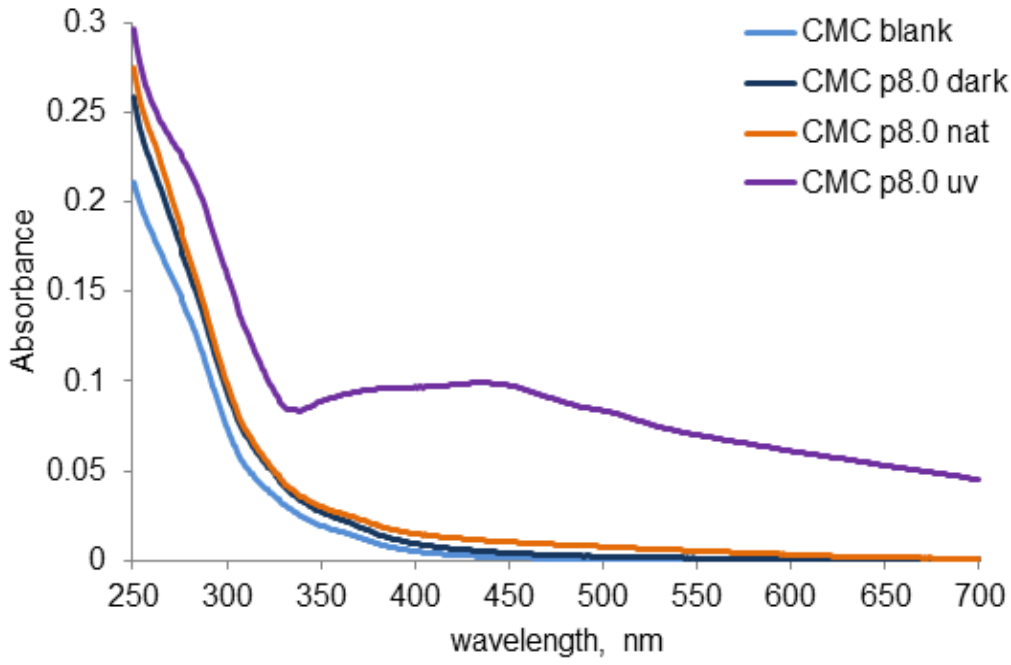

Figure 4.38 UV-Vis spectra of CMC-stabilized silver nanoparticles colloids synthesized at pH of 8.0 using different light sources: a) pure CMC solution, b) at dark, c) natural light (indoor) and d) UV lamp

The reduction mechanism can be explained as follows. CMC can reduce very small amount of silver ions by itself. It is probably due to the fact that CMC is cellulose derivatives. The aldehyde end groups are reductive site for silver ions, and the presence of aldehyde group can be occurred by two paths. The first path can be occurred by the acid hydrolysis to form open-chain end structure that contained aldehyde end groups [89]. The second path can be explained with lower molecular weight cellulose and also amorphous part consists of hemicellulose which is weak and easily hydrolyzed by dilute acid or base [90]. Hemicellulose are composed of xylose as major component [90]. Xylose is one of glucose structure with aldehyde functional group [90].

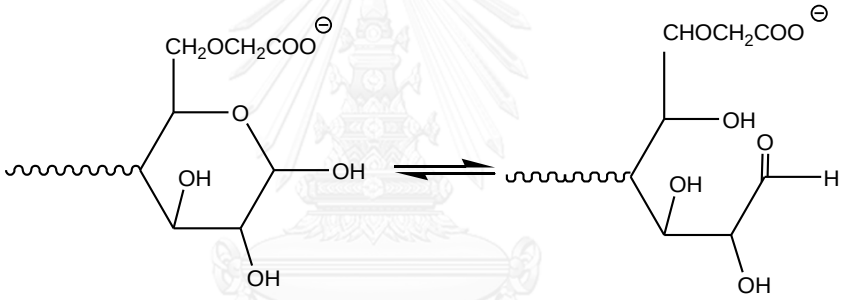

However, the maximum absorbance of the dark condition was very low compared to the absorbance of UV radiation condition. This can be concluded that UV radiation promotes the reduction of silver ions to silver atom in the synthesis of CMC-stabilized silver nanoparticles.

4.3.2 Morphology

Figure 4.39 shows TEM images of CMC-stabilzed silver nanoparticles. The results confirm that there were silver nanoparticles occurred in all conditions. However, there were less amount of silver nanoparticles than the silver nanoparticles synthesis in the presence of TA and PMA even the same method was used. Moreover, TEM images show that nanoparticles synthesized using initial pH of CMC at 5.0, 6.0 and 7.0 are non-uniform and have larger particles compared to those obtained from other two conditions. There were triangonal plate and spherical nanoparticles. Previous work suggested that the slow rate growth of the silver nanoparticles yield non-uniform and nano plate particles [44]. In addtion, TEM images confirm the UV-Vis results that silver nanoparticles synthesized with initial pH of CMC at 8.0 and 9.0 were more uniform, spherical and smaller particles than the others. Those two conditions yielded the spherical silver nanoparticles which suggested that elevated initial pH of CMC solution to alkali condition, reduced silver ions faster than the others.

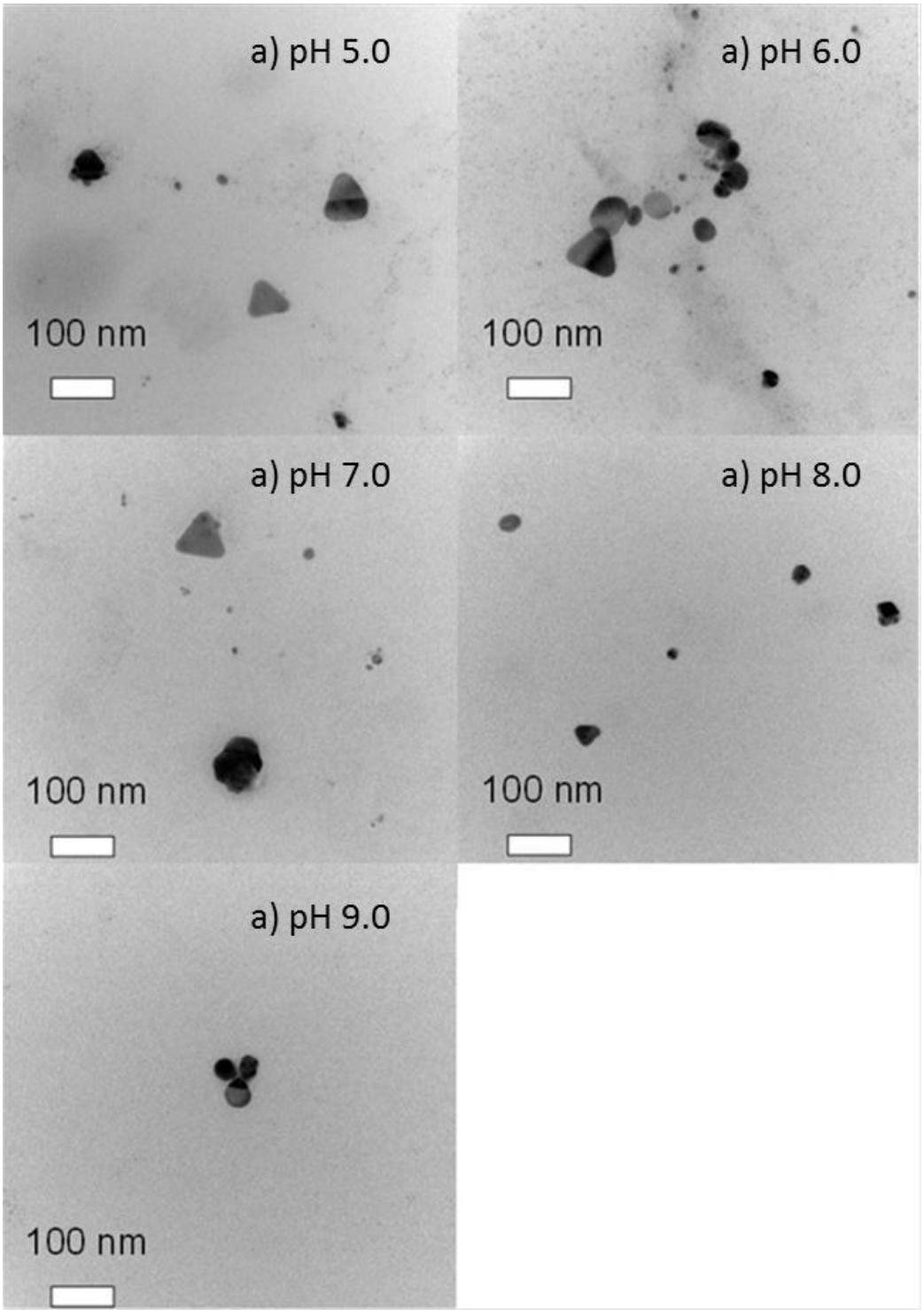

Figure 4.39 TEM images of CMC-stabilized silver nanoparticles synthesized using different initial pH of CMC solution and molar ratio of CMC to silver ions at 1:10

4.3.3 Stability

The stability of the synthesized silver nanoparticles was observed after stored for one month at room temperature. As shown in Figure 4.40, CMC-stabilized silver nanoparticles colloids synthesized using initial pH of CMC at 7.0, 8.0 and 9.0, changed from very pale color to darker yellow, as the pH of CMC elevated, after storage. This indicates the continuous reduction of silver ions into silver nanoparticles.

On the other hand, samples synthesized using initial pH of CMC at 5.0 and 6.0 were not changed much. This may be because at low pH condition, CMC dissociated into anionic species less than at higher pH due to the acid dissociation equilibrium [91]. Neutral form of CMC has slower reduction rate than the dissociated form then after one month storage, the sample of pH at 5.0 and 6.0 showed less change in color than those of higher pH conditions. These observations can be confirmed by UV-Vis spectra as shown in Figure 4.41. The intensities of the characteristic peaks of silver nanoparticles increase with increasing pH value.

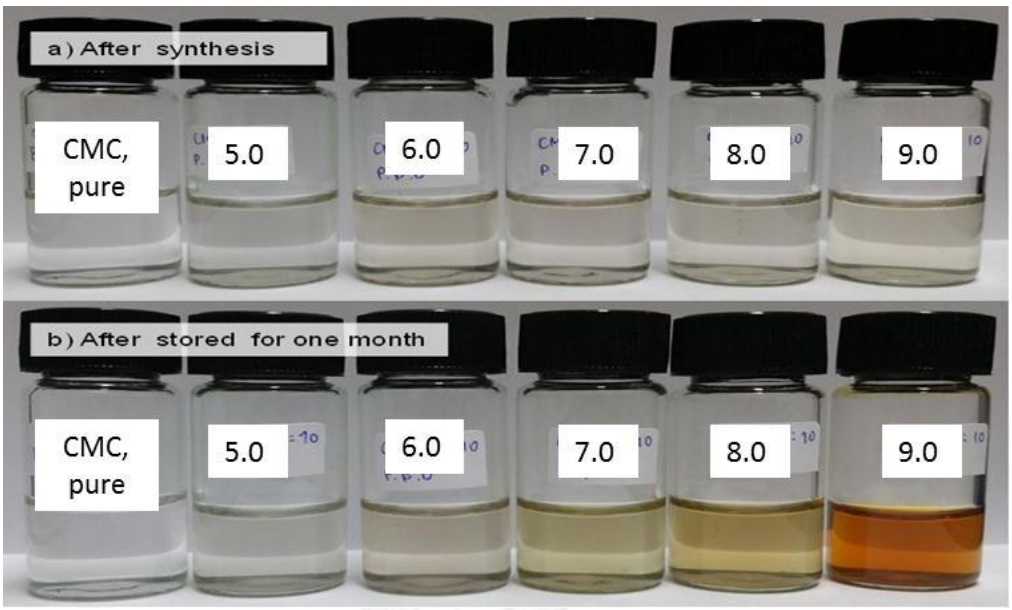

Figure 4.40 Appearances of CMC-stabilized silver nanoparticles colloids synthesized using molar ratio of CMC to silver ions at 1:10 after synthesis and after stored for one month

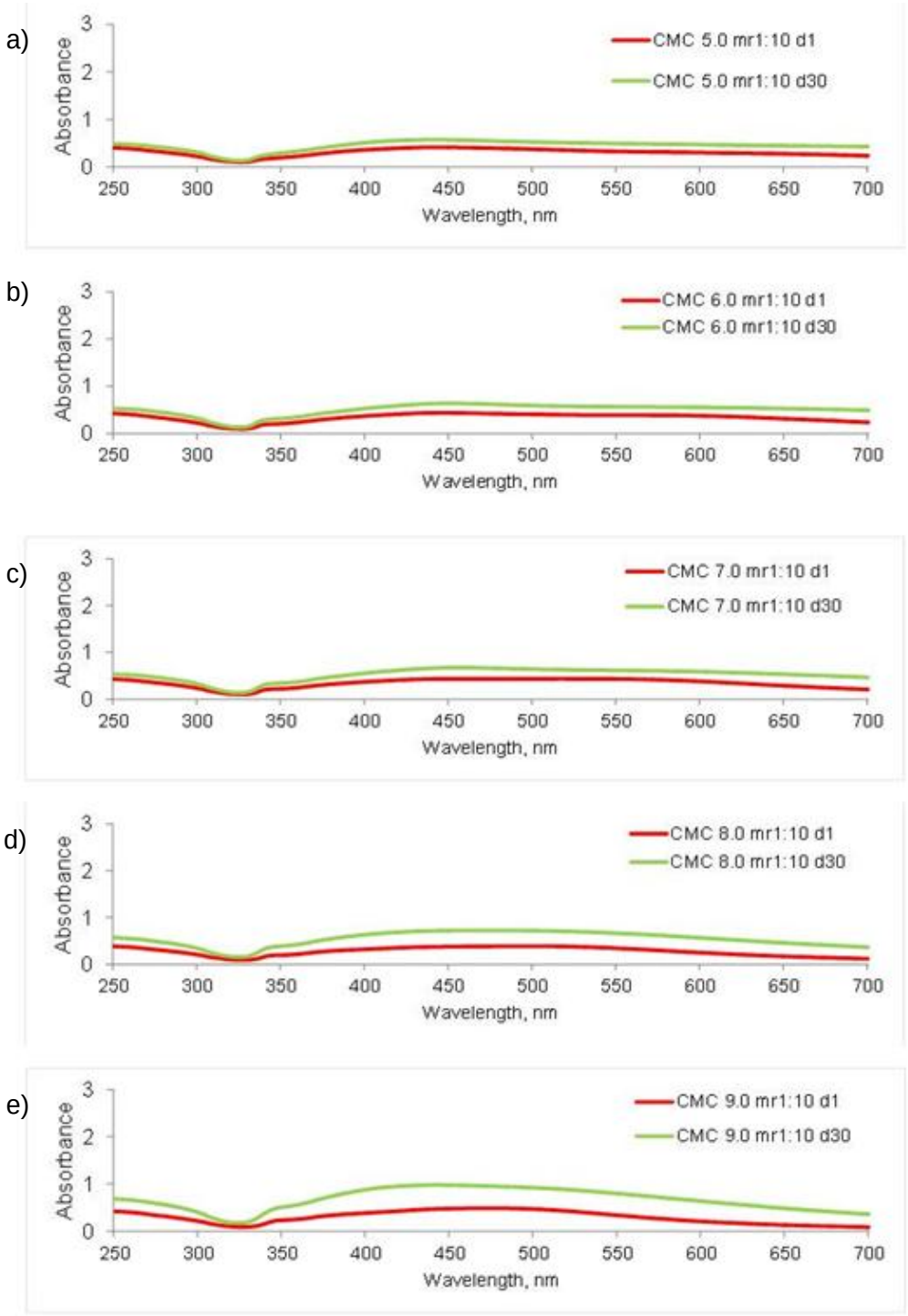

Figure 4.41 UV-Vis spectra of CMC-stabilized silver nanoparticles colloids synthesized using molar ratio of CMC to silver ions at 1:10 after synthesis and after stored for one month

4.4 Characteristics of silver nanoparticles stabilized by chitosan

Chitosan (CS) is readily soluble in dilute acidic solution below pH of 6.0. It is considered as a strong base since it has primary amino groups with pKa value of 6.3 [57]. At acidic condition, the amines are protonated and become positively charged making CS to be water-soluble cationic polyelectrolytes. On the other hand, if pH is above 6.0, deprotonation of these amine groups occurs causing CS to lose its charge and become insoluble [57]. Therefore, in this research, only pH of 5.0 and 6.0 were used to study because CS was completely dissolved as shown in Figure 4.42 a). In addition, due to high molecular weight of CS used in this research, only MR of 1:10 was employed.

Figure 4.43 shows that only the sample synthesized using pH of 5.0 showed significant in color change as a result of silver nanoparticles formation whereas at pH of 6.0, no evidence of silver nanoparticles formed after 1 hour of UV radiation. It can be explained that why CS did not reduce silver ions at pH of 6.0, because chitosan acted like a strong base. Its pKa is around 6.3 [57], then at pH of 6.0 chitosan probably was less protonated than pH of 5.0. Moreover, it was observed that at pH of 5.0, the samples exhibited the color change from colorless to purple and then brown-greyish color as shown in Figure 4.44. This may be due to its long chain structure that can cause the difficulty in the reduction as it slow down the reduction rate. For this reason, the formation of silver nanoparticles stabilized with CS was observed as a function of the radiation time as shown in Figure 4.44.

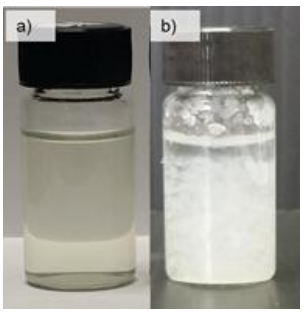

Figure 4.42 Appearance of 0.1 mM of chitosan in 1.0 % v/v of acetic acid solutions at pH of a) 6.0 and b) 7.0

Figure 4.43 Appearances of silver nanoparticles colloids synthesized using initial pH of chitosan at 5.0 (left), and 6.0 (right) after UV radiation for one hour

4.4.1 Optical characteristics

4.4.1.1 Effect of radiation time

Figure 4.44 shows the silver nanoparticle colloids synthesized using 0.1 mM CS in 1.0 % v/v acetic acid solution at initial pH of CS solution of 5.0 at various radiation times of 1, 2, 4, 8, 15, 20, 25, 30, 40, 50 and 60 minutes. It can be seen that CS-stabilized silver nanoparticles were formed right after UV radiation as the color of mixture changed from colorless to purple. Then after 20 minutes of radiation, its color changed to greyish color as shown in Figure 4.44. Their UV-Vis spectra given in Figure 4.45 show that the purple silver nanoparticles have the characteristic peaks around 490-518 nm. However, after UV radiation for 8 minutes the spectra shows

broaden curved from 330-700 nm. These results confirmed the appearance in greyish color observed above.

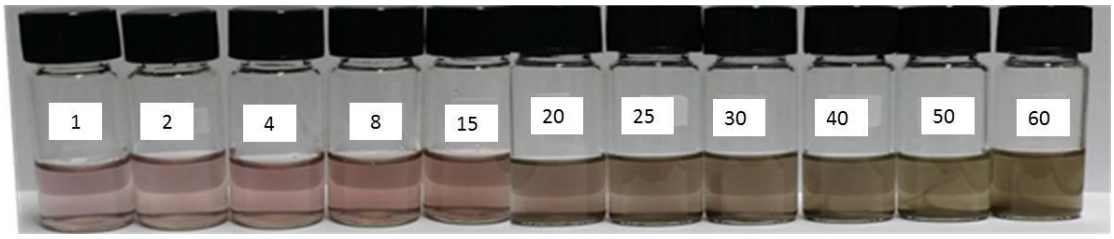

Figure 4.44 Appearances of silver nanoparticles colloids synthesized using 0.1 mM CS in 1.0 % v/v acetic acid solution at initial pH of 5.0 at various radiation times of 1, 2, 4, 8, 15, 20, 25, 30, 40, 50 and 60 minutes

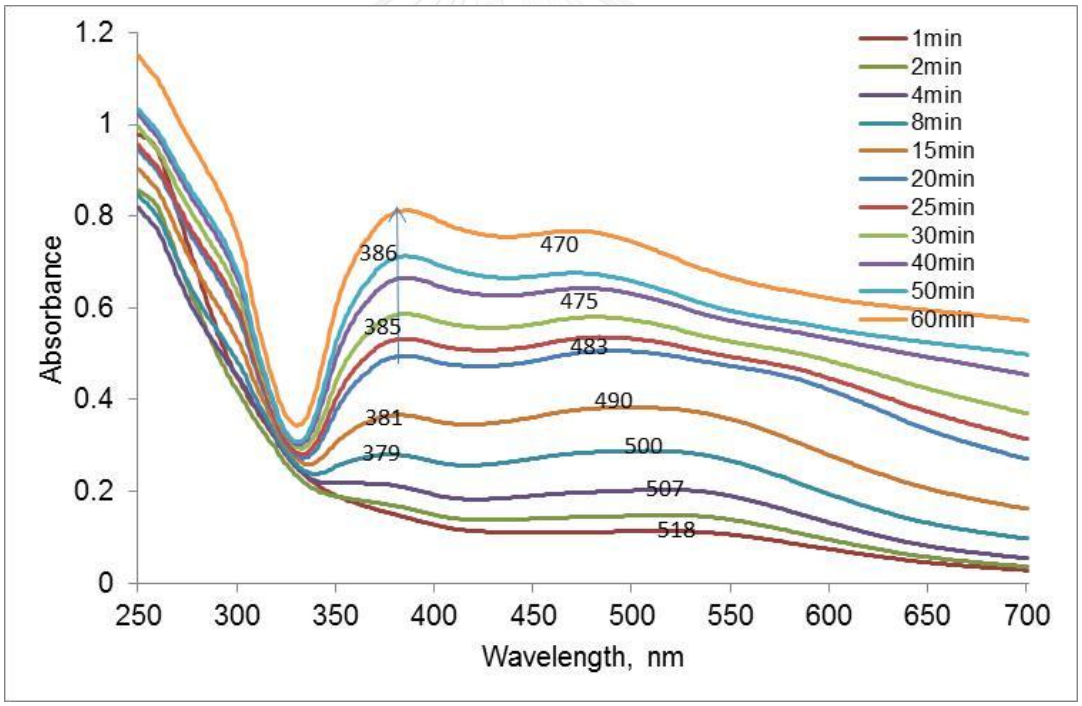

Figure 4.45 UV-Vis spectra of silver nanoparticles colloids synthesized using 0.1 mM CS in 1.0 % v/v acetic acid solution at initial pH of 5.0 at various radiation times of 1, 2, 4, 8, 15, 20, 25, 30, 40, 50 and 60 minutes

4.4.1.2 Role of UV radiation in the synthesis

Figure 4.46 shows that without UV radiation, CS can reduce little amount of silver ions to form silver nanoparticatles by itself. However, there is no characteristic peak ofsilver nanoparticles shown in its spectrum as shown in Figure 4.47. CS is also known as polysaccharide biopolymer. It has same backbone as CMC. Then one reducing mechanism of CS was the aldehyde functional group at the open chain ends of the glucose unit same as CMC mechanism. Another mechanism was due to the reduction of silver ions to silver atom assisted by UV radiation reduced [87, 92].

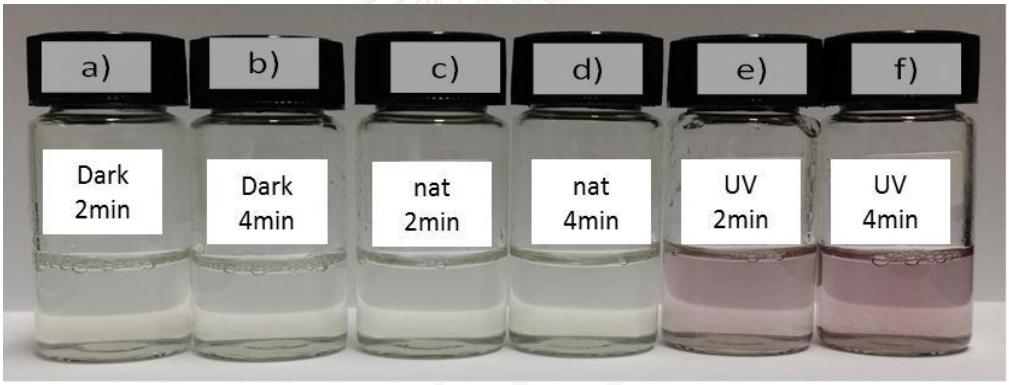

Figure 4.46 Appearances of CS-stabilized silver nanoparticles colloids synthesized at pH of 5.0 using different light sources: a) at dark for 2 min, b) at dark for 4 min, c) natural light for 2 min, d) natural light for 4 min, e) UV lamp for 2 min and f) UV lamp for 4 min

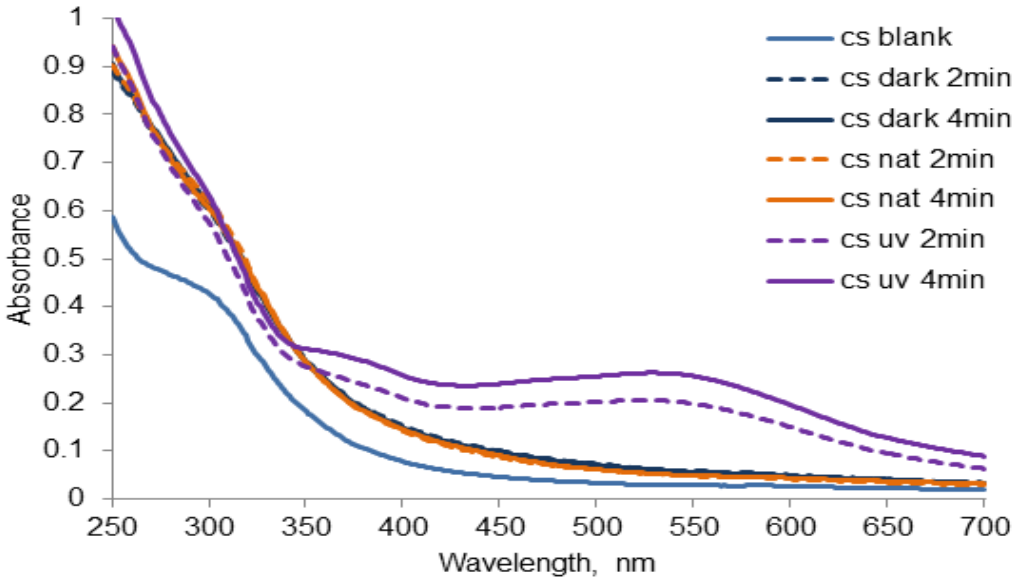

Figure 4.47 UV-Vis spectra of CS-stabilized silver nanoparticles colloids synthesized at pH of 5.0 using different light sources: a) at dark for 2 min, b) at dark for 4 min, c) natural light for 2 min, d) natural light for 4 min, e) UV lamp for 2 min and f) UV lamp for 4 min

4.4.2 Morphology

From UV-Vis spectroscopic results, in order to choose one sample to analyze with TEM, two criteria for selecting were: it showed the characteristic peak of the purple silver nanoparticles, and it had less agglomeration of the nanoparticles (lower absorbance intensities on the right hand side of the characteristic peak) or size distribution of the nanoparticles was more uniform. Therefore, the sample synthesized using 2 minutes of radiation time was selected to analyze with TEM and the results were shown in Figure 4.48.

It can be seen from this figure that in the same sample, there were two shapes of silver nanoparticles. These results confirmed UV-Vis absorbance spectra that there were two characteristic peaks at 370 and 507 nm. The former represents the spherical particles and the latter represents the rod-like particles. Similar rod-like shape was also found in PMA- stabilized silver nanoparticles (MR of 1:10, pH of 6.0) which exhibited purple color and the characteristic peak around 501 nm.

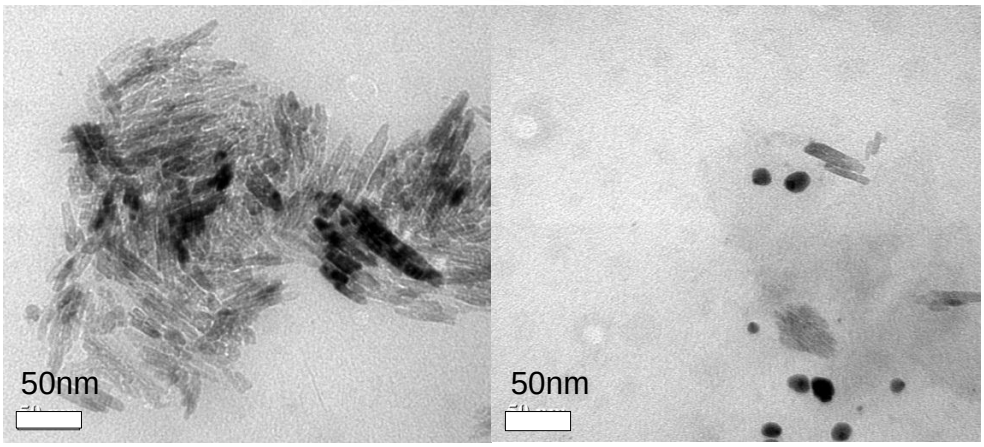

Figure 4.48 TEM images of CS-stabilized silver nanoparticles colloids synthesized using 0.1 mM CS in 1.0 % v/v acetic acid solution at initial pH of 5.0 and radiation time of 2 minutes

4.4.3 Stability

The stability of the synthesized silver nanoparticles was performed with the same procedure as was done in section of TA-stabilized silver nanoparticles. Figure 4.49 shows the appearance of the obtained nanoaparticles after one month storage. Figure 4.50 shows that after stored for one month, the intensity of the absorption spectra increase compared to those of after synthesis. The most different spectra after stored for one month were observed from the sample exposed to 1.0 min of UV radiation because it had highest amount of silver ions left in the mixture that can undergo the reduction after radiation was stopped.

Figure 4.49 Appearances of CS-stabilized silver nanoparticles colloids synthesized using 0.1 mM CS in 1.0 % v/v acetic acid solution at initial pH of 5.0 at various radiation times of 1, 2, 4, 8, 15, 20, 25, 30, 40, 50 and 60 minutes after synthesis and after stored for one month

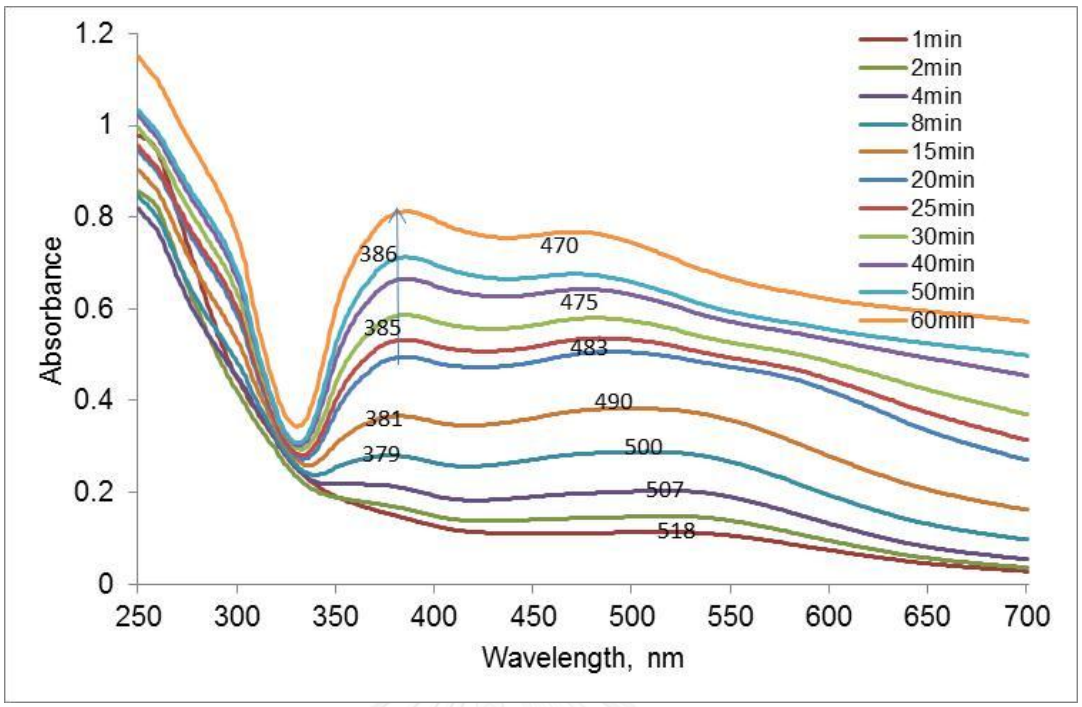

Figure 4.50 UV-Vis spectra of silver nanoparticles colloids synthesized using 0.1 mM CS in 1.0 % v/v acetic acid solution at initial pH of 5.0 at various radiation times of 1, 2, 4, 8, 15, 20, 25, 30, 40, 50 and 60 minutes

4.4.1.2 Role of UV radiation in the synthesis

Figure 4.46 shows that without UV radiation, CS can reduce little amount of silver ions to form silver nanoparticatles by itself. However, there is no characteristic peak of silver nanoparticles shown in its spectrum as shown in Figure 4.47. CS is also known as polysaccharide biopolymer. It has same backbone as CMC. Then one reducing mechanism of CS was the aldehyde functional group at the open chain ends of the glucose unit same as CMC mechanism. Another mechanism was due to the reduction of silver ions to silver atom assisted by UV radiation reduced [87, 92].

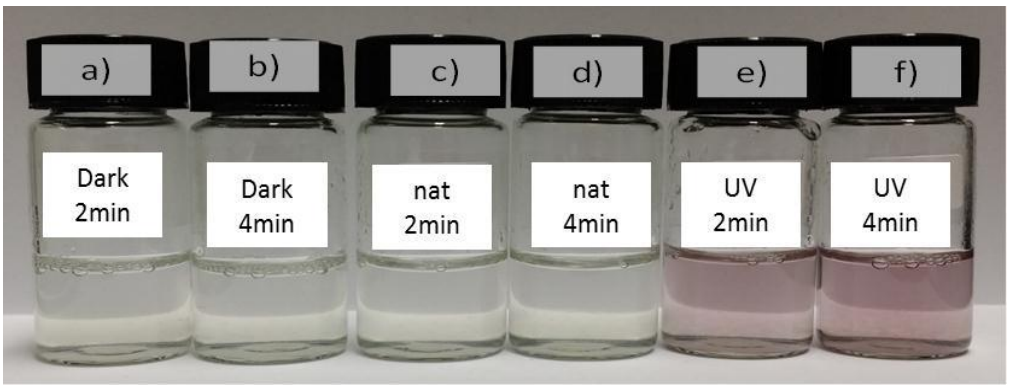

Figure 4.51 Appearances of CS-stabilized silver nanoparticles colloids synthesized at pH of 5.0 using different light sources: a) at dark for 2 min, b) at dark for 4 min, c) natural light for 2 min, d) natural light for 4 min, e) UV lamp for 2 min and f) UV lamp for 4 min

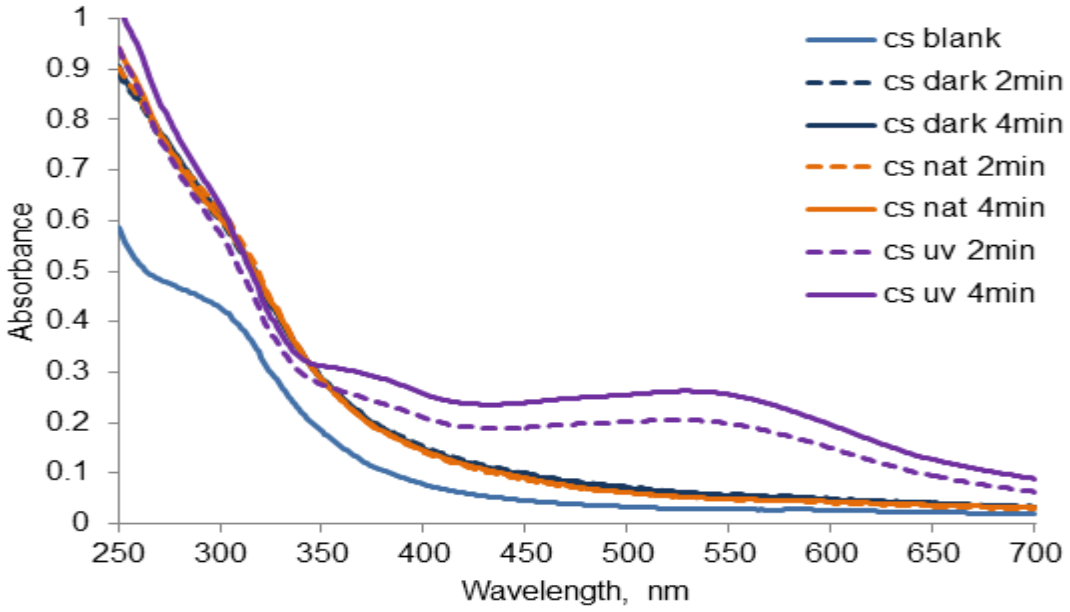

Figure 4.52 UV-Vis spectra of CS-stabilized silver nanoparticles colloids synthesized at pH of 5.0 using different light sources: a) at dark for 2 min, b) at dark for 4 min, c) natural light for 2 min, d) natural light for 4 min, e) UV lamp or 2 min and f) UV lamp for 4 min

4.4.2 Morphology

From UV-Vis spectroscopic results, in order to choose one sample to analyze with TEM, two criteria for selecting were: it showed the characteristic peak of the purple silver nanoparticles, and it had less agglomeration of the nanoparticles (lower absorbance intensities on the right hand side of the characteristic peak) or size distribution of the nanoparticles was more uniform. Therefore, the sample synthesized using 2 minutes of radiation time was selected to analyze with TEM and the results were shown in Figure 4.48.

It can be seen from this figure that in the same sample, there were two shapes of silver nanoparticles. These results confirmed UV-Vis absorbance spectra that there were two characteristic peaks at 370 and 507 nm. The former represents the spherical particles and the latter represents the rod-like particles. Similar rod-like shape was also found in PMA- stabilized silver nanoparticles (MR of 1:10, pH of 6.0) which exhibited purple color and the characteristic peak around 501 nm.

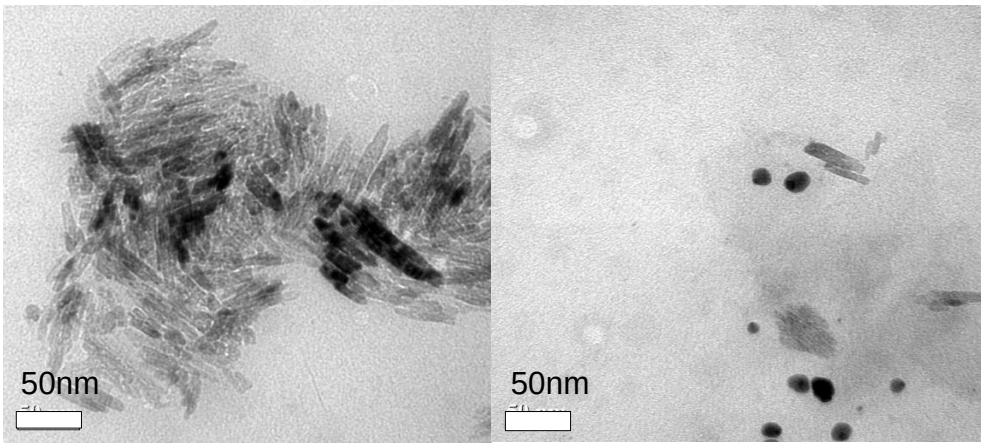

Figure 4.53 TEM images of CS-stabilized silver nanoparticles colloids synthesized using 0.1 mM CS in 1.0 % v/v acetic acid solution at initial pH of 5.0 and radiation time of 2 minutes

4.4.3 Stability

The stability of the synthesized silver nanoparticles was performed with the same procedure as was done in section of TA-stabilized silver nanoparticles. Figure 4.49 shows the appearance of the obtained nanoaparticles after one month storage. Figure 4.50 shows that after stored for one month, the intensity of the absorption spectra increase compared to those of after synthesis. The most different spectra after stored for one month were observed from the sample exposed to 1.0 min of UV radiation because it had highest amount of silver ions left in the mixture that can undergo the reduction after radiation was stopped.

Figure 4.54 Appearances of CS-stabilized silver nanoparticles colloids synthesized using 0.1 mM CS in 1.0 % v/v acetic acid solution at initial pH of 5.0 at various radiation times of 1, 2, 4, 8, 15, 20, 25, 30, 40, 50 and 60 minutes after synthesis and after stored for one month

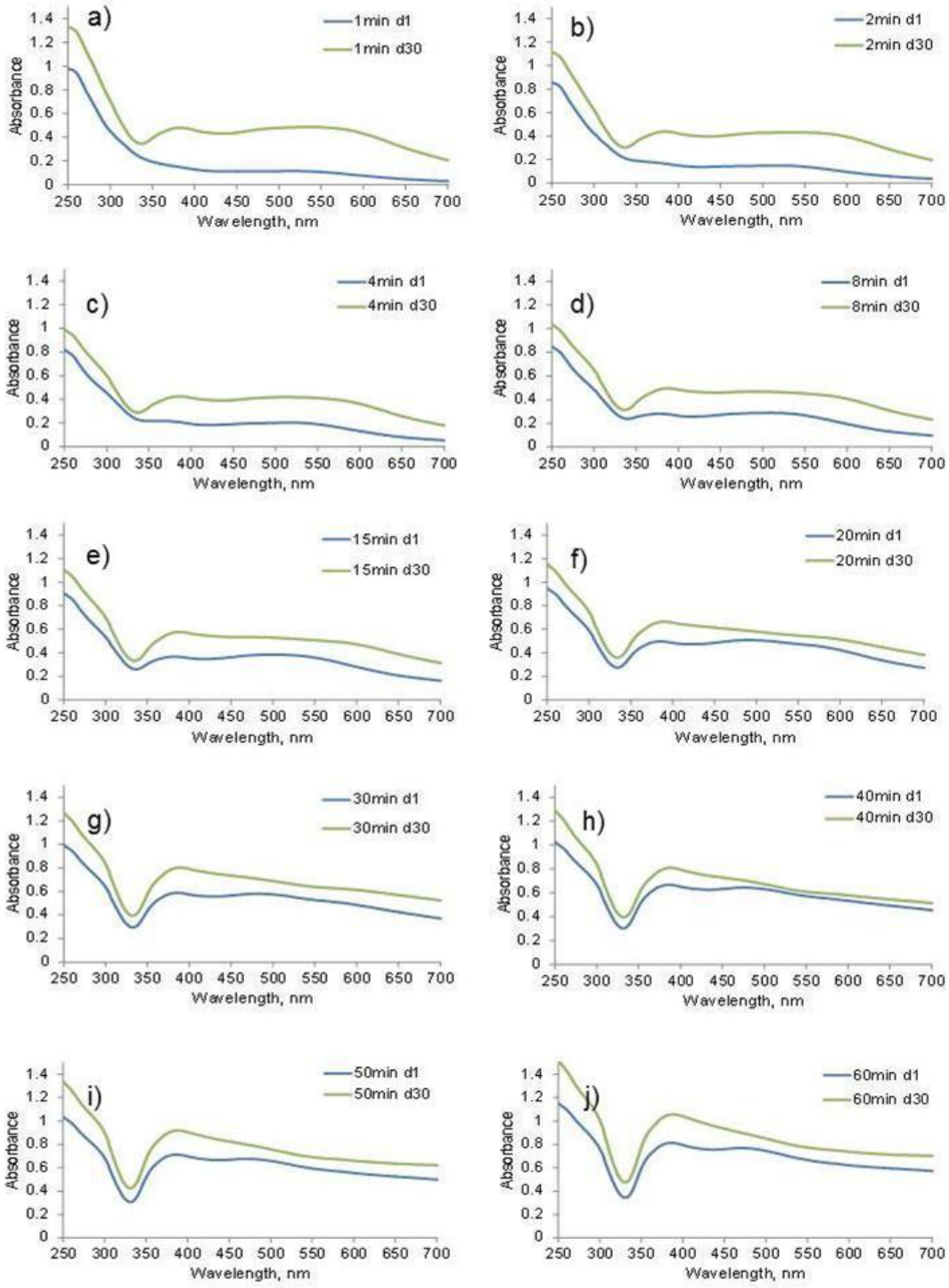

Figure 4.55 UV-Vis spectra of CS-stabilized silver nanoparticles colloids synthesized using 0.1 mM CS in 1.0 % v/v acetic acid solution at initial pH of 5.0 at various radiation times of 1, 2, 4, 8, 15, 20, 25, 30, 40, 50 and 60 minutes after synthesis and after stored for one month

4.5 Characteristics of silver nanoparticles stabilized by humic acid

HA is macromolecular which have broad range of molecular weight (MW), it's MW is range from 2,000-500,000 [82]. HA was analyzed with GPC technique. The result shows that it has M_w =124,758 g/mol, M_n = 47,594 g/mol and polydispersity index = 2.62. HA was prepared as 0.0721 mM at first. However, at this concentration, HA cannot completely dissolved. Then 0.0072 and 0.0007 mM HA were prepared and their appearances were shown in Figure 4.51. It can be seen that 0.0072 mM HA solution was too dark to observe the evidence of the formation of silver nanoparticles. However, UV-Vis spectroscopy can be evaluated the formation of silver nanoparticles in that system.

Figure 4.56 Appearances of humic acid solutions at different concentrations

4.5.1 Optical characteristics

4.5.1.1 Effect of initial pH of humic acid solution

Figure 4.52 a) shows that the colors of the obtained nanoparticles colloids at every pH are dark brown almost the same color as pure 0.0072 mM of HA solution. Those colloids were too dark to observe the formation of silver nanoparticles or any color change. Figure 4.53 a) shows that there are not much different between

UV-Vis spectra of those colloids. Moreover, there are no characteristic peaks of silver nanoparticles. These results confirm the above observation.

Figure 4.52 b) shows that the color of the obtained nanoparticles synthesized using 0.0007 mM of HA solution were lighter than those synthesized using 0.0072 mM of HA solution. Their color allowed the observation of silver nanoparticles formation. However the results show no difference in color of those colloids. Figure 4.53 b) shows UV-Vis spectra of those silver nanoparticles colloids. It can be seen that there are not much different between the spectra of those colloids. Moreover, there are no characteristic peaks of silver nanoparticles.

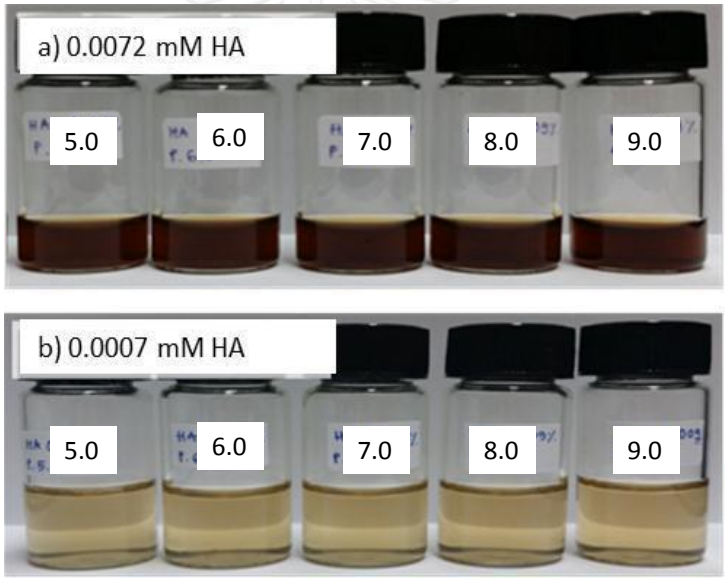

Figure 4.57 Appearances of silver nanoparticles colloids synthesized using different initial pH of HA solution and two concentrations of HA: a) 0.0072 mM and b) 0.0007 mM.

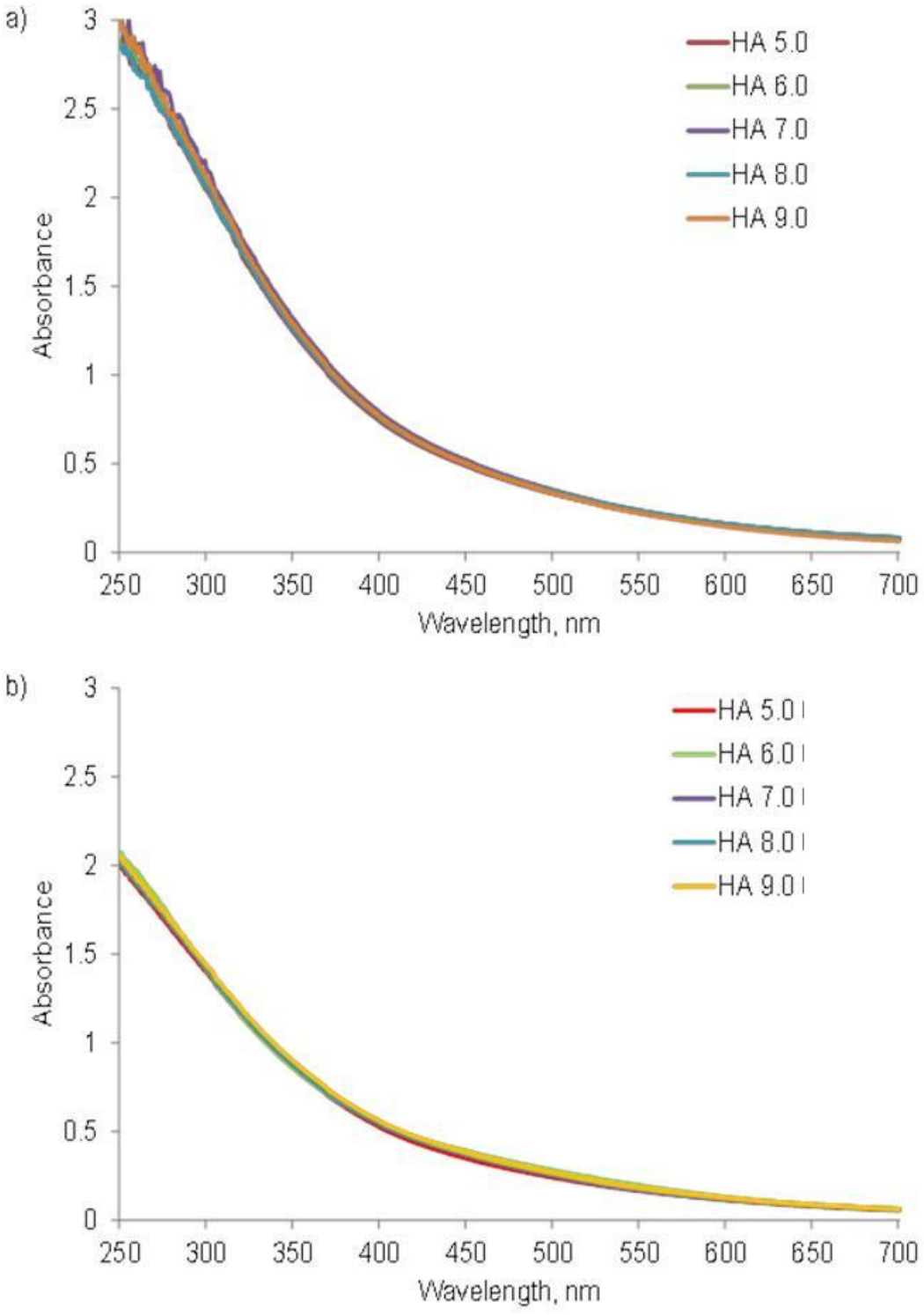

Figure 4.58 UV-Vis spectra of silver nanoparticles colloids synthesized using different initial pH of HA solution and two concentrations of HA: a) 0.0072 mM and b) 0.0007 mM.

4.5.1.2 Role of UV radiation in the synthesis

Figures 4.54 and 4.55 show that there are no difference among the appearances and UV-Vis spectra of the samples synthesized with or without UV radiation. There was no clear evidence of silver nanoparticles formation in all UV-Vis spectra as shown in Figure 4.55. This may be because the molecular weight of HA used in this research is too high; as a result, the functional groups that can reduce silver ions are very low compared to other four stabilizers used in this research. Though there might be some nanoparticles formed but due to the dark color of HA itself and its strong absorbance, the formation of the nanoparticles may be difficult to detect.

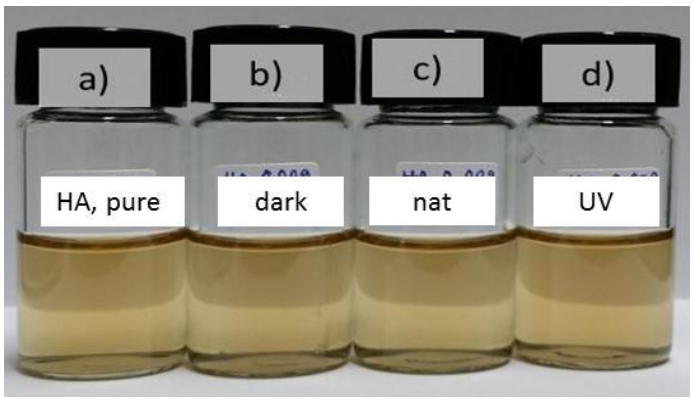

Figure 4.59 Appearances of HA-stabilized silver nanoparticles colloids synthesized at pH of 9.0 and 0.0007 mM of HA solution using different light sources: a) pure CMC solution, b) at dark, c) natural light (indoor) and d) UV lamp

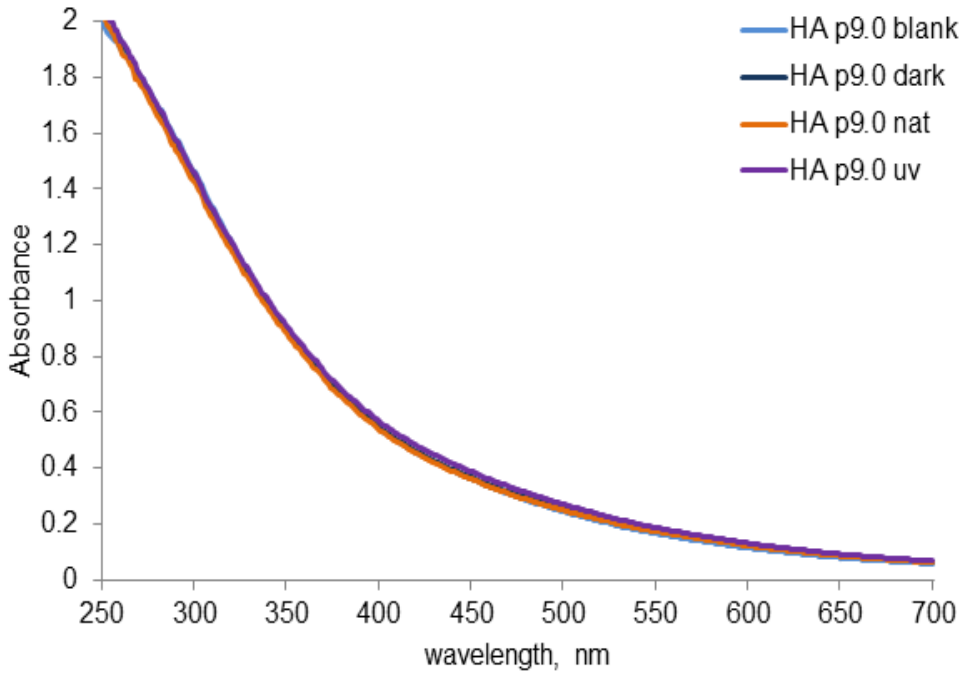

Figure 4.60 UV-Vis spectra of HA-stabilized silver nanoparticles colloids synthesized at pH of 9.0 and 0.0007 mM of HA solution using different light sources: a) pure CMC solution, b) at dark, c) natural light (indoor) and d) UV lamp

4.5.2 Morphology

TEM images of HA-stabilzed silver nanoparticles using 0.0072 mM of HA solution shown in Figure 4.56 indicate that there were silver nanoparticles formed at every condition though their characteristic peaks did not appear in UV-Vis spectra. However, silver nanoparticles synthesized using pH of 7.0, 8.0 and 9.0 were more uniform and smaller than those obtained from the other two conditions. This can explained that there are silver nanoparticles formation in the samples but probably the absorption of the HA with high intensities block the very low absorption intensities of the synthesized silver nanoparticles. However, TEM technique is the very powerful sensitivity to detect the very small particles in range of nanosize. However, TEM results showed that the samples of the initial pH of HA at 5.0 and 6.0 were bigger particles and un-uniformity in size. While the samples of the initial pH of HA at 8.0 and 9.0 showed smaller size particles with uniformity. This can be concluded that at alkali condition the formation of silver nanoparticles in the presence of HA was faster than the acidic condition. This can be explained with the acid dissociation equilibrium as mention before. When HA dissociated into anionic species in the condition of less hydrogen cations, it can be easily give electron to silver ions than its neutral form.

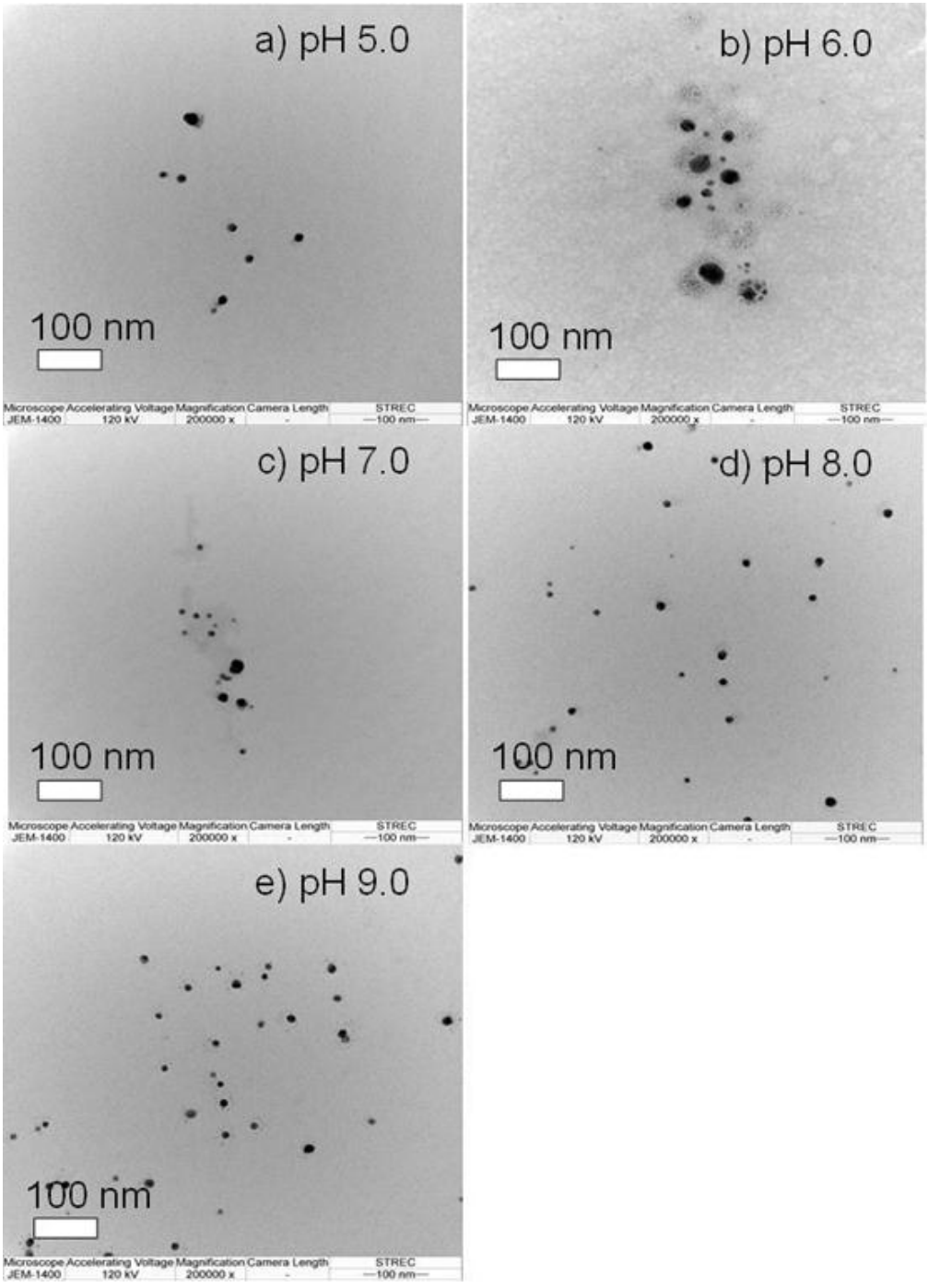

Figure 4.61 TEM images of HA-stabilized silver nanoparticles colloids synthesized using 0.0072 mM of HA solution

5.2 Stability

The stability of HA-synthesized silver nanoparticles was observed after one month storage. Figure 4.57 b1) shows that at 0.0072 mM of HA, silver nanoparticles colloids exhibit no significant change in their colors due to the dark color of HA solution itself. However, UV-Vis measurement indicates a slight change in the absorption spectra. The silver nanoparticles synthesized at pH of 5.0, 6.0, 7.0, 8.0 and 9.0 exhibit small characteristic peaks at 425, 450, 450, 421 and 425 nm, respectively, as shown in Figure 4.58. This can be concluded that there were silver nanoparticles formed during storage.

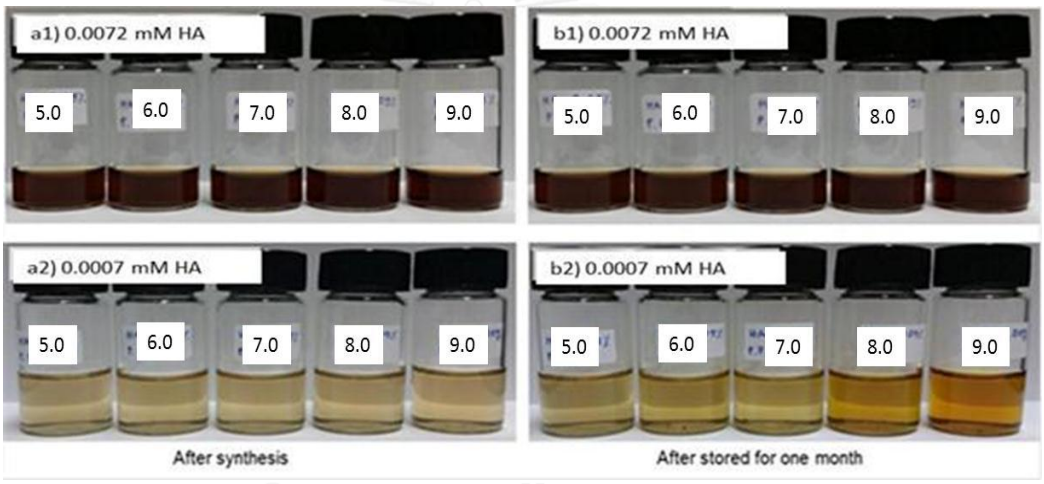

Figure 4.62 Appearances of HA-stabilized silver nanoparticles colloids after synthesis and after stored for one month

Figure 4.57 b2) shows that silver nanoparticles colloids synthesized with 0.0007 mM of HA solutions, after stored for one month, exhibit significantly change in color. UV-Vis spectra confirm this change as shown in Figure 4.59. All samples show the characteristic peaks around 420 nm. However, the absorbance intensities increase with increasing initial pH of HA solution. This may be due to the acid dissociation equilibrium as mentioned before that higher pH condition generated dissociated HA as anionic HA and this anionic form can reduce silver ions faster than the neutral form [93].

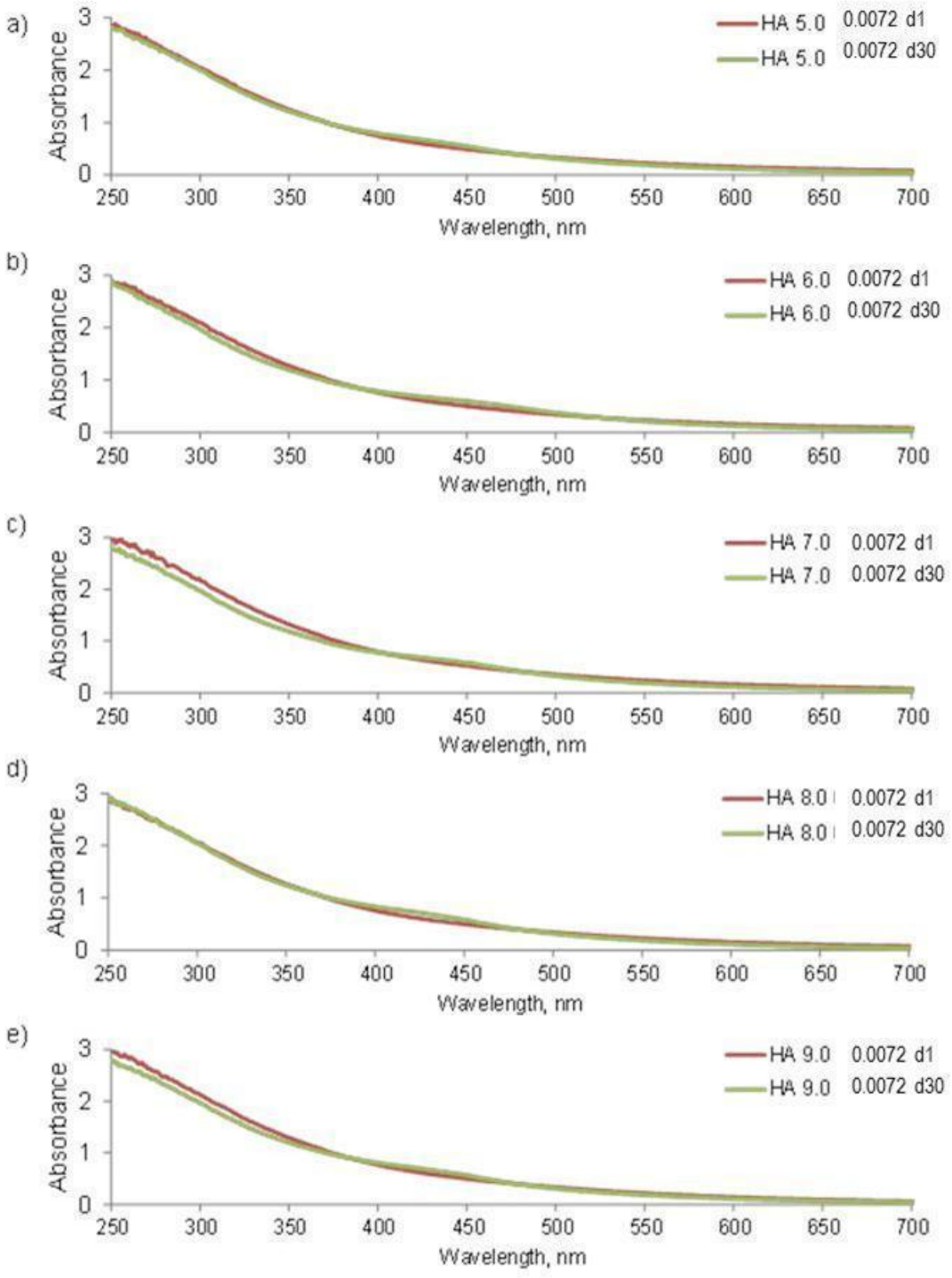

Figure 4.63 UV-Vis spectra of HA-stabilized silver nanoparticles colloids synthesized using 0.0072 mM of HA solution after synthesis and after stored for one month

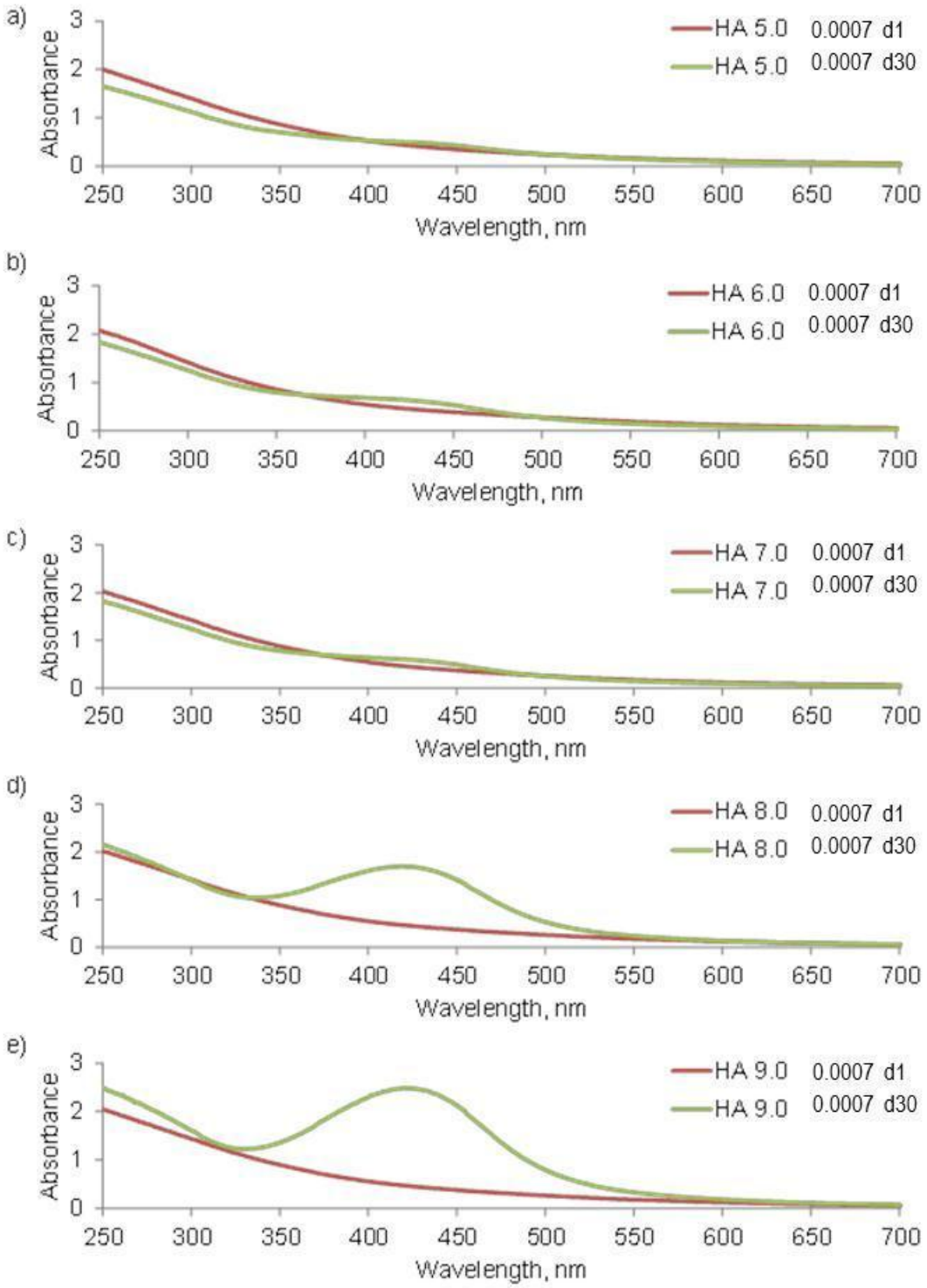

Figure 4.64 UV-Vis spectra of HA-stabilized silver nanoparticles colloids synthesized using 0.0007 mM of HA solution after synthesis and after stored for one month

4.6 Herbicide sensing ability of silver nanoparticles

4.6.1 Sensing to pyrazosulfuron-ethyl herbicide

The appearances of some silver nanoparticles colloids after mixing with various amounts of PSE herbicide as 0, 50, 100, 200 and 400 ppm are shown together with their UV-Vis spectra in Figures 4.60 to 4.77.

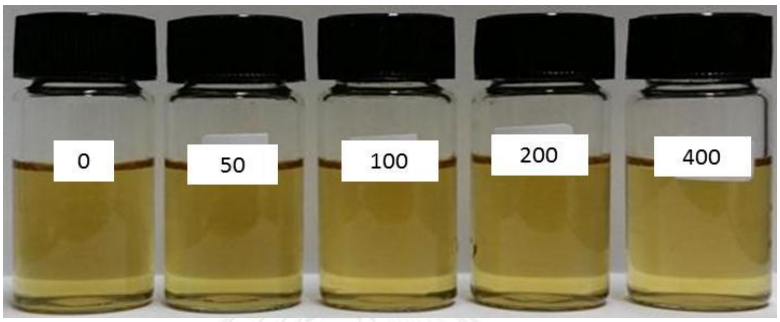

Figure 4.65 Appearances of TA-stabilized silver nanoparticles colloids synthesized using initial pH of 6.0 and MR of 10:1 exposed to various amount of PSE herbicide (ppm)

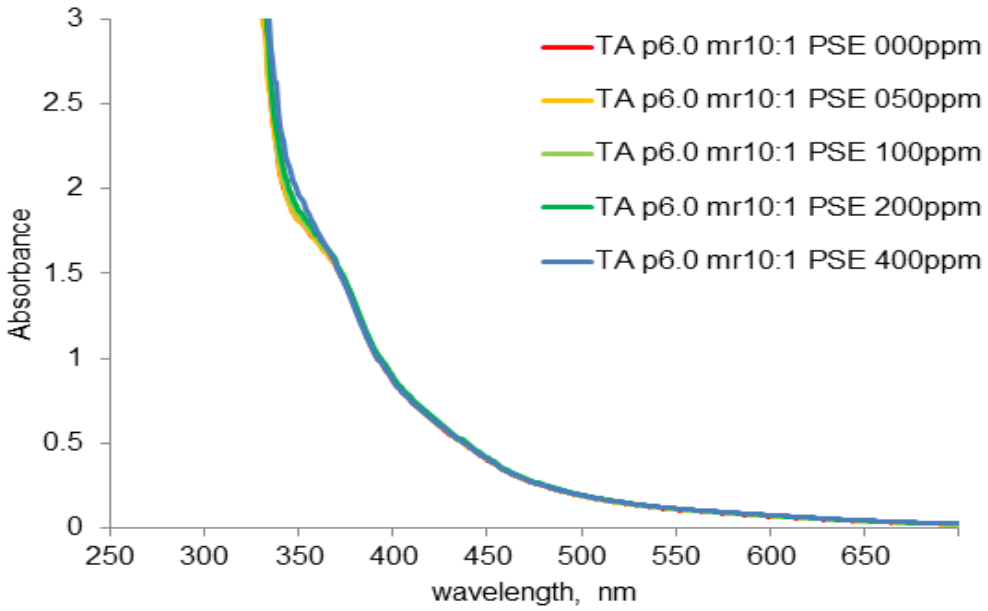

Figure 4.66 UV-Vis spectra of TA-stabilized silver nanoparticles colloids synthesized using initial pH of 6.0 and MR of 10:1 exposed to various amount of PSE herbicide (ppm)

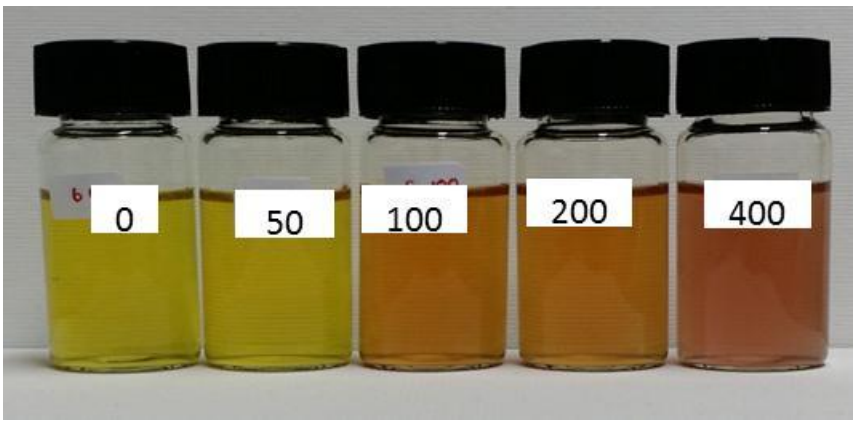

Figure 4.67 Appearances of TA-stabilized silver nanoparticles colloids synthesized using initial pH of 6.0 and MR of 1:1 exposed to various amount of PSE herbicide (ppm)

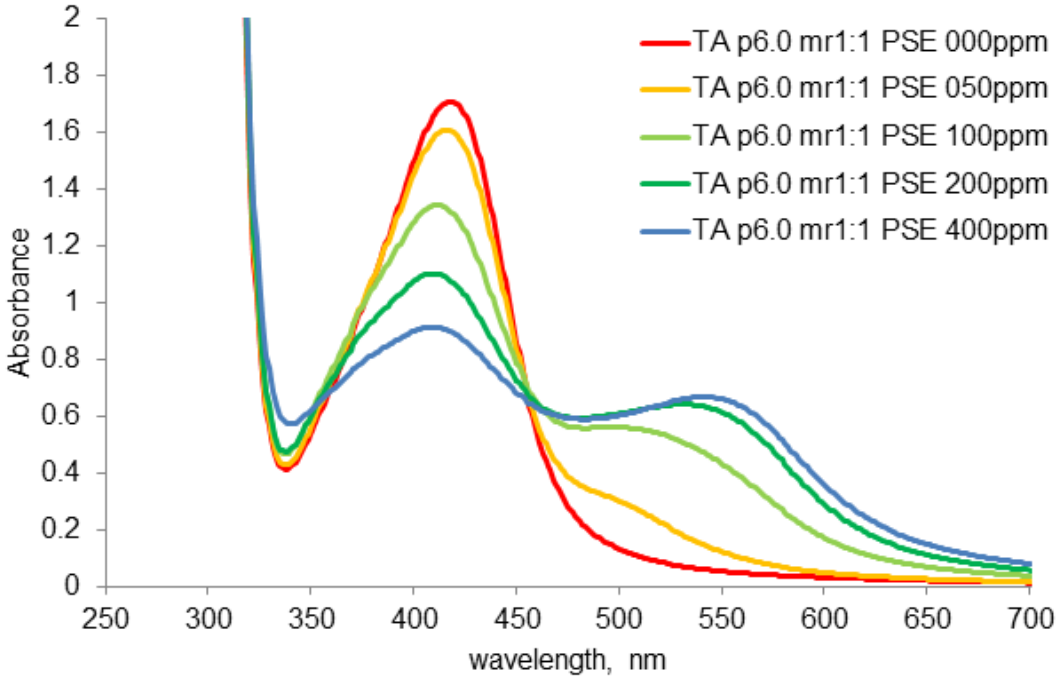

Figure 4.68 UV-Vis spectra of TA-stabilized silver nanoparticles colloids synthesized using initial pH of 6.0 and MR of 1:1 exposed to various amount of PSE herbicide (ppm)

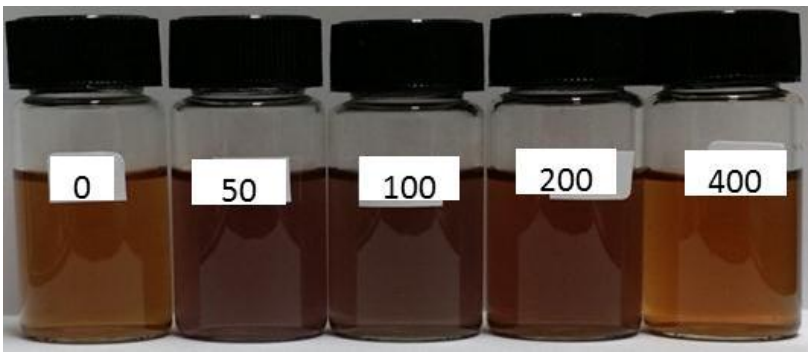

Figure 4.69 Appearances of TA-stabilized silver nanoparticles colloids synthesized using initial pH of 6.0 and MR of 1:10 exposed to various amount of PSE herbicide (ppm)

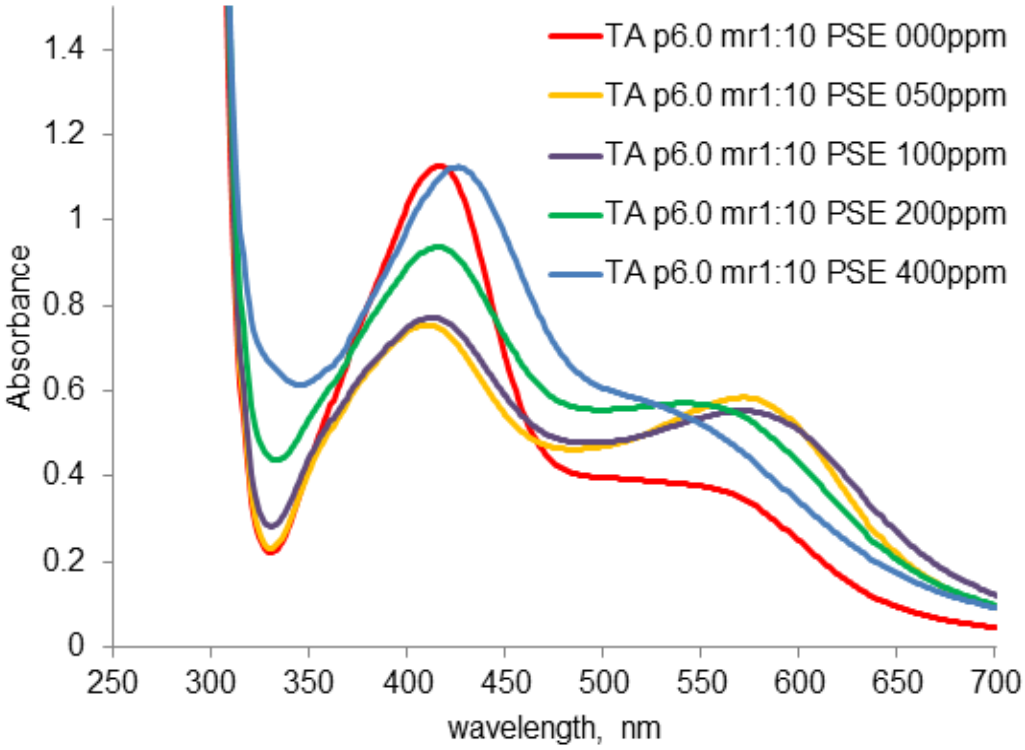

Figure 4.70 UV-Vis spectra of TA-stabilized silver nanoparticles colloids synthesized using initial pH of 6.0 and MR of 1:10 exposed to various amount of PSE herbicide (ppm)

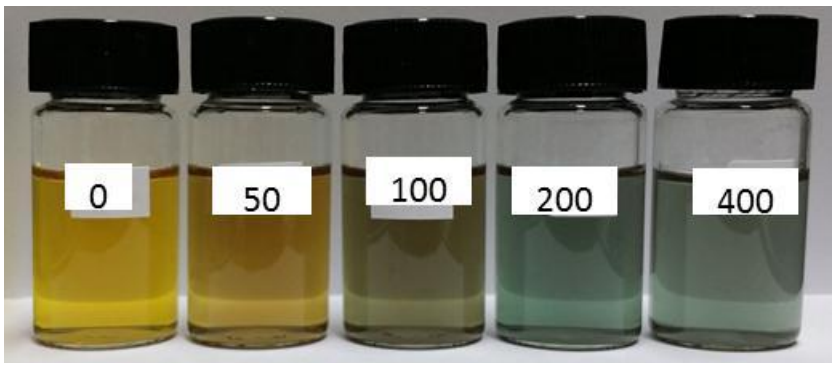

Figure 4.71 Appearances of TA-stabilized silver nanoparticles colloids synthesized using initial pH of 5.0 and MR of 1:1 exposed to various amount of PSE herbicide (ppm)

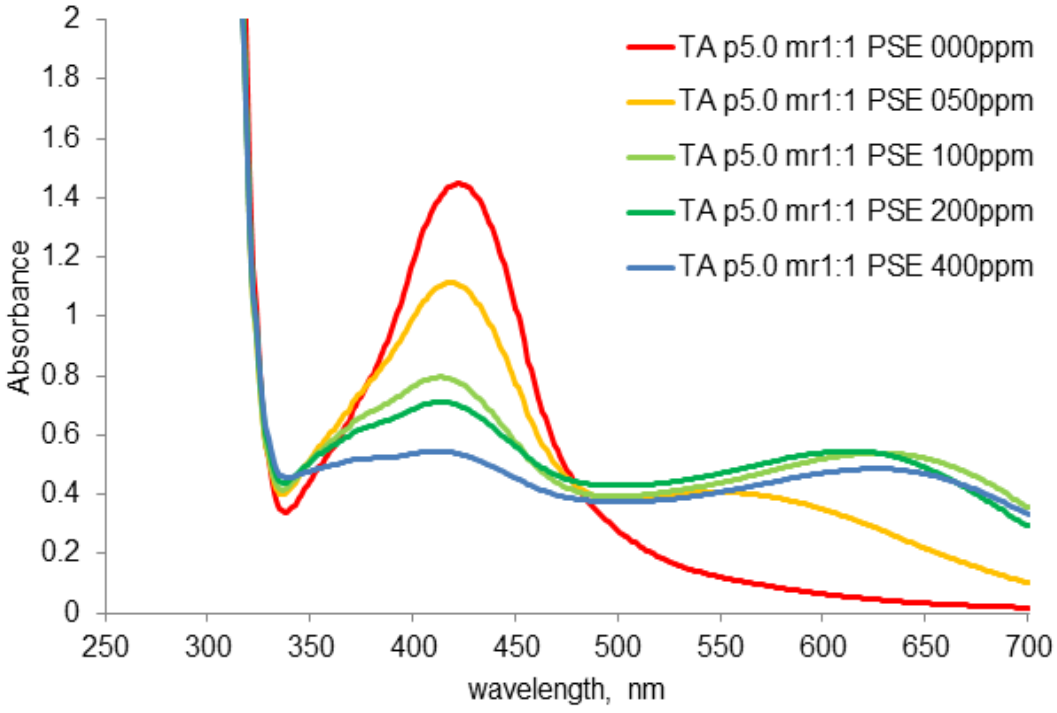

Figure 4.72 UV-Vis spectra of TA-stabilized silver nanoparticles colloids synthesized using initial pH of 5.0 and MR of 1:1 exposed to various amount of PSE herbicide (ppm)

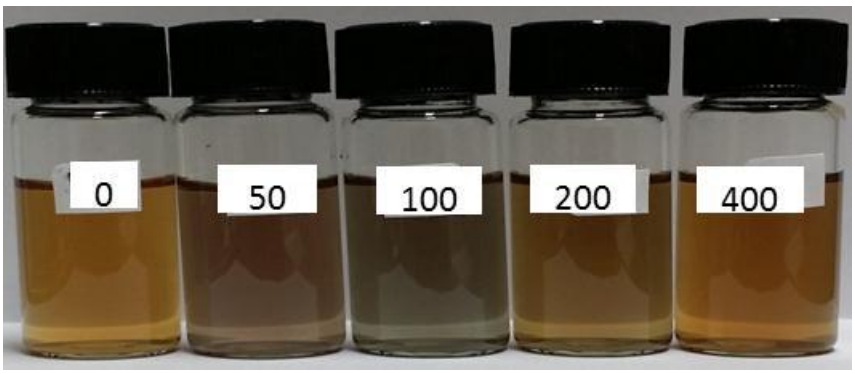

Figure 4.73 Appearances of TA-stabilized silver nanoparticles colloids synthesized using initial pH of 6.0 and MR of 1:10 exposed to various amount of PSE herbicide (ppm)

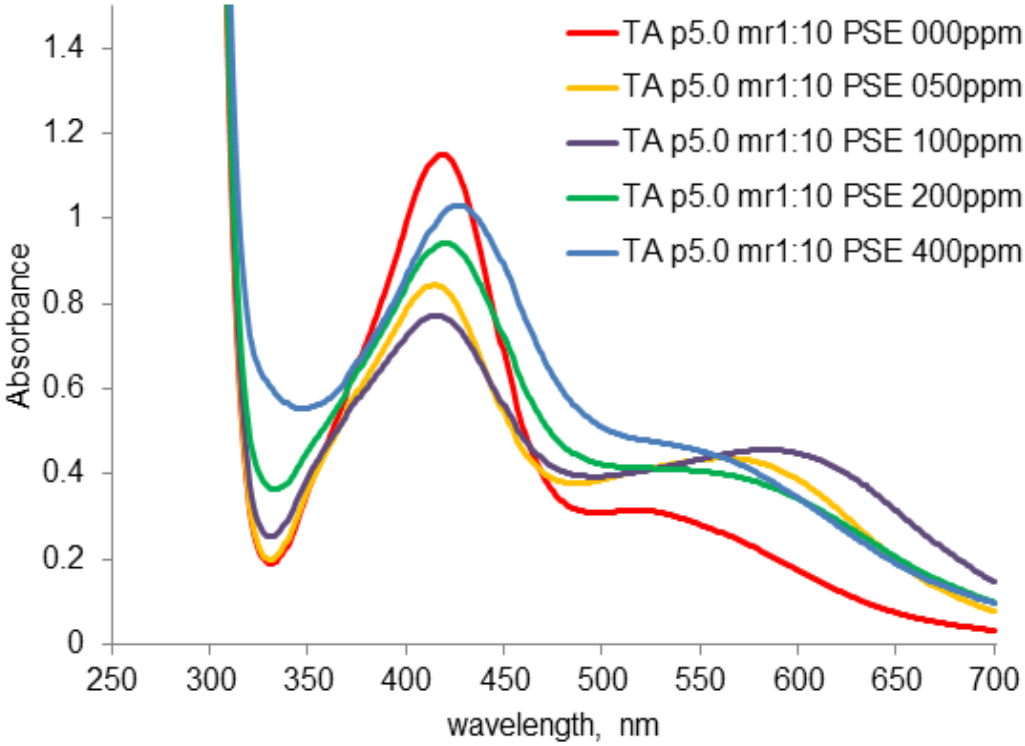

Figure 4.74 UV-Vis spectra of TA-stabilized silver nanoparticles colloids synthesized using initial pH of 6.0 and MR of 1:10 exposed to various amount of PSE herbicide (ppm)

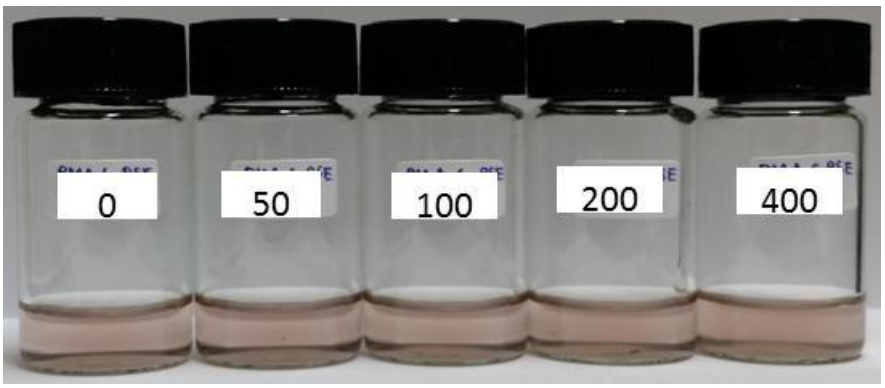

Figure 4.75 Appearances of PMA-stabilized silver nanoparticles colloids synthesized using initial pH of 6.0 and MR of 1:10 exposed to various amount of PSE herbicide (ppm)

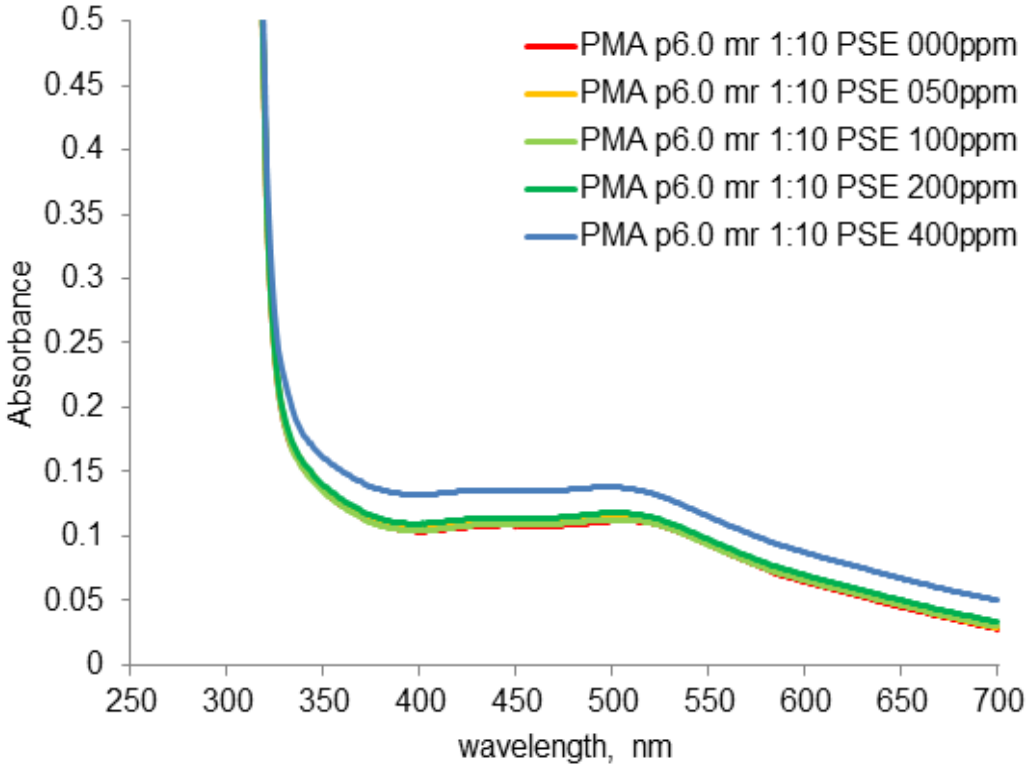

Figure 4.76 UV-Vis spectra of PMA-stabilized silver nanoparticles colloids synthesized using initial pH of 6.0 and MR of 1:10 exposed to various amount of PSE herbicide (ppm)

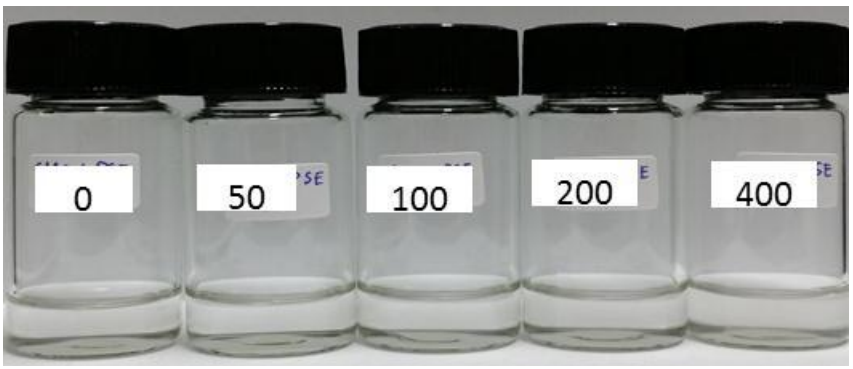

Figure 4.77 Appearances of CMC-stabilized silver nanoparticles colloids synthesized using initial pH of 6.0 and MR of 1:10 exposed to various amount of PSE herbicide (ppm)

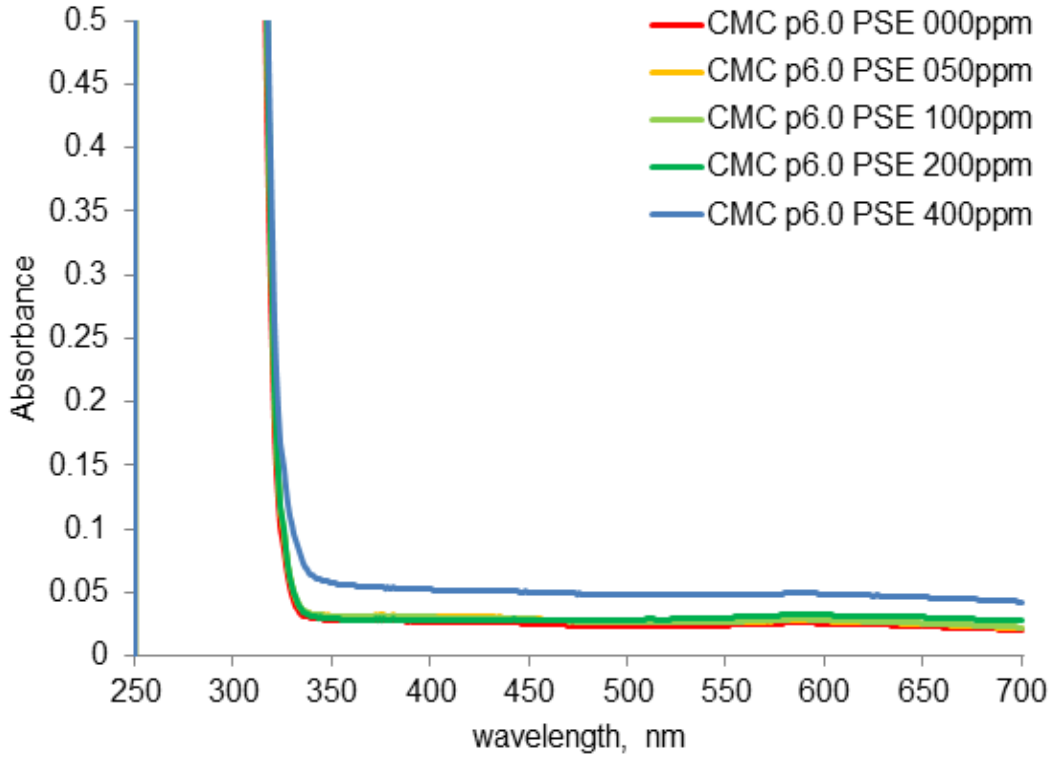

Figure 4.78 UV-Vis spectra of CMC-stabilized silver nanoparticles colloids synthesized using initial pH of 6.0 and MR of 1:10 exposed to various amount of PSE herbicide (ppm)

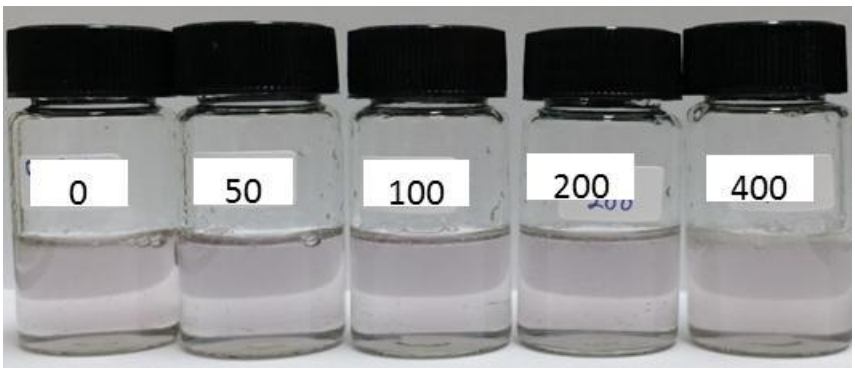

Figure 4.79 Appearances of CS-stabilized silver nanoparticles colloids synthesized using initial pH of 5.0, radiation time of 4 mins and MR of 1:10 exposed to various amount of PSE herbicide (ppm)

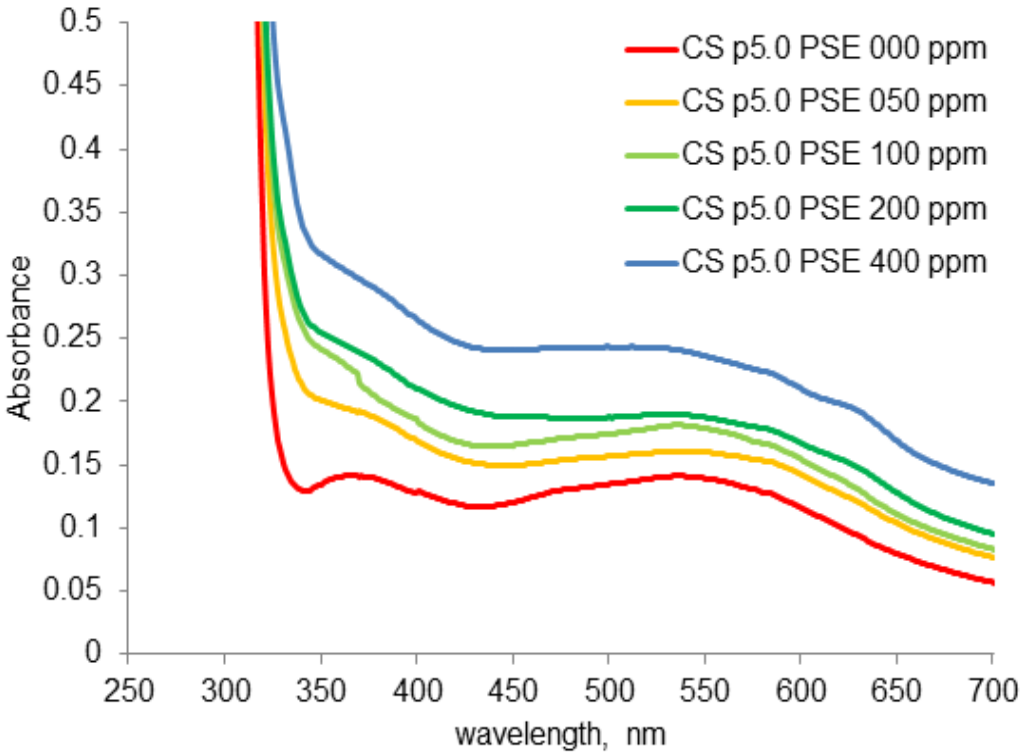

Figure 4.80 UV-Vis spectra of CS-stabilized silver nanoparticles colloids synthesized using initial pH of 5.0, radiation time of 4 mins and MR of 1:10 exposed to various amount of PSE herbicide (ppm)

Figure 4.81 Appearances of HA-stabilized silver nanoparticles colloids synthesized using 0.0007 mM of HA at initial pH of 6.0 exposed to various amount of PSE herbicide (ppm)

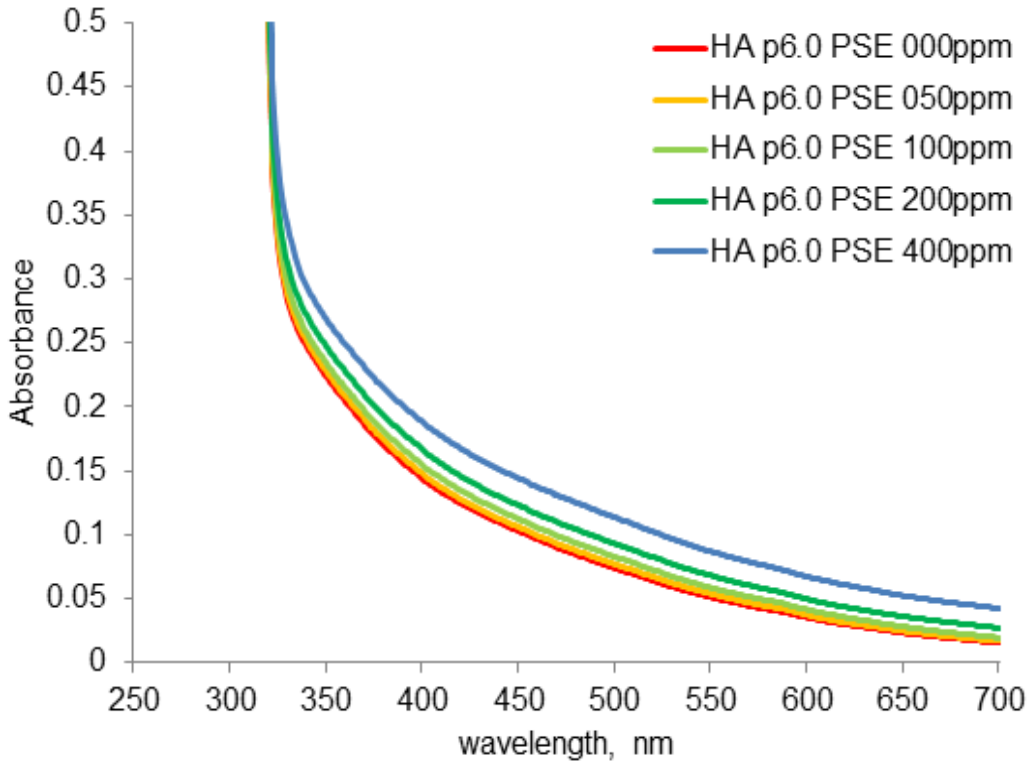

Figure 4.82 UV-Vis spectra of HA-stabilized silver nanoparticles colloids synthesized using 0.0007 mM of HA at initial pH of 6.0 exposed to various amount of PSE herbicide (ppm)

The above results suggest that only TA-stabilized silver nanoparticles in acidic condition exhibit sensing ability to PSE herbicide. The following discussion is explained about this phenomenon.

PSE is one of sulfonylurea herbicides. They were weak acids and have pKa values ranging from 3 to 5. These herbicides typically exist in neutral form at pH levels above pKa. Therefore, they are anionic in most agriculture soils and the relative concentrations of the neutral form are greatest in soil of low pH [94], their acid dissociation equilibrium is showed as the following equation [95, 96].

$$R_1 - SO_2 - NH\text{-}CO - NH - R_2 \leftrightarrow [R_1 - SO_2 - N\text{-}CO - NH - R_2]^- + H^+ \quad ...(\text{eq. } 4.4)$$

Then PSE exists as an equilibrium mixture of neutral form and dissociated form as shown in Figure 4.78.

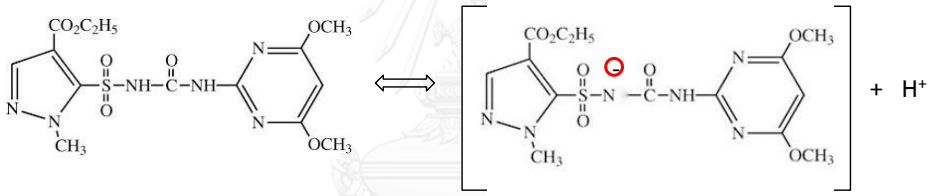

(eq. 4.5)

Figure 4.83 Dissociation of pyrazosulfuron-ethyl acid

Several studies showed that sulfonylurea herbicide is pH-dependent [97]. The sulfonylurea herbicide can be hydrolysis in acidic condition. These compounds hydrolyze more rapidly in water at acidic pH but remained stable in neutral solution [96, 97] the mechanism of hydrolysis under mild acidic condition is cleavage of sulfonylurea bridge, producing CO_2 and the sulfonamide and heterocyclic amine as shown in following equation [96].

$$R_1 - SO_2 - NH\text{-}CO - NH - R_2 \leftrightarrow R_1 - SO_2 - NH_2 + R_2 - NH_2 + CO_2 \quad ...(\text{eq. } 4.6)$$

Previous works revealed that hydrolysis of PSE in aqueous solution was much faster in acidic than under neutral [98] and the suggested mechanism was shown in Figure 4.79. Moreover, it was reported that sulfonylurea exist as an equilibrium mixture of the neutral form and dissociated form less subject to the hydrolysis reaction [96, 98].

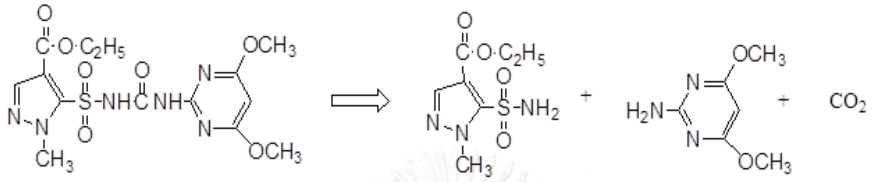

(eq. 4.7)

Figure 4.84 Hydrolysis of pyrazosulfuron-ethyl herbicide

The products of the hydrolysis of PSE were two primary amines which were primary sulfonamide and heterocyclic amine. Moreover, primary amine was concerned as a basic substance. However, the primary sulfonamide generally was concerned as relatively unreactive compounds [99]. Moreover heteroclic amine was concerned as a basic substance. These are considered using the Bronsted-Lowry theory of acids and bases - the base is a hydrogen ion acceptor [100]. Then the heterocyclic amines are probably accepted hydronium ions in acidic condition as shown in Figure 4.80. And these heterocyclic amines showed the interaction with the TA stabilized silver nanoparticle and made the color of the silver nanoparticles changed. Figure 4.81 showed the schematic of the interaction between TA stabilized silver nanoparticles and heterocyclic amines.

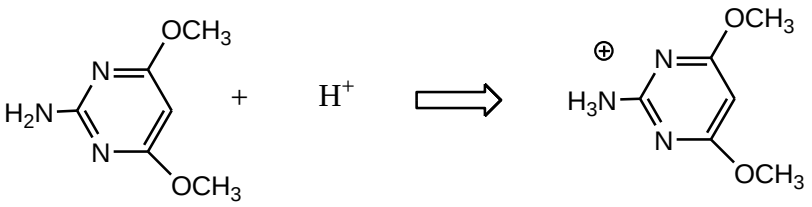

(eq. 4.8)

Figure 4.85 Reaction showing the role of heterocyclic amine as basic substance.

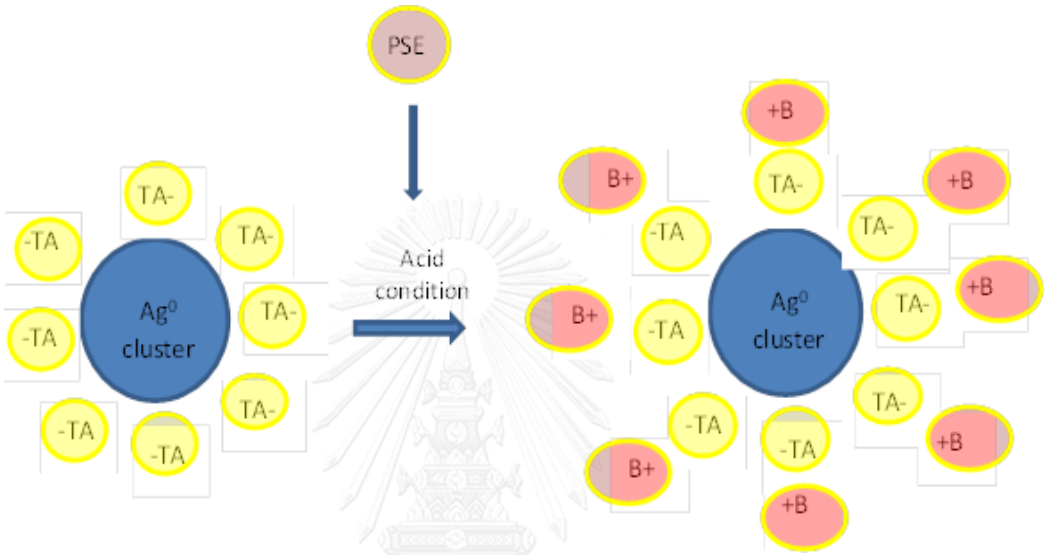

Figure 4.86 Schematic interaction between pyrazosulfuron ethyl and TA-stabilized silver nanoparticles. (TA= Tannic acid, PSE= pyrazosulfuron ethyl, B^+= cationic of heterocyclic amine).

TA is natural weak acid, polyphenol plant extract, macromolecule [43]. While it act as stabilizer, it has to turn nonpolar part toward silver nanoparticles and let the ionic part outside the particles. To be polyphenol substance, TA will turn polyphenol outside of the nanoparticles to make the particles stable in aqueous solution. However TA has a pKa value between seven and eight [43]. Then it dissociated at pH above pKa. At acidic condition TA stay in neutral form with their polyphenol groups.

The schematic represents how PSE interacts with silver nanoparticles is shown in Figure 4.78. When PSE stays in acidic solution, it is hydrolyzed as mentioned

before. Then the cationic hetercyclic amines surround the TA stabilized silver nanoparticles with the electrostatic attraction. This probably resulted in formation of the bigger nanoparticles. This made UV-Vis spectra showed that the original peak was decreased and a new peak formed at the longer wavelength due to bigger particles formation.

It can be seen that there were two different patterns of color shifted of the synthesized silver nanoparticles. Figure 4.62 and 4.66, silver nanoparticles synthesized with MR 1:1, with initial pH of tannic acid at 6.0 and 5.0, changed their color from bright yellow to red, and yellow to bluish green. Moreover, the differences between silver nanoparticles synthesized with initial pH of TA at pH of 5.0 and 6.0 changed after added PSE solutions were explained with the increasing in acidic condition. Consequently, increasing in acidic condition of silver nanoparticles (pH 5.0) made more amount of heterocyclic amine. This yields a denser layer of heterocyclic amine on the surface of silver nanoparticles, which showed in UV-Vis spectra shifted to longer wavelength at 640 nm while the UV-Vis spectra of the pH of 6.0 samples shifted to the wavelength of 550 nm. These results can be confirmed with TEM images which show that after exposed to 400 ppm of PSE herbicide solution, the nanoparticles of pH of 5.0 are bigger than the nanoparticles of pH of 6.0 as shown in Figure 4.82.

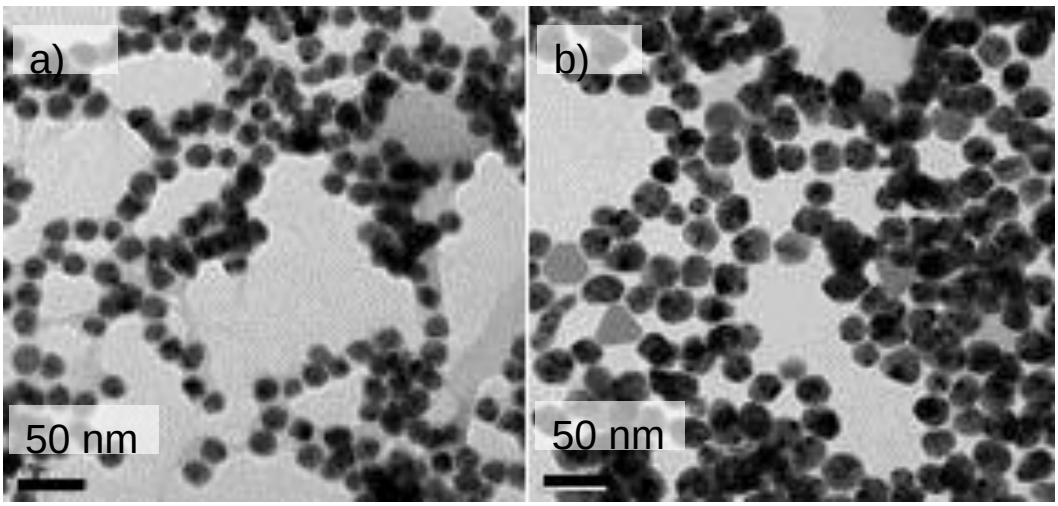

Figure 4.87 TEM images of TA-stabilized silver nanoparticles synthesized using molar ratio of TA to silver ions at 1:1 with different initial pH of TA after exposed to 400 ppm of PSE herbicide; a) pH of 6.0 and b) pH of 5.0

However, with MR 1:10, for TA-stabilized silver nanoparticles at pH of 6.0, as amount of PSE herbicide increased, the original peak around 420 nm decreased. A new shoulder appears around 500-600 nm as shown in Figure 4.65. However, it was shown that without any of PSE herbicide in this sample, its UV-Vis spectrum exhibits a shoulder around 460-570 nm, while sample of MR 1:1 pH of 6.0, has no this shoulder. This phenomenon was also observed in the sample of MR 1:10 at pH of 5.0 compared to their MR 1:1. These resulted in dull color of the samples on MR 1:10 than MR 1:1. From those results, it can be concluded that the best synthesized silver nanoparticles that showed the ability to be PSE herbicide detection application was the sample synthesized in the presence of TA with MR of 1:1 at pH of 6.0.

However, it can be explained how the silver nanoparticles stabilized with other stabilizers were not show the sensing ability to PSE herbicide. It is because the other stabilizers are macromolecules with long chain structures. These phenomena were probably occurred as in the case of high amount of TA as in MR 10:1 samples which were very good stabilized silver nanoparticles. Therefore, the heterocyclic amines

from PSE hydrolyzation cannot affect those silver nanoparticles as shown in Figures 4.70 – 4.77.

4.6.2 Sensing to paraquat herbicide

The appearance of the silver nanoparticles colloids exposed to various amounts of PQ herbicide as 0, 50, 100, 200 and 400 ppm are shown together with their UV-Vis spectra in Figures 4.83 to 4.92. It can be seen that TA-stabilzed silver nanoparticles synthesized at initial pH of 6.0 with MR of 1:1 and PMA-stabilzed silver nanoparticles synthesized at initial pH of 6.0 MR1:10 show good respond to PQ herbicide solution. Their color changes are easily detected by eye as shown in Figure 4.83 and 4.85, respectively.

For TA-stabilized silver nanoparticles sample of pH 6.0 MR 1:1, the color of the mixtures changed from yellow to darker orange to lighter orange. The UV-Vis spectra showed that as PQ increased to 50 ppm, the original peak around 420 nm was decreased and a new peak appeared around 440-500 nm. This may be because there were PQ^{2+} ions surrounded on TA-stabilized silver nanoparticles which showed anionic part of polyphenol groups on their surface. This case is different from PSE sensing of the same sample. UV-Vis spectra of PQ sensing test showed that the original peaks were decreased and shifted to the longer wavelength, there were no new peaks showing up as in PSE sensing results because there were no new particles formed as in PSE sensing test.

Figure 4.83 shows that after adding more amount of PQ, the absorbance peak shifted to the shorter wavelength because more amount of PQ increased the cations of PQ^{2+} in the mixture. This is probably caused higher electrostatic repulsion to the silver nanoparticles surrounded with PQ^{2+} and this causes the contraction of the particles. However, when PQ concentration was increased to 400 ppm, UV-Vis spectra showed lower peak intensity.

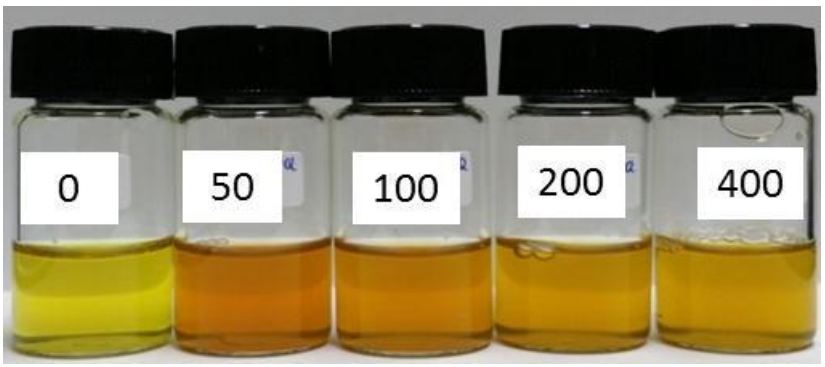

Figure 4.88 Appearances of TA-stabilized silver nanoparticles colloids synthesized using initial pH of 6.0 and MR of 1:1 exposed to various amount of PQ herbicide (ppm)

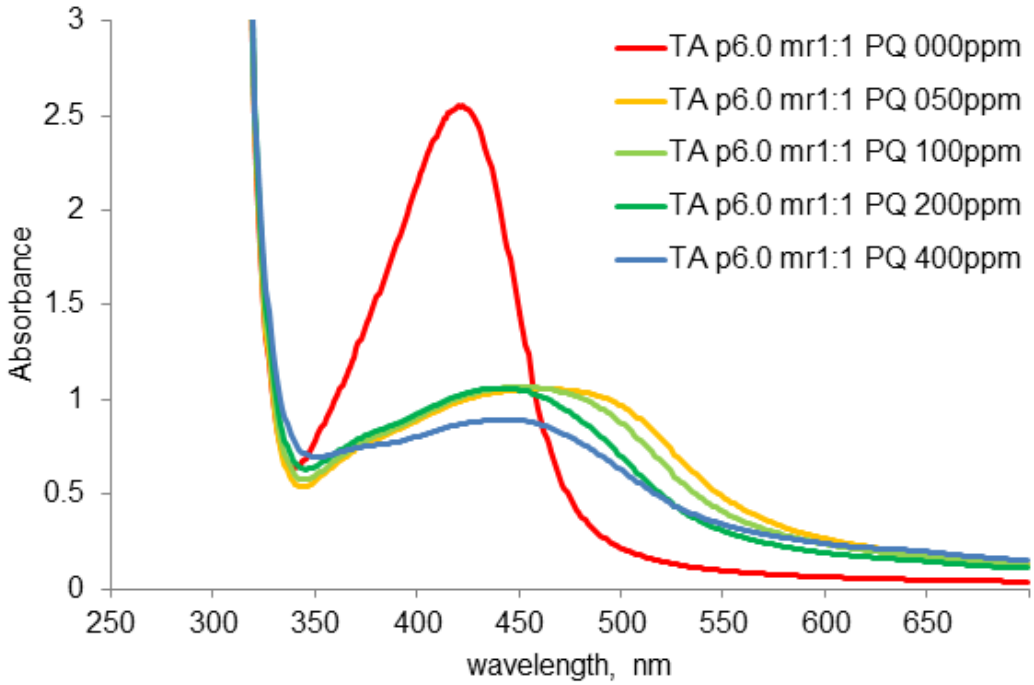

Figure 4.89 UV-Vis spectra of TA-stabilized silver nanoparticles colloids synthesized using initial pH of 6.0 and MR of 1:1 exposed to various amount of PQ herbicide (ppm)

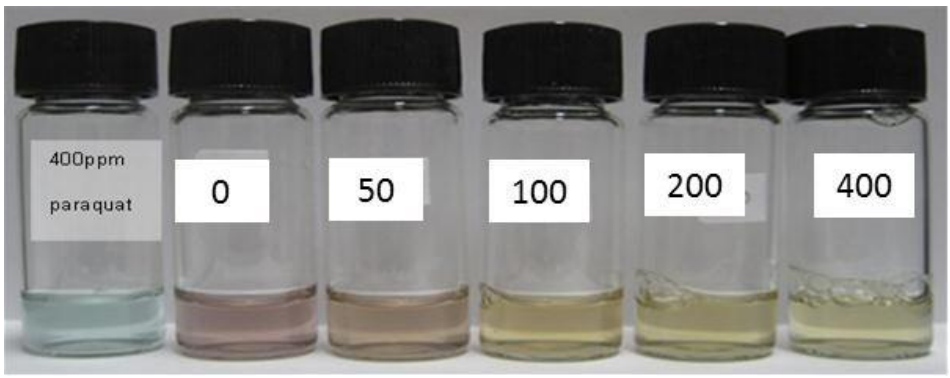

Figure 4.90 Appearances of PMA-stabilized silver nanoparticles colloids synthesized using initial pH of 6.0 and MR of 1:10 exposed to various amount of PQ herbicide (ppm)

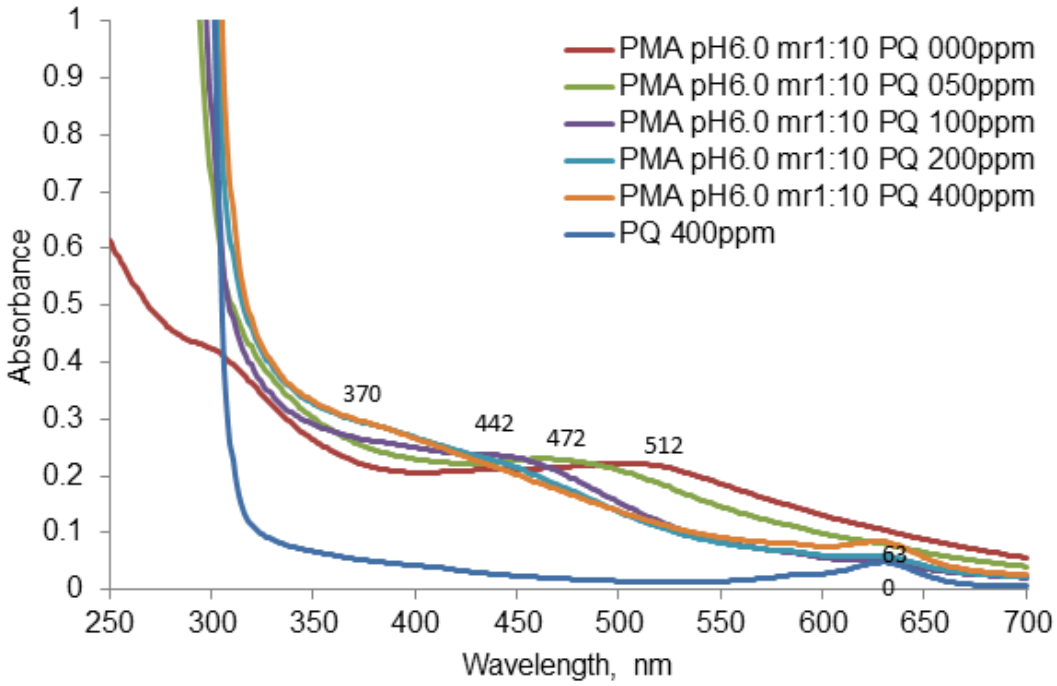

Figure 4.91 UV-Vis spectra of PMA-stabilized silver nanoparticles colloids synthesized using initial pH of 6.0 and MR of 1:10 exposed to various amount of PQ herbicide (ppm)

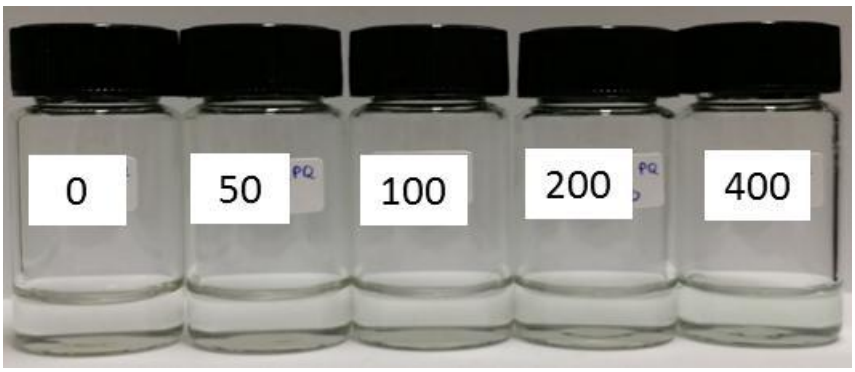

Figure 4.92 Appearances of CMC-stabilized silver nanoparticles colloids synthesized using initial pH of 6.0 and MR of 1:10 exposed to various amount of PQ herbicide (ppm)

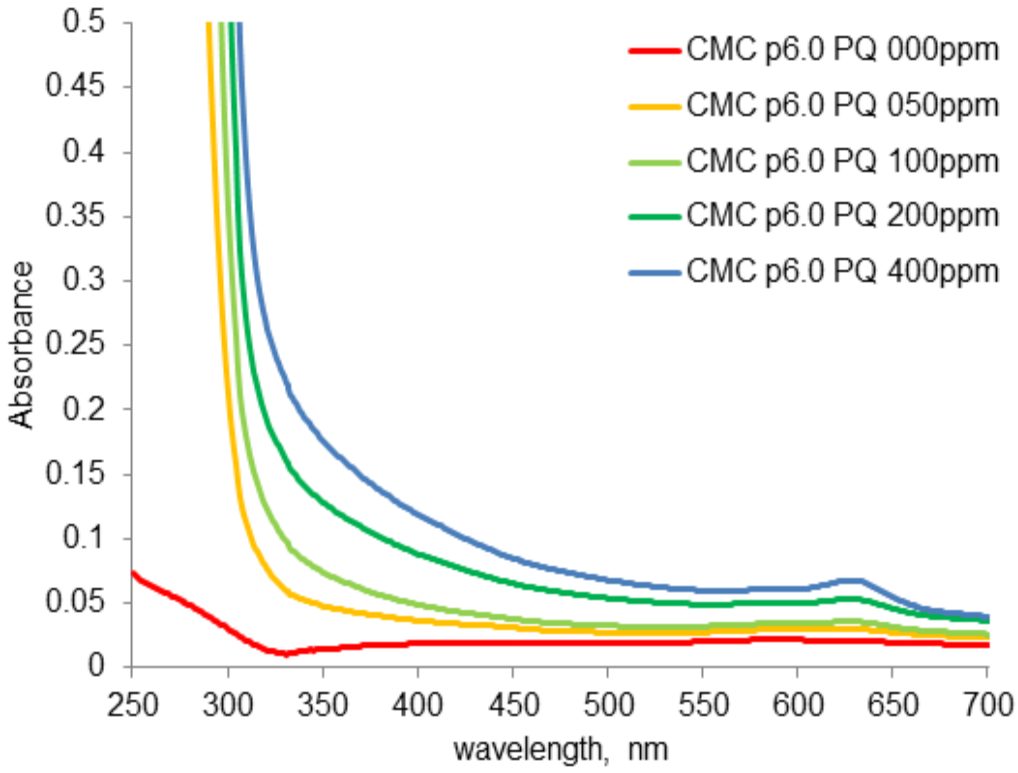

Figure 4.93 UV-Vis spectra of CMC-stabilized silver nanoparticles colloids synthesized using initial pH of 6.0 and MR of 1:10 exposed to various amount of PQ herbicide (ppm).

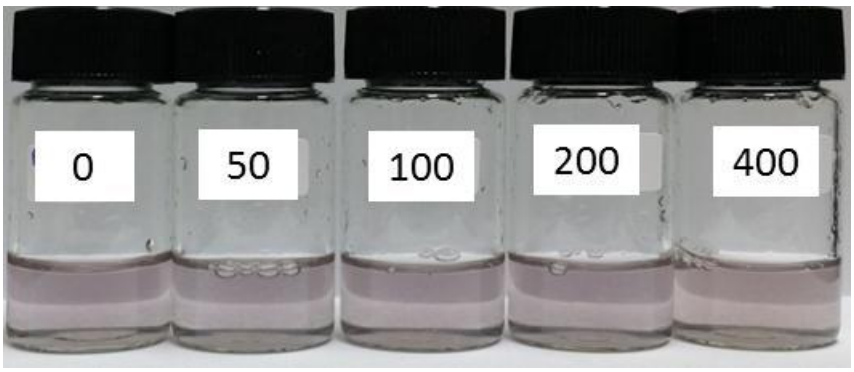

Figure 4.94 Appearances of CS-stabilized silver nanoparticles colloids synthesized using initial pH of 5.0, radiation time of 4 mins and MR of 1:10 exposed to various amount of PQ herbicide (ppm)

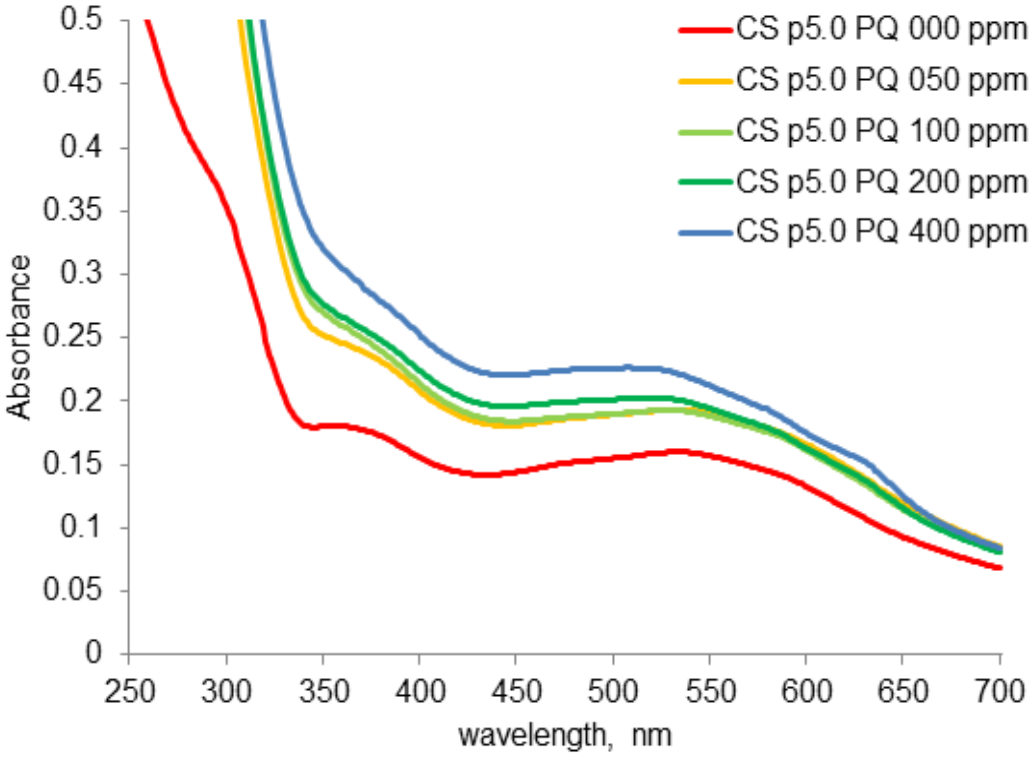

Figure 4.95 UV-Vis spectra of CS-stabilized silver nanoparticles colloids synthesized using initial pH of 5.0, radiation time of 4 mins and MR of 1:10 exposed to various amount of PQ herbicide (ppm)

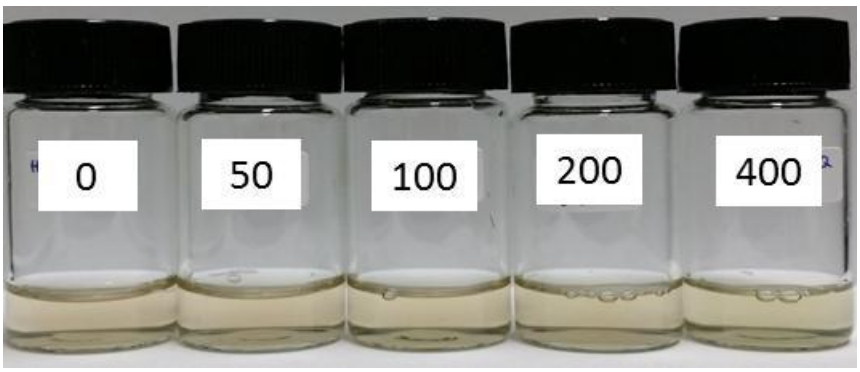

Figure 4.96 Appearances of HA-stabilized silver nanoparticles colloids synthesized using 0.0007 mM of HA at initial pH of 6.0 exposed to various amount of PQ herbicide (ppm)

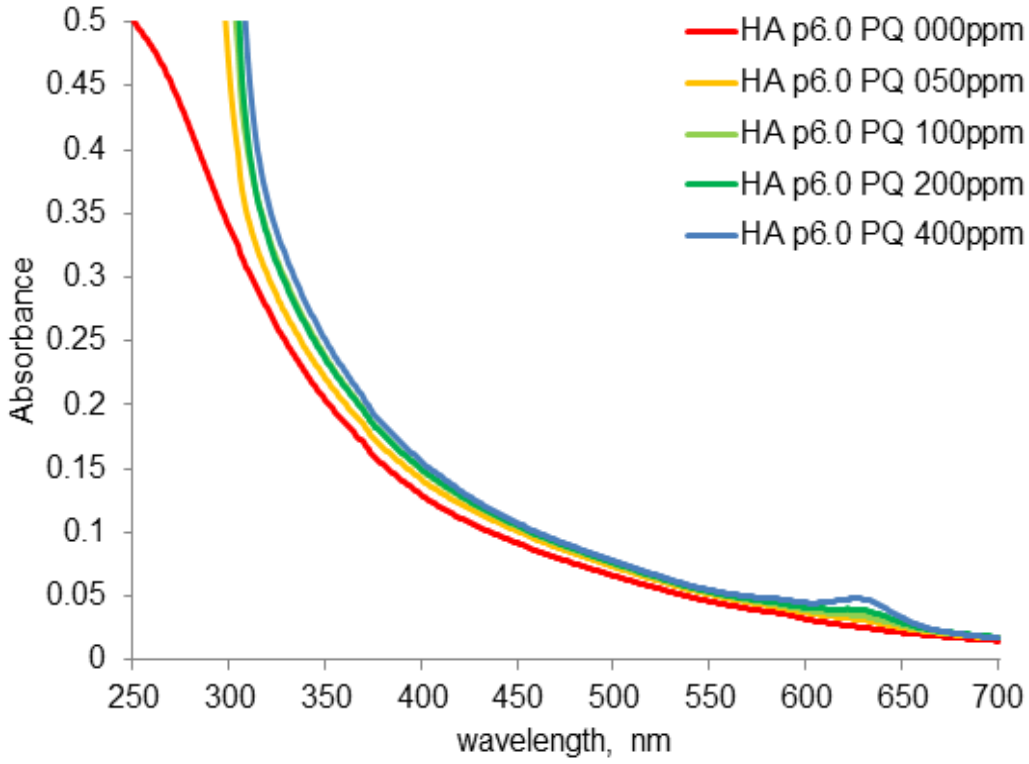

Figure 4.97 UV-Vis spectra of HA-stabilized silver nanoparticles colloids synthesized using 0.0007 mM of HA at initial pH of 6.0 exposed to various amount of PQ herbicide (ppm)

For PMA-stabilized silver nanoparticles synthesized using pH of 6.0 and MR of 1:10, the absorbance spectra of the nanoparticles colloids shifted upon mixing with PQ herbicide and the color of the mixtures changed from purple to yellow. The changes of the absorbance spectra can be monitored as a function of the PQ herbicide content. The absorbance characteristic peak shifted from 512 to 472, 442, 370 and 370 nm, respectively, as amount of PQ increased from 0, 50, 100, 200 and 400 ppm. It can be seen that the initial absorbance peak intensity at 512 nm decreases and is replaced with another peak appearing at the shorter wavelength position as PQ herbicide content is increased. This can be explained with the particle at 512 nm decreased and the formation of the particles around 350 to 400 nm more. Which can be confirmed with smaller particles after exposed to the PQ herbicide. TEM images in Figure 4.93 shows that after exposed to 400 ppm of PQ herbicide solution, the size of PMA- stabilized silver nanoparticles synthesized using MR of 1:10 at initial pH of PMA at 6.0 is smaller than the original size. Moreover, their shape changes from nanorod to mostly spherical shape as shown in the same figure.

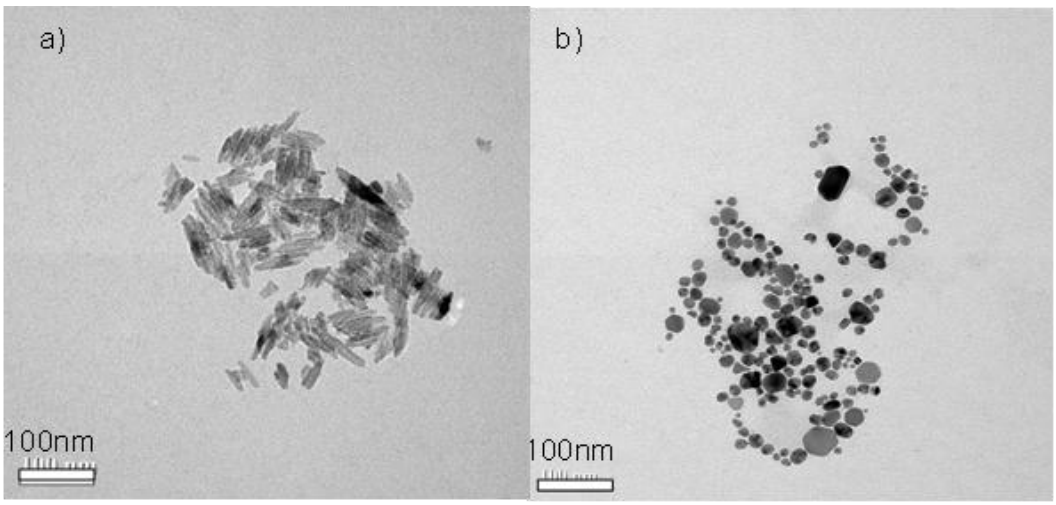

Figure 4.98 TEM images of PMA stabilized silver nanoparticles synthesized with molar ratio of PMA to silver ions at 1:10 with initial pH of PMA at 6.0 after exposed to PQ herbicide; a) 0 ppm and b) 400 ppm

This sensing mechanism can be explained with charge-transfer interactions at nanoparticles surface [13]. Instead of the nanoparticles aggregation as the results of PSE sensing test with TA stabilized silver nanoparticles, PQ sensing test showed different pattern. Previous worked reported that metal ions can interact with ionic pesticides/herbicides such as PQ by an ion-exchange mechanism for example, Ca-Smecite exchanges with PQ as followed [101, 102].

$$\text{Paraquat}_{(aq)} + \text{Ca-Smecite}_{(s)} \Longleftrightarrow \text{Paraquat-Smecite}_{(s)} + Ca^{2+}_{(aq)} \qquad \text{(eq. 4.9)}$$

As mentioned in the section of PMA-stabilized silver nanoparticles, the unreacted silver ions adsorbed on the surface of the silver nanoparticles and formed Ag^{+}/COO^{-} complex with carboxylic groups of PMA adjacent to silver atom cluster. When PQ herbicide solution was added to these colloids, silver ions were let go from COO^{-} on the surface of the nanoparticles. This resulted in the decreased of Ag^{+}/COO^{-} complexes that formed on the surface of silver nanoparticles before. It can be seen that this complexes decreased as the absorbance intensity at 512 nm

decreased as shown in Figure 4.86. Then the sensing mechanism of PMA-stabilized silver nanoparticles to PQ herbicide could be charge-transfer interactions at nanoparticles surface. Moreover, the results indicate that there were new nanoparticles formed as can be seen by an increase in the intensities at the wavelength around 350-400 nm. This may be due to the reduction of free silver ions after charge transfer with PQ^{2+}. This can be illustrated as shown in Figure 4.94.

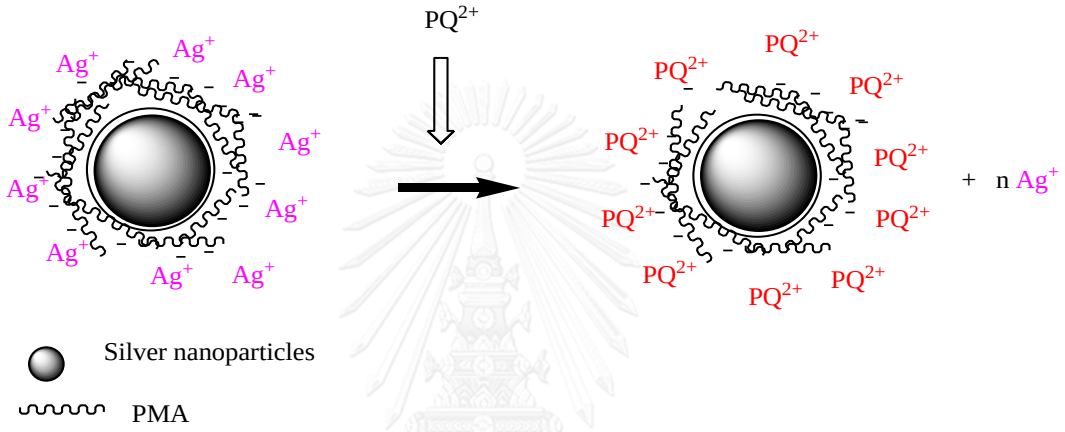

Figure 4.99 The illustration of the charge-transfer interaction at nanoparticles surface between PMA-stabilized silver nanoparticles and PQ herbicide.

From those results, it can be concluded that the best synthesized silver nanoparticles that show sensing ability to PQ herbicide was the sample synthesized in the presence of PMA with MR of 1:10 at pH of 6.0. This is because the color change of PMA-stabilized silver nanoparticles from purple to yellow was easier to detect with naked eye than the color change of TA-stabilized silver nanoparticles which was from yellow to orange.

CHAPTER V
CONCLUSIONS AND RECOMMENDATIONS

5.1 Conclusions

This research emphasized on the synthesis of silver nanoparticles using UV irradiation in the presence of five stabilizers. The optical characteristics, the morphology and the herbicide sensing ability of the synthesized silver nanoparticles were studied. Their stability after one month storage was also investigated. The results can be concluded as follows.

1. Successful synthesis of silver nanoparticles using 8 watts of UV irradiation was developed. The size, shape and amount of the nanoparticles can be controlled by selecting the suitable stabilizers, adjusting the pH of the stabilizer solution, and adjusting the molar ratio of the stabilizer to silver ions.

2. When the type of the stabilizer was considered, the stabilizers having lower molecular weight (TA, PMA) can reduce silver ions to silver nanoparticles without the assistance of UV irradiation at specific pH. However, using UV irradiation promoted the reduction of silver ions in to silver nanoparticles at every pH. On the other hand, it was necessary to use UV irradiation when the stabilizers having high molecular weight such as CMC and CS were employed in order to assist the synthesis. In the case of HA, since its molecular weight was too high, UV-Vis spectra of the obtained nanoparticles did not show the characteristic peak but their formation was confirmed by TEM images indicating very low amount of silver nanoparticles was formed even though UV irradiation was applied.

It was found that type of stabilizer affected the size and shape of the obtained nanoparticles. While using TA, PMA and HA resulted in only spherical particles, using CMC resulted in spherical and trigonal particles. On the other hand, spherical and rod-like particles were found when chitosan was used. In addition, it was found

that the reduction of the silver ions still occurred after finish UV irradiation for all stabilizers.

3. For studying the effect of the pH of stabilizer solution, CS was not used in the study since it can only dissolve at pH of 5.0. It was found that when TA, PMA, CMC and HA were used, the higher formation of the silver nanoparticles was achieved with increasing initial pH of stabilizer solution. In addition, it was observed that more uniform and smaller spherical nanoparticles were mostly obtained when pH of 8.0 and 9.0. At specific condition such as using initial pH of PMA solution at 6.0 with MR 1:10 resulted in the nanoparticles having the mixture of rod-like shape and spherical shape.

The effect of the pH of stabilizer solution on the stability of the obtained nanoparticles was associated with the type of the stabilizer. This is due to the fact that each stabilizer has its own characteristics when it dissolves in acidic, neutral or alkali conditions. Most of the results indicated that the nanoparticles obtained when low pH of stabilizer solutions was used showed higher stability than those obtained from other pH conditions. The reduction of the silver ions still occurred after finish UV irradiation especially when the initial pH of 8.0 and 9.0 were used.

4. For studying the effect of the molar ratio of stabilizers to silver ions, only TA and PMA which are low molecular weight stabilizers were applied due to their ease of dissolving when higher amounts were used. It was found that for TA-stabilized silver nanoparticles, their size increased with increasing the amount of TA except for those of pH 8.0 and 9.0. All the samples were in spherical shape.

On the other hand, different MR resulted in different morphology of PMA-stabilized silver nanoparticles. While the silver nanoparticles obtained with MR of 10:1 showed the bigger size compared to the others, the silver nanoparticles obtained with MR of 1:1 were the smallest particles. For MR of 1:10, most of

the obtained nanoparticles had spherical shape except for those synthesized at pH of 6.0 which exhibited rod-like and spherical shapes.

It was also found that increasing the molar ratio of TA or PMA to silver ions resulted in poor stability of the obtained nanoparticles. Especially in the case of PMA-stabilized silver nanoparticles synthesized using MR of 10:1 at most of the pH conditions except for 5.0, the sediments were observed after one month storage.

5. The suitable conditions for synthesizing silver nanoparticles were determined based on their stability after one month storage and their characteristics of being silver nanoparticles such as color and size. It was found that the suitable conditions were at pH of 6.0 when TA was used as a stabilizer at MR of 1:1 and at pH of 6.0 when PMA was used as a stabilizer at MR of 1:10.

6. Two criteria were used to determine the highest sensing ability to herbicide solution of the obtained nanoparticles. First criterion was that the color of the silver nanoparticles colloids must be significantly changed and can be easily observed by naked eye. Second criterion was that those color changed can be confirmed by UV-Vis spectroscopy. The sample that exhibited the highest sensing ability to PSE herbicide was the silver nanoparticles synthesized in the presence of TA with MR of 1:1 at pH of 6.0. On the other hand, the sample that showed the highest sensing ability to PQ herbicide was the silver nanoparticles synthesized in the presence of PMA with MR of 1:10 at pH of 6.0.

The above results suggest that the silver nanoparticles obtained from this environmental friendly synthesis using UV irradiation combined with a stabilizer that can also act as a reducing agent can be applied for sensing of various types of herbicide by selecting a stabilizer, pH of the stabilizer and its molar ratio to silver ions which are suitable for each herbicide.

5.2 Recommendations

Based on above conclusions, the following topics were recommended for further study.

1) The possibility of using the silver nanoparticles stabilized by TA for detection of other chemicals might be studied.
2) The possibility of using the silver nanoparticles stabilized by PMA for detection of other chemicals might be studied.

REFERENCES

1. Dubas, S. T., and Pimpan, V., Humic acid assisted synthesis of silver nanoparticles and its application to herbicide detection. Mater. Lett. 62 (2008): 2661-2663.
2. Akaighe, N., MacCuspie, R. I., Navarro, D. A., Aga, D. S., Banerjee, S., Sohn, M., *et al.*, Humic Acid-Induced Silver Nanoparticle Formation Under Environmentally Relevant Conditions. Environ. Sci. Technol. 45 (2011): 3895–3901.
3. Chen, J., Wang, J., Zhang, X., and Jin, Y., Microwave-assisted green synthesis of silver nanoparticles by carboxymethyl cellulose sodium and silver nitrate. Mater. Chem. Phys. 108 (2008): 421-424.
4. Dubas, S. T., and Pimpan, V., Green synthesis of silver nanoparticles for ammonia sensing. Talanta 76 (2008): 29-33.
5. Spadaro, D., Barletta, E., Barreca, F., Curro, G., and Neri, F., PMA capped silver nanoparticles produced by UV-enhanced chemical process. Appl. Surf. Sci. 255 (2009): 8403-8408.
6. Hu, B., Wang, S. B., Wang, K., Zhang, M., and Yu, S. H., Microwave-assisted rapid facile "Green" synthesis of uniform silver nanoparticles: Self-assembly into multilayered films and their optical properties. J. Phys. Chem. C 112 (2008): 11169-11174.
7. Solomon, S. D., Bahadory, M., Jeyarajasingam, A. V., Rutkowsky, S. A., Boritz, C., and Mulfinger, L., Synthesis and study of silver nanoparticles. J. Chem. Educ. 84 (2007): 322-325.
8. Kreibig, U., Vollmer, M., and Toennies, J. P., Optical Properties of Metal Clusters, . Springer-Verlag, Berlin, (1995)
9. Stewart, M. E., Anderton, C. R., Thompson, L. B., Maria, J., Gray, S. K., Rogers, J. A., *et al.*, Nanostructured plasmonic sensors. Chem. Rev. 108 (2008): 494-521.

10. Link, S., and El-Sayed, M. A., Shape and size dependence of radiative, non-radiative and photothermal properties of gold nanocrystals. Int. Reviews in Physical Chemistry 19 (2000): 409- 453.
11. Petryayeva, E., and Krull, U. J., Localized surface plasmon resonance: nanostructures, bioassays and biosensing--a review. Analytica Chimica Acta 706 (2011): 8-24.
12. Haes, A. J., Zou, S., Schatz, G. C., and Van Duyne, R. P., Nanoscale Optical Biosensor: Short Range Distance Dependence of the Localized Surface Plasmon Resonance of Noble Metal Nanoparticles. J. Phys. Chem. B 108 (2004): 6961-6968.
13. Haes, A. J., and Van Duyne, R. P., A Nanoscale Optical Biosensor: Sensitivity and Selectivity of an Approach Based on the Localized Surface Plasmon Resonance Spectroscopy of Triangular Silver Nanoparticles. J. Am. Chem. Soc. 124 (2002): 10596-10604.
14. Huang, T., and Xu, X. H. N., Synthesis and characterization of tunable rainbow colored colloidal silver nanoparticles using single-nanoparticle plasmonic microscopy and spectroscopy. J. Mater. Chem. 20 (2010): 9867-9876.
15. Pillai, Z. S., and Kamat, P. V., What factors control the size and shape of silver nanoparticles in the citrate ion reduction method? J. Phys. Chem. B 108 (2004): 945-951.
16. Dadosh, T., Synthesis of uniform silver nanoparticles with a controllable size. Mater. Lett. 63 (2009): 2236-2238.
17. Tian, X. L., Wang, W. H., and Cao, G. Y., A facile aqueous-phase route for the synthesis of silver nanoplates. Mater. Lett. 61 (2007): 130-133.
18. Pal, S., Tak, Y. K., and Song, J. M., Does the antibacterial activity of silver nanoparticles depend on the shape of the nanoparticle? A study of the Gram-negative bacterium Escherichia coli. Appl. Environ. Microbiol. 73 (2007): 1712-1720.
19. Sun, Y., and Xia, Y., Shape-controlled synthesis of gold and silver nanoparticles. Science 298 (2002): 2176-2179.

20. Lee, G. P., Bignell, L. J., Romeo, T. C., Razal, J. M., Shepherd, R. L., Chen, J., *et al.*, The citrate-mediated shape evolution of transforming photomorphic silver nanoparticles. Chem. Commun. 46 (2010): 7807-7809.

21. Qin, Y. Q., Ji, X. H., Jing, J., Liu, H., Wu, H. L., and Yang, W. S., Size control over spherical silver nanoparticles by ascorbic acid reduction. Colloid Surf., A 372 (2010): 172-176.

22. Desai, R., Mankad, V., Gupta, S. K., and Jha, P. K., Size Distribution of Silver Nanoparticles: UV-Visible Spectroscopic Assessment. Nanosci. Nanotechnol. Lett. 4 (2012): 30-34.

23. Limsavarn, L., Sritaveesinsub, V., and Dubas, S. T., Polyelectrolyte assisted silver nanoparticles synthesis and thin film formation. Mater. Lett. 61 (2007): 3048-3051.

24. de Oliveira, J. F., and Cardoso, M. B., Partial aggregation of silver nanoparticles induced by capping and reducing agents competition. Langmuir 30 (2014): 4879-4886.

25. Yoksan, R., and Chirachanchai, S., Silver nanoparticles dispersing in chitosan solution: Preparation by γ-ray irradiation and their antimicrobial activities. Mater. Chem. Phys. 115 (2009): 296-302.

26. Chen, P., Song, L., Liu, Y., and Fang, Y.-e., Synthesis of silver nanoparticles by γ-ray irradiation in acetic water solution containing chitosan. Radiat. Phys. Chem. 76 (2007): 1165-1168.

27. Janata, E., Structure of the trimer silver cluster Ag-3(2+). J. Phys. Chem. B. 107 (2003): 7334-7336.

28. Janata, E., Henglein, A., and Ershov, B. G., First Clusters of Ag-solution (ion reduction in aqueous) J. Phys. Chem. 98 (1994): 10888 - 10890

29. Huang, L., Zhai, M. L., Long, D. W., Peng, J., Xu, L., Wu, G. Z., *et al.*, UV-induced synthesis, characterization and formation mechanism of silver nanoparticles in alkalic carboxymethylated chitosan solution. J. Nanopart. Res. 10 (2008): 1193-1202.

30. Zhai, M., Kudoh, H., Wu, G., Wach, R. A., Muroya, Y., Katsumura, Y., *et al.*, Laser photolysis of carboxymethylated chitin derivatives in aqueous solution. Part 1. Formation of hydrated electron and a long-lived radical. Biomacromolecules 5 (2004): 453-457.

31. Ershov, B. G., Janata, E., Henglein, A., and Fojtik, A., Silver atoms and clusters in aqueous solution: absorption spectra and the particle growth in the absence of stabilizing Ag+ ions. J. Phys. Chem. 97 (1993): 4589-4594.

32. Ershov, B. G., Janata, E., and Henglein, A., Growth of silver particles in aqueous solution: long-lived "magic" clusters and ionic strength effects. J. Phys. Chem. B 97 (1993): 339-343.

33. Ershov, B. G., and Henglein, A., Time-Resolved Investigation of Early Processes in the Reduction of Ag+on Polyacrylate in Aqueous Solution. J. Phys. Chem. B 102 (1998): 10667-10671.

34. Hebeish, A. A., El-Rafie, M. H., Abdel-Mohdy, F. A., Abdel-Halim, E. S., and Emam, H. E., Carboxymethyl cellulose for green synthesis and stabilization of silver nanoparticles. Carbohydr. Polym. 82 (2010): 933-941.

35. Bin Xue, P. C., Qi Hong, Jianyi Lina, Kuang Lee Tana Growth of Pd, Pt, Ag and Au nanoparticles on carbon nanotubes. J. Mater. Chem. 11 (2001): 2378-2381.

36. Aswathy, B., Avadhani, G. S., Sumithra, I. S., Suji, S., and Sony, G., Microwave assisted synthesis and UV-Vis spectroscopic studies of silver nanoparticles synthesized using vanillin as a reducing agent. J. Mol. Liq. 159 (2011): 165-169.

37. Martinez-Castanon, G. A., Nino-Martinez, N., Martinez-Gutierrez, F., Martinez-Mendoza, J. R., and Ruiz, F., Synthesis and antibacterial activity of silver nanoparticles with different sizes. J. Nanopart. Res. 10 (2008): 1343-1348.

38. Watcharaporn, K., Opaprakasit, M., and Pimpan, V., Effects of UV radiation and pH of tannic acid solution in the synthesis of silver nanoparticles. Adv. Mater. Res. 911 (2014): 110-114.

39. Dong, X., Ji, X., Wu, H., Zhao, L., Li, J., and W., Y., Shape control of silver nanoparticles by stepwise citrate reduction. J. Phys. Chem. C 113 (2009): 6573–6576.

40. LaMer, V. K., and Dinegar, R. H., Theory production and mechanism of formation of monodispersed hydrosols. J. Am. Chem. Soc. 72 (1950): 4847–4854.

41. Hagerman, A. E., Riedl, K. M., Jones, G. A., Sovik, K. N., Ritchard, N. T., Hartzfeld, P. W., *et al.*, High molecular weight plant polyphenolics (tannins) as biological antioxidants. J. Agric. Food Chem. 46 (1998): 1887–1892.

42. Ling, J., Sang, Y., and Huang, C. Z., Visual colorimetric detection of berberine hydrochloride with silver nanoparticles. J. Pharm. Biomed. Anal. 47 (2008): 860-864.

43. Sivaraman, S. K., Elango, I., Kumar, S., and Santhanam, V., A green protocol for room temperature synthesis of silver nanoparticles in seconds. Curr. Sci. India 97 (2009): 1055-1059.

44. Yi, Z., Li, X. B., Xu, X. B., Luo, B. C., Luo, J. S., Wu, W. D., *et al.*, Green, effective chemical route for the synthesis of silver nanoplates in tannic acid aqueous solution. Colloid Surf., A 392 (2011): 131-136.

45. Liu, J., Qin, G., Raveendran, P., and Ikushima, Y., A facile and green synthesis, characterization, and catalytic function of b-Dglucose stabilized Au nanocrystals Chem. Eur. J. 12 (2006): 2131–2138.

46. Yoosaf, K., Ipe, B. I., Suresh, C. H., and Thomas, K. G., In situ synthesis of metal nanoparticles and selective naked-eye detection of lead ions from aqueous media. J. Phys. Chem. C 111 (2007): 12839–12847.

47. Dutta, A., and Dolui, S. K., Tannic acid assisted one step synthesis route for stable colloidal dispersion of nickel nanostructures. Appl. Surf. Sci. 257 (2011): 6889–6896.

48. Dubas, S. T., Kumlangdudsana, P., and Potiyaraj, P., Layer-by-layer deposition of antimicrobial silver nanoparticles on textile fibers. Colloid Surf., A 289 (2006): 105-109.

49. Cardenas, G., Munoz, C., and Carbacho, H., Thermal properties and TGA-FTIR studies of polyacrylic and polymethacrylic acid doped with metal clusters. Eur. Polym. J. 36 (2000): 1091–1099.

50. Patakfalvi, R., Papp, S., and Dekany, I., The kinetics of homogeneous nucleation of silver nanoparticles stabilized by polymers. J. Nanoparticles Res. 9 (2007): 353–364.

51. Luo, C., Zhang, Y., Zeng, X., Zeng, Y., and Wang, Y., The role of poly(ethylene glycol) in the formation of silver nanoparticles J. Colloid Interf. Sci. 288 (2005): 444–448.

52. UC Davis ChemWiki. Oxidizing and Reducing Agents. [online]. 2014. source: http://chemwiki.ucdavis.edu/.../Oxidizing_and_Reducing_Agents

53. Spadaro, D., Barletta, E., Barreca, F., Curro, G., and Neri, F., Synthesis of PMA stabilized silver nanoparticles by chemical reduction process under a two-step UV irradiation. Appl. Surf. Sci. 256 (2010): 3812-3816.

54. Singh, V., and Ahmad, S., Synthesis and characterization of carboxymethyl cellulose-silver nanoparticle (AgNp)-silica hybrid for amylase immobilization. Cellulose 19 (2012): 1759-1769.

55. Peterson, E. A., and Sober, H. A., Chromatography of Proteins. I. Cellulose Ion-exchange Adsorbents. J. Am. Chem. Soc. 78 (1956): 751-755.

56. Dong, Y. M., Xu, C. Y., Wang, J. W., Wu, Y. S., Wang, M., and Ruan, Y. H., Influence of degree of deacetylation on critical concentration of chitosan/dichloroacetic acid liquid-crystalline solution. J. Appl. Polym. Sci. 83 (2002): 1204-1208.

57. Pillai, C. K. S., Paul, W., and Sharma, C. P., Chitin and chitosan polymers: Chemistry, solubility and fiber formation. Prog. Polym. Sci. 34 (2009): 641-678.

58. Dong, T. Y., Chen, W. T., Wang, C. W., Chen, C. P., Chen, C. N., Lin, M. C., *et al.*, One-step synthesis of uniform silver nanoparticles capped by saturated decanoate: direct spray printing ink to form metallic silver films. Phys. Chem. Chem. Phys. 11 (2009): 6269-6275.

59. Ravi Kumar, M. N. V., A review of chitin and chitosan applications. React. Funct. Polym. 46 (2000): 1-27.

60. Božanić, D. K., Trandafilović, L. V., Luyt, A. S., and Djoković, V., 'Green' synthesis and optical properties of silver–chitosan complexes and nanocomposites. React. Funct. Polym. 70 (2010): 869-873.

61. Chen, Z., Wang, Z., Chen, X., Xu, H., and Liu, J., Chitosan-capped gold nanoparticles for selective and colorimetric sensing of heparin. J. Nanopart. Res. 15 (2013): 1930.

62. Huang, H., Yuan, Q., and Yang, X., Preparation and characterization of metal-chitosan nanocomposites. Colloids Surf., B Biointerfaces 39 (2004): 31-37.

63. Yi, H., Wu, L. Q., Bentley, W. E., Ghodssi, R., Rubloff, G. W., Culver, J. N., *et al.*, Biofabrication with chitosan. Biomacromolecules 6 (2005): 2881-2894.

64. Peter, K. J. P., Manu, N., Chacko, J., and Nair, S. M., Synthesis of silver nanoparticles and of self assembled supramolecules from marine humic acid. J. Exp. Nanosci. (2012): 1-9.

65. von Wandruszka, R., Ragle, C., and Engebretson, R., The role of selected cations in the formation of pseudomicelles in aqueous humic acid. Talanta 44 (1997): 805-809.

66. Bauer, M., Heitmann, T., Macalady, D. L., and Blodau, C., Electron transfer capacities and reaction kinetics of peat dissolved organic matter. Environ. Sci. Technol. 41 (2007): 139-145.

67. Kang, C. A., Kim, M. R., Shen, J. Y., Cho, I. K., Park, B. J., Kim, I. S., *et al.*, Supercritical Fluid Extraction for Liquid Chromatographic Determination of Pyrazosulfuron-Ethyl in Soils. Bull. Environ. Contam. Toxicol. 76 (2006): 745-751.

68. Central Agricultural Pesticides Laboratory. Pyrazosulfuron-ethyl [online]. 2009. source: http://www.capl.sci.eg/ActiveIngredient/Pyrazosulfuron-ethyl.html

69. Kamel, F., Epidemiology. Paths from pesticides to Parkinson's. Science 341 (2013): 722-723.

70. Durán, N., Marcato, P. D., De Souza, G. I. H., Alves, O. L., and Esposito, E., Antibacterial Effect of Silver Nanoparticles Produced by Fungal Process on Textile Fabrics and Their Effluent Treatment. J. Biomed. Nanotechnol. 3 (2007): 203-208.

71. Yeo, S. Y., Preparation of nanocomposite fibers for permanent antibacterial effect. J. Mater. Sci. 38 (2003): 2143-2147.

72. Lee, H. J., Yeo, S. Y., and Jeong, S. H., Antibacterial effect of nanosized silver colloidal solution on textile fabrics. J. Mater. Sci. 38 (2003): 2199-2204.

73. Lee, H. J., and Jeon, S. H., Bacteriostasis of Nanosized Colloidal Silver on Polyester Nonwovens. Text. Res. J. 74 (2004): 442-447.

74. Jain, P., and Pradeep, T., Potential of silver nanoparticles-coated polyurethane foam as an antibacterial water filter. Biotechnol. Bioeng. 90 (2005): 59-63.

75. Kim, D., and Moon, J., Highly Conductive Ink Jet Printed Films of Nanosilver Particles for Printable Electronics. Electrochem. Solid St. 8 (2005): J30.

76. Manno, D., Filippo, E., Di Giulio, M., and Serra, A., Synthesis and characterization of starch-stabilized Ag nanostructures for sensors applications. J. Non-Cryst. Solids 354 (2008): 5515-5520.

77. Köhler, J. M., Abahmane, L., Wagner, J., Albert, J., and Mayer, G., Preparation of metal nanoparticles with varied composition for catalytical applications in microreactors. Chem. Eng. Sci. 63 (2008): 5048-5055.

78. InTech. Silver Nanoparticles: Sensing and Imaging Applications. [online]. 2010. source: http://www.intechopen.com/books/silver-nanoparticles/silver-nanoparticles-sensing-and-imaging-applications

79. Hormozi Nezhad, M. R., Tashkhourian, J., and Khodaveisi, J., Sensitive spectrophotometric detection of dopamine, levodopa and adrenaline using surface plasmon resonance band of silver nanoparticles. J. Iran. Chem. Soc. 7 (2010): S83-S91.

80. Paulson, G. W., Addiction to nicotine is due to high intrinsic levels of dopamine. Med. Hypoth. 38 (1992): 206-207.

81. Kelly, K. L., Coronado, E., Zhao, L. L., and Schatz, G. C., The optical properties of metal nanoparticles: The influence of size, shape, and dielectric environment. J. Phys. Chem. B 107 (2003): 668-677.

82. Sigma-Aldrich. FAOs, Chemical synthesis, Humic acid H16752. [online]. 2014. source: http://sigma-aldrich.custhelp.com/app/answers/list/p/128,249

83. Polewski, K., Kniat, S., and Slawinska, D., Gallic acid, a natural antioxidant, in aqueous and micellar environment: spectroscopic studies. Curr. Top. Biophys 26 (2000): 217-227.

84. Palaniswamy, R., Wang, C., Tam, K. C., and Gan, L. H., Association Behavior of Poly(methacrylic acid)-block-Poly(methyl methacrylate) in Aqueous Medium: Potentiometric and Laser Light Scattering Studies. (2003):

85. Cesarano, J., Aksay, I. A., and Bleier, A., Stability of Aqueous alpha-Al2O3 Suspensions with Poly(methacrylic acid) Polyelectrolyte. J. Am. Ceram. Soc. 71 (1988): 250-255.

86. UC Davis ChemWiki. Introduction to carboxylic acid derivatives and the nucleophilic acyl substitution reaction. [online]. 2014. source: http://chemwiki.ucdavis.edu/.../Section_12.1%3A_Introduction_to_carboxylic_acid_derivatives_and_the_nucleophilic_acyl_substitution_reaction

87. Wikimedia Foundation, Inc. Tollens' reagent. [online]. 2014. source: http://en.wikipedia.org/wiki/Tollens%27_reagent

88. Reactions Involving Aldehydes and Ketones. 1997, North Lake College.

89. Wikimedia Foundation, Inc. Reducing sugar. [online]. 2012. source: http://en.wikipedia.org/wiki/Reducing_sugar

90. Univ. Mass. Amherst. Carbohydrates. [online]. 2013. source: https://www2.chemistry.msu.edu/faculty/reusch/virttxtjml/carbhyd.htm

91. Theo van de Ven and Louis Godbout. Electric Properties of Carboxymethyl Cellulose. 2013.

92. Le, A. T., Le, T. T., Phuong, D. T., Huy, P. T., Tran, Q. H., Nguyen, V. H., *et al.*, Synthesis of oleic acid-stabilized silver nanoparticles and analysis of their antibacterial activity. Mat. Sci. Eng. C-Mater. 30 (2010): 910-916.

93. Columbia University. Acidity, Basicity and pKa. [online]. 2006. source: http://www.columbia.edu/~crg2133/Files/CambridgeIA/Chemistry/AcidityBasicitykPa.pdf [Oct. 23, 2014]

94. Sarmah, A. K., Kookana, R. S., and Alston, A. M., Leaching and degradation of triasulfuron, metsulfuron-methyl, and chlorsulfuron in alkaline soil profiles under field conditions. Aust. J. Soil Res. 38 (2000): 617-631.

95. Sulfonylurea herbicides. 1988.

96. Sarmah, A. K., and Sabadie, J., Hydrolysis of sulfonylurea herbicides in soils and aqueous solutions: a review. J. Agric. Food Chem. 50 (2002): 6253-6265.

97. Brown, H. M., Mode of action, crop selectivity, and soil relations of the sulfonylurea herbicides. Pestic. Sci. 29 (1990): 263-281.

98. Singh, S. B., and Singh, N., Degradation behaviour of pyrazosulfuron-ethyl in water as affected by pH. J. Environ. Sci. Health B 48 (2013): 266-271.

99. Auburn. Carboxylic Acid Structure and Chemistry. [online]. 2005. source: http://www.auburn.edu/~deruija/pda1_acids1.pdf

100. Chem guide. Amines as bases [online]. 2004. source: http://www.chemguide.co.uk/organicprops/amines/base.html

101. Environmental chemistry of soils. . 63. 1994.

102. Rhoda, O. M., Rufus, S., and Nnadozie, N. N., The Role of Paraquat (1,1-dimethyl-4,4-bipyridiniumchloride) and Glyphosate (n-phosphonomethyl glycine) in Translocation of Metal Ions to Subsurface Soils. Pak. J. Anal. Environ. Chem. 10 (2009): 19-24.

APPENDIX

APPENDIX A

Table A-1 List of abbreviations

Abbrevation	Full name
TA	Tannic acid
PMA	poly (methacrylic acid sodium salt)
CS	Chitosan
CMC	Carboxylmethyl cellulose sodium salt
HA	humic acid sodium salt

APPENDIX B

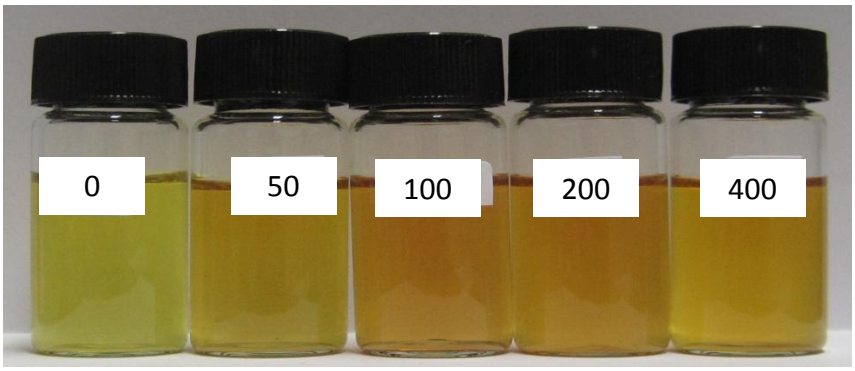

Figure B-1 Appearances of TA-stabilized silver nanoparticles colloids synthesized using initial pH of 7.0 and MR of 1:10 exposed to various amount of PSE herbicide (ppm)

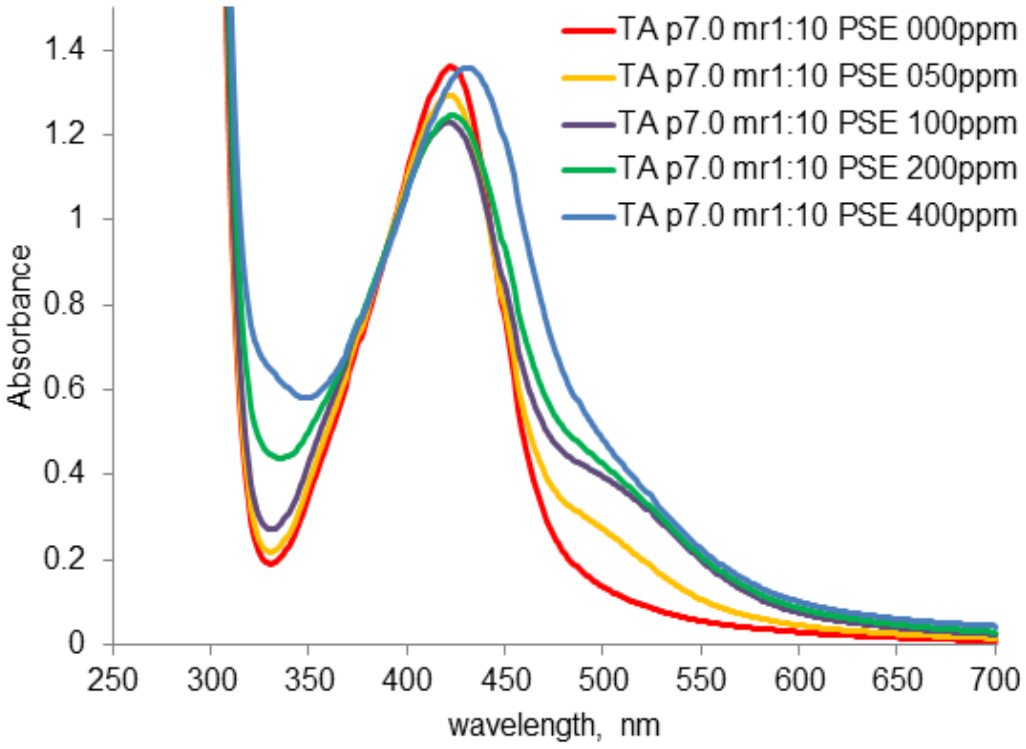

Figure B-2 UV-Vis spectra of TA-stabilized silver nanoparticles colloids synthesized using initial pH of 7.0 and MR of 1:10 exposed to various amount of PSE herbicide (ppm).

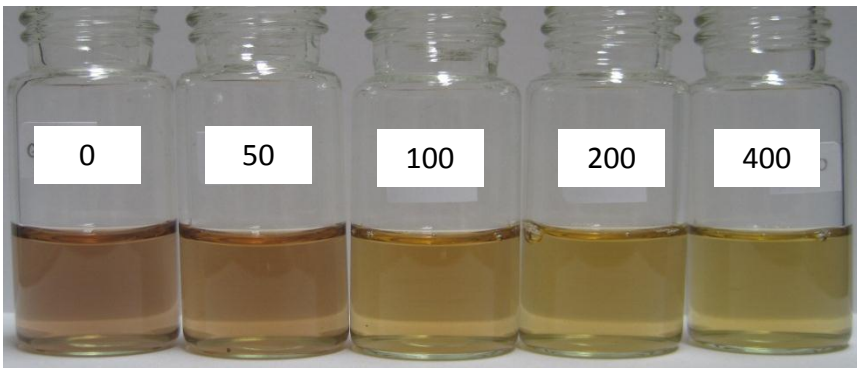

Figure B-3 Appearances of PMA-stabilized silver nanoparticles colloids synthesized using initial pH of 7.0 and MR of 1:10 exposed to various amount of PQ herbicide (ppm)

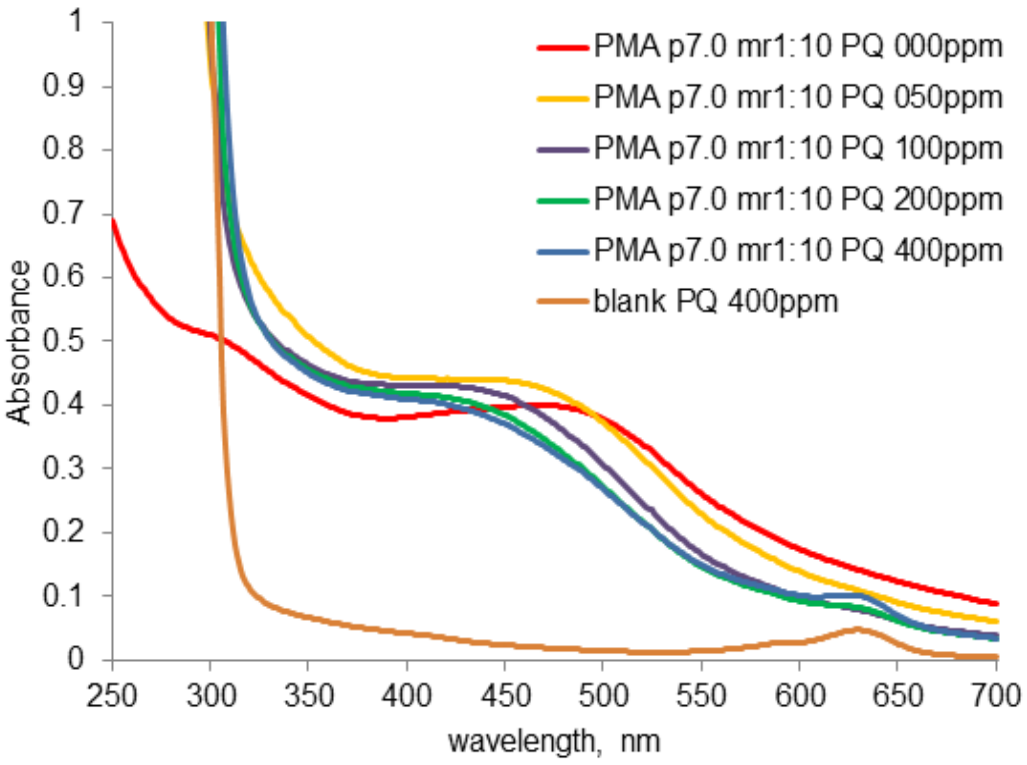

Figure B-4 UV-Vis spectra of PMA-stabilized silver nanoparticles colloids synthesized using initial pH of 7.0 and MR of 1:10 exposed to various amount of PQ herbicide (ppm).

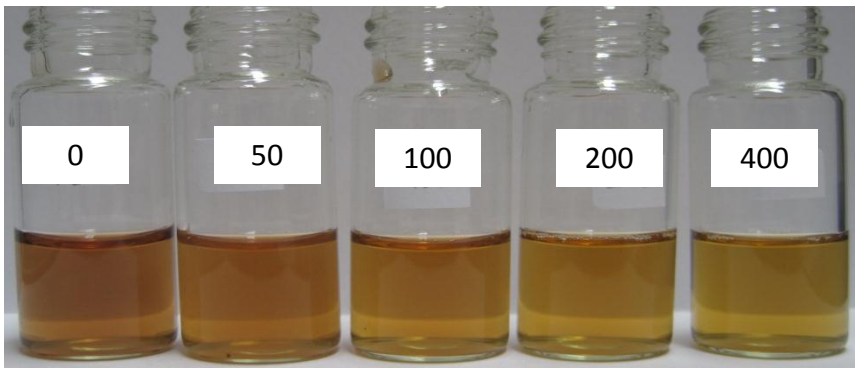

Figure B-5 Appearances of PMA-stabilized silver nanoparticles colloids synthesized using initial pH of 8.0 and MR of 1:10 exposed to various amount of PQ herbicide (ppm)

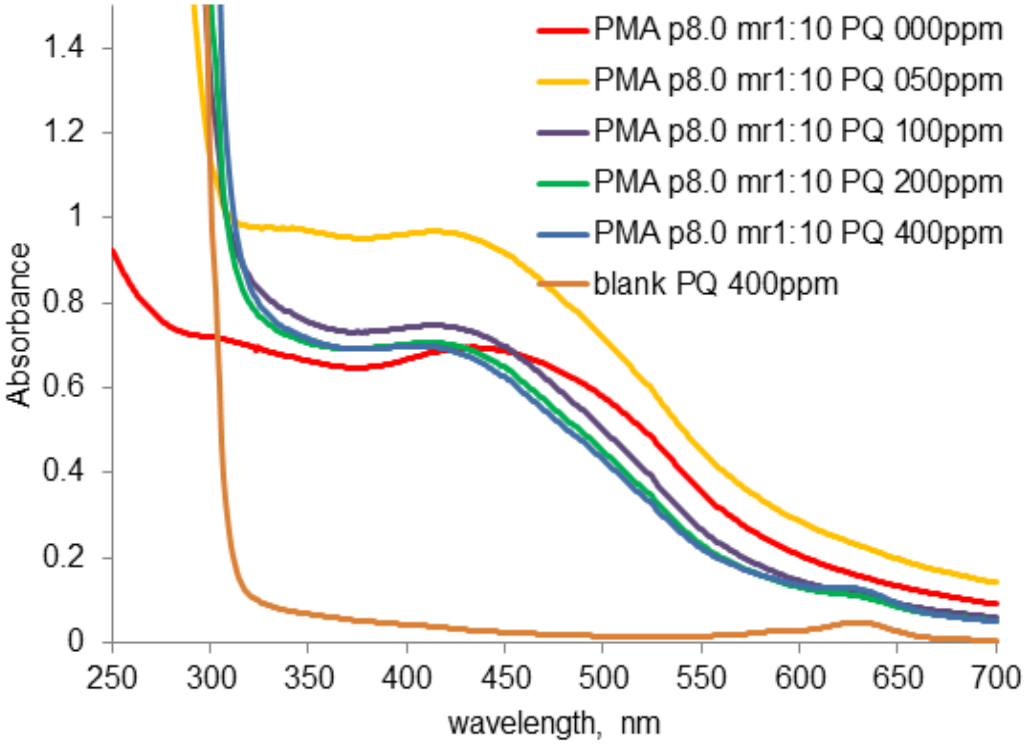

Figure B-6 UV-Vis spectra of PMA-stabilized silver nanoparticles colloids synthesized using initial pH of 8.0 and MR of 1:10 exposed to various amount of PQ herbicide (ppm).

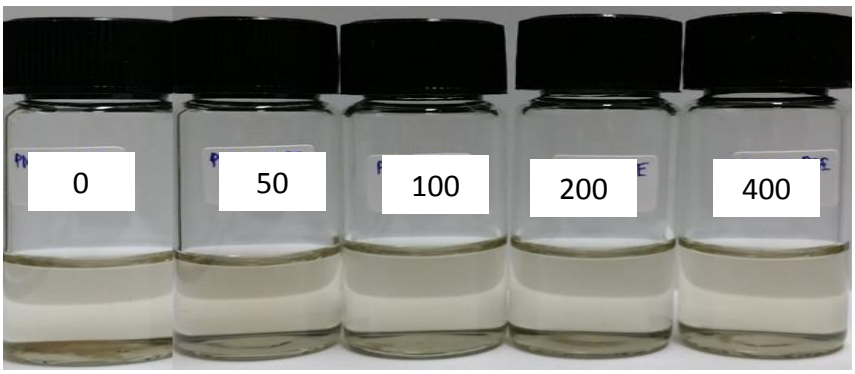

Figure B-7 Appearances of PMA-stabilized silver nanoparticles colloids synthesized using initial pH of87.0 and MR of 1:1 exposed to various amount of PSE herbicide (ppm)

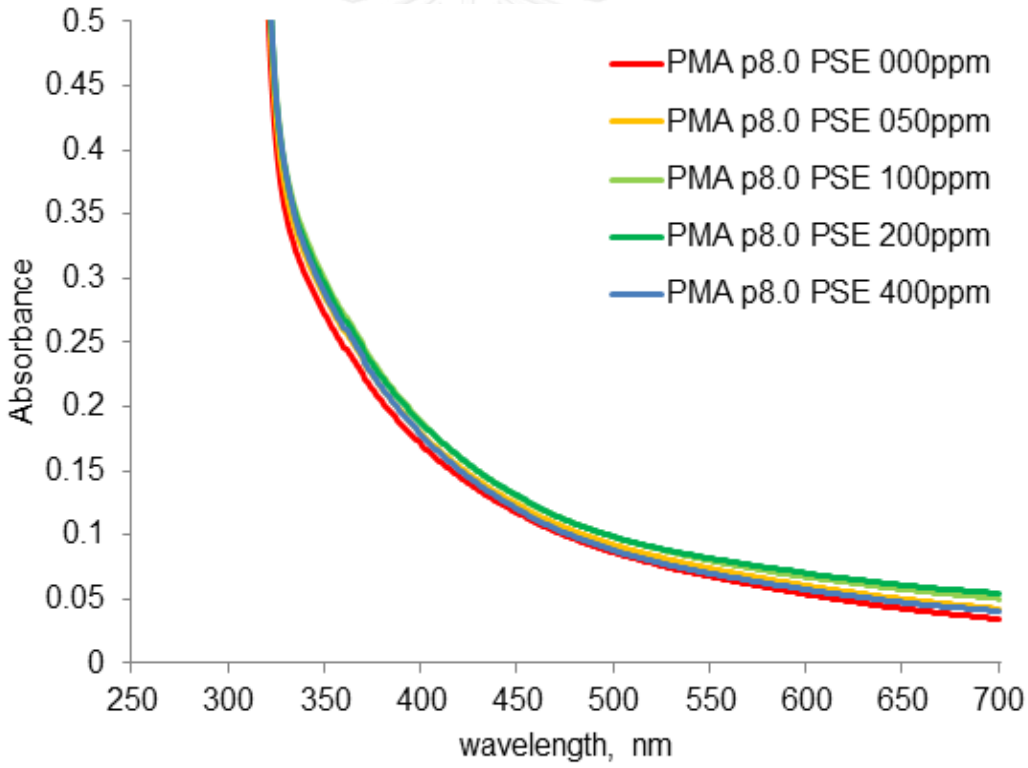

Figure B-8 UV-Vis spectra of PMA-stabilized silver nanoparticles colloids synthesized using initial pH of 8.0 and MR of 1:1 exposed to various amount of PSE herbicide (ppm).

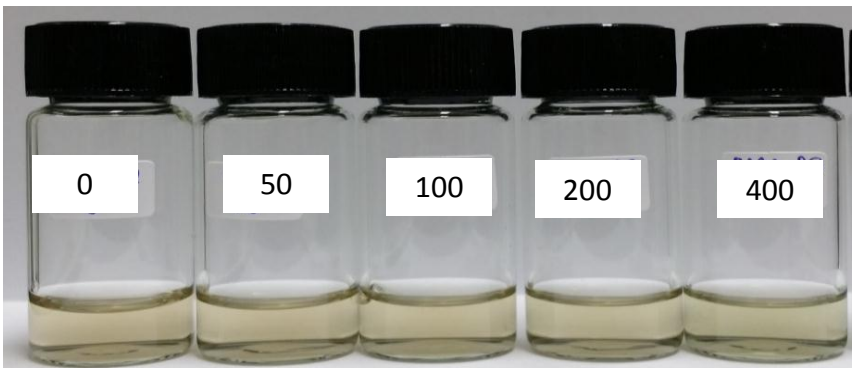

Figure B-9 Appearances of PMA-stabilized silver nanoparticles colloids synthesized using initial pH of 8.0 and MR of 1:1 exposed to various amount of PQ herbicide (ppm)

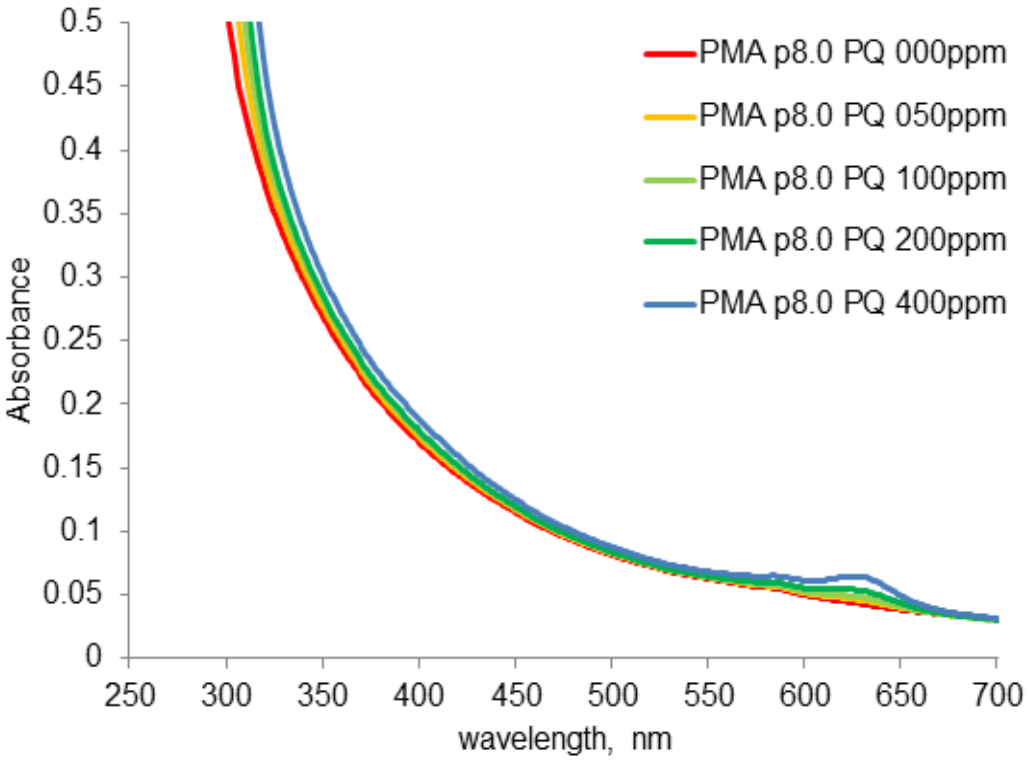

Figure B-10 UV-Vis spectra of PMA-stabilized silver nanoparticles colloids synthesized using initial pH of 8.0 and MR of 1:1 exposed to various amount of PSE herbicide (ppm).

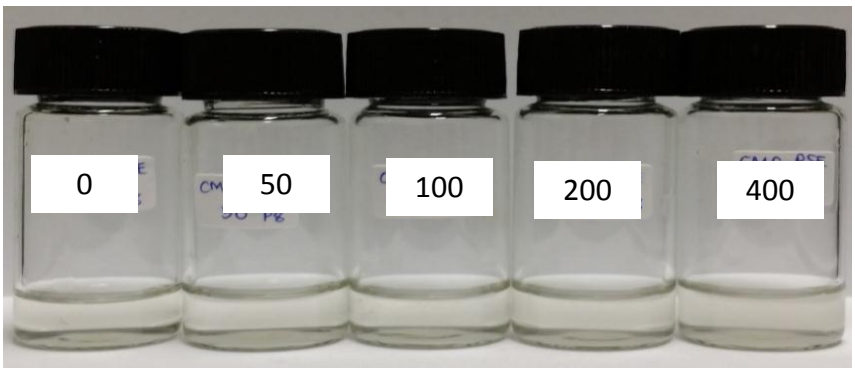

Figure B-11 Appearances of CMC-stabilized silver nanoparticles colloids synthesized using initial pH of 8.0 and MR of 1:10 exposed to various amount of PSE herbicide (ppm)

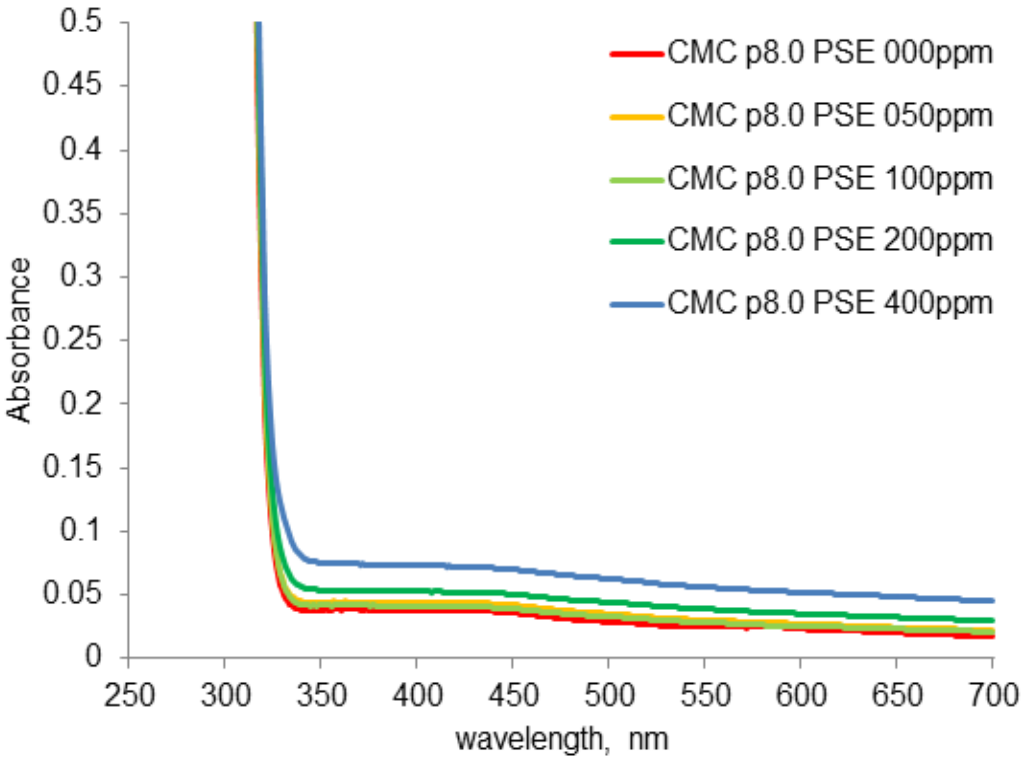

Figure B-12 UV-Vis spectra of CMC-stabilized silver nanoparticles colloids synthesized using initial pH of 8.0 and MR of 1:10 exposed to various amount of PSE herbicide (ppm).

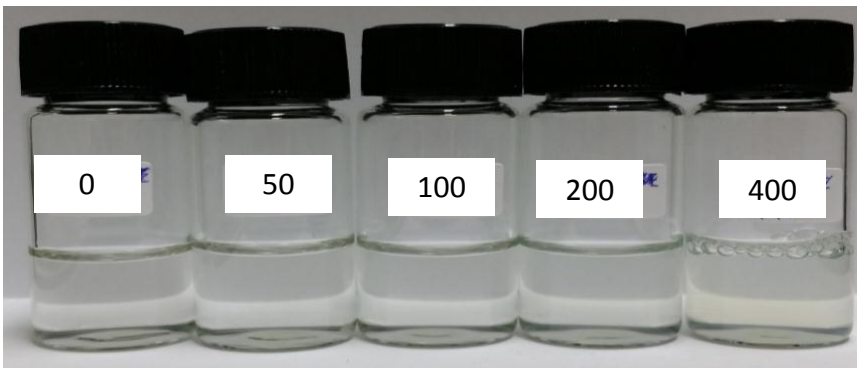

Figure B-13 Appearances of CMC-stabilized silver nanoparticles colloids synthesized using initial pH of 8.0 and MR of 1:10 exposed to various amount of PQ herbicide (ppm)

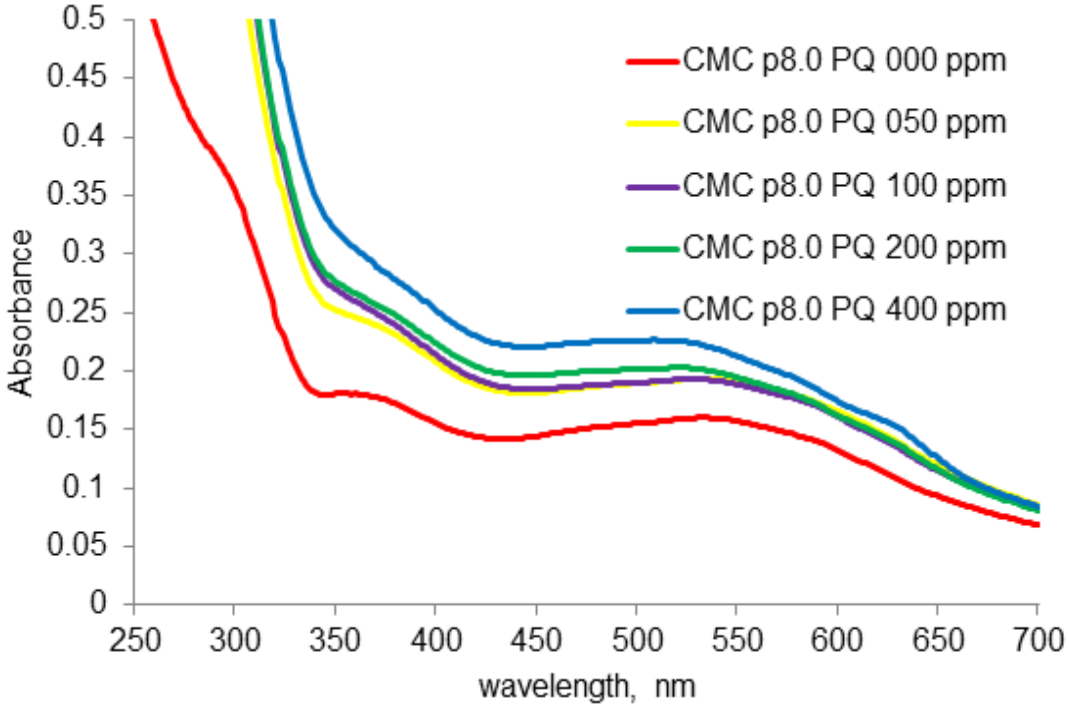

Figure B-14 UV-Vis spectra of CMC-stabilized silver nanoparticles colloids synthesized using initial pH of 8.0 and MR of 1:10 exposed to various amount of PQ herbicide (ppm).

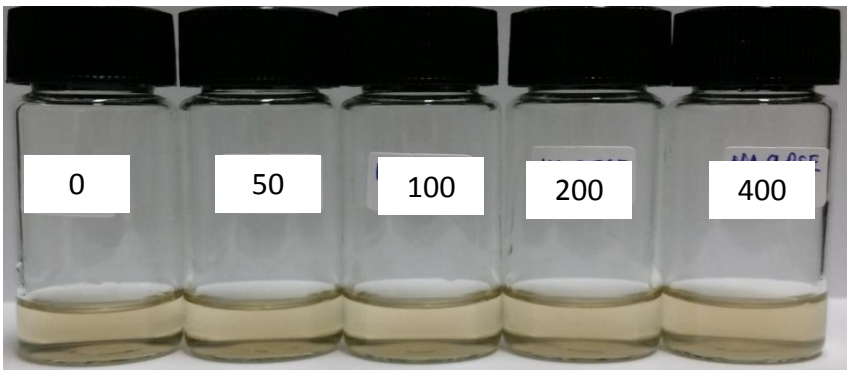

Figure B-15 Appearances of HA-stabilized silver nanoparticles colloids synthesized using initial pH of 9.0 with 0.009 %w/v HA solutions exposed to various amount of PSE herbicide (ppm)

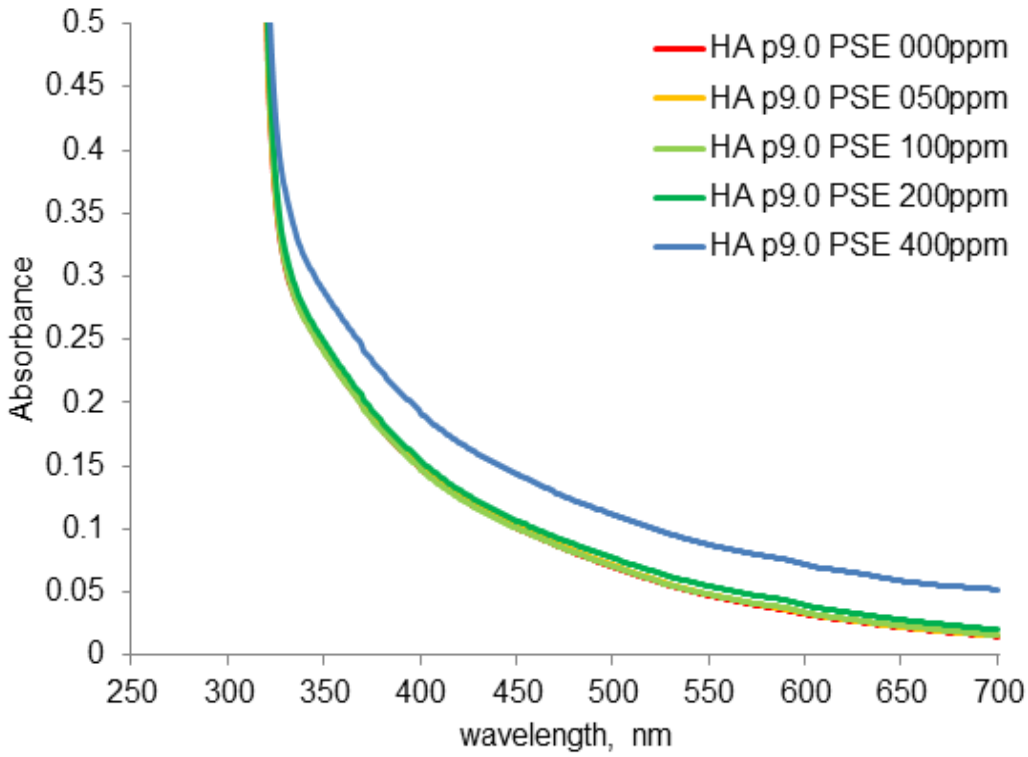

Figure B-16 UV-Vis spectra of HA-stabilized silver nanoparticles colloids synthesized using initial pH of 9.0 with 0.009 %w/v HA solutions exposed to various amount of PSE herbicide (ppm).

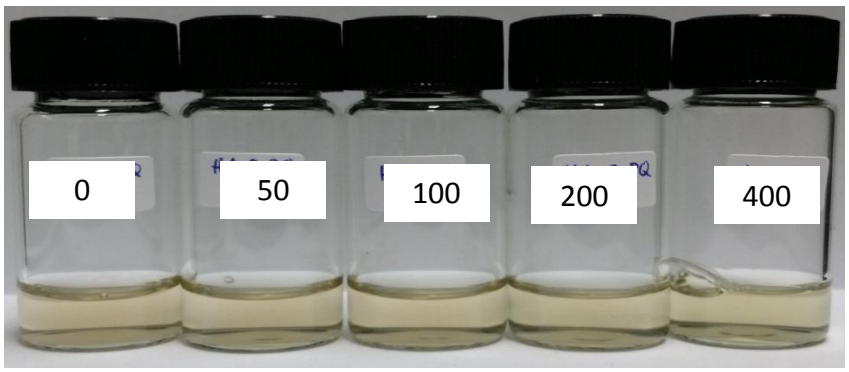

Figure B-17 Appearances of HA-stabilized silver nanoparticles colloids synthesized using initial pH of 9.0 with 0.009 %w/v HA solutions exposed to various amount of PQ herbicide (ppm)

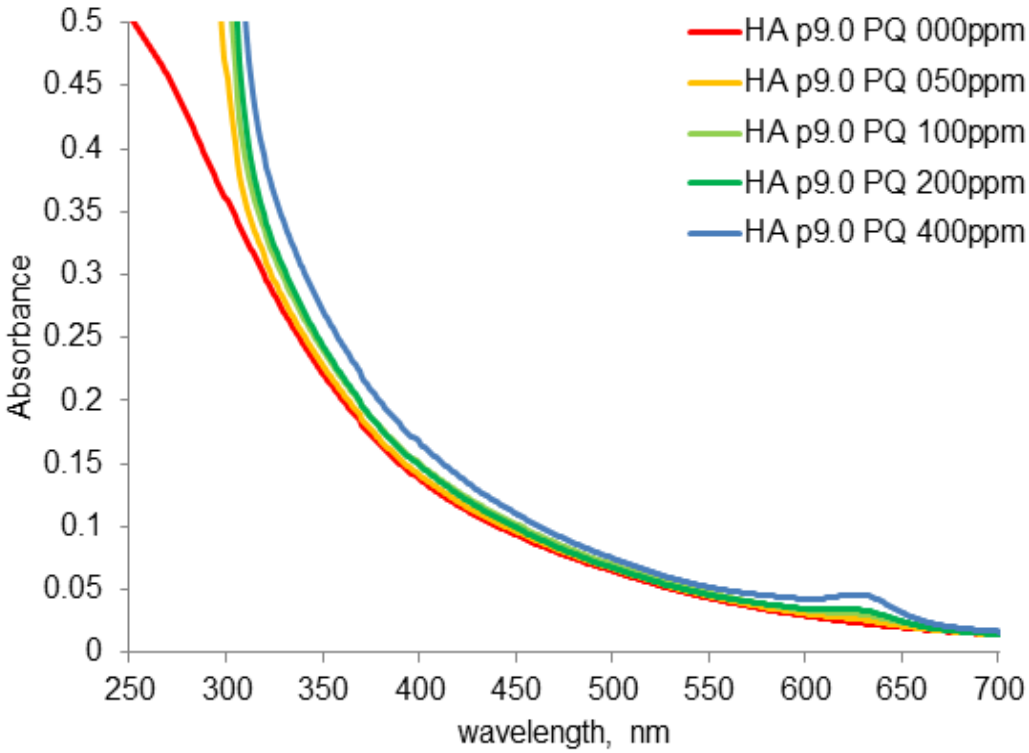

Figure B-18 UV-Vis spectra of HA-stabilized silver nanoparticles colloids synthesized using initial pH of 9.0 with 0.009 %w/v HA solutions exposed to various amount of PQ herbicide (ppm).

VITA

Mrs. Kanitta Watcharaporn was born in Bangkok, Thailand on November 18, 1971. She received Bachelor's Degree of Science in Material Science from Department of Materials Science, Chulalongkorn University in 1994. After that she started working as quality control supervisor, at Teijin Polyester, Ltd., Thailand and then moved to work as lab analyst for Kimberly & Clark, Asia Pacific Headquarters. In 1997, she got scholarship from Thai government to pursue her master degree in Textile Chemistry, at Clemson University, USA. After graduated in 2000, she started her new carrier as lecturer in Textile department, Agro-industry faculty, Kasetsart University. Later in 2008, she continued her further study of Doctoral program in Materials Science, Chulalongkorn University, and graduated in 2014.

PUBLICATION:

1. Kanitta Watcharaporn, Mantana Opaprakasit, and Vimolvan Pimpan, Effects of UV Radiation and pH of Tannic Acid Solution in the Synthesis of Silver Nanoparticles. Advanced Materials Research, Volume 911, 2014: p110-114.